Phosphorus removal and induced precipitation in aerobic granular sludge process for wastewater treatment

Angela Manas Llamas

Université de Toulouse

THÈSE

En vue de l'obtention du

DOCTORAT DE L'UNIVERSITÉ DE TOULOUSE

Délivré par :
Institut National Polytechnique de Toulouse (INP Toulouse)

Discipline ou spécialité :

Génie des procédés et de l'environnement

Présentée et soutenue par :
Angela Mañas Llamas

le : vendredi 16 décembre 2011

Titre :

Immobilisation du phosphore par précipitation induite dans un procédé aérobie à biomasse granulaire

---

Ecole doctorale :
Mécanique, Energétique, Génie civil et Procédés (MEGeP)

Unité de recherche :
LISBP - INSA, Toulouse

Directeur(s) de Thèse :
Mathieu SPERANDIO (LISBP, Toulouse), directeur de thèse
Béatrice BISCANS (LGC, Toulouse) Co-directrice de thèse

Rapporteurs :

Eberhard MORGENROTH (EAWAG, Zürich)
Aurora SECO (Universidad Politécnica, Valencia)

Membre(s) du jury :
Eberhard MORGENROTH (EAWAG, Zürich), Rapporteur
Aurora SECO (Universidad Politécnica, Valencia), Rapporteur
Christèle COMBES (CIRIMAT, Toulouse), Examinateur
Marie-Line DAUMER (CEMAGREF, Rennes), Examinateur
François DECKER (VALBIO, Toulouse) Examinateur

MANUSCRIT FINAL DE THESE

Issu de l'obtention du doctorat en:

GENIE DES PROCEDES ET DE L'ENVIRONNEMENT

à: INSTITUT NATIONAL POLYTECHNIQUE de Toulouse

et: INSTITUT NATIONAL DES SCIENCES APPLIQUEES de Toulouse

Angela Mañas Llamas

Immobilisation du phosphore par précipitation induite dans un procédé aérobie à biomasse granulaire

Co-encadrants:

Mathieu Spérandio (Laboratoire d'Ingénierie des Systèmes Biologiques et des Procédés –LISBP-, INSA, Toulouse)

Béatrice Biscans (Laboratoire de Génie Chimique –LGC-, INP, Toulouse)

Soutenue le **16 décembre 2011** à l'INSA Toulouse.

Commission d'examen:

Eberhard MORGENROTH (EAWAG, Zürich)	Rapporteur
Aurora SECO (Universidad Politécnica, Valencia)	Rapporteur
Christèle COMBES (CIRIMAT, Toulouse)	Examinateur
Marie-Line DAUMER (CEMAGREF, Rennes)	Examinateur
François DECKER (VALBIO, Toulouse)	Examinateur
Béatrice BISCANS (LGC, Toulouse)	Co-directrice
Mathieu SPERANDIO (LISBP, Toulouse)	Co-directeur

A mis abuelas, Adela y Ángela por todo el cariño y dedicación que siempre me dieron.

REMERCIEMENTS

"On n'est curieux qu'à proportion qu'on est instruit" (Jean-Jacques Rousseau, Emile ou de l'éducation, 1762)

Cette thèse a pu être aboutie grâce à tous les gens qui au bout de ces trois années m'ont accueilli, dirigé, corrigé, appris et soutenu dans les moments les plus difficiles.

Tout d'abord, je tiens à remercier mes encadrants, M. Spérandio et B. Biscans, à qui je leur dédie la phrase de Rousseau du début, preuve de mon respect pour leurs connaissances et de ma gratitude.

Merci aussi à François et à Sandra, de Valbio, pour leur support pour leurs contributions dans les aspects pratiques de la thèse.

Merci à toute l'équipe technique qui a contribué à la mise en oeuvre des différents pilotes, avec une mention speciale à S. Julien et D. Auban (et ses trains ratés à cause du MEB ☺) etpour letemps qu'ils m'ont accordé à realiser mes expériences.

Chers Yoan, Mathieu Po., Ahlem, Paula, c'est un vrai plaisir de travailler avec vous; merci beaucoup pour votre aide à la construction de ces chapitres. Merci aux collègues (Sophie, Laetitia, Mathieu Pe., Pong) pour votre soutien et je vous souhaite beaucoup de succès bien mérité dans vos thèses.

Merci Sebastien car tu m'as poussé à faire cette thèse lorsque je découpais du papier-carton☺. Et merci à Jungfeng, pour avoir laissé la base de ton travail ouverte aux nouveaux horizons pour Cedric, Ahlem et moi.

Merci "querida" Irene, pour avoir été toujours à côté de moi toujours dans les moments les plus difficiles, ainsi que Sarah, Caroline, Cédric,… et autant d'autres que j'oublie peut être de mentionner maintenant, mais dont leurs chemins se sont croisés pendant ce temps à Toulouse et avec lesquels j'ai partagé des moments importants.

Comme vous dites, *un coucou* pour Fatima, "obrigada" pour les pauses partagées et tes mots pendant la rédaction à l'INP, ainsi qu'à Baptiste et à Nicolas: merci de m'avoir aidé à m'intégrer là-bas et à me désintégrer avec le RAMAN ☺.

Merci aux rapporteurs et aux examinateurs pour vos commentaires et pour l'intêret que vous avez porté dans ce travail.

Y finalmente, quiero agradecer a mis padres, el esfuerzo continuo que han hecho siempre para poder ayudarme, y el haberme transmitido esa curiosidad por las cosas; a mi hermana por su admiración y devoción y por último, quiero agradecerte a ti, Alfonso, el que me hayas apoyado en todo momento.

A todos vosotros, MUCHAS GRACIAS.

GENERAL INTRODUCTION

This dissertation makes part of a Ph.D program financed by the French government (*Ministère de l'Education Nationale*) in cooperation with the **Laboratoire d'Ingénierie des Systèmes Biologiques et des Procédés (LISBP)**, at the Institut National des Sciences Appliquées, and the **Laboratoire de Génie Chimique (LGC)** at the Institut National Polytechnique, in Toulouse, France. The work developed during this Ph.D has also contributed to some tasks in two different national projects: VALORCAP (2009-2010) and PHOSPH'OR (2010-2011) aiming the *Valorisation of Carbon, Nitrogen and Phosphorus, from agriculture and Industry wastes: modelling of nitrogen and phosphorus transformation processes*", being this thesis focused on the phosphorus transformation processes.

Phosphorus is a non-renewable resource and an important macronutrient on which life depends and for which there is no substitute. Reserves are unevenly spread on the Earth, but almost all phosphorus used by society is mined from a comparatively small number of commercially exploitable deposits in the world, making phosphorus recovery necessary in the coming decades. On the other hand, in response to the increasing eutrophication phenomena in aquatic systems all over the world, phosphorus is a target nutrient on which legislation is becoming more stringent.

Aerobic granulation technology has been proven to withstand high organic loads in compact systems, as well as a promising technology regarding the performances of simultaneous nitrification, denitrification and phosphate (SNDP) removal process. Previous work in the laboratory (Wan J. thesis in 2009), with a hybrid aerobic granulation process, revealed that stable aggregates could form by alternating anoxic/aerobic conditions in a SBR, identifying 3 main research axis to overcome: the first one, consists on the comprehension of the nitrogen removal processes involving a floccular and granular hybrid sludge process (Thesis of A. Filali, 2011); the second one consists on the characterization of the EPS (exopolymeric substances) and its role in the granular aggregation mechanism (Thesis of C. Caudan, 2011); and the third one, implicates the study of the phosphorus processes that take place in a granular sludge batch reactor (GSBR).

This thesis has focused in particular on a biomineralization phenomenon of phosphorus immobilization inside the aerobic granules, and the particular objectives will be specified in section I.5. The thesis is structured in four result chapters, each of them, aimed to constitute the basis of a peer-reviewed publication in different international scientific journals (see section *List of publications and collaborations* below).

EDUCATION

- 2002-2008: CHEMICAL ENGINEER (bac+5). UNIVERSITY OF VALLADOLID, Spain.
- 2008: Master Pro Internal Auditor in Quality Management (ISO 9000). BUREAU VERITAS, Madrid, Spain.
- 2008-2011: Ph.D fellow in Environmental Engineering Processes at INSA-INP, Toulouse, France.

TRAINING EXPERIENCE

- 2008-2011: Research activity as Ph.D student on thesis entitled: *Immobilisation du phosphore par précipitation induite dans un procédé aérobie à biomasse granulaire* at LISBP-LGC, Toulouse, France.
- 2009-2011: Practical work teaching in the field of Chemical Engineering, Thermodynamics and Biological water treatment, Hydraulic Engineering, Thermal Transfer (IUT-Dépt. Génie Chimique, INSA/125h.) Co-supervision of initiation to research work on the topics of the adsorption of ammonium on activated sludge (12h, INSA).
- 2007-2008: Research activity during a Master Research at LISBP (6months). *Measure of aqueous diffusional coefficients for the anaerobic biodegradability of paper/cardboard wastes in landfills.*
- 2006: Internship in R&D Laboratory in METAROM (Agro-food industry). Amiens, France/1month. *Study* of the optimization parameters in a solid-solid vanillin extraction process applied for food flavors.
- 2005: Internship in a Quality & Control Laboratory (METAROM). Amiens, France/1month**.** *Security Protocols and Management of chemical products. Analytical methods for evaluating end-product conformity.*

ACCEPTED PUBLICATIONS:

- Mañas A., Spérandio M., Biscans B. (2011). *Biologically induced phosphorus precipitation in aerobic granular sludge process. Water Research* 45(12):3776-3786.
- Mañas A., Pocquet M., Biscans B., Spérandio M. *Parameters influencing calcium phosphate precipitation in granular sludge sequencing batch reactor.* (Submitted on 1st October 2011 à Chemical Engineering Science, Accepted: DOI 10.1016-CES-D-11-01301).
- Mañas A., Biscans B., F. Decker, Spérandio M. *Location and chemical composition of microbially induced phosphorus precipitates in anaerobic and aerobic granular sludge*. (Submitted on 4th November 2011 at Environmental Technology, accepted on may 2012: DOI-TENT-OA-2012-0106).
- Pommier S., Mañas A., Lefebvre X. (2008). *Analysis of the outcome of shredding pretreatment on the anaerobic biodegradability of paper and cardboard materials*. Bioresource Technology 101(2): 463-468.
- Filali A. Mañas A. Bessière Y., Biscans B., Spérandio M. *Stability and performances of two GSBRs operated with alternating anoxic/aerobic or anaerobic/aerobic conditions for nutrient removal* (submitted at Biochemical Engineering Journal, accepted on may 2012: *BEJ-D-11-00811R1).*

PUBLICATIONS SUBMITTED/IN SUBMISSION:

- Pocquet M., Mañas A., Spérandio M. *Integrated modelling and optimization of phosphorus recovery in high-strength wastewater treatment* (in course of submission at Water Research).

PATENT IN COLLABORATION WITH VALBIO- LGC-LISBP:

Procedé de Traitement biologique d'eaux uses par biomasse granulaire aérobie. (Registered on January 2011; FR 1150469).

ORAL PRESENTATIONS AND PROCEEDINGS:

Mañas A., Spérandio M., Biscans B. *Phosphorous recovery by inducing mineral phosphate precipitation in aerobic granular sludge process*. Société Française de Génie des Procédés SFGP (Marseille, 2009).

Mañas A., Spérandio M., Biscans B. *Etude de la précipitation du phosphore induite par réaction biologique dans un procédé de traitement d'effluent industriel par granulation aérobie.* APTEN (Poitiers, 2010)

Mañas A., Spérandio M., Biscans B. *Phosphorous precipitation in aerobic granules induced by biological reaction in a wastewater treatment process*. WEF-IWA Nutrient Removal. (Miami, 2011)

Pocquet M., Mañas A., Spérandio M. *Integrated modelling and optimization of phosphorous recovery in high-strength wastewater treatment*. Watermatex (San Sebastián, 2011)

Mañas A., Biscans B., Spérandio M. *Microbially induced phosphorous crystallization inside aerobic granules for wastewater treatment*. ISIC 18 (Zurich 2011).

POSTERS:

- Mañas A., Filali A., Spérandio M., Bessière Y., Biscans B. *Procédé de granulation aérobie pour l'élimination des pollutions DCO, N et P, ainsi que le recyclage sous forme valorisable du phosphore*. Price Pollutec, Lyon 2010.
- Mañas A., Spérandio M., Biscans B., Filali A., Bessiere Y., Decker F. *Phosphorous precipitation in aerobic granules induced by biological reaction in a wastewater treatment process.* WEF-IWA Nutrient Removal. Introduced at IWA Conference, Amsterdam 2011.
- Mañas A., Pocquet M., Decker F., Biscans B., Spérandio M. *Analysis of Mineral Precipitation inside anaerobic or aerobic granules*. SFGP 2011, Lille.

COLLABORATIONS AND PROJETCS INVOLVED:

VALORCAP: (Regional Project - Midi-Pyrinées- involving 3 laboratories and 3 companies). Collaboration in tasks 2 and 3 (aerobic granulation reactor performance and Phoshorous crystallization processes).

PHOSPH'OR: (Project from the Agence Nationale de Recherche). Collaboration in tasks 3 and 4 (Mechanisms of precipitation and modelling).

RÉSUMÉ:

Depuis une dizaine d'années, les procédés de granulation aérobie sont apparus comme une technologie prometteuse pour le traitement des effluents fortement chargés en azote, phosphore et carbone, tels que ceux issus de l'agro-industrie. La complexité microbienne de ces granules et les mécanismes qui leur donnent des propriétés exceptionnelles de décantation et de cohésion, constituent encore des axes de recherche importants. Dans cette thèse, le travail s'est axé sur un mécanisme encore non étudié : les processus de précipitation des phosphates au cœur des granules microbiennes.

Différentes techniques d'analyses spectrales, parfois adaptés pour la première fois à ce type de systèmes, comme la spectroscopie Raman, ont permis de caractériser la nature de ces minéraux formés au cœur des granules. L'analyse menée sur des réacteurs de laboratoires a démontré la présence des phosphates de calcium sous forme d'hydroxyapatite [$Ca_5(PO_4)_3(OH)$]. Cette précipitation est potentiellement induite par les variations locales de pH et de sursaturation provoqués par les réactions microbiennes à l'intérieur des granules. L'étude des phénomènes de biominéralisation à été étendu aux granules anaérobies issus des réacteurs de type UASB de l'industrie laitière. Un modèle physico-chimique sur les processus de précipitation sous forme matriciel sur AQUASIM®, couplé avec des bases de calcul de sursaturation (PHREEQC®), ont permis d'avancer des hypothèses sur les mécanismes influençant ces processus de biominéralisation, tels que la formation d'un précurseur amorphe de l'hydroxyapatite (ACP), ainsi que d'identifier les constantes de précipitation thermodynamiques ($pKsp_{|20ºC}$=28.07±0.58) et cinétiques dans différentes conditions opératoires.

Grâce au suivi d'un système biologique GSBR (*Granular Sludge Sequenced Batch Reactor*) pendant plus de 900 jours, la contribution de ce phénomène aux processus de déphosphatation a été estimé (46% dans les conditions testées). L'utilisation de ce processus pour immobiliser efficacement le phosphore et apporter des propriétés physiques stables aux granules a été également discutée. Une évaluation des performances et de la stabilité du réacteur à été mis en œuvre en alternant des cycles anoxies/aérobies ou anaérobies/aérobies vis-à-vis d'une future application industrielle. L'induction locale de la précipitation par les variations de pH et par le relargage des phosphates par les réactions microbiennes, nécessite une modélisation appropriée, qui a été également initiée dans cette thèse.

SUMMARY:

Over the last decade, aerobic granulation processes have araised as a promising technology for treating wastewater effluents containing high nitrogen, phosphorus and carbon concentrations. The microbial complexity of granules and the mechanisms by which they acquire excellent settleability properties, still constitute important research goals to investigate. This thesis is focused on a mechanism that has been little addressed in literature, that is, phosphate precipitation in the core of aerobic granules.

Different analytical techniques, sometimes adapted for the first time to this type of systems, like Raman spectroscopy, have let an exhaustive characterization of biominerals in the core of granules. Analyses performed on aerobic granules grown with synthetic fed in a lab-scale SBR (Sequential Batch Reactor), revealed a calcium phosphate core made of hydroxyapatite [$Ca_5(PO_4)_3(OH)$]. This precipitation phenomenon is induced by local pH and supersaturation gradients issued of biological reactions inside granules. The study of the biomineralization phenomenon has been extended into anaerobic granules coming from UASB reactors at different cheese wastewater treatment plants. A physico-chemical model has been described in a form of matrix with AQUASIM® software, and coupled with a thermodynamic database (PHREEQC®), in an attempt to hypothesize the mechanisms that influence the biomineralization phenomena. It has been proposed the formation of an amorphous precursor (ACP) prior hydroxyapatite precipitation in the core of granules, suggesting the thermodynamic constant ($pK_{sp|20ºC}$=28.07±0.58) and kinetic constants at different operating conditions.

It has been also estimated the contribution of the biomineralization to the overall phosphorus removal process (up to 46% at the operating conditions tested), thanks to the development and study of a GSBR (Granular Sludge Batch Reactor) in lab-scale, for more than 900 days. The fate of the biomineralization process in granules, regarding the contribution to their stabilization and physical properties, has been also dealt in this thesis. The reactor stability and performances have been assessed by alternating anoxic/aerobic and anaerobic/aerobic cycles, in sights of a future industrial application. The induction of precipitation by local variation of pH and supersaturation issued of biological reactions has been here introduced, although it will need further investigation.

RESUMEN:

Los procesos de granulación aerobia han emergido durante la última década como una tecnología eficaz para el tratamiento de efluentes con elevado contenido en nitrógeno, fósforo y materia orgánica. La complejidad microbiana de los gránulos, así como los mecanismos por los cuales adquieren excelentes propiedades de agregación y decantación, constituyen aún importantes líneas de investigación en el seno del tratamiento de aguas residuales. Esta tesis se focaliza en un mecanismo aún poco estudiando en profundidad, que consiste en la precipitación de fosfatos en el núcleo de los gránulos aerobios.

Para ello, diferentes técnicas analíticas han sido empleadas, y algunas de ellas como la espectroscopia Raman, adaptadas por primera vez en estos sistemas, con el fin de llevar a cabo una caracterización exhaustiva de los biominerales precipitados en el interior de los gránulos. Estos análisis en gránulos aerobios cultivados en reactores de tipo SBR alimentado con un efluente sintético, revelan la precipitación en el interior de los agregados, de fosfato de calcio en forma de hidroxiapatita [$Ca_5(PO_4)_3(OH)$]. Dicho fenómeno de precipitación se debe a la aparición de gradientes locales de pH y supersaturación, inducidos por las mismas reacciones biológicas y productos metabólicos.

El estudio del fenómeno de la biomineralización se ha extendido a los gránulos anaerobios provenientes de digestores anaerobios UASB de diferentes plantas de fabricación de derivados lácteos. Un modelo físico-químico ha sido descrito en forma matricial con AQUASIM®, junto con un programa de cálculo de disociación de especies (PHREEQC®), con el objetivo de proponer hipótesis sobre los mecanismos que influencian los fenómenos de biomineralización. La formación de hydroxyapatita mediante un precursor amorfo (ACP) ha sido propuesto, así como la determinación de la constante temodinámica (pKsp|20ºC=28.07±0.58) y cinéticas en diferentes condiciones de operación.

También se ha estimado la contribución de la biomineralización a la eliminación total del fósforo (hasta un 46% en las condiciones testadas), gracias al seguimiento de un piloto GSBR durante más de 900 días de operación. La importancia de los procesos de biomineralización en los gránulos ha sido abordada igualmente en la tesis.

En vista de la aplicación industrial del proceso, la estabilidad del reactor y los rendimientos alcanzados se han evaluado mediante un estudio comparativo entre dos reactores, trabajando con ciclos anóxicos/aerobios y anaerobios/aerobios, respectivamente.

INDEX

NOMENCLATURE

Abbreviation	Meaning	Units/ Formula
ACP	Amorphous calcium phosphate	$Ca_3(PO4)_2$
AOB	Ammonium Oxidizing Bacteria	
ARAG	Aragonite	$CaCO_3$
BARDENPHO	Barnard Denitrification Phosphorus Removal Process	
BMP	Biological Methane Potential	
CAL	Calcite	$CaCO_3$
COD	Chemical Oxygen Demand	(mg /L)
DCPA	Phosphate dicalcic anhydrous, Monetite	$CaHPO_4$
DCPD	Brushite	$CaHPO_4$: $2H_2O$
D_G	Mean equivalent diameter of granule	(mm)
DM	Dried Matter	
DO	Dissolved oxygen concentration	mg/L
DOL	Dolomite	$CaMg(CO_3)_2$
EBPR	Enhanced biological phosphate removal	
EPS	Extracellular Polymeric Substances	
GSBR	Granular sludge Sequencing Batch Reactor	
HAP	Hydroxyapatite	$Ca_5(PO_4)_3(OH)$
HDP	Hydroxy dicalcium phosphate	$Ca_2HPO_4(OH)_2$
HRT	Hydraulic Retention Time	h
IAP	Ionic Activity Product	
Ic	Ionic strength	mol/kg
ISAH	Institut für Siedlungswasserwirtschaft und Abfalltechnik der Universität Hannover	
JHB	Johannesburg process	
K_{sp}	Thermodynamic equilibrium of precipitation constant	
LMF	Mineral matter fraction contained in the mixed liquor	(%)
MAG	Magnesite	$MgCO_3$
MAP	Struvite (Magnesium Ammonium Phosphate)	$MgNH_4PO_4 \cdot 6H_2O$
MF	Mineral Matter in the mixed liquor	g/L
MIPP	Microbially Induced Phosphate Precipitation	
MKP	Potassium struvite	$MgKPO_4$: $6H_20$
MLSS	Mixed Liquor Suspended Solids	g/L
MLVSS	Mixed Liquor Volatile Suspended Solids	g/L
MM	Mineral Matter	g/L
MUCT	Modified University of Cape Town Process	
MWH	Magnesium whitlockite	$Ca_{18}Mg_2H_2(PO_4)_{14}$
NEW	Newberite	$MgHPO_4$: $3H_2O$
NOB	Nitrite Oxidizing Bacteria	
OCP	Octacalcium Phosphate	$Ca_8(HPO_4)_2(PO_4)_4$:$5H_2O$
OLR	Organic Loading Rate	$kgCOD \cdot m^{-3} \cdot d^{-1}$
PAO	Polyphosphate Accumulating Organisms	
PCA	Cold Perchloric Acid	
PE	Population Equivalent	

PHOREDOX	Phosphorus Reduction Oxidation Process	
PP	Polyphosphate	
SAV	Superficial Air Velocity	cm/s
SBR	Sequencing Batch Reactor	
SI	Saturation Index	Log Ω
SMF	Sludge Mineral Fraction/ash content	(%)
SNDP	Simultaneous nitrification, denitrification and Phosphorus Removal	
SRT	Solid Retention Time	d
SVI	Sludge Volume Index	mL/g
TCP	Tricalcium Phosphate	$Ca_3(PO_4)_2$
TIC	Total Inorganic Carbon	
TKN	Total Kjeldahl Nitrogen	mgN/L
TN	Total Nitrogen	mgN-/L
TSS	Total Suspended Solids	g/L
UASB	Upflow Anaerobic Sludge Blanket	
UCT	University of Cape Town Process	
VER	Volume Exchange Ratio	
VFA	Volatile Fatty Acids	mg/L
VSS	Volatile Suspended Solids	g/L
WWTP	Wastewater Treatment Plant	
ϋ	Raman shift	(cm^{-1})
Ω	Supersaturation ratio	

CHAPTER I:

GENERAL OBJECTIVES AND LITERATURE OVERVIEW

‘‘Life can multiply until all the phosphorus has gone and then there is an inexorable halt which nothing can prevent. We may be able to substitute nuclear power for coal, and plastics for wood, and yeast for meat, and friendliness for isolation - but for phosphorus there is neither substitute nor replacement.”

Isaac Asimov, 1974

I.1. PHOSPHORUS: FROM EXCESS TO SCARCITY

Phosphorus was discovered by the German alchemist Hennig Brandt in 1669 (Ashley et al., 2011). During his search for the legendary "Philosopher's Stone", he made experiments by boiling urine but what he found was the glowing molecules of oxidized phosphorus, immortalized in Joseph Wright's painting (figure I.1). Phosphorus has three allotropes (white, red and black), but due to its extremely high reactivity, it is always found in nature combined with other elements (HPO_4^{2-}, PO_4^{-3}, P_2O_5, etc…), although only the inorganic ortho-phosphate is bioavailable.

Figure I. 1: The Alchemist in Search of the Philosopher's Stone, Joseph Wright (1771.)

Phosphorus is a key element of life for which there is no substitute. Human adults contain approximately 0.7 Kg of phosphorus in their bodies, around 85% in the form of calcium phosphate salts forming bones and teeth (Lehninger, 1988). It also makes part of the polynucleotide structures (DNA, RNA), as well as being present in the lipids of its membranes. It also plays an essential role in photosynthesis as it is part of the ATP, a key molecule involved in the energy transport in the metabolic functions of living beings. From the basis, phosphorus is incorporated in feed (around 1.7 g/day, according to FAO annual report, 2004), and its presence in the soil is one of the main requirements in intensive agriculture. As shown in figure I.2, the 95% of the phosphorus used for fertilizing purposes comes from the phosphate rock deposits which contain on average around 33% of P_2O_5 (Vaccari, 2011). However, it is a non-renewable source of phosphorus that takes between 10 to 15 million years to form (White, 2000).

At the annual consumption rate in 2011 (19 million tonnes per year), current phosphate rock resources are estimated to run-off in the coming century, and this

depletion could be exacerbated by growing crop demand linked to the population increase, which implies between 2.7 to 4.4% of P annual growing demand (CEEP, 2011).

Not so far from the Malthussian concern about food scarcity for a growing population, Hubbert (1949) anticipated the actual fuel oil crisis that we are suffering nowadays, and that similarly, could implicate phosphorus as well in the next years. Furthermore, 85% of the major mining deposits are shared by only among 5 countries all over the Globe, namely: Marocco, United States, China, South Africa and Jordan, being the first three, the principal phosphate exporters (Cordell et al., 2011).

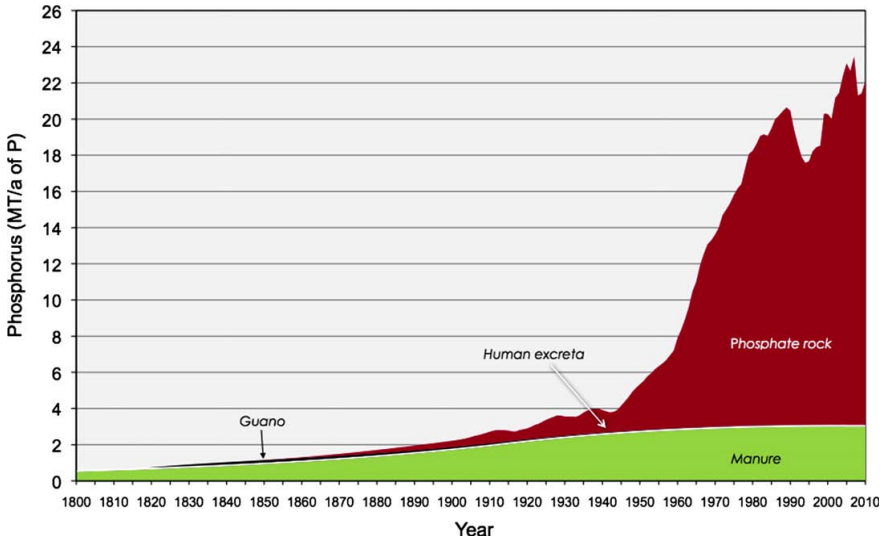

Figure I. 2: Extent of P sources for agriculture since 1800-2010. (Cordell et al., 2009)

On the opposite side of scarcity, phosphorus has been reported together with nitrogen, as targeted elements responsible for the eutrophication phenomenon (Golterman and De Oude, 1991), which affects more than 50% of the lakes and reservoirs all over the world (WRC, 2008). In Europe, the regulation of P released into the aquatic systems is integrated in the frame of a 2000/60/EC directive, being, the maximum concentrations allowed are between 2-0.5 mgP/L. However, green tides and algae bloom problems have been increasingly reported over the last few years, harming touristic landscapes and constituting a toxicological danger for humans and animals (Charlier et al., 2008; CEVA, 2011).

I.2. PROBLEMATIC OF THE AGRO-INDUSTRIAL EFFLUENTS

I.2.1. Effluent characteristics

Faced with the need of making efforts for phosphorus removal on the one hand, and, for its recycling through valuable ores, on the other hand, special attention has been paid to the agro-food wastewater treatment. According to a CEEP report (2004), more than half of the phosphorus coming from wastewater, has an agro-industrial origin (see figure I.3).

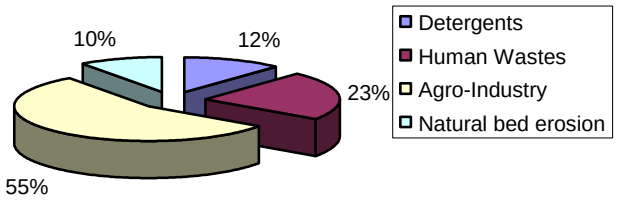

Figure I. 3: Sources of P sewage according to Centre d'Etudes Européen des Phosphates, 2004.

In fact, agro-food wastewaters are usually rich in proteins and other bio-molecules, which make up an important source of organic nitrogen and phosphorus, especially those from the animal industry. One of the complexities linked to agro-industrial wastewater treatment is the broad diversity of effluent characteristics. Table I.1 collects some agro-food wastewater effluents characteristics of different origins.

Table I. 1: wastewater characterization from different agro-industrial sectors.

Origin	*COD**	*BOD_5**	*VFA**	*TKN**	*NH_4^{+}**	*Pt**	*TSS**	*BOD/ COD*	*BOD/ NTK*	*BOD/ Pt*	*Reference*
Dairy Factory	4000	2600	400	55	-	35	675	0.7	47.3	74.3	[1]
Whey	61250	-	-	2500	-	533	5077	-	-	46	[1]
Cheese and whey recover	3500	2000	-	50	-	0.1**	500	0.6	40.0	30-90	[2]
Milk powder	2800	1600	-	80	-	0.04**	-	0.6	20.0	-	[2]
Milk, derivates, Egg	3390	1855	253	120	83	4.72	-	0.5	15.5	393.0	[3]
General Slaughterhouse	4200-8500	1600-300	100-200	114-148	65-87	20-30	-	-	-	-	[1]
Thin piggery manure fraction	3969	1730	-	1700	-	147	-	0.4	1.0	11.8	[4]
Pig Slaughterhouse	5200	2000	1100	300	-	60	2250	0.4	6.7	33.3	[2]
Primary treated abattoir wastewater	2000-6200	-	40-600	-	20-30	15-40	-	-	-	-	[5]
Primary treated abattoir wastewater	490-2050	-	250-990	105-170	26-116	25-47	-	-	-	-	[6]
Wine	25000	10000	-	150	-	50	1600	0.4	66.7	200.0	[2]
Cidrery	4718			42.95		14.52	1487	0.0	0.0	0.0	[2]
Coke, soda and beer factory	3256	1639	189	-	11.3	114.11	688	0.5	-	14.4	[3]
ERU	544	248	-	31	-	12.8	195	0.5	8	19.4	[7]

*Concentrations in mg/L ; **gP/L dry milk

References: *[1]- Doble et al., 2005 [2]- Moletta (2006) [3]- Confidential (industrial data) [4]- Obaja et al., 2003 [5]- Caixeta et al., 2002 [6]- Thayalakumaran et al., 2003b [7]- ERU Aoste de Granieu*

I.2.2. Dairy and cheese wastewater treatment

Agro-food effluents, and particularly dairy and cheese effluents show a high COD and BOD concentration, being favorable for organic matter valorization via anaerobic treatment for methane production, coupled with a post-treatment of nutrients. However, the need for nutrient removal should be carefully evaluated. The fraction of the incoming easily biodegradable organic load is uneven. For some types of effluents (e.g.: abattoir), between 40 to 70 % of the COD is slowly biodegradable and not directly available for denitrification or biological P removal (Yilmaz et al., 1997). In the case of cheese and whey wastewaters, the BOD/N and BOD/P ratios are low, compared to the bacteria DBO:N:P needs (Metcalf and Eddy, 1991; Henze et al., 1997), and the concentrations depend on the ratio of whey (highly concentrated) and white washing waters (diluted) in the final effluent (Perle et al., 1995).

Organic loads from dairy and cheese wastewater treatment plants come from degradable carbohydrates, mainly lactose, and from the less biodegradable proteins and lipids (Hwang and Hansen, 1998). Casein is the major protein found in these effluents and it is usually quickly hydrolyzed, in contrast to lipids (Perle et al., 1995). The latter are less bioavailable and their degradation produces glycerol and low fatty acid chains that can be inhibitory to certain methanogenic bacteria, overall the unsaturated ones (Koster, 1987; Komatsu et al., 1991).

The main organic nitrogen source comes from the organic proteins, oligopeptides, nucleic acids and some additive ingredients (Law, 1997). High nitrogen concentrations constitute a source of disturbance for Biological Nutrient Removal (BNR) processes, causing for instance ammonia inhibitory effects over nitrification/denitrification populations (Anthonisen et al., 1976; Hawkins et al., 2010). Indeed, although high concentrations of NH_3 and HNO_2 can affect both nitrifying microbial populations, Nitrite Oxydising Bacteria (NOB) are more sensitive to this factor (Vazquez-Rodríguez et al., 1997; Pambrun, 2005).

Another problem linked to the agro-industrial and dairy wastewater is the settling sludge problems related to the presence of suspended solids and of fats and grease, causing the development of filamentous bacteria, which have competitive advantages over other strains when oxygen limitation is present (Danalewich et al., 1998). Although it has been reported that high organic loading rates an short SRT reduce bulking problems, high SRT implies higher reactor volumes, leading to a rise in the operating and fixed costs. High total suspended solids mainly originate from the coagulated milk, cheese curd fines or flavoring ingredients (Demirel et al., 2005). Indeed, high sodium, calcium, and potassium concentrations appear in these effluents; e.g.: $[Ca^{2+}]$ = 35-55 mg/L, for dairy industry (Demirel et al., 2003) and between 150-950 mg Ca^{2+}/L, in cheese wastewater (Monroy et al., 1995). Most calcium concentrations derive from casein and additives like calcium phosphate (to improve texture and consistency of cheese) or calcium sulphate (acting as desiccant).

A typical wastewater treatment plant for the cheese industry is schematized in the figure I.4. It is constituted by an anaerobic treatment unit, followed by an activated sludge process including nitrification (aerobic reactor), denitrification (anoxic reactor) and simultaneous P removal by either biological or physical-chemical treatment (Fe or Al precipitation).

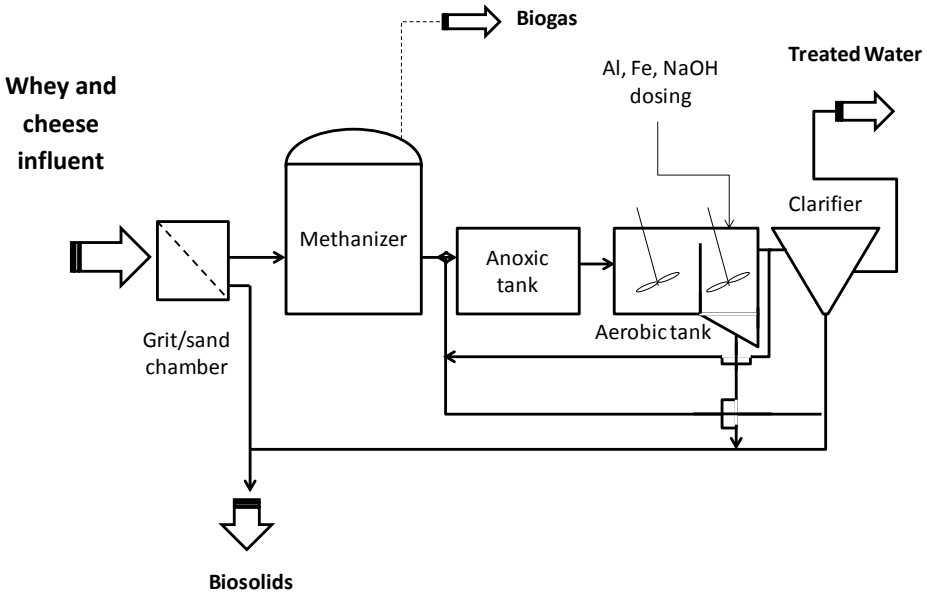

Figure I. 4: General Scheme of a WWTP for cheese processing manufacture.

Upflow Anaerobic Sludge Blanket reactors (UASB) have been reported since the 1970's as an efficient technology for treating high COD loading rates, and for maintaining high stable biomass concentrations in more compact facilities compared to a completely mixed anaerobic reactor (Lettinga et al., 1980). These systems are energetic efficient and produce low sludge volumes even if it could be difficult to degrade proteins based on particulate substrate if residence time is too short, as the hydrolysis of fats is usually a limiting step compared to the fatty acids conversion rate to acetic acid (Batstone et al., 2000). Obviously the UASB processes need complementary nitrogen and phosphorus facilities because nutrient requirements of anaerobic organisms are ten times lower than those of aerobic ones (Henze et al., 1997), and most of N and P is present in the outlet of the anaerobic process in ammonium (due to the proteins hydrolysis) and ortho-phosphate forms.

A first observation is that the surface and volume needs for nutrients post-treatment is very important (more than that necessary for methanization). A second observation is that phosphate is mainly removed with secondary sludge and cannot be exploited independently. Finally, a last point is that high phosphorus content in wastewater can cause precipitation in the different units. Location of precipitation is still difficult to predict. On the one hand, it will cause hydraulic disturbances if they appear on walls, pipes, stirrers, etc. On the other hand, the consequence of P precipitation in

anaerobic or aerobic sludge requires more attention in order to avoid loss of bacterial activity due to external mineralization.

I.2.3. Case study in France

In the field of agro-industrial wastewater, we have studied the case of a cheese factory wastewater treatment plant (WWTP) in the south of France (see figure I.5). According to figure I.5, black, white and process wastewaters coming form the dairy factory are first collected in a buffer tank where pH and flow rates are adjusted prior physico-chemical treatment. After a primary treatment, where most of the incoming fats and grease are removed by aeroflotation, the main stream effluent and the sludge from the primary step are treated in methanizers I and II. During the anaerobic digestion, most of organic nitrogen is hydrolyzed, resulting in a high ammonium concentration at the outlet of both methanizers, but most of the organic load is removed during the anaerobic stage. Ammonium is afterwards oxidized during the aerobic stage into nitrates and nitrites (nitrification), and finally converted to N_2, leading to 84% removal yields for organic nitrogen. The pH of effluents coming from the factory is quite acidic (3.5), and it is adjusted in the methanizer to control the acetogenesis and methanogenic steps after the VFA production. Some of the biogas produced is then collected, purified and cogenerated for steam and electricity production for supporting the plant's energy demand (in the line of milk boilers and heating devices).

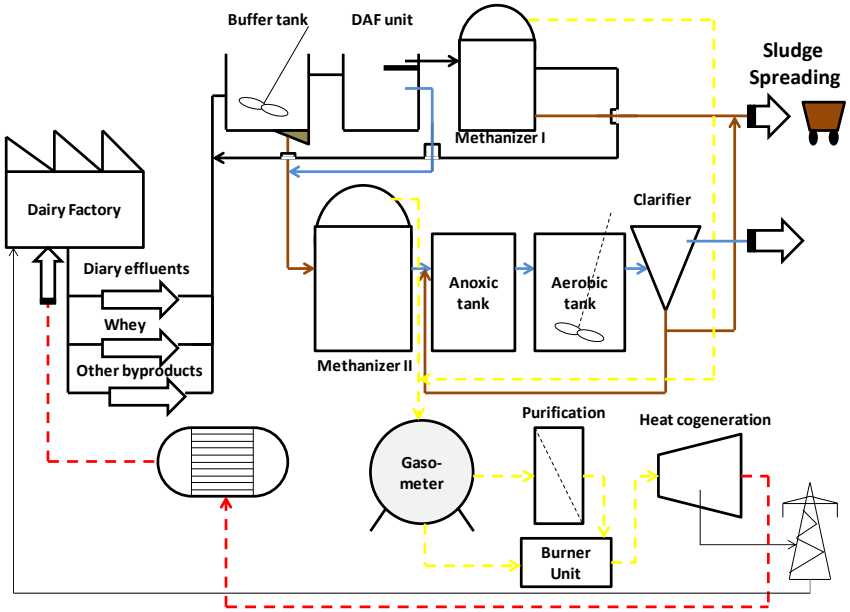

Figure I.5.: Block diagram of the industrial wastewater treatment plant exploited by VALBIO Company.

Table I.2 shows the characteristics of the raw influent coming into the WWTP. Most of the incoming phosphorus originates from the whey, proteins, additives and from the products used in the *Clean-In-Place* (CIP) units (phosphoric acid solutions). For its treatment, secondary precipitation in the aerobic reactor takes place resulting in 40% of the removal yield. The remaining phosphorus (32%) is probably removed by spontaneous precipitation in the methanizer tank enhanced by high pH (>7.4), raising the question about how and which phosphate compounds are formed during this stage.

Table I. 2: Wastewater characterization of the influent from the industrial WWTP

Parameter	***Value***	***Parameter***	***Value***
Total Chemical Oxygen Demand (mg/L)	59300	Nitrates (mg NO_3^-/L)	0.49
Soluble Chemical Oxygen Demand (mg/L)	37760	Ca^{2+} (mg/L)	211.55
Inorganic Phosphorus (mg PO_4^{3-}/L)	165	Mg^{2+} (mg/L)	44.3
Total Phosphorus (mg Pt/L)	320	K^+ (mg/L)	822
Ammonium Nitrogen (mg NH_4^+/L)	175	Na^+ (mg/L)	200
Total Kjeldahl Nitrogen (mg TKN/L)	945	Cl^- (mg/L)	965
Nitrites (mgNO_2^-/L)	0.00	TSS(g/L)	38
Nitrates (mg NO_3^-/L)	0.49	pH (15°C)	4.91

Indeed, several mineral deposits were found to precipitate in different locations of the plant, as shown in figure I.6. Although the analytical tools for mineral characterization will be part of the results of this thesis, preliminary tests revealed that a part of the phosphorus was removed as calcium phosphates precipitated on the walls of some devices (See chapter II).

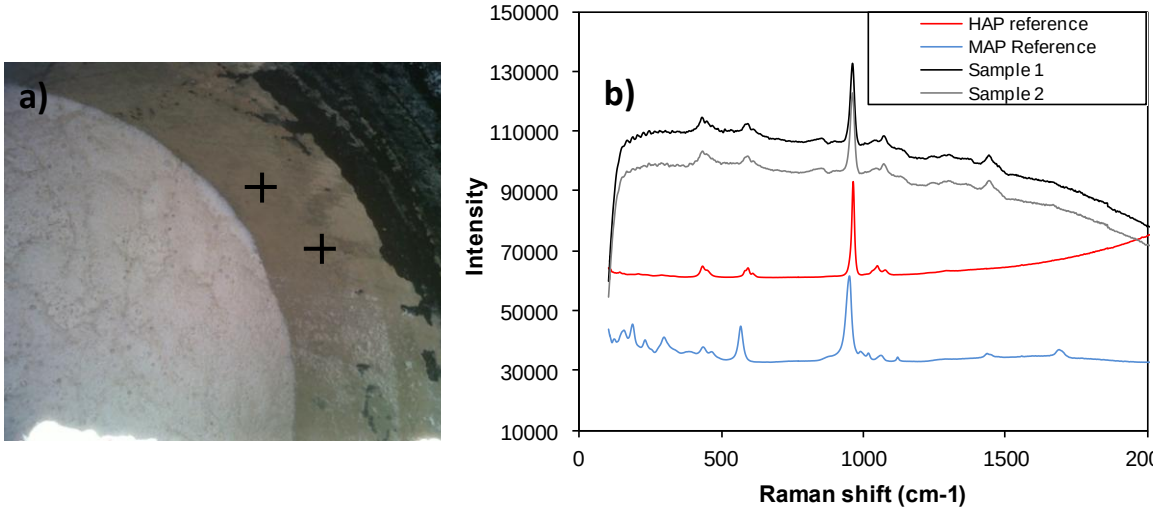

Figure I. 6: a) Mineral deposits found in anoxic tank walls of industrial site; b) Raman Analysis over two precipitated samples.

I.3. SCOPE OF PHOSPHORUS REMOVAL AND/OR RECOVERY

Precipitation and enhanced biological phosphorus removal (EBPR) are the main mechanisms on which the available technologies for phosphorus wastewater treatment rely on. Crystallization of phosphate minerals like struvite (MAP) and hydroxyapatite (HAP) are the most common minerals researched for valorization purposes.

I.3.1. Conventional physico-chemical precipitation

The development of full scale technologies for phosphorus removal started in the 1950s in response to a reduction in the levels of phosphorus entering surface waters leading to eutrophication. But it was long before, that phosphorus removal had been achieved by chemical precipitation. In particular, several wastewater streams were treated with lime in the XIX century (Wardle, 1893), followed by the use of iron salts (Wakeford, 1911). The obtaining of a fertilizer as an end-product was conceived in 1944 by Sawyer. According to this, and continuing in the line of precipitation, different plant configurations were designed, depending on the stage in which reactants were applied (Balmer and Hultman, 1988). Conventional chemical precipitation was simple and cheap, but produced huge quantities of sludge difficult to manage and handle. However, due to its simplicity, nowadays it is still widely used in a lot of Municipal Plants.

Via precipitation, a conversion of dissolved phosphates into solid insoluble phosphates is obtained. Phosphate precipitation through ferrous or alums salts ($Al_n(OH)_n^{(3-n)}$) has been well-known for decades, and depending on the stage where chemicals are added, we can talk about *primary precipitation* (before primary sedimentation), *secondary or simultaneous precipitation* (directly to the aeration tank of an activated sludge process) and *tertiary precipitation* (where dosing follows a secondary treatment), (Omoike and van Loon, 1999). The most common chemicals used for conventional precipitation are: $Al_2(SO_4)_3 \cdot 16\ H_2O$, $FeCl_3 \cdot H_2O$, $FeSO_4 \cdot 7H_2O$ and $Al_n(OH)_n^{(3-n)}$, because of their relatively low price. They are usually sub-products coming from other industries, and lead to high phosphorus removal efficiency (95-99%). However, due to the high metal content and low free disposal (Yeoman et al., 1988), the use of these chemicals makes the precipitate unrecoverable for possible industrial processing into a fertilizer. Another disadvantage that promotes the investment in other technologies, is the huge quantity of sludge produced by chemical precipitation, due to parasite reactions that even if they enhance flocculation, consume a lot of reagents. The following example shows the type of products achieved:

Primary reaction: $Me^{3+} + H_nPO_4^{n-3} \rightarrow MePO_4 + nH^+$ Equation I.1

Side reaction: $Me^{3+} + 3HCO_3^- \rightarrow Me(OH)_3 + 3CO_2$ Equation I.2

Where "*Me*" indicates a common metal use

I.3.2. Biological Phosphorus Removal

It was not until the middle of the XX century that *Enhanced Biological Phosphorus Removal* (EBPR) seemed feasible, with the concomitant *luxury uptake* concepts (Levin and Shapiro, 1965). Phosphorus is enclosed in the general formula of the biomass constitution: $C_{106}H_{180}O_{45}N_{16}P$ (Perry and Green, 1999), implicating up to 1.38 % of phosphorus in their weight (Cardot, 1999). Thus, between 0.01-0.02 g P/g VSS can be expected from a classical assimilation, which is not enough for legal reject requirements with high strength effluents. However, an over accumulation of phosphorus of up to 0.38 gP/ g MVS higher than their normally growing needs (Wentzel et al., 1989) can be achieved by *Phosphorus Accumulating Organisms* (PAOs) when alternating anaerobic/aerobic conditions. These organisms are a compendium of bacteria like *Acinetobacter spp* (Cloete and Steyn, 1988), *Microlunatus Phosphovorus, Lampropedia spp, Rhodocyclus, Aeromonas sp. (Pasteurella, Pseudomonas, Moraxella), Acinetobacter sp. (A.calcoaceticus, A. euthrophus)*, *Phormidi um*

bonheri, P. Laminosum, P. Tenue, Oscillatoria, Staphilococcus auricularis, Rhodobacter capsulatus, Rh. Sphaeroides, Rh. Sphaeroides NR-3, Rh. Seudomonas palustris, Chlorella vulgaris, Scenedesmus dimorphus and Spirulina platensis (Mino, 2000; Blackal et al., 2002; Seviour et al., 2003), and any of each isolated strain has a 100% PAO metabolism (Wong et al., 2005), which is described in Figure I.7. They can absorb low-weight molecular organic chains (acetate, propionate) thanks to exopolymeric substances (EPS) under anaerobic conditions through Polyhydroxyalkanoates (PHA), which is the general denomination of a type of lipids including PHB (Poly-β-hydroxybutirate) and PHV (Poly-β-hydroxyvalerate). According to Smolders et al. (1994), they can be quickly metabolized (between 4-6 hours at 20°C). Glycogen is a carbohydrate which is also stored by these micro organisms in counter-phase to PHA, as one is being built up, the other is being degraded. It supplies energy for 1-2 days, as well as acting as a regulator on the cell's red-ox balance. The energy required is obtained by hydrolysis of the intracellular polyphosphate stored bounds. Polyphosphate is accumulated thanks to the *polyphosphatase kinase* enzyme, while its release is catalyzed by the *polyphosphatase*. Then, in the aerobic phase, the organic matter can be oxidized and the energy released is used for cell growth as well as for the re-accumulation of phosphates into polyphosphates in their protoplasm.

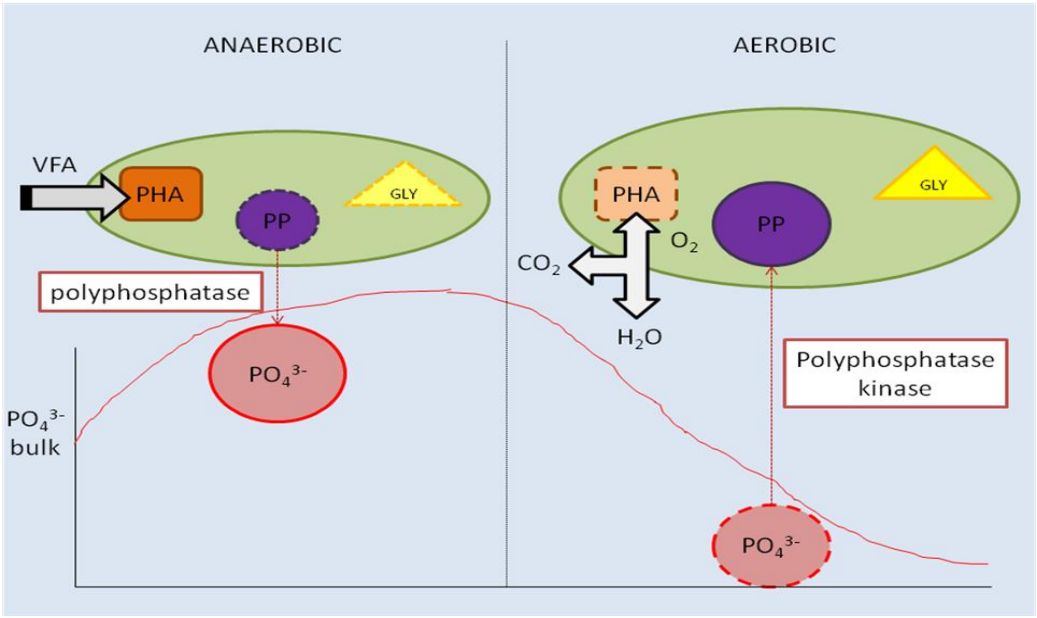

Figure I.7.: Scheme of EBPR mechanism carried out by PAOs.

The net effect is a surplus of phosphorus content in the bacteria, and hence, a phosphate concentration drop in the effluent (Eckenfelder, 1997; Wong et al., 2005). The

yields achieved is linked to the ratio between easily biodegradable COD and phosphate in the wastewater ((between 60- 75% of P removal with common domestic wastewater), which does not always achieve the legal requirements). In fact, phosphorus net removal is directly linked to the phosphorus content in PAOs, and in the other bacteria that coexist in the bioreactor.

Panswad et al., (2007) reported the different phosphorus content in PAOs regarding the P:COD feeding ratio. Thus, for increasing ratios from 0.02 to 0.16, P sludge content varied from 5.3 to 20.5 % in weight, which is not negligible regarding valorization.

Disruption of EBPR in wastewater treatment plants by the presence of other microorganisms called GAO (glycogen accumulating organisms) has been largely investigated in the last decade. They compete with PAO for VFA uptake under anaerobic conditions, but at the expense of glycogen accumulation instead of polyphosphate as the energy source. With regards to the phylogenetic groups of bacteria forming GAOs, Oehmen et al., 2010 highlighted *Candidatus Competibacter* and *Defluviicoccus vanus*, both having several sub-groups with denitrifying capacities. Moreover, they have been reported to be the first bacterial group responsible for denitrification in SNDPR processes in granules (Zeng et al., 2003a; 2003b), and according to Lemaire (2007), he found GAOs preferentially in the center of the granules (coinciding with the anoxic local conditions), while PAOs were found mostly in the outer part at 200µm depth. The parameters that favour the selection of one phenotype or another have been studied: the type of VFA present in the influent (e.g. acetate or propionate) (Pijuan et al., 2004; Oehmen et al., 2005a, 2006), pH (Filipe et al., 2001; Oehmen et al., 2005b), temperature (Whang and Park, 2006), the phosphorus to VFA ratio (Liu et al., 1997) and the combined effect of such parameters (Lopez-Vazquez et al., 2009).

Technical configurations like ***BIODENIPHO*** (Bungaard et al., 1988)***, A/O, ISAH, JHB, Unitank*** (Janssen et al., 2002)***, PhoRedox (3 stage A²/O),*** or ***5-stage BARDENPHO*** (Barnard et al., 1990) were developed in order to produce a P-rich sludge production with lower chemical consumption. However, some technical downsides appeared, concerning NO_3^- presence in the anaerobic phase, which led to the switch electron acceptor for consuming VFA, instead of accumulating as PHB. Moreover most of these processes had been originally conceived for biological nitrogen removal, like *BARDENPHO*, and phosphorus removal yields were not satisfactory with high P loads in the influent. In order to solve the nitrate problem, ***UCT*** (Siebritz et al., 1983; Brett et al., 1997) and then, ***MUCT***

(Farnell et al., 1990) processes were successfully applied full scale for an anaerobic liquor digester from a vegetable processing plant in the UK (Upton et al., 1996; Brett et al., 1997). Problems related to the necessity of a post sludge treatment for P-extracting or strong regulations for sludge spreading, encouraged combined biological-chemical processes, like ***PHOSTRIP*** -shown in figure I.8- (Levin and Shapiro, 1965; Brett et al., 1997; Upton et al., 1996), or ***BCFS*** (van Loosdrecht et al., 1998). Although these technologies were more environmental-friendly they presented some disadvantages like rich-nutrient sludge management and spontaneous struvite accumulation in pipelines (Borgerding, 1972).

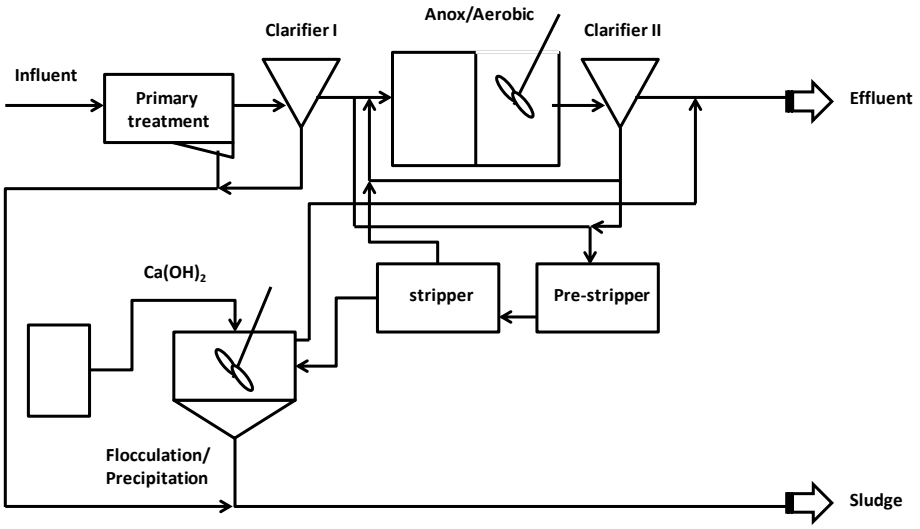

Figure I. 8: Scheme of a PHOSTRIP WWTP in Caorle, Italy (Szpyrkowicz and Zilio-Grandi, 1995)

I.3.3. Crystallization in specific reactors for phosphorus recovery

The latest trends in phosphorus removal are focused on recovering phosphates as marketable fertilizers like hydroxyapatite (HAP) or struvite (MAP) via controlled crystallization in specific reactors.

I.3.3.1. Struvite precipitation

Struvite or magnesium ammonium phosphate (MAP), was first regarded as a piping fouling problem, as it precipitates spontaneously in waste water treatment environments where high concentrations of soluble phosphorus and ammonium are present under pH higher than 7.5 (Borgerding et al., 1972). The first modelling efforts were focused on

avoiding its formation which had been reported to cause high economical impact in facilities all over the world (Ohlinger et al., 1998; Doyle et al., 2000). As struvite contains both phosphorus and nitrogen, its precipitation will affect the content of both elements in the leftover sludge, used by farmers as a soil improvement agent and fertilizer. The relation between phosphorus and nitrogen removal is linked to the mass balance; since sewage has a typical N:P ratio of 8:1 and struvite 1:1, a theoretical maximum of 12.5% of the nitrogen load could be removed as struvite (Bashan et al., 2004).

Moreover, while sewage sludge applied directly to fields has phosphorus content higher than the need of plants, struvite recovery should achieve the legal requirements of fertilizers (gathered in the U.E. Directive 97/622). In addition, struvite is an excellent slow-release fertilizer that does not burn the roots when over applied, unlike ammonium-phosphate fertilizers (Hu et al., 1996).

But other products can be synthesized using recovered struvite crystals. For example, the most common used fertilizer, diammonium phosphate (Khan and Jones, 2009), which is produced by neutralizing phosphoric acid with ammonia, can be replaced by mixing struvite with phosphoric acid. And this might even yield a superior fertilizer made partly of slow release: $MgHPO_4$ and partly of fast-release: $(NH_4)_2HPO_4$.

As struvite purification technology is still unknown, its use for the cement industry, as a fire-resistant material (Sarkar, 1990), or cosmetics or pharmaceutical applications, seems not likely in the short term.

However, the potential of struvite as a fertilizer (Wilsenach et al., 2003; Brett et al., 1997; Bashan et al., 2004) has reoriented processes and modelling towards its recovery. Thus, its crystallization in specific reactors has been widely developed, leading to full scale commercial processes, like **Kurita®** (Joko, 1984) or **Phosnix®** (Unitika, 1994).

Struvite is an orthorhombic crystal the formation of which depends on the concentration of the constituting ions present in the solution and on other factors, like T, pH, solvent nature, hydrodynamic conditions and the presence of other ions (Ali et al., 2005). Crystallization is a thermodynamic-dependent phenomenon that implicates a stable nucleus formation first, followed by a crystal growth. In the processes mentioned above, different chemicals are needed to modify the inlet ions concentrations and/or the pH. Although the stoichiometry establishes a relation $1(Mg^{2+}):1(NH_4^+):1(PO_4^{3-})$, experiments have shown that an excess of Mg^{2+} is required, at least in municipal

wastewater (and in most of industrial wastewaters), where this ion is lacking. Some strategies to precipitate struvite consist on:

i) Adding $Mg(OH)_2$ or the more effective $MgCl_2$ (Wu and Bishop., 2004).

ii)Adding a counter current sea-water flow, and adjusting pH to 8.2-8.8, with NaOH (Stratful et al., 2004).

iii)Carrying out air stripping, which is a cheaper method to increase pH (Battistoni et al., 1997) or by CO_2 stripping based on pH change (Saidou et al., 2009).

Struvite precipitation can be inhibited by the use of $FeCl_3$, zeolites, NaH_2PO_4 or sodium polyphosphate, as well as a pH or an ion concentration decrease.

I.3.3.2. Hydroxyapatite precipitation

Hydroxyapatite precipitation by P-rich sludge can be achieved by adding $Ca(OH)_2$/CaO to the influent, but also with $CaCl_2$ without the need of a pH adjustment and prior heating of the sludge in order to release the phosphorus. The precipitate contains more phosphorus and less Ca^{2+} than the conventional phosphate rock, but it is a poorly-soluble phosphate as a fertilizer, so effective means like the use of PSB and PSF (Phosphorus solubilising bacteria and fungi), may be required. But problems linked to other ions presence, reveal that amorphous apatite does really appear instead of the crystalline hydroxyapatite. The significance of encouraging the second form rather than the amorphous one, relies on the better availability for metabolism of plants.

Hydroxyapatite formation has also been pursued and widely developed in crystallization reactors, like the DHV Crystalactor® technology (Morse et al., 1998; Montastruc, 2003). Calcium added in the form of lime ($Ca(OH)_2$/CaO) leads to the formation of hydroxyapatite (HAP), according to the following formula:

Primary reaction: $5Ca^{2+} + 7OH^- + 3H_2PO_4^- \rightarrow Ca_5(PO_4)_3OH + 6H_2O$ Equation I.3

Side reaction: $Ca^{2+} + CO_3^{2-} \rightarrow CaCO_3$ Equation I.4

The crystalline solid obtained can also precipitate and be formed by the same mechanisms as for struvite, but in practice, its production is due to the final stage of a series of reactions in which a number of more easily soluble calcium phosphates (precursors) are produced, which really determine the phosphate solubility according to Henze (1997). Thus, phosphorus removal yields can decrease if other apatite formations

take place, by the substitution of OH^- ion by F^- present in the water, or when PO_4^{3-} is substituted by CO_3^- and Ca^{2+} is replaced by Na^+, Fe^{3+}, Al^{3+}, $Mg^{2+}$and Zn^{2+} ions. But not only apatites can spoil the desired crystalline hydroxyapatite formation, as more amorphous and soluble compounds can arise: $CaHPO_4$, $Ca_4H(PO_4)_3$, $Ca_3(PO_4)_2$. These last components will determine the phosphate solubility if high concentration of Mg^{2+}, poly-phosphate or HCO_3^- are present in the wastewater.

EBPR and crystallisation-precipitation processes can be combined in order to improve total P removal efficiency and for recovering phosphorus in a valuable mineral form. It is thus possible to take advantage of the biological process to concentrate on a phosphate stream (enhance the ion supersaturation) and facilitate precipitation in a relatively soluble form (magnesium or calcium phosphate instead of metallic ones). Precipitation can be provoked either during the phosphate release at the anaerobic stage of the activated sludge system, or in a parallel stream after the anaerobic digestion of the sludge. Here, four possibilities are shown for MAP or HAP crystallization:

i) **Selective Ion Exchange**, like the ***RIM-NUT®*** process (Liberti et al., 1986), in which first ammonium and then phosphate are concentrated from the influent thanks to a cationic and anionic resin respectively. The main drawbacks of this process are the lack of phosphate ions selective sorbents, and thus, the competition with NO_3^-, HCO_3^{2-} and SO_4^{2-} ions, on the one hand, and the long resin regeneration times with NaCl, on the other hand.

ii) **Precipitation in a continuous stirred reactor**, has up to date only been performed on a pilot and laboratory scale. Phosphate precipitation and crystallization takes place in a mechanical stirred tank where $MgCl_2$ generally is dosed for compensating Mg^{2+} deficiencies (Stratful et al., 2004), as well as NaOH for pH rise. The precipitation of struvite in the previous **RIM-NUT®** process takes place directly in this kind of reactor. Another crystallization process using a stirred reactor is the **P-ROC®** process, developed full-scale in Germany (patent from Forschungszentrum Karlsruhe). It produces calcium phosphates, HAP and brushite in a stirred reactor seeded with tobermorite and Calcium Silicate Hydrates pellets. This type of crystallization reactor usually requires a collector and settling zone, and can operate with or without seeding materials (Le Corre, 2006).

iii) Crystallization in **Fluidized bed Reactors** is the most common technology for recovering phosphorus like MAP or HAP from wastewaters. A column filled with seed materials is provided to promote crystal nucleation and growth, and different chemicals are added, like NaOH, for pH rising, or magnesium and calcium salts (Seckler et al., 1996). Processes like **PHOSNIX** (Katsuura et al., 1998; Münch et al., 2001), **CRYSTALACTOR®** shown in figure I.9 (Eggers et al., 1991; Piekema and Giesen, 2001), or **CSIR** (Momberg et al., 1992), have been adapted full-scale for a broad type of effluent, mainly from anaerobic digester supernatant, abattoir and swine wastes (Brett et al., 1997). In some cases, air is pulled upwards not only to favor contact but also for pH control (Suzuki et al., 2006), like in **Air-Prex** process (Stratful et al., 2004). Most of them recover phosphorus through MAP, HAP or amorphous phosphates and achieve phosphorus removal yields higher than 85%. The recent case of the **OSTARA®** process (Baur et al., 2008). The main advantage of this process is that it provides a phosphorus rich product (27% P_2O_5, 5% N, 10% Mg), commercialized as Crystal Green™, as well as struvite, both marketable slow-release fertilizers.

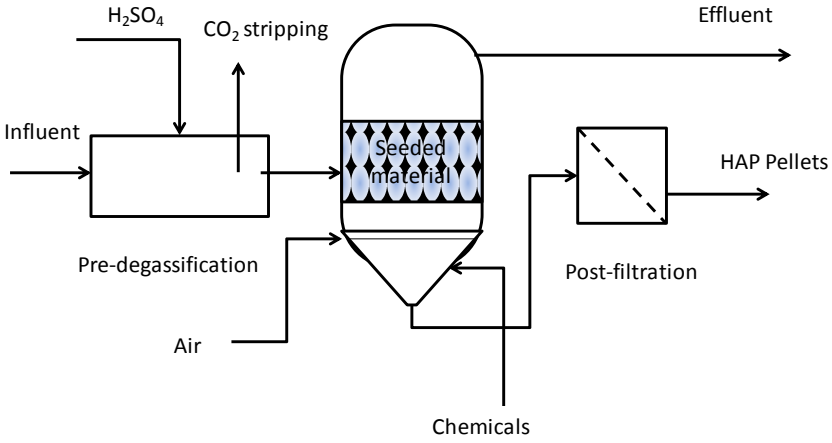

Figure I. 9: Scheme of Crystallactor process (Morse et al., 1998)

iv) Crystallization in **Packed or Fixed Bed reactors**. Processes like **KURITA®** (Joko, 1984 ; Brett et al., 1997), where high phosphorus removal yields up to 90% are achieved in a fixed packed column seeded with phosphate rock, produces HAP as a recovering product, without the need of chemicals. The *Organic Fraction Municipal Waste and Biological Nutrient Removal* process **OFMWBNR** developed in Italy and Spain (Llabres et al., 1999; Cecchi et al., 1994; Battistoni et al., 1997) recovers phosphorus from an anaerobic digester of a municipal wastewater plant 100000 PE, in

the form of HAP and MAP. In this case, quartz is required as seeding material. Finally, other authors focus on the fixed bed column technology for phosphorus removal, although instead of recovering it as a crystallize form, it is removed using adsorbents coming from other industrial wastes, like the case of the red mud adsorption (Huang et al., 2008).

Another path for recovering phosphate consists on treating the P-enriched sludge, for example, from EBPR processes previously mentioned. When sludge characteristics are not suitable for field spreading (high Cd, Zn or iron content, low nitrogen, magnesium or potassium content, etc.), some technologies for extracting and recycling phosphorus are developed, like ***KEPRO*** process (Sweden), although it produces an iron phosphate difficult to solubilise (Kemira Kemi AB patent), ***Cambi/KEPRO*** and ***Bio-Con*** process. Most of them use a thermal/chemical treatment path.

Although most of the recycling processes are based on Fluidized bed reactors (Montastruc, 2003), phosphorus recovery through struvite or hydroxyapatite in these systems present some economic drawbacks. On the one hand, there is not a clear phosphorus-bench market position, and prices of the recovered minerals are local-dependent (Shu et al., 2005; Weikard, 2010). On the other hand, the 97% of the operating costs come from the pH adjustment and from reagent dosing (CEEP, 2001), and efforts must be addressed towards more economical and environmental-friendly sustainable processes for P recovery.

I.4. AEROBIC GRANULAR SLUDGE: AN INNOVATIVE PROCESS

Due to the impossibility of anaerobic granules to perform nutrient removal, aerobic granular sludge process emerges as an interesting alternative or complement to the UASB process. Mishima and Nakamura first reported aerobic granules in 1991, and the first patent of an aerobic granulation sludge process in a SBR was claimed by van Loosdrecht and co-workers (1998). Aerobic granulation has been reported as a suitable biological technology to treat industrial wastewater due to its small footprint and its capacity to withhold high organic loading rates and simultaneous nutrient removal (Morgenroth et al., 1997; Beun et al., 1999; Etterer and Wilderer, 2001; Liu and Tay., 2004). This is due to their capacity to concentrate the biomass in the reactors (ten times

more than in conventional activated sludge systems, where VSS concentration is between 3-5 mg/L. A granule is considered as a dense bio-aggregate involving a lot of different types of microorganisms that agglomerate under certain hydrodynamic and feeding conditions (De Kreuk et al., 2005). Aerobic granules are conceived as dense spherical stratified bio aggregates of 0.2-5 mm diameter. Their specific gravity varies from 1.004 to1.065 (Etterer and Wilderer, 2001), being the smallest ones, to the denser ones. They have a negative-charged porous surface, with porosity channels up to 900μm depth below the surface that peak up to 300-500μm above the surface (Liu et al., 2004). Confocal laser scanning microscopy combined with different oligonucleotide probes, has served to determine a 70-80 μm depth layer from the granule surface, constituted mainly of aerobically nitritant microorganisms (*Nitrosomonas spp)*, whereas typical anaerobic bacteria were detected at a depth of 800-900 μm (Tay et al., 2002). Heterotrophs are classically located in the periphery, followed by autotrophs depending on the oxygen diffusion conditions (Lemaire, 2007). Finally a layer of dead microbial cells was located at 800-1000 μm from the surface (Toh et al., 2003). EPS matrix wrapped the granules and penetrated to 400μm depths. Aerobic granules result from the bio-aggregation of different types of microbial communities under specific conditions, and have been widely developed in Sequencing Batch Reactors, mostly under acetate or glucose synthetic feed. Nevertheless, they have also been satisfactory for treating dairy wastewater (Arrojo et al., 2004; Schwarzenbeck et al., 2005; Wichern et al., 2008), abattoir wastewater (Cassidy et al., 2005, Lemaire, 2007), domestic wastewater (De Kreuk, 2006; Coma et al., 2011), soy-bean processing wastewater (Su and Yu., 2005), brewery wastewater (Wang et al., 2007), paper-making wastewater (Wang et al., 2006), heavy metals and dye wastewater (Zhang et al., 2005).

One advantage of aerobic granules compared to flocculated sludge is that they have higher settling velocities than flocs: Uaer_g = 18-60 m/h > Uanaer_g = 10 m/h > Uflocs = 1-3 m/h (Liu et al., 2003; Qin et al., 2004), enabling the former to settle in the same reactor without the need of secondary clarifiers (Etterer et al., 2001). Another advantage comes from their dense structure that favors the simultaneous nitrification denitrification and phosphorus removal (SNDPR), thanks to the different reactions that take place with the stratified microorganisms. In particular, this last is facilitated thanks to the DPAOs presence that allows simultaneous NOx reduction (denitrification) and P

uptake (Kuba et al., 1993; Lemaire, 2006). The particularity of granules to maintaining aerobic and anaerobic zones play a crucial role in the SND process.

However, incomplete coupling leads to N_2O production (Meyer et al., 2005), which has been recently targeted as one of the WWTP impacts needing to be further attended regarding its contribution to the greenhouse effect. In fact, one of the most suitable scenarios for N_2O production coincides with that of the better SND operating conditions at low oxygen concentrations (0.3-0.5 mg/L), (Kampschreur et al., 2008), both nitrification and denitrification producing N_2O in this intermediary DO range. Lemaire (2007) proposed the limitation of GAOs presence, that appeared to be related to the major N_2O accumulation, by the enrichment of other carbon sources promoting the growth of another denitrifier strains that would minimize the N_2O production, for example by bypassing a municipal wastewater stream during the anoxic phase. It would appear that the advantage of aerobic granules relies on its dense structure, allowing the formation of strict anaerobic or anoxic zones thanks to the oxygen-limiting conditions in the center of the granules.

Although the knowledge of the exact parameters that influence densification of floccular mass to form aerobic aggregates still remains ambiguous, here are some simplified guidelines from the literature:

- High Organic Loading Rates (OLRs), (Liu et al., 2005).

- High Volume Exchange Ratio (VER), (Coma, 2011; Liu et al., 2005).

- Short settling times to select pressure over the denser aggregates (Adav et al., 2008; de Kreuk et al., 2007).

- Long feast/famine periods (Lemaire, 2007; Liu et al., 2005).

- Alternating anoxic feast/aerobic famine periods (Wan et al., 2009).

- High presence of particulate matter as nucleation sites on which bacteria could start aggregating (Coma, 2011).

Promoting shear forces in the reactor by aeration (Liu and Tay., 2002), as it enhances polysaccharides production leading to heavier sludge particles (Tay et al., 2001; Gao et al., 2011). Coma (2011) recently pointed out that one of the effects of increasing the OLR would be the enriched PAOs granules obtained, leading to dense packed heterotrophs in sludge enhancing granulation.

Up to now, phosphorus treatment in aerobic granules has been assessed within the PAO-GAO development conditions. It is intimately linked with nitrification/denitrification processes, as the success of biological phosphorus removal by PAO, depends on the

availability of easily degradable organic carbon sources (VFA) and the capacity of PAO to use nitrate as electron acceptor (Lemaire, 2007). However, Tchobanouglous et al., (2003) pointed out that both nitrite and nitrate enabled P uptake at similar rates, nitrite electron acceptor was more effective in bio-P removal when organic matter limitations took place.

Simultaneously to biological P removal, a parallel phosphorus precipitation process in the supernatant of activated sludge has been assessed by several authors (Lan et al., 1982; Maurer et al., 1999a and 1999b; Pambrun, 2005; Barat et al., 2008 and 2011). Phosphate precipitation in a granular sludge process was assumed (but not directly demonstrated) by Yilmaz (2007) and De Kreuk (2005, 2007). Lemaire (2007) predicted struvite precipitation in the supernatant of granules in treating abattoir wastewater with high ammonium content. By estimating its supersaturation index, Yilmaz et al. (2007) suggested that struvite could be transiently formed during the anaerobic phase of the SBR cycle. The contribution of this process to overall P removal was estimated to be less than 10% on the basis of a perchloric acid extraction method (PCA), (Haas et al., 1990; Daumer et al., 2008). Similarly, experimental results by De Kreuk (2005) suggest that P-removal occurs partly by biologically induced precipitation in granular sludge. Extraction techniques indicated that 2.6% of the sludge mass was due to precipitates (P/VSS), but the whole contribution of this process compared to biological P removal processes was not quantified. For simplicity, precipitation was not included when modelling the process but De Kreuk et al. (2007) proposed to increase the maximum fraction of poly-phosphate in PAO from 0.35 (Hu et al., 2002) to 0.65 assuming that about 46% of the P removal could be due to P precipitation and 54% due to polyphosphate accumulating bacteria. Finally this side mechanism has never been quantified directly but has been supposed to contribute significantly to P removal in EBPR processes, thus, requiring further attention.

In addition, some actors have also mentioned the possible accumulation in aerobic granules of calcium carbonate (Ren et al., 2008); or calcium and iron phosphates (Juang et al., 2010), thanks to simulation tools (for calculating the saturation index of different mineral phases regarding the concentrations in the bulk) or VSS/TSS ratio assessment. But little work has been done on the possible role of phosphate minerals precipitated inside granules over the whole P removal process, and the triggering mechanisms, in spite of its possible contribution to the high settling velocity of granules as well as to the particular self-immobilized feature. This will be the particular topic of this thesis.

I.5. RESEARCH OBJECTIVES

In the final aim of increasing the phosphorus removal yields as well as nitrification/denitrification in a single step (without needing metals for precipitation) the implementation of an aerobic granular sludge process has been proposed.

In the case of a dairy wastewater treatment plant this process could be placed after the methanizer unit (UASB). Simultaneous carbon, nitrogen and phosphorus removal in a granular sequenced batch reactor (GSBR) could substitute the actual activated sludge process (Anoxic and aerobic tanks + secondary clarifier) as a more compact unit (see figure I.10).

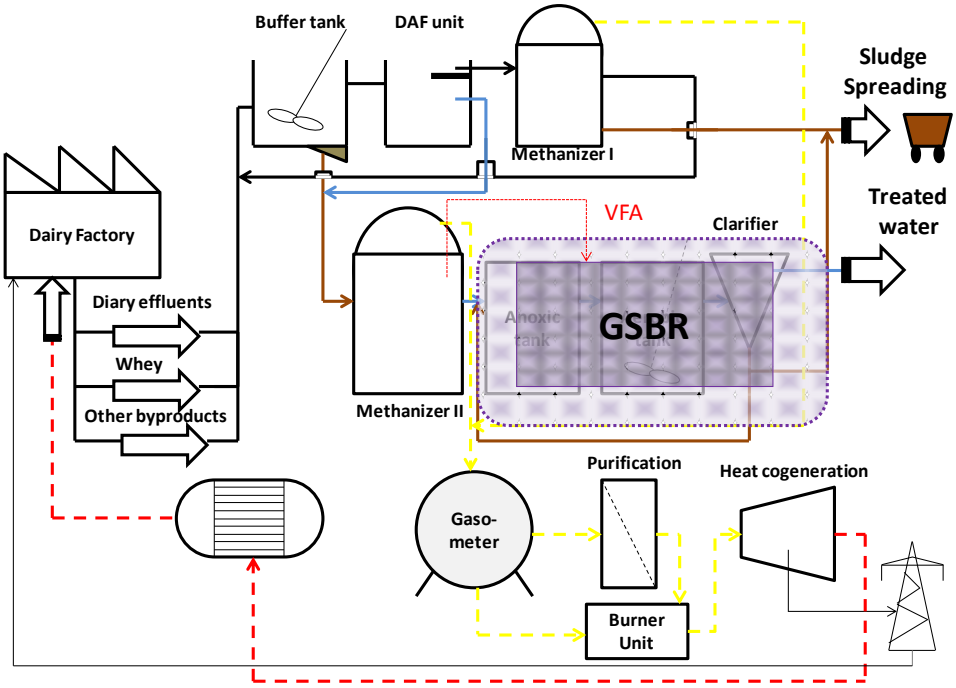

Figure I. 10: Block diagram of the industrial wastewater treatment plant exploited by VALBIO Company.

Previous work at LISBP laboratory (Wan, 2009), focused on the stability and formation of aerobic granules under anoxic/aerobic cycle conditions, also in a GSBR, finding that low oxygen flow rate (SAV=0.63cm/s) as well as the introduction of a pre-anoxic feast phase, can favor the densification of aggregates and thus, stable granular sludge retention (MLSS=10g/L). However, phosphorus removal in this system was not further analyzed, constituting one of the starting points of the thesis. Therefore, the following 5 chapters aim to study the phosphorus processes that take place in this system,

for the sake of accomplishing legal reject requirements, and recovering it in an easy-handling form in response to the growing phosphorus global demand. The main challenges (corresponding to each chapter) that will be dealt in this dissertation are:

1. ***Demonstrating the biological induced precipitation process inside aerobic granules*.** For that, a stable GSBR system was used for treating synthetic wastewater with similar COD/P ratios to that of the high strength effluents (whey, slaughterhouse). In fact, Wan (2009) had before assessed the performances and stability of a GSBR operated with a pre-anoxic feast phase, during more than 250 days, and microscopic images on granules arise the first question of the possible mineral precipitation inside (figure I.11). Therefore, Chapter II aims to confirm by mass balance and analytical techniques, the possible precipitation phenomenon, as well as the nature of the bioliths precipitated.

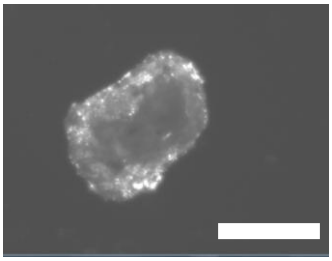

Figure I. 11: Microscopic observation of an aerobic granule from the GSBR at the beginning of the thesis dissertation (Scale bar represents 400 µm-length)

2. ***Studying GSBR process at different operating conditions focusing in particular, into the phosphorus removal processes with a synthetic fed lab-scale reactor.*** The reactor performances will be mainly assessed in Chapter III, in which two GSBRs operating with anoxic/aerobic cycles and anaerobic/aerobic cycles, will be compared regarding COD, nitrogen, and phosphorus removal. Several studies with GSBR run at anaerobic/aerobic cycles have been carried out by different actors regarding with the improvement of biological phosphorus removal, but up to the present, no studies with similar COD/N and COD/P ratios had been compared, nor any process with MIPP inside granules.

3. ***Analyzing the local formation of minerals in granules from aerobic and anaerobic processes.*** Chapter IV aims to extend the analytical tools (for assessing biological induced mineralization in aerobic granules) on anaerobic granules coming from the UASB (Methanizer II) from the cheese WWTP study case (figure I.5). Here, the biomineralization phenomenon in granules is compared regarding the different operating conditions that take place in the different reactors, establishing different hypothesis for mineral occurrence and discussing the pros and cons of this process regarding nutrient and carbon removal. An important question will be discussed: the consistency between the saturation indexes calculated with thermodynamical database and the observed minerals. This constitutes the first step for developing a prediction approach.
4. ***Analyzing the calcium phosphate precipitation and its interactions with bioreactions in a granular sludge process.*** The final information that this work tries to provide in chapter V, relies on the influence of the operating conditions that can encourage the mineral precipitation in aerobic granules, as well as the information necessary (stoichiometry and kinetics) in sights of modeling later, the Mineral Induced Phosphorus Precipitation (MIPP) inside aerobic granules.

Nota: Due to the structure of the dissertation (each chapter has been adapted to constitute a published article), some literature staples may be repeated during the different chapters. Otherwise, each chapter can be read separately.

I.6. REFERENCES

Adav, SS., Lee, D-J., Show, K-Y., Tay, J-H. (2008). Aerobic granular sludge: Recent advances. Biotechnology Advances. 26 (5):411-423.

Anthonisen A.C., Loehr R.C., Prakasam T.B.S., Srinath E.G. (1976). *Inhibition of nitrification by ammonia and nitrous-acid*. Journal of Water Pollution Control. Fed., 48 : 835–852.

Ali M.I., Schneider P. (2005). Crystallization of struvite from metastable region with different types of seed crystal, J. Non-Equilib. Thermodyn., 30 (2)95-111.

Arrojo B., Mosquera-Corral A., Garrido J.M. (2004). *Aerobic Granulation with industrial wastewater in Sequencing Batch Reactors*. Water Research. 38 (14-15): 3389-3399.

Ashley K, Cordell D., Mavinic D. (2011). *A brief history of phosphorus: From the philosopher's stone to nutrient recovery and reuse*. Chemosphere 84 (6): 737–746.

Balmer P., Hultman B. (1988). *Control of phosphorus discharges: present situation and trends.* Hydrobiologia (170):305-319.

Barat R., Montoya T., Seco A., Ferrer J. (2011). *Modelling biological and chemically induced precipitation of calcium phosphate in enhanced biological phosphorus removal systems*, Water Research, 45(12) : 3744-3752.

Barat R., Montoya T., Borrás L., Ferrer J., Seco A. (2008). *Interactions between calcium precipitation and the polyphosphate-accumulating bacteria metabolism.* Water Research, 42 (13): 3415-3424.

Barnard J.L. (1990). *Full scale BNR plant overview: putting theory into practise*. Proceedings of IAWPRC Conference, Bendigo, Victoria, pp. 205-218.

Batstone, D.J., Keller, J., Newell, R.B., Newland, M. (2000). *Modelling anaerobic degradation of complex wastewater. I: model development*. Bioresource Technology, 75: 67–74.

Battistoni P., Fava G., Pavan P., Musacco A., Cecchi F. (1997). *Phosphate removal in anaerobic liquors by struvite crystallization without addition of chemicals: Preliminary results*. Water Research. 31(11): 2925-2929.

Baur R., Prasad R., Britton A. (2008). *Reducing Ammonia and Phosphorus Recycle Loads by Struvite Harvesting.* Ostara Nutrient Recovery Processes Brochure for WEFTEC 2008.

Beun J.J., Hendriks A., Van Loosdrecht M.C.M., Morgenroth E., Wilderer P. A. and Heijnen J.J. (1999). *Aerobic granulation in a sequencing batch reactor.* Water Research 33(10): 2283-2290.

Blackall L.L., Crocetti G.R., Saunders A.M., Bond P.L. (2002). *A review and update of the microbiology of enhanced biological phosphorus removal in wastewater treatment plants*. Antonie van Leeuwenhoek, 81:(681- 691).

Borgerding J. (1972). *Phosphate deposits in digestion systems*. Journal of the water pollution control federation. 44: 813-819.

Brett S., Guy J., Morse G.K., Leister N. (1997). *Phosphorus Removal and recovery Technologies*. Selper Publications, London.

Bundgaard E. (1988). *Bundgaard, Nitrogen and phosphorus removal by the BIO-DENITRO and BIO-DENIPHO processes* Proc. Int. Workshop on Wastewater Treat. Technol.Copenhagen

Caixeta E.T., Cammarota M., Alcina X. (2002). *Slaughterhouse wastewater treatment: evaluation of a new three-phase separation system in a UASB reactor*. Bioresource Technology, 81 (1):61-69.

Cardot Claude (1999). *Les traitements de l'eau*. Procédés Physico-chimiques et biologiques. Ed. Ellipses.

Cassidy DP, Belia E. (2005). *Nitrogen and phosphorus removal from an abattoir wastewater in a SBR with aerobic granular sludge*. Water Res., 39:4817–23.

Cecchi F., Battistoni P., Pavan P., Fava G., Mata-Alvarez J. (1994). *Anaerobic digestion of OFMSW - organic fraction of municipal solid waste and BNR_biological nutrient removal- processes: a possible integration and preliminary results*. Water Sci Technol., 30:65-72.

CEEP: Centre d'Etudes Européen des Polyphosphates. (2011). ScopeNewsletter, N°79.

CEEP: Centre d'Etudes Européen des Polyphosphates. (2004). ScopeNewsletter, N°55.

Centre d'Etude et de valorisation des algues (CEVA), 2011. Brittany, France report.

Charlier Roger H., Morand P., Finkl C.W. (2008). *How Brittany and Florida coasts cope with green tides*, International Journal of environmental studies, 65(2):197-214 .

Cloete T.E., Steyn P.L. (1988).*The role of Acinetobacter as a phosphorus removing agent in activated sludge*, Water Research, 22(8): 971-976.

Coma M., Verawaty M., Pijuan M., Yuan Z., Bond P.L. (2011). *Enhancing Aerobic Granulation For Biological Nutrient Removal From Domestic Wastewater*. Bioresource Technology (in press).

Coma M., Biological Nutrient Removal in SBR Technology: from floccular to granular sludge (2011). Ph.D. Thesis, University of Girona, Spain.

Cordell, D., Rosemarin, A., Schröder, J., Smit, A. (2011). *Towards global phosphorus security: a systemic framework for phosphorus recovery and reuse options*. Special Issue on the phosphorus cycle. Chemosphere 84, 747–758.

Danalewich J.R., T.G. Papagiannis, R.L. Belyea, M.E. Tumbleson, L. Raskin (1998). Characterization of dairy waste streams, current treatment practices, and potential for biological nutrient removal. Water Research, 32 (12):3555-3568

Daumer M.-L., Béline F., Spérandio M. and Morel C. (2008). *Relevance of a perchloric acid extraction scheme to determine mineral and organic phosphorus in swine slurry*. Bioresource Technology 99(5): 1319-1324.

De Bashan L.E., Bashan Y. (2004). *Recent advances in removing phosphorus from wastewater and its future use as a fertilizer*. Water Research 38(19): 4222-4246.

Demirel B. (2003). *Acidogenesis in two-phase anaerobic treatment of dairy wastewater*. Ph.D. Thesis dissertation. Bogazici University, Istabul, Turkey.

Demirel B., Yenigun O., T. Onay (2005). *Anaerobic treatment of dairy wastewaters: a review*. Process Biochemistry, 40 (8): 2583-2595.

Doble M., KuChapter A. (2005). *Treatment of Municipal Waste*. Biotreatment of Industrial Effluents, Ed. Elsevier, chp.27, pp. 275-283.

Doyle J.D, Oldring K, Churchley J, Parsons S.A. (2002). *Struvite formation and the fouling propensity of different materials*. Water Research, 36(16): 3971-3978.

Eckenfelder Jr. Weley W. (1997). Industrial Water Polution Control. Mc Graw Hill International Editions (2nd edition).

Eggers E., Dirkzwager A.H., van der Honing H. (1991). *Full-scale experiences with phosphate crystallisation in a crystalactor*. Water Sci Technol., 24:333-334.

Etterer T. and Wilderer P.A. (2001). *Generation and properties of aerobic granular sludge*. Water Science and Technology. 43 (3): 19-26

FAO report (2004). *The state of food insecurity in the world*. Available on ftp://ftp.**fao**.org/docrep/**fao**/007/y5650e/y5650e00.pdf

Farnell BA., Loockwood G., Murdoch W.C., Lefebvre S., Lindrea K.C. (1990). *Comparison of biological phosphorus removal activated sludge configurations*. Proceedings of IWAPRC Conference, Bendigo, Victoria. pp. 177-184.

Filipe C.D.M., Daigger G.T., Grady Jr. C.P.L. (2001). *A metabolic model for acetate uptake under anaerobic conditions by glycogen-accumulating organisms: stoichiometry, kinetics and effect of pH*. Biotechnol. Bioeng. 76 (1): 17–31.

Gao D., Liu L., Liang H., Wu W.M. (2011). *Comparison of four enhancement strategies for aerobic granulation in sequencing batch reactors*. Journal of Hazardous Materials, 186(1):320-327.

Golterman H.L, De Oude N. (1998). *Eutrophication of lakes, rivers and coastal seas*. The handbook of environmental chemistry 5 (Part A): 79–124.

Haas D.W., Lötter DW., Dubery IA. (1990). *An evaluation of the methods used for the determination of ortho-phosphate and total phosphate in activated sludge extracts*. Water Science 15(4), 257-260.

Hawkins S. , K. Robinson, A. Layton, G. Sayler (2010). Limited impact of free ammonia on *Nitrobacter spp.* inhibition assessed by chemical and molecular techniques. Bioresource Technology, 101 (12): 4513-4519.

Henze, Harremöes, La Cour, Arvin (1997). *Waste Water Treatment*. Biological and Chemical Processes. Ed. Springer, 2nd edition.

Hubbert M.K.. (1949). *Energy from fossil fuels*. Science, 109:103-109.

Hu H., Li X., Liu J., Xu F. (1996). *The effect of direct application of phosphate rock on increasing crop yield and improving properties of red soil*. Nutrient Cycling in Agro-ecosystems, 46: 235-239.

Hu Z.R.., Wentzel M. C. and Ekama G. A. (2002). *Anoxic growth of phosphate-accumulating organisms (PAOs) in biological nutrient removal activated sludge systems*. Water Research 36(19): 4927-4937.

Huang W., Wang S., Zhu Z., Li L. Yao X., Rudolph V., Haghseresht F. (2008). *Phosphate Removal from wastewater using red mud*. Journal of Hazardous Materials, 158: 35-42.

Hwang S., Hansen C.L., (1998). *Characterization of and bioproduction of short-chain organic acids from mixed dairy-processing wastewater*. Trans. Am. Soc. Agric. Engineering, 41:795–802.

Janssen M.J., Meinema K., van der Roest H.F. (2002). *Biological Phosphorus Removal: Manual for Design and Operation*. STOWA-IWA Publisher. pp. 186-196.

Joko I. Phosphorus removal from wastewater by the crystallization method. Water Sci. Technol. (17):121-132.

Juang Y.C., Adav S.S., Lee D.J., Tay J.H. (2010). *Stable aerobic granules for continuous-flow reactors: precipitating calcium and iron salts in granular interiors*. Bioresource Technology, 101 (21): 8051-8057.

Kampschreur M.J., van der Star W.R.L., Wielders H.A., Mulder J.W., M.S.M. Jetten, M.C.M. van Loosdrecht (2008). *Dynamics of nitric oxide and nitrous oxide emission during full-scale reject water treatment.* Water Research, 42(3):812-826.

Katsuura H. (1998). *Phosphate recovery from sewage by granule forming process (full scale struvite recovery from a sewage works at Shimane Prefecture, Japan)*. In International conference on phosphorus recovery from sewage and animal waste, Warwick University, UK.

Komatsu T, Hanaki K, Matsuo T. (1991). *Prevention of lipid inhibition in anaerobic processes by introducing a two-phase system*. Water Science and Technology, 23:1189–200.

Koster I. (1987). *Abatement of long-chain fatty acid inhibition of methanogenic by calcium addition*. Biol. Wastes, 25:51–9.

Kuba T., Smolders G. J. F., van Loosdrecht M. C. M. and Heijnen J.J. (1993). *Biological phosphorus removal from wastewater by anaerobic and anoxic sequencing batch reactor*. Water Science and Technology, 27: 241-252.

de Kreuk, M., Heijnen, J.J. and van Loosdrecht, M.C.M. (2005). *Simultaneous COD, nitrogen, and phosphate removal by aerobic granular sludge*. Biotechnol Bioeng. 90: 761-769.

de Kreuk, MK. (2006). *Aerobic Granular Sludge: Scaling up a new technology*. Ph.D. Thesis, Technical University of Delft, Delft, The Netherlands. ISBN: 978-90- 9020767-4.

de Kreuk, MK., Kishida, N., van Loosdrecht, MCM. (2007). *Aerobic granular sludge- state of the art*. Water Sci Technol. 55 (8-9): 75-81.

Lan J.C., Benefield L., Randall C.W. (1982).*Phosphorus removal in the activated sludge process.* Water Research, 17(9): 1193-1200.

Law (1997). *Microbiology and biochemistry of cheese and fermented milk*. Second edition, Chapman and Hall.

Le Corre K. (2006). *Understanding struvite crystallization and recovery*. Ph. Thesis, Cranfield University, School of Applied Science.

Lehninger (1988). *Biochemistry*. Worth Publishers, Ed. Omega. p: 807.

Lemaire R. (2007). *Development and fundamental investigations of innovative technologies for biological nutrient removal from abattoir wastewater*. Ph.D Thesis. University of Queensland, Australia.

Lemaire R., Meyer R., Taske A., Crocetti G. R., Keller J. and Yuan Z. G. (2006). *Identifying causes for N2O accumulation in a lab-scale sequencing batch reactor performing simultaneous nitrification, denitrification and phosphorus removal*. Journal of Biotechnology. 122(1): 62-72.

Lettinga, G., van Nelsen, A.F.M., Hobma, S.W., de Zeeuw, W., Klapwijk, A., (1980). Use of the upflow sludge blanket (USB) reactor concept for biological wastewater treatment, especially for anaerobic treatment. Biotechnology and Bioengineering, 22 : 699-734.

Levin G.V., Shapiro J. (1965). *Metabolic uptake of phosphorus by wastewater organisms*. Journal Water Pollution Control Fed. 37: 800-821.

Liberti L., Limoni N., Lopez A., Passino R., Boari G. (1986). *The 10m^3/h RIM-NUT demonstration plant at West Bari for removing and recovering N and P from wastewater*. Water Research. 20: 800-821.

Liu, W.T., Nakamura, K., Matsuo, T., Mino, T. (1997). *Internal energy-based competition between polyphosphate- and glycogen-accumulating bacteria in biological phosphorus removal reactors-effect of P/C feeding ratio*. Water Research, 31(6): 1430–1438.

Liu Y., Tay J.H. (2004). *State of the art of biogranulation technology for wastewater treatment*. Biotechnology Advances, 22(7): 533-563.

Liu Y. Q., Liu Y. and Tay J. H. (2004). *The effects of extracellular polymeric substances on the formation and stability of biogranules*. Applied Microbiology and Biotechnolog, 65(2):143-148.

Liu Y, Lin YM, Yang SF, Tay JH. (2003). *A balanced model for bio.lms developed at different growth and detachment forces*. Process Biochem. ,38:1761–1765.

Liu, Y., Wang, Z-W., Qin, L., Liu, Y-Q., Tay, J-H. (2005). *Selection pressure-driven aerobic granulation in a sequencing batch reactor*. Appl Microbiol Biotechnol., 67: 26-32.

Liu Y., Tay J.H.. (2002). *The essential role of hydrodynamic shear force in the formation of biofilm and granular sludge*, Water Res., 36 : 1653–1665.

Llabres P., Pavan P., Battistoni P., Cecchi M. F., Mata-Alvarez J. (1998). *The use of organic fraction of municipal solid waste hydrolysis products for biological nutrient removal in wastewater treatment plants.* Water Research 33(1). 214-222.

van Loosdrecht M.C.M., Brandse F.A., de Vries A.C. (1998). *Upgrading of wastewater treatment processes for integrated nutrient removal- the BCFS® process*, Water Science and Technology, 37 (9): 209-217.

Lopez-Vazquez C.M., Oehmen A., Hooijmans C.M., Brdjanovicc D., Gijzenad H.J., Yuane Z., M.C.M. van Loosdrecht. (2009). *Modeling the PAO–GAO competition: Effects of carbon source, pH and temperatur*e. Water Research, 43: 450-462.

Maurer M., Boller M. (1999a). *Modelling of phosphorus precipitation in wastewater treatment plants with enhanced biological phosphorus removal*. *Water Science and Technology* 39(1):147-163.

Maurer M., Abramovich D., Siegrist H., Gujer W. (1999b). *Kinetics of biologically induced phosphorus precipitation in waste-water treatment*. Water Research 33(2):484-493.

Metcalf & Eddie (1991). *Wastewater engineering: treatment, disposal, reuse*. (3rd edition). Ed. Mc. Graw Hill international.

Meyer R. L., Zeng R. J. X., Giugliano V. and Blackall L. L. (2005). *Challenges for simultaneous nitrification, denitrification, and pH aggregates: mass transfer limitation and nitrous oxide production*. FEMS Microbiology Ecology. 52(3): 329-338.

Mino T. (2000). *Microbial Selection of Polyphosphate-Accumulating Bacteria in Activated Sludge Wastewater Treatment Processes for Enhanced Biological Phosphate Removal*. Biochemistry, 65:(341- 348).

Mishima K., Nakamura M. (1991). *Self-immobilization of aerobic activated sludge-a pilot study of the process in municipal sewage treatment*. Water Science Technology, 23:981-990.

Monroy O.H., Vazquez F.M., Derramadero J.C., Guyot J.P. (1995). *Anaerobic–aerobic treatment of cheese wastewater with national technology in Mexico: the case of 'El Sauz'*. Water Sci Technol., 32:149–56.

Mostastruc L. (2003). *Modélisation et optimisation d'un réacteur en lit fluidisé de déphosphatation d'effluents aqueux*. Ph.D. Thesis at INPT and UPS Toulouse III.

Moletta R. (2006). *Gestion des problèmes environnementaux dans les industries agro-alimentaires*. Ed. Lavoisier.

Momberg G.A., Oellermann R.A. (1992). *The removal of phosphate by hydroxyapatite and struvite crystallisation in South Africa*. Water Sci Technol., 26:987-996.

Morgenroth E., Sherden T., van Loosdrecht M.C.M., J.J. Heijnen, P.A. Wilderer. (1997). *Aerobic granular sludge in a sequencing batch reactor*. Water Research, 31(12):3191-3194.

Morse G.K, Brett S.W., Guy J.A., Lester J.N. (1998). *Review: Phosphorus removal and recovery technologies*. Science of The Total Environment, 212(1):69-81.

Münch E.V., Barr K. (2001). *Controlled struvite crystallisation for removing phosphorus from anaerobic digester sidestreams*, Water Research, 35(1) :151-159.

Obaja D., Macé S., Costa J., Sans C., Mata-Alvarez J. (2003). *Nitrification, denitrification and biological phosphorus removal in piggery wastewater using a sequencing batch reactor*. Bioresource Technology, 87(1):103-111.

Oehmen, A., Carvalho G., Lopez-Vazquez C.M., van Loosdrecht M.C.M., Reis MAM. (2010). *Incorporating microbial ecology into the metabolic modelling of polyphosphate accumulating organisms and glycogen accumulating organisms*. Water Research, 44(17):4992-5004.

Oehmen, A., Yuan, Z., Blackall, L.L., Keller, J. (2005a). *Comparison of acetate and propionate uptake by polyphosphate accumulating organisms and glycogen accumulating organisms*. Biotechnology Bioengineering. 91 (2): 162–168.

Oehmen, A., Vives, M.T., Lu, H., Yuan, Z., Keller, J. (2005b). *The effect of pH on the competition between polyphosphateaccumulating organisms and glycogen-accumulating organisms*. Water Research, 39 (15): 3727–3737.

Oehmen, A., Saunders, A.M., Vives, M.T., Yuan, Z., Keller, J. (2006). *Competition between polyphosphate and glycogen accumulating organisms in enhanced biological phosphorus removal systems with acetate and propionate as carbon sources*. J. Biotechnol., 123 (1): 22–32.

Ohlinger K.N., Young T.M., Shroeder E.D. (1998). *Predicting struvite formation in digestion*. Water Research, 32(12): 3607-3614.

Omoike A.I., van Loon G. W. (1999). *Removal of phosphorus and organic matter removal by alum during wastewater treatment*. Water Research (33):3617- 3627.

Pambrun V. (2005). *Analyse et modélisation de la nitrification partielle et de la précipitation concomitante du phosphore dans un réacteur à alimentation séquencé*. INSA (Toulouse).

Panswad T., Tongkhammak N., Anotai J. (2007). *Estimation of intracellular phosphorus content of phosphorus-accumulating organisms at different P:COD feeding ratios*. Journal of Environmental Management, 84(2):141-145.

Perle M,Kimchie S, Shelef G. (1995). *Some biochemical aspects of the anaerobic degradation of dairy wastewater*. Water Research, 29:1549–54.

Perry R., Green D. (1999). *Wastewater treatment*. The Perry's Chemical Engineers Handbook. Mc Graw Hill.

P. Piekema, A. Giesen. (2001). *Phosphate recovery by the crystallization process: experience and developments*. Second international conference on Recovery of Phosphate from sewage and animal wastes, Holland, 12th and 13th march 2001.

Pijuan Y.Z., Saunders A.M., Guisasola A., Baeza J.A., Casas C. And Blackall L.L. (2004). *Enhanced Biological Phosphorus Removal in a sequencing batch reactor using propionate as the sole carbon source*. Biotechnology and Bioengineering, 85(1): 56-67.

Qin L, Liu Y, Tay JH. (2004). *Effect of settling time on aerobic granulation in sequencing batch reactor.* Biochem Eng. J., 21:47–52.

Ren T.-T., Liu L., Sheng G.-P., Liu X.-W., Yu H.-Q., Zhang M.-C. and Zhu J.-R. (2008). *Calcium spatial distribution in aerobic granules and its effects on granule structure, strength and bioactivity*. Water Research 42(13): 3343-3352.

Saidou H., Korchef A., Ben Moussa S., Ben Amor M. (2009). *Struvite precipitation by the dissolved CO_2 degasification technique: impact of the airflow rate and pH*. Chemosphere. 74(2): 338-343.

Sarkar, A.K. (1990). *Phosphate cement-based fast setting binders*. J.Am. Ceram. Soc. Bull., 69: 234–238.

Sawyer C.N. (1944). *Biological Engineering in sewage treatment*. Sewage Works Journal (16):925-935.

Schwarzenbeck N, Borges JM, Wilderer PA. (2005). *Treatment of dairy effluents in an aerobic granular sludge sequencing batch reactor*. Appl. Microbiol. Biotechnol., 6:711–8.

Seviour R.J., Mino T., M. Onuki. (2003). *The microbiology of biological phosphorus removal in activated sludge systems*. FEMS Microbiology Reviews, 27(1): 99-127.

Shu L., Schneider P., Jegatheesan V., Johnson J. (2005). *An economic evaluation of phosphorus recovery as struvite from disgester supernatant*. Bioresources Technology. 97(17): 2211-2216.

Siebritz I.P., Ekama G.A. Marais G.V.R. (1983). *A parametric model for biological excess phosphorus removal*. Water Science Technology. 15:127-152.

Smolders G.J.F., van der Meij J., van Loosdrecht M. C. M., HeijnenJ. J. (1994). *Stoichiometric model of the aerobic metabolism of the biological phosphorus removal process*. Biotechnol. Bioenginering 44: 837-848.

Szpyrkowicz L., F. Zilio-Grandi. (1995). Seasonal phosphorus removal in a Phostrip process—I. Two-years' plant performance. Water Research, 29(10): 2318-2326.

Stratful I., Scrimshaw M.D., Lester J.N. (2004). *Removal of Struvite to Prevent Problems Associated with its Accumulation in Wastewater Treatment Works*. Water Environment Research, 76, (5):437-443

Su K.Z., Yu H.Q. (2005). *Formation and characterization of aerobic granules in sequencing batch reactor treating soybean-processing wastewater*. Environmental Science and Technology, 39:2818-2828.

Suzuki K., Tanaka Y., Kuroda K., Hanajima D., Fukumoto Y., Yasuda T. (2006). *The technology of phosphorus removal and recovery from swine wastewater by struvite crystallization reaction*. JARQ. 40(4): 341-349.

Tay J. H., Liu Q. S. and Liu Y. (2002). *Characteristics of aerobic granules grown on glucose and acetate in sequential aerobic sludge blanket reactors*. Environmental Technology. 23(8): 931-936.

Tay J.H., Liu Q.S., Liu Y.. (2001). *The effects of shear force on the formation, structure and metabolism of aerobic granules*, Appl. Microbiol. Biotechnol. 57: 227–233.

Tchobanoglous, G., Burton, F.L. and Stensel, H.D. (2003). *Wastewater engineering: treatment and reuse*, 4th ed. Metcalf and Eddy Inc. McGraw-Hill Higher Education, New York, USA.

Thayalakumaran N., Bhamidimarri R., Bickers P.O. (2003). *Biological nutrient removal from meat processing wastewater using a sequencing batch reactor*. Water Science & Technology,47 (10): 101–108.

Toh S.K., Tay J.H., Moy B.Y.P., Ivanov V., Tay S.T.L. (2003). *Size effect on the physical characteristics of the aerobic granule in a SBR*. Applied Microbiology Biotechnology. 60: 687-695.

Unitika Ltd. (1994). *Fertiliser produced from wastewater*. Jpn Chem Wkly. 35:2.

Upton J., Hayes E., Churchley J. (1996). Biological phosphorus removal at Stratford Upon Avon, UK: The effect of influent wastewater characteristics on effluent phosphate. Water Science Technology, 33:73-80.

Vaccari David A. (2011). *Phosphorus Cycle Issue*. Chemosphere 84(6): 735–736.

Vazquez-Rodríguez G.A., Rols J.L. (1997). *Etude du processus de nitratation avec des boues activées: effet inhibiteur de l'ammoniac sur les bactéries nitratantes*. Revue des Sciences de l'eau. 3: 359-375.

Wakeford J.P. (1911). *Trials of sewage precipitants at Wakefeield.* Eng. Record 64, str. 355.

Wan J., Bessière Y., Spérandio M. (2009). *Alternating anoxic feast/aerobic famine condition for improving granular sludge formation in sequencing batch airlift reactor at reduced aeration rate*, Water Research, 43 (20): 5097-5108.

Wan J. (2009). *Interaction entre l'élimination des polluants azotées et la formation des granules aérobies en réacteur biologique séquencé*. PhD thesis, INSA (Toulouse).

Wang Z. W., Liu Y. and Tay J. H. (2005). Distribution of EPS and cell surface hydrophobicity in aerobic granules. Applied Microbiology and Biotechnology 69(4): 469-473.

Wang S.G., Liu X.W., Gong W.X., Gao B.Y. Zhang D.H., Yu H.Q. (2007). *Aerobic granulation with brewery wastewater in a sequencing batch reactor*. Bioressources Technology, 98:2142-2147.

Water Research Commission Report (WRC), *Water Wheel*, issue Sept/Oct., 2008, pp.14-17.

Wardle, T. (1893). *On Sewage Treatment and Disposal*, John Heywood, London, p. 43.

Weikard. (2010). *Phosphorus Use: Resource economics and ethics. A research Agenda. Conference workshop Phosphorus form excess to shortage. Can technology solve the problem?, IHE-UNESCO Conference, Delft, November 2010.*

Wentzel M.C., Ekama G.A., Loewenthal R.E., Dold P.L., Marais G.R. (1989). *Enhanced polyphosphate organism cultures in activated sludge systems*. *Part II: experimental behaviour*. Water SA 15(2):71-88.

Whang L.M., Park J.K. (2006). *Competition between polyphosphate- and glycogen-accumulating organisms in enhanced biological phosphorus removal systems: effect of temperature and sludge age*. Water Environmental Research, 78 (1): 4–11.

White, J. (2000). *Introduction to Biogeochemical Cycles (Ch. 4)*. Department of Geological Sciences. University of Colorado, Boulder.

Wichern M., Lubken M., Horn H. (2008). *Optimizing Sequencing Batch Reactor Operation for treatment of diary wastewater with aerobic granular sludge*. Water Science Technology. 58(6): 1199-1206

Wilsenach J.A., Maurer M. Larsen T., van Lososdrecht M.C.M. (2003). *From wastewater treatment to integrated resource management*. Water Science Technology. 48(1): 1-9.

Wong M.T, Mino T., Seviour R.J., Onuki M., Liu W.T.. (2005). *Situ identification and characterization of the microbial community structure of full-scale enhanced biological phosphorous removal plants in Japan.* Water Research, 39(13): 2901-2914.

Wu Q., Bishop P.L. (2004). *Enhancing struvite crystallization from anaerobic supernatant*. Journal of Environmental Engineering and Science. 3(1): 21-29.

Yilmaz G., Lemaire R., Keller J., Yuan Z., (2007). *Effectiveness of an alternating aerobic, anoxic/anaerobic strategy for maintaining biomass activity of BNR sludge during long-term starvation*. Water Research, 41: 2590-2598.

Yeoman S., Stephenson T., Lesten J.N., Perry R. (1988). *Removal of phosphorus during wastewater treatment : a review*. Environmental Pollution. 49 (3): 183-233.

Zeng R.J., Lemaire R., Yuan Z., Keller J. (2003a). *Simultaneous Nitrification, Denitrification, and Phosphorus Removal in a Lab-Scale Sequencing Batch Reactor*. Biotechnology Bioengineering, 84(2):170-178.

Zeng R.J., van Loosdrecht M.C.M., Yuan Z., Keller J. (2003b). *Metabolic model for glycogen-accumulating organisms in anaerobic/aerobic activated sludge systems*. Biotechnol. Bioeng. 81(1):92-105.

Zhang LL, Feng XX, Xu F, Xu S, Cai WM. (2005). *Biosorption of rare earth metal ion on aerobic granules*. J Environ Sci Health A Tox/Hazard Subst Environ Eng., 40(4):857–67.

CHAPTER II:

MICROBIALLY INDUCED PHOSPHORUS PRECIPITATION (MIPP) IN AEROBIC GRANULAR SLUDGE PROCESS

In this chapter, different analytical techniques are investigated to assess, for the first time, the biologically induced precipitation of phosphorus in the core of granules. Mineral precipitation of hydroxyapatite (calcium phosphate) is demonstrated by direct spectral and optical analysis: Raman spectroscopy, Energy dispersive X-ray (EDX) coupled with Scanning Electron Microscopy (SEM), and X-ray diffraction analysis are performed simultaneously on aerobic granules cultivated in a batch airlift reactor working with anoxic feast/aerobic famine cycles for 500 days. The limitations of the different analytical techniques, as well as the mineral implications on the phosphorus removal process will also be evaluated in this chapter.

This chapter corresponds to the article:

Mañas A., Spérandio M., Biscans B. (2011). Biologically induced phosphorus precipitation in aerobic granular sludge process. Water Research 45(12):3776-3786.

II.1. INTRODUCTION

Phosphorous is a key nutriment for the development of life, constituting one of the major nutrients necessary for agricultural activity. However, the quantities of mineral phosphorus resources (phosphate rock) are decreasing in the world, making phosphorus recovery necessary in the coming century. On the other hand, the high phosphorus and nitrogen content of wastewaters leads to serious problems of eutrophication in ponds, rivers and seas. Therefore, research is now focusing increasingly on combined processes that remove phosphorous from wastewaters and simultaneously recover it in the form of a valuable product, for example, struvite (MAP) or hydroxyapatite (HAP), (de-Bashan and Bashan 2004; Shu et al., 2006, Suzuki et al., 2006). Phosphorous recovery techniques are particularly suited to high strength wastewaters produced by anaerobic sludge digestion (Demirel et al., 2005; Lemaire, 2007). Calcium or magnesium phosphates can be formed by crystallization and recovered in specific reactors via pH control and chemical dosing (Seckler et al., 1996; Katsuura et al., 1998; Münch et al. 2001; Giesen et al., 1999; Baur et al., 2008). The spontaneous phenomenon has been reported to cause economic damage related to pipe clogging when it is not controlled (van Rensburg et al., 2003). In activated sludge systems, biologically induced phosphate precipitation has also been reported but less investigated (Maurer et al., 1999; Pambrun, 2005; De Kreuk et al, 2005). Calcium phosphate precipitation is thought to contribute to P removal in Enhanced Biological Phosphorous Removal processes (EBPR) and it is considered to enhance biological P removal efficiency (Maurer et al., 1999). Local precipitation is naturally induced when the pH and ion concentrations lead to mineral supersaturation. In the case of calcium or magnesium phosphate, their formation can be caused by phosphate release due to Polyphosphate Accumulating Organisms (PAO) during the anaerobic phase, but also clearly depends on pH. Bioreactions (e.g. nitrification and denitrification) or aeration (CO_2 stripping) lead to pH gradients which can be responsible for mineral precipitation in biological sludge (Pambrun et al., 2005; Bogaert et al., 1997; Saidou et al., 2009; Zhu et al., 2007). These processes still need to be clarified in granular sludge systems.

The aerobic granular sludge process is a promising technology for wastewater treatment because of its small footprint and capacity to treat high organic loading rates and its simultaneous nutrient removal through nitrification, denitrification and Bio-P accumulating processes (Morgenroth et al., 1997; Etterer and Wilderer, 2001; De Kreuk et al., 2005 ; Lemaire, 2007). The dense-spherical structure of granules leads to transfer

limitations (Liu et al., 2004; Adav et al., 2008), promoting not only DO gradients but also local pH gradients coming from biological reactions, especially in the case of enhanced denitrification (Wan and Spérandio, 2009; Wan et al., 2009). As phosphate accumulating bacteria can also be present inside the granules (Lemaire et al., 2007), anaerobic phosphate release can encourage P precipitation within the core of the microorganisms, where subsequent solubilization of the crystals would be more difficult than in the bulk. Phosphate precipitation in a granular sludge process was assumed (but not directly demonstrated) by Yilmaz (2007) and De Kreuk (2005, 2007). By estimating its supersaturation index, Yilmaz et al. (2007) suggested that struvite could be transiently formed during the anaerobic phase of the SBR cycle. The contribution of this process to overall P removal was estimated to be less than 10% on the basis of a perchloric acid extraction method (PCA), (Haas et al., 1990; Daumer et al., 2008). Similarly, experimental results by De Kreuk (2005) suggest that P-removal occurs partly by biologically induced precipitation in granular sludge. Extraction techniques indicated that 2.6% of the sludge mass was due to precipitates (P/VSS), but the whole contribution of this process compared to biological P removal processes was not quantified. For simplicity, precipitation was not included when modelling the process but De Kreuk et al. (2007) proposed to increase the maximum fraction of poly-phosphate in PAO from 0.35 (Hu et al., 2002) to 0.65 assuming that about 46% of the P removal could be due to P precipitation and 54% due to polyphosphate accumulating bacteria. In 1999, Maurer et al. have proposed a model for naturally induced P precipitation in activated sludge, which is based on the assumption that hydroxyapatite (HAP) and hydroxydicalcium phosphate (HDP) are formed. The model can predict calcium and phosphate concentrations at different pH. However, in all these studies, phosphate minerals formed in biological granules or flocs have never been directly characterized, and the nature of the phosphate precipitate is not demonstrated but only indirectly deduced from stoichiometry of soluble species.

The characterization of precipitates inside aerobic granules is still a relatively unexplored field. Minerals involved in phosphorus immobilization have been poorly qualified in biological sludge because traditional techniques (like X-ray diffraction) are difficult to apply directly in such organic matrices (Cloete and Oosthuizen, 2001). SEM-EDX analysis has recently been applied to determine calcite formations in granules and in nacre shells (Ren et al., 2008). However, calcium or magnesium phosphates have not been quantified in previous studies of aerobic granules (Wang et al., 2006; Ren et al., 2008).

Therefore, the aim of this study is to reveal the nature of P minerals which can accumulate in EBPR granular sludge systems. In an attempt to determine the chemical composition of precipitates in granules, RAMAN spectroscopy, EDX (Energy Dispersive X-ray) technique coupled with Scanning Electron Microscopy (SEM), and X-ray Diffraction analysis (XRD) are evaluated.

II.2. MATERIAL AND METHODS

II.2.1. Reactor operating conditions

Aerobic granules were cultivated in a Sequencing Airlift Batch Reactor (SBAR), with a working volume of 17 L, consisting of an airlift column (D=15 cm, H/D ratio = 7) with a baffle plate (length/width = 83/15-cm-). An aerating diffuser providing fine bubbles 3 mm in diameter was inserted at the bottom of the reactor at one side of the baffle plate, achieving mixing during both anoxic and aerobic phases (using nitrogen gas for the anoxic phase and air for the aerobic one). Oxygen concentration and pH were measured and recorded online with selective probes (WTW TriOxmatic 701). Temperature was maintained constant at 20 °C thanks to a water jacket. Details of the system schematization can be seen in figure II.1. Process batch cycles of 4 hours length were established as follows: anoxic phase (20 minutes), aerobic reaction (145 minutes), idle (30 minutes), withdraw (30 minutes) and feed (15 minutes). Hydraulic Retention Time (HRT) was fixed at 8.5 hours, with a volumetric exchange ratio of 50%. The column was fed at the bottom with a synthetic substrate (details in Wan et al., 2009) having the following composition: COD of 1000 mg/L (25% contribution each of glucose, acetate, propionic acid and ethanol); $[PO_4^{3-}]$ = 30 mgP/L , $[Ca^{2+}]$ = 46 mg/L, $[HCO_3^-]$ = 100 mg/L, $[MgSO_4 \cdot 7H_2O]$ = 12 mg/L, $[NH_4^+]$ = 50 mgN/L, $[NO_3^-]$ = 100 mgN/L. Therefore, a COD/N-NH_4^+ ratio of 20 was maintained, and nitrate was dosed in order to maintain an anoxic phase after feeding. Similarly, a COD/P ratio of 33 in feed was imposed. Influent loading rates coming into the reactor were as follows: 0.14 gN/L·d for ammonium, 0.08 gP/L·d for ortho-phosphate and 2.82 gCOD/L·d for organic substrate.

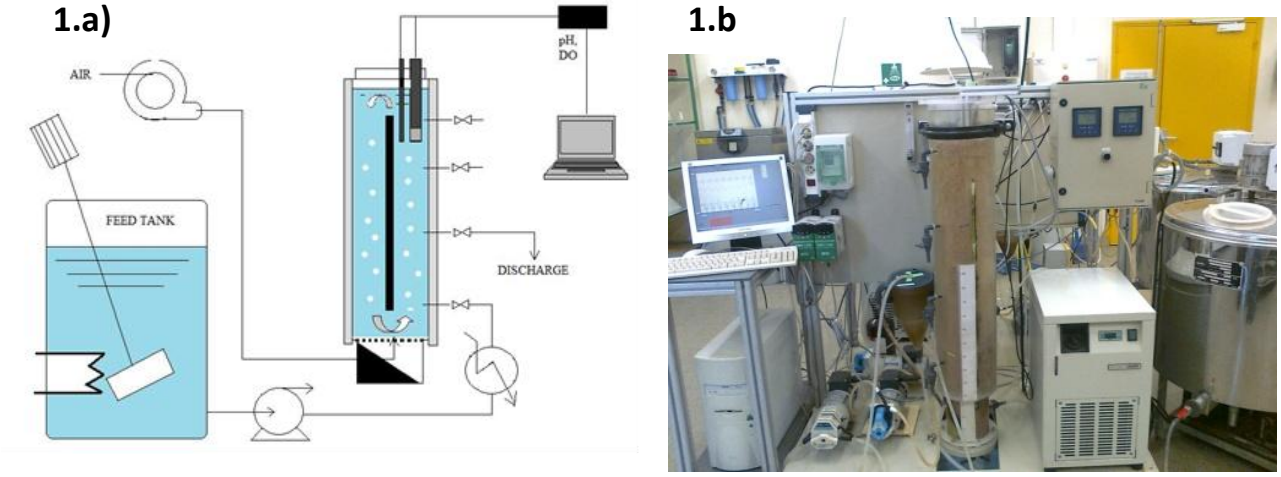

Figure II. 1: a) Scheme of the GSBR device; b) Picture of the laboratory GSBR

II.2.2. Analytical characterization of the liquid and solid phases

Chemical analyses were conducted according to standard methods (AFNOR, 1994). COD (NFT 90-101), MLSS (NFT 90-105) and MLVSS (NFT 90-106). NO_2^-, NO_3^-, PO_4^{3-}, NH_4^+, Ca^{2+}, K^+, Mg^{2+} concentrations were analyzed by Ion Chromatography after being filtered with 0.2 µm pore-size acetate filters. Microscopic observations over the whole sludge sample were performed with a Biomed-Litz® binocular photonic microscope. Particle size distribution was measured with a Malvern 2000 Mastersizer® analyser. Granules were sampled at the end of the aerobic phase. Those analyzed by EDX or Raman Spectroscopy had been previously cut into thin slices of 100 µm using a cryo-microtome (Leica CM 30505 Kryostat). Those analysed by XRD had been previously dried and calcined in an oven at 500°C for 2 hours, in order to remove the organic fraction.

Raman Spectroscopy was performed with an RXN Kaiser Optical Systems INC at a wavelength of 785 nm in the visible range. Two different optical fibres were used for the incident (50 µm) and collected (100 µm) rays. EDX analysis was performed with a photon X analyzer (Quantax Technology Silicon Drift) having a detection limit of 127 eV. It was coupled to a SEM (JEOL 5410 LV) which allowed working in a partial pressure chamber. The reference samples used for comparing the mineral spectra were: struvite (CAS N.13478-16-5), calcite (CAS N. 72608-12-9), magnesite (CAS N. 235-192-7), hydroxyapatite (CAS N. 12167-74-7) and brushite (CAS N. 7789-77-7).

XRD analyses were performed with a BRUKER D5000 diffractometer, with a cobalt tube scattering from 4-70° in 2θ.

Chemical nitrogen and total phosphorus extractions were performed in accordance with standard methods (NFT 90-110 and NFT 90-136 respectively) adapted for the granular samples: first a physical separation was made between flocs and granules by means of a 315 *μm* shiver, then granules were rinsed with a volume of ultrapure water and the volume of sample extracted was re-established with ultrapure water before analysis.

The Supersaturation Index (SI) for each mineral considered (equation I.1) was calculated as the logarithm of supersaturation ratio:

$$SI = \log \Omega = \log\left(\frac{IAP}{K_{sp}}\right)^{1/j} \qquad \text{Equation I.1}$$

where *IAP* is the Ionic Activity Product of the ion activities involved in the mineral precipitation, in which the ionic activity coefficients, and the ionization fractions of each component (Snoeyink and Jenkins, 1980; Burriel et al., 1985) were considered; *j* is the number of ions of the mineral and K_{sp} refers to the thermodynamic mineral precipitation constant at a given temperature (25ºC). The PHREEQC® software (Parkhurst, 2000) and Minteq.v4 database was used to calculate the chemical equilibrium for each sample collected in the reactor. Ionic Strength was taken into account as well as the ionic activity coefficients by the Davies approach (Parkhurst et al., 1980; Burriel et al., 1985; Montastruc, 2003). pK_{sp} of struvite (MAP), hydroxyapatite (HAP), brushite (DCPD), amorphous calcium phosphate (ACP) and hydroxyl dicalcium phosphate (HDP) considered were respectively: 13.26, 57.5, 6.6, 26.52 and 22.6 (Ohlinger et al., 1998). Supersaturating conditions were considered to be achieved when SI > 0.5 (theoretically zero but a security margin is usually given (Burriel et al., 1985; Rahaman et al., 2006).

II.3. RESULTS

II.3.1. Reactor performance and kinetics assessment

The sequencing batch reactor was operated for 540 days. Mean efficiencies of COD, total Nitrogen and Phosphorous removal, as well as MLSS, MLVSS and SVI_{30} values are shown in table II.1. An SVI_5/SVI_{30} ratio closer to 1, indicates a major presence of granules in the whole sludge.

Table II. 1: Mean values measured during 500 days of reactor performance, for MLSS; soluble COD, Total Nitrogen and Phosphorous efficiencies; MLVSS/MLSS ratio, SVI after 30 min and SVI_5/SVI_{30} ratio.

Period of Time	**MLSS**	**η COD**	**η TN**	**η P**	**MLVSS/MLSS**	**SVI_{30}**	**SVI_5/SVI_{30}**
(days)	*(g/L)*	*(%)*	*(%)*	*(%)*	-	*(mL/g)*	-
0-100	14	94	92	62	78	33	2.0
100-200	13	97	100	31	83	34	1.7
200-300	22	93	96	56	77	22	1.5
300-400	28	93	96	67	67	15	1.0
400-500	34	97	97	50	65	15	1.0

MLVSS and MLSS of the whole sludge were measured regularly in the reactor with time, values of 30-35 and 21-25 g/L being achieved for MLSS and MLVSS respectively at the end of the study. The MLVSS/MLSS ratio of granules progressively decreased from 80% to 67%, whilst size and biomass concentration increased, indicating mineral accumulation. Final SVI_5 achieved was 15 mL/g. As shown in figure II.2, the mixed liquor in the reactor was composed of granules and flocs, the latter disappearing progressively with time. Particle size distribution analyses (not shown here) revealed that 800µm was the most probable diameter for granules. At the end of the 540 days of reactor run, removal efficiencies achieved were 100% for ammonium, 100% for nitrate, 82% for ortho-phosphates and 99% for soluble COD.

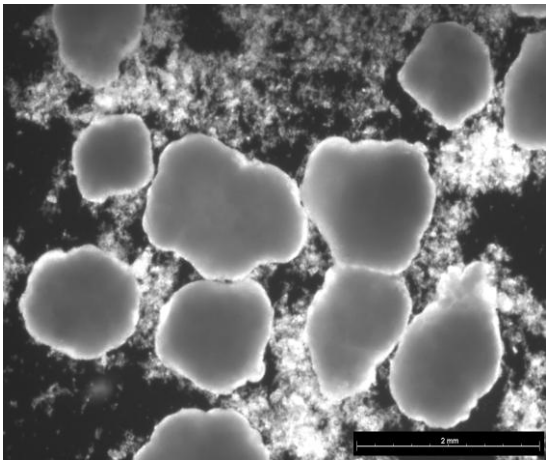

Figure II. 2: granules and flocs in the GSBR after 520 days of operation. The bar dimension is 2 mm.

Kinetic analyses were performed during the batch cycle to assess ammonium, nitrate, COD and phosphate removal rates. Figures II.3 and II.4 show typical time-series profiles in the reactor obtained with two different aeration flow rates (160 L/h and 350 L/h respectively). The separation between the anoxic/aerobic phases is depicted by a dotted vertical line. Ammonium was first partially removed during the non-aerated phase and then during the aerobic phase via nitrification.

Ammonium consumption during the anoxic phase was due to heterotrophic assimilation but it could also be explained by other, non-biotic processes like adsorption (because of high MLSS) or precipitation (as struvite for example). Nitrate and nitrite concentration remained negligible at all times, confirming that simultaneous nitrification and denitrification (SND) occurs in granular sludge. Regarding phosphorus, several mechanisms seemed to take place simultaneously. Kinetics in figures II.3.a and II.3.b, show slightly phosphorus release during the anaerobic phase and P uptake during the aerobic period.

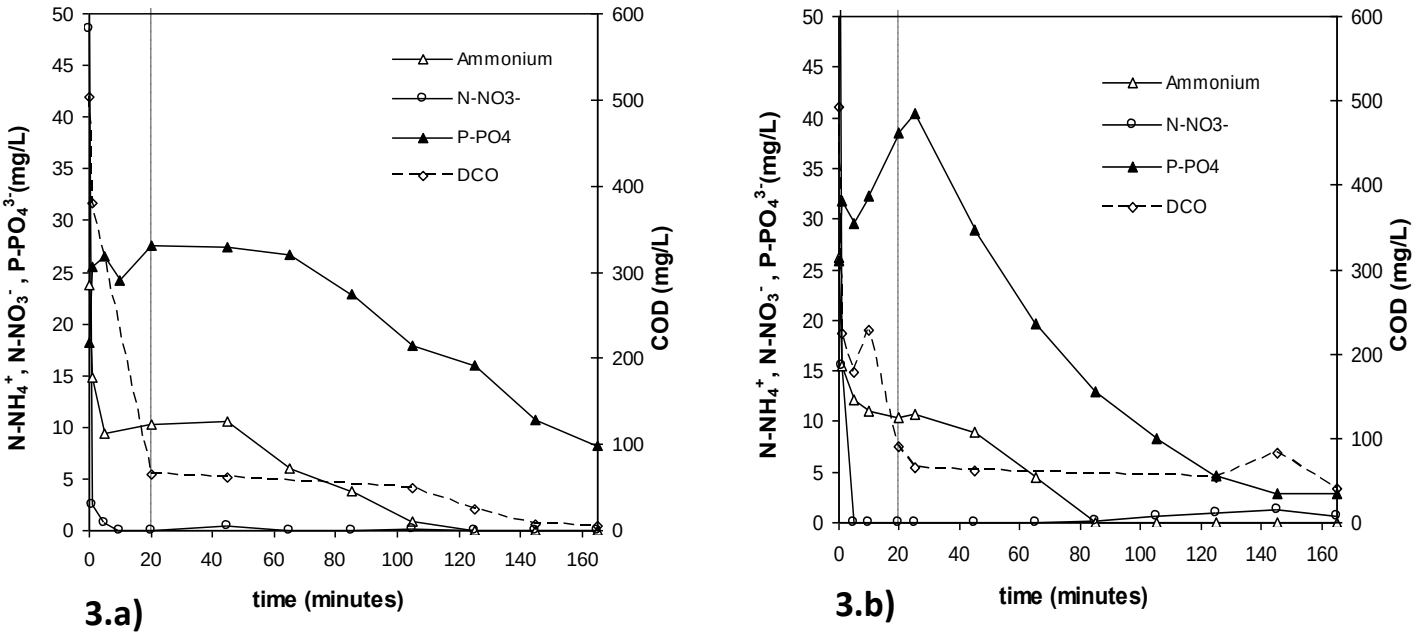

Figure II. 3: Variation of NO_3^-, PO_4^{3-}, NH_4^+ and COD in the reactor bulk during a cycle operation with weak aeration (160 L/h) (3.a) and high aeration (350 L/h) (3.b) rates

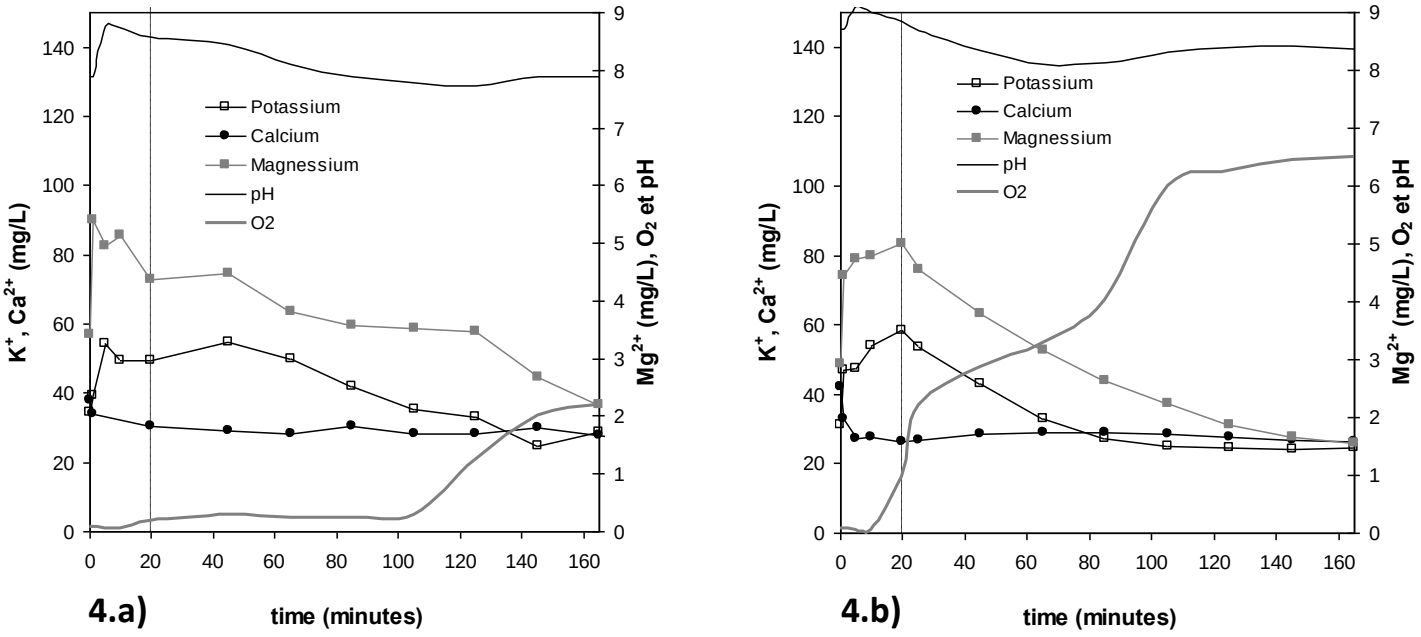

Figure II. 4: Variation of K^+, Mg^{2+}, Ca^{2+}, pH and O_2 in the reactor bulk during a cycle operation with weak aeration (160 L/h) (4.a) and high aeration (350 L/h) (4.b) rates

Meanwhile, biological staining with *sudan black* and *safranin* was carried out according to the method reported in Pandolfi et al., 2007, revealing lipid and PHB accumulations in different granules samples taken during the anoxic phase (results shown in chapter III). Both kinetics and color staining results, suggested the presence and activity of Polyphosphate Accumulating Organisms (PAO). Figures II.3.a and II.3.b show that phosphate uptake rate was higher for higher aeration rate, because dissolved oxygen was limiting at low aeration rate (DO being maintained at 0.3 mg/L). Final phosphate concentration was thus lower at the high air flow rate (2.5 mgP/L) compared to the low aeration rate (8 mgP/L). Mg^{2+} and K^+ fluctuations followed those of P (figure II.4.a. and II.4.b). This was related to poly-phosphate synthesis, which general formula is $Me_{n+2}P_nO_{3n+1}$, where *n* indicates the chain length, and *Me* represents a metal cation (*Jardin and Pöpel, 1996*). In contrast, Ca^{2+} concentration showed a very different trend. It decreased rapidly during the non-aerated period following wastewater feeding. This behavior can be explained by a rapid formation of calcium complexes or precipitates, which will be demonstrated in the following section.

Total phosphorus was extracted from granular sludge samples collected at the end of the aerobic cycle. It was carried out in triplicate after 520 days of reactor operation

(according to the method detailed in section II.2.2). Results indicated that P content was 56 ± 7.3 mgP/gVSS. This value is not really different from values usually reported for EBPR sludge. In EBPR systems, this value is related to the polyphosphate content of sludge, which depends on various parameters: fraction of PAO in the sludge, wastewater COD/P ratio and fraction of volatile fatty acids in wastewater. Li et al. (2005) reported a similar P content at a similar P/COD ratio. Indeed, Panswad et al., (2007), reported similar P content in sludge enriched with PAOs (5.3-20.5 % P in weight), when P:COD ratios varied from 0.02-0.16 respectively. However, the following section will show that phosphorus is not only accumulated in poly-phosphate form but also as a precipitated mineral compound.

In the research of non-destructive techniques for determining the chemical composition of minerals in granules, four criteria were established:

1- Mineral's chemical structure should not be modified within the sample preparing and/or analyze performance.

2- Precipitated minerals inside granules are in solid phase, so are the mineral references used for comparison. The chosen analytical technique should provide results in the same physico-chemical state.

3- The analysis must allow focusing in the microscopic scale, hence, apparatus and probes must be able to point at the microns-scale.

4- The last criterion relates to the rapidity of the analysis, in order to avoid changes or degradation of the sample with time.

II.3.2. Raman analysis

Raman Analysis is a non-destructive analytical technique that requires limited sample preparation (*Hollas, 1996* ; *Skoog et al., 2003*) and that full-filled the aforementioned criteria. It was chosen because of its low water background, as well as for providing sharper and clearer bands than IR spectra (*Barbillat, 2009*). It has already been proved for the characterization and identification of different biological systems since the biologically associated molecules can exhibit a unique spectrum (*Ivleva et al., 2009*). In an attempt to determine the internal structure of the granules, samples were cut into slices of 100 µm width, prepared as described in section (II.2.2). Previous tests were carried out varying the sample slice widths (50-150-200-250 and 300 µm) and different time of exposure to the light source (10s-2 min), showing that 100 µm and 30s were respectively

the optimal conditions to obtain a clear spectrum for the internal part of granules. Then, a central slice was chosen and observed with a binocular microscope before being analyzed by Raman Spectroscopy. As shown in Figure II.5.a, microscopic observation with polarized light of a typical central slice, revealed a white crystalline precipitate in the centre of the granule. Spectroscopic analysis was performed at different points of the mineral core (as indicated on figure II.5.a). An initial set of tests (not shown) were also conducted beforehand with different samples: granules taken at different batch cycle times, dehydrated flocs separately, different cuts and thicknesses sliced from the same granule. Finally, some pure minerals used as reference products (struvite, hydroxyapatite, brushite, calcite and magnesite), were also analyzed with Raman Microscopy and compared to the sample spectra. The following conclusions were drawn: (i) Both flocs and external granule slices showed a noisy signal (due to organic matter) with no remarkable matching peaks (ii) All spectra obtained in the core of granules showed a common and reproducible pattern of 8 peaks of different intensities (see figure II.5.b), considering that a peak is noted when its intensity is three times the mean background noise; (iii) All granule central slices had the same typical peaks regardless of the cycle time.

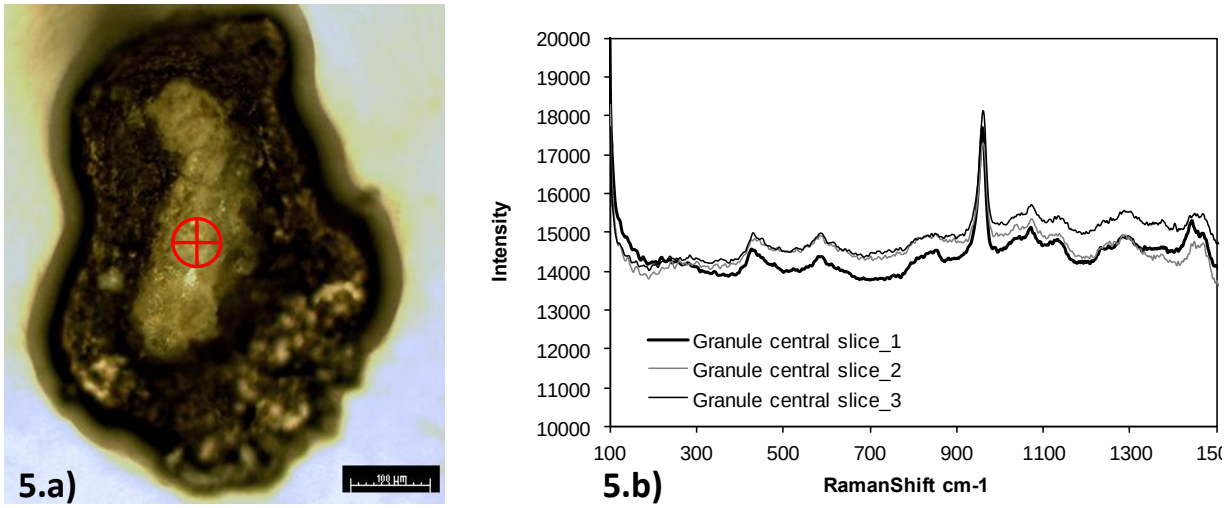

Figure II. 5: a) Central slice from a mature granule after 450 days of reactor run. The bar length is 100 µm; b) Spectra of core aerobic granule slices.

According to figure II.5.b., the most important peaks in the sample were found at the following Raman shifts (cm^{-1}): 430, 588, 850, 962, 1072, 1135, 1295, 1448. The spectra of granule core samples were compared with those obtained with reference minerals. After an individual comparison of frequency-intensity coincidence, it was

concluded that calcite and magnesite spectra (not shown) did not match the sample at all. In figure II.6, the most similar mineral spectra have been depicted in order to compare the coincidence of their peaks. Only those which where suspected to form due to high SI indexes and occurrency in litterature references, were chosen.

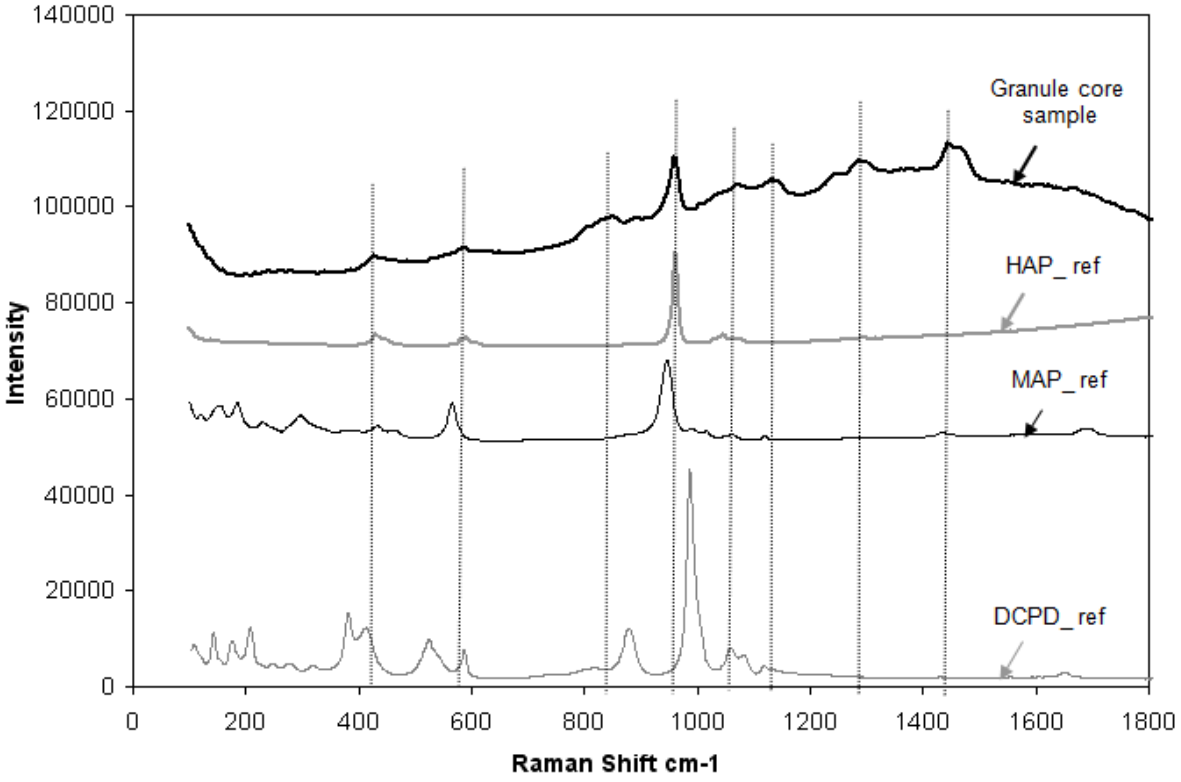

Figure II. 6: Raman spectra of reference minerals compared to a granule central slice

Brushite shows two or three peaks not far from those of granule spectra, but most of the major peaks do not coincide (407, 586, 986, 1056 and 1114 cm^{-1}). Struvite spectrum indicates five peaks (421, 563, 944, 1053, 1112 cm^{-1}) which are very similar to those of the granule sample, but differences in the Raman shifts are statistically significant. The hydroxyapatite spectrum shows 4 peaks, which all match the granule spectra (427, 589, 962, 1072 cm^{-1}) with differences lower than 3 cm^{-1}. Globally, among all the different pure mineral patterns compared, the hydroxyapatite spectrum best fitted the sample in intensity and wave number but could not explain all the peaks observed in the granule spectra. These results suggest that hydroxyapatite is a major mineral precipitated in the aerobic granule cores but the presence of other minerals cannot be totally discounted and further techniques must be compared.

II.3.3. SEM-EDX analysis

Scanning Electron Microscopy (SEM) coupled with Energy Dispersive X-ray detector (EDX) analyses were carried out on cut mature granules. Typical images are shown in figure II.7 for two typical central slices of different granules. It was found that inorganic precipitates occupied an important fraction of the total volume of the granule, located in different zones, mainly close to the centre. A first scanning map of carbon (Figures II.7.c and II.7.d) revealed that the central inorganic zones did not contain large amounts of carbon in contrast with peripheral organic biofilm. Similar results were observed for nitrogen and magnesium (not shown). In contrast, Ca and P were mainly found together in the central precipitates and comparatively poorly in the organic biofilm (figures II.7.e-II.7.h). This result again supports the idea that calcium phosphates are formed in the core of the granules. Phosphorus was also detected but with lower concentration in the organic biofilm zone. It probably came from polyphosphates in PAO clusters. Figures II.7.i and II.7.j, focus on the inorganic precipitate with a higher objective. Figure II.7.i reveals porous, ordered holes in the solid mineral phase. This could be related to the mechanism of precipitate formation around bacterial cells, in relation with gaseous transfers between the microorganisms and the extracellular medium. Another interesting result can be seen in figure II.7.j, where some prismatic structures appear stacked, similar to hydroxyapatite, which crystallizes in the hexagonal system (Morgan et al., 2000), although this last information is not conclusive. Furthermore, several localized EDX spectral analyses were made, pointing the probe at different locations of the precipitate. The spectrum obtained was very reproducible in different locations of the central mineral zone. Analysis spectra clearly showed that calcium, phosphate and oxygen were the major components observed in the mineral zone whereas magnesium and potassium were definitively absent.

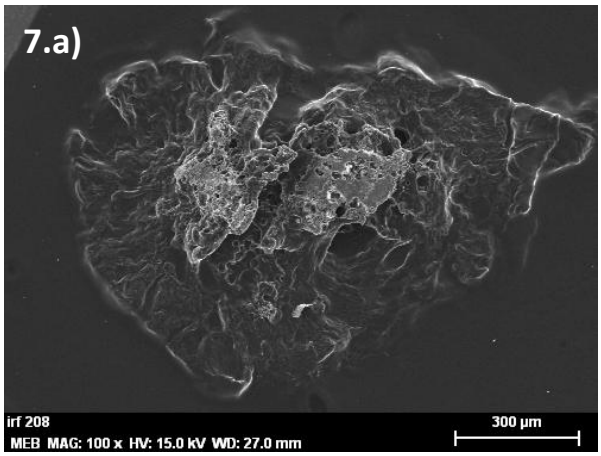
7.a)
irf 208
MEB MAG: 100 x HV: 15.0 kV WD: 27.0 mm
300 µm

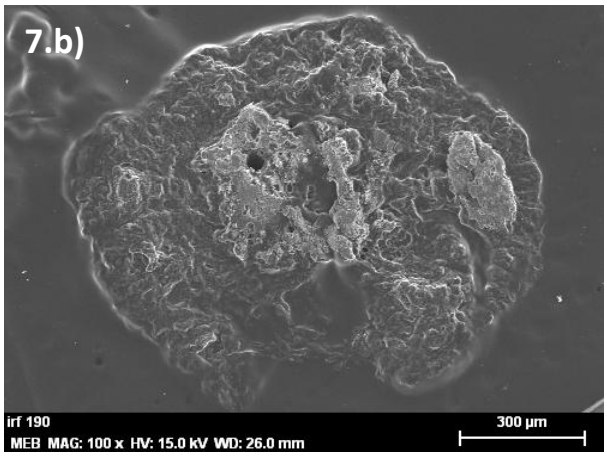
7.b)
irf 190
MEB MAG: 100 x HV: 15.0 kV WD: 26.0 mm
300 µm

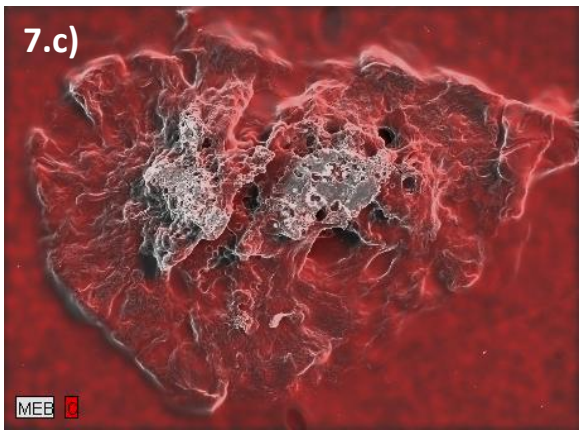
7.c)
MEB C

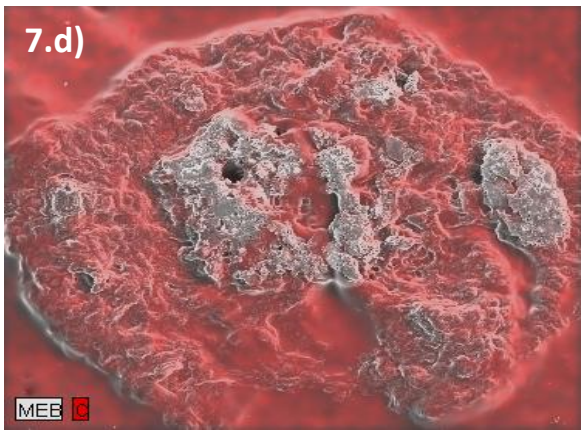
7.d)
MEB C

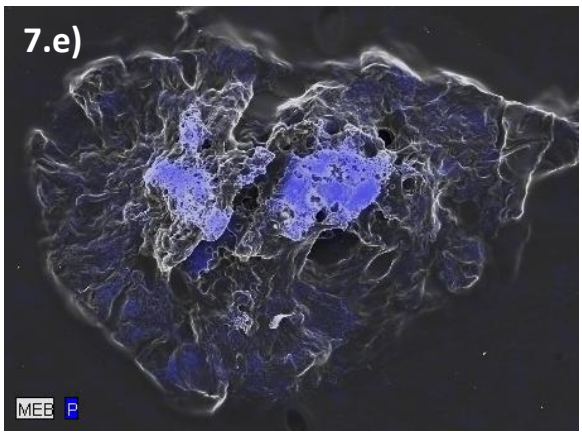
7.e)
MEB P

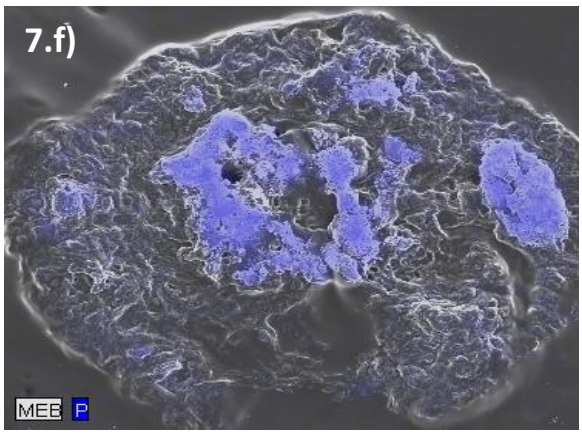
7.f)
MEB P

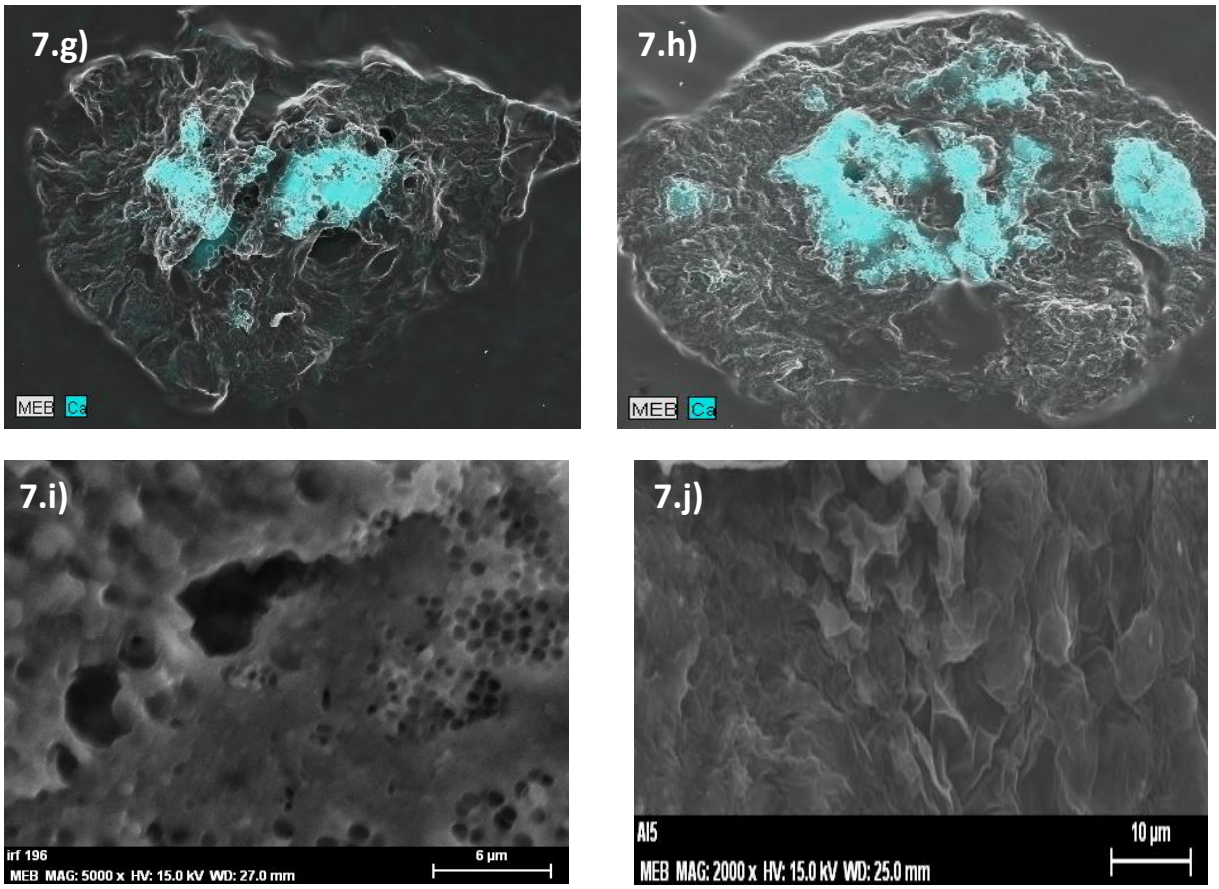

Figure II. 7: 7.a, b) SEM image of a granule central slice; Fig.7.c, d) Carbon (red) scanning with EDX; Fig.7.e, f) P (dark blue) scanning with EDX; Fig.7.g,h) Ca (light blue) scanning with EDX; Fig.7.i, j) granule mineral core SEM images

Figure II.8 shows an external SEM analysis on the granule's surface. EDX probes show a different elemental composition with regards to the mineral core (see table II.2).

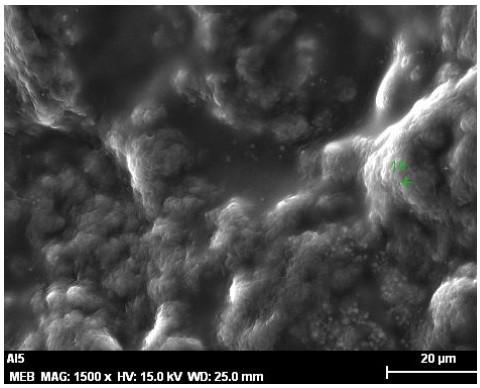

Figure II. 8: SEM image of a granule's surface

Element	External (%w)	Internal (%w)
C	60	18
O	36	35
P	2	10
Mg	0	0
Ca	1	28
K	0	0

Table II. 2: Comparison of the different composition according to the location of the EDX probes (surface of the granule or on the mineral core)

According to table II.2, the most abundant components on average present in the periphery of the granule are carbon and oxygen, both making up the most part of the surface composition. The remainder elements are split between phosphorus, calcium and some traces (not sown) of basically, sulphur. However, calcium and phosphorus are more abundant in the core of the granule, being the former, one of the most abundant elements (almost 30 times more than on the surface), counting up for the 30% in weight. Quantitative analysis over five different samples showed that the Ca/P mean atomic ratio obtained for the mineral precipitate in the core was 1.63 ±0.05, which is quite close to the theoretical one for hydroxyapatite (1.67).

In parallel, scanning analyses on the flocs and supernatant (figure II.9) did not reveal any similar calcium phosphates but some sparse mineral particles with high K, Mg and P content were found (circled in figure II.9.b). These analyses indicated that calcium phosphates were exclusively accumulated in the granules whereas other minerals could be formed in the bulk, e.g. magnesium phosphate, ammonium struvite ($MgNH_4PO_4{\cdot}6H_2O$) or potassium struvite ($KMgPO_4{\cdot}6H_2O$). However, they were detected in much smaller amounts than hydroxyapatite.

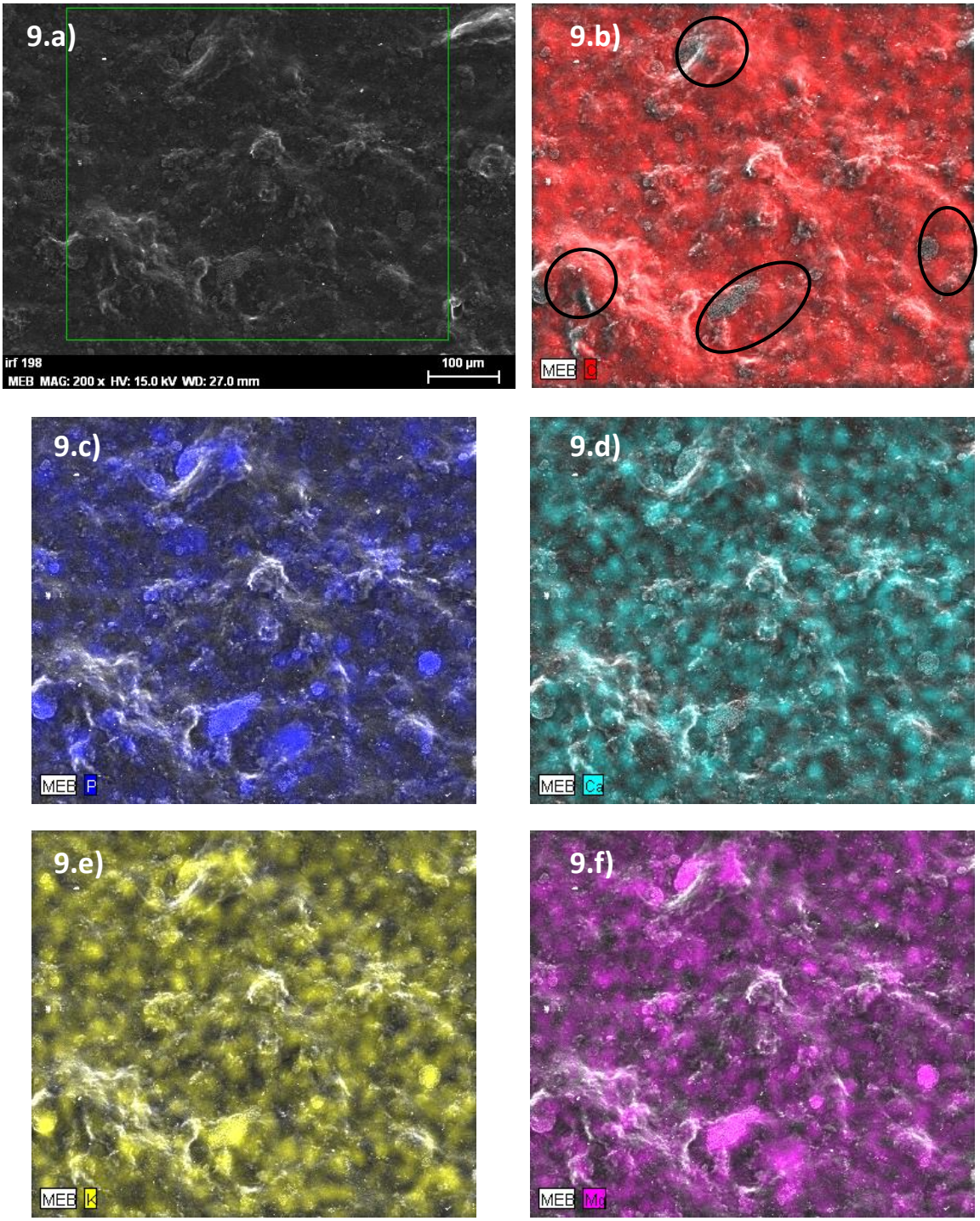

Figure II. 9: a) SEM image of flocs from the GSBR; b) carbon (red) scanning with EDX; c) phosphorus scanning (dark blue) with EDX; d) calcium scanning with EDX probe; e) potassium scanning with EDX; f) magnesium scanning with EDX

II.3.4. XRD analysis

XRD analysis is an efficient tool for distinguishing crystalline minerals from those of amorphous structure, so it was also carried out on some granule samples. Three different preparations of granular samples were tested. Results of two sample analyses (not shown), i.e. a sample of dried pulverized granules and a wet sludge sample, revealed a major peak coinciding with calcium phosphate patterns. However, high noise due to the organic fraction was present, making any interpretation difficult. Thus, a third granular sludge sample was treated to remove the organic matter (described in section II.2.2*)*, leading to the diffractogram presented in figure II.10. A number of distinct rays indicate the presence of crystalline forms. By comparison with reference spectra, most of the peaks, and in particular the bigger ones, coincided with those of the hydroxyapatite ($Ca_5(PO4)_3(OH)$). The remaining minor peaks coincided with whitlockite ($Ca_{18}Mg_2H_2(PO_4)_{14}$). The large central peaks indicate the possible presence of amorphous mineral species.

It should not be forgotten that, for XRD analysis, the sample was heated to 500°C and so some hydroxylation phenomena could have taken place. Considering that hydroxyapatite dehydroxilation does not occur under 800°C (Wang et al., 2004), changes of this mineral in the original sample, due to heating, would not take place. However, in the range of 200-400°C, dehydratation of the lattice and adsorbed water of some other minerals could be possible according to *Kohutova et al.* (2010). The magnesium and phosphorus initially present in organic polymers (polyphosphate) could precipitate in a new form during heating. Despite the fact that XRD again confirmed the major formation of hydroxyapatite, it is still difficult to know whether other intermediates were present or not and, in the case of whitlockite (WHT), it might have been formed during the heating process.

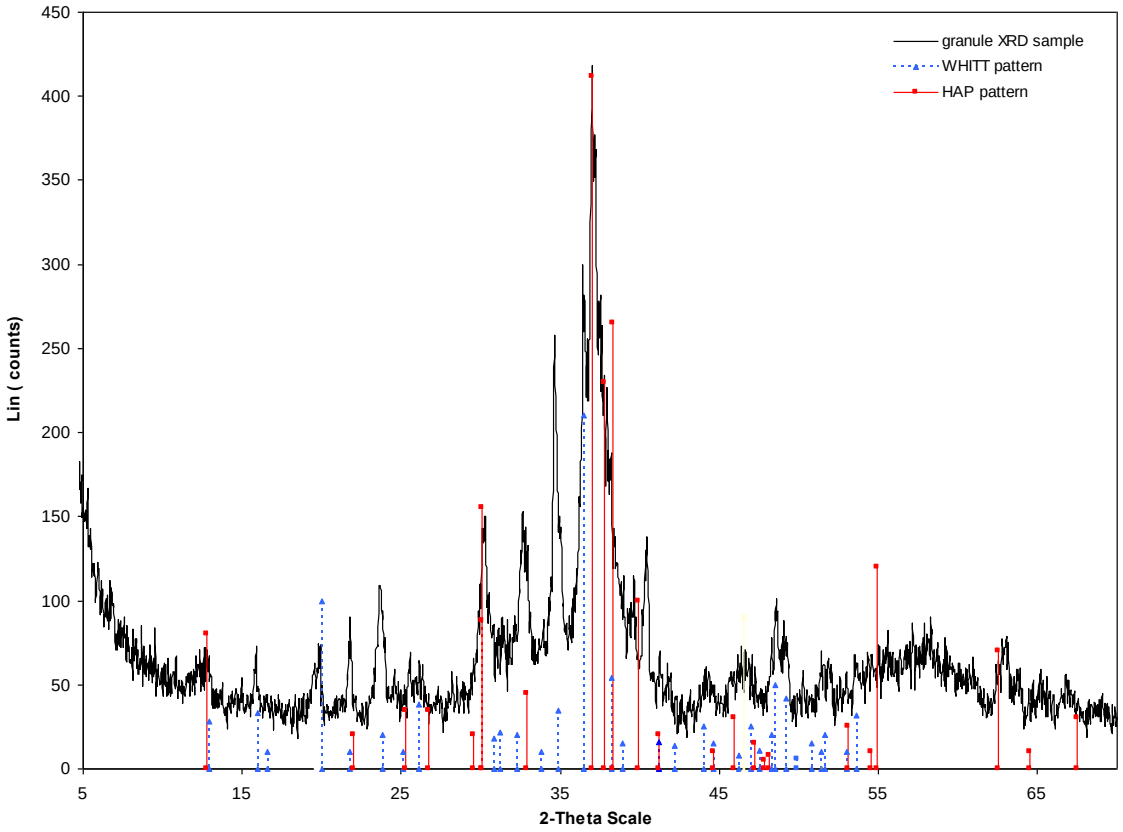

Figure II. 10: XRD diffractogram of a granule sample compared to HAP and WHT pattern.

II.4. DISCUSSION

II.4.1. Hydroxyapatite: a major phosphate mineral in aerobic granules

All the results (Raman spectroscopy, SEM-EDX, and XRD) support the same conclusion: hydroxyapatite (HAP) was the major mineral found inside the phosphorus-rich granules in this study. Both Raman and SEM-EDX analysis allowed calcium phosphate mineral to be identified and XRD analysis confirmed its crystalline form, but also suggested the presence of other amorphous minerals. SEM-EDX analysis in Figs II.7.e and II.7.f, pointed out that P was also present in the organic fraction of the aggregates, probably linked to polyphosphate stored in bacterial biofilm. This last statement may be supported by the fact that Mg and K elements, which are linked to polyphosphate constitution, were also found sparsely in this area. SEM-EDX indicates very reproducible

Ca/P ratios (1.63±0.05) close to that of hydroxyapatite's (1.67), and notably different from other calcium phosphates (e.g. amorphous calcium phosphate: 1.50; hydroxyl dicalcium phosphate: 2; whitlockite: 1.3). Considering that most of the calcium was immobilized with phosphorus (as indicated by SEM-EDX images) with a Ca/P ratio of 1.67 (hydroxyapatite), it is possible to estimate the contribution of precipitation to global P removal. As Ca^{2+} removal yield of 46 % was obtained (0.488 mmol/L), it means that about 0.292 mmolP/L was removed via hydroxyapatite precipitation. This represents about 45% of the total P removal in the process (82% of P was removed which represents 0.68 mmol/L), the rest being explained by biological mechanisms. The precipitation contribution is hence much more significant than those estimated in flocculated sludge (*Haas et al., 1990*). But this is in accordance with the data obtained with granular sludge by *De Kreuk et al. (2005, 2007),* which suggest that P accumulation in EBPR granules can double the accumulation achieved in flocs, because of precipitation.

In the calcium phosphate family, hydroxyapatite (HAP) is commonly considered as the most stable phase and the most insoluble one. According to Ostwald's ripening theory (*Mullen et al., 2001*), precursors such as brushite (DCPD), octacalcium phosphate (OCP), and amorphous calcium phosphate (ACP) contribute to its formation, brushite being the most soluble phase. Hydroxyapatite and brushite were both considered in this study as reference samples but brushite was not detected (Raman). In one sense, our results confirm the first assumption of Maurer et al. (1999) who supposed that hydroxyapatite can be accumulated in EBPR systems. However Maurer et al. (1999) also supposed that HDP was formed as an intermediate without any convincing explanation for that choice, and this assumption is difficult to confirm in our case.

Of all the minerals that could be found in wastewater treatment (*Musvoto et al., 2000*; van *Rensburg et al., 2003*; *Larsdotter et al., 2007*), only a few were expected to precipitate in granular sludge, in particular calcium carbonate (*Ren at al., 2008*; *Wang et al., 2006*), or struvite (*Yilmaz et al., 2007*). Calcium carbonate in calcite form, was previously detected in biological aggregates and aerobic granules (*Ren at al., 2008; Wang et al., 2006*). Due to their competition for calcium (Lin and Singer, 2006) mineral phosphate and carbonate can inhibit each other. According to several authors (*Montastruc, 2003*), pH plays an important role, favoring phosphate precipitation at pH 7-8.5, whereas both carbonates and phosphates co-precipitate at pH 9-11. In our case, absence of calcite could be explained simultaneously by low calcium availability due to hydroxyapatite

formation and inappropriate pH inside the granules. In contrast with the assumption of *Yilmaz et al. (2007)*, no struvite was detected in the granules and struvite precipitation seems to have played a minor role in phosphate immobilization in our study. However, samples were taken at the end of the aerobic period, and it is possible that struvite had been transiently formed in the previous anaerobic phase and afterwards solubilized as ammonia was consumed during nitrification, as could be also suggested with results in figure 9. These last results could raise a question about the transient precipitation of potassium struvite in flocs, but it is difficult to assess, as on the one side, no quantitative analyses had been done; and on the other hand, the analysis scaling-frame was too little compared to a representative sample of the reactor, and several heterogeneities could arise.

II.4.2 Parameters controlling P precipitation in EBPR granular sludge

Supersaturation index calculations (SI) for the different minerals in the supernatant, and for each time of the kinetic cycle, are shown in figure II.11. Saturation index was calculated using the Minteq.v4 default database (PHREEQC, software) with the pH and concentrations measured in the bulk. Struvite saturation index was negative throughout the batch cycle and lessened progressively with ammonia consumption by nitrification. This indicates that the ammonium and magnesium concentrations were too low to cause struvite precipitation in those conditions. Concerning calcium phosphates, the saturation index for brushite and hydroxyl dicalcium phosphate were close to zero, i.e. these minerals were not considerably supersaturated. This suggests that the latter were poorly or very briefly formed, only during the feeding period. SI for amorphous calcium phosphate varied from around 1 to less than 0.5. Finally, the highest value of SI (from 1.7 to 1.2) was obtained for hydroxyapatite, i.e. the most stable phase among the calcium phosphates showed supersaturation conditions throughout the experiment. In addition, for all the compounds studied, SI decreased during the aerobic phase, because phosphate concentration lessened (due to P uptake) and pH decreased (due to nitrification). This result confirms that precipitation of calcium phosphate is more probable during the initial anoxic period, which is in accordance with the tendency observed for calcium (figure II.4).

Additionally, hydroxyapatite precipitate was observed in the core of granules. This means that confined conditions were more favorable for hydroxyapatite formation or

accumulation than conditions in the bulk. Three explanations can be proposed: (1) higher local phosphate concentration, (2) higher local pH and (3) higher retention time for granules. Firstly, higher local phosphate concentration is probably reached during the anaerobic period due to phosphate release by PAO in the internal part of granules. Simultaneously, calcium was also provided during the anaerobic period by means of wastewater feeding. In parallel, observed phosphate release was relatively moderate and would probably have been more significant if precipitation had not occurred. This suggests that feeding anaerobically is a method that encourages P precipitation (this issue will make part of the following chapter). Secondly, pH is obviously an important parameter controlling phosphate precipitation (high pH increases hydroxyapatite supersaturation). Therefore, another possible explanation for hydroxyapatite accumulation in the core of granules is the fact that internal pH can be higher than bulk pH, because of denitrification. A last mechanism is the fact that high retention time of granules encourages the formation of the most stable calcium phosphate (HAP) due to low solubilization rates, whereas other calcium phosphates mentioned before can be transiently produced and resolubilized.

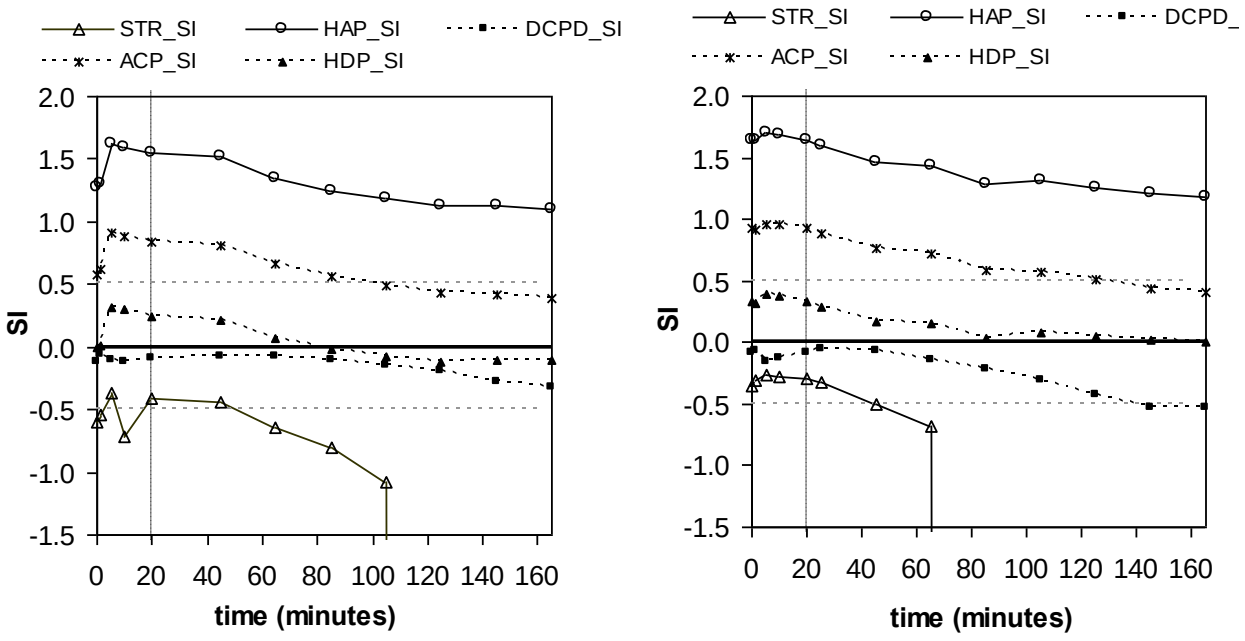

Figure II. 11: a) Saturation Index for several minerals in the bulk during a cycle with weak aerating conditions; b) Saturation Index for several minerals in the bulk during a cycle with strong aerating conditions

More generally, the importance of calcium precipitate depends on influent characteristics. In this work, the range of phosphate concentration was similar to those explored by *Maurer et al. (2000)*. It was higher than those found in conventional domestic wastewater, but lower than those reported for high strength wastewater like agro-food industry waste (*Yilmaz et al., 2007*). However, COD:P feeding ratios were similar to those found for high-strength effluents. Calcium, magnesium, and ammonium concentrations were at moderate levels, similar to those found in domestic wastewater. Comparatively to other studies, pH was relatively high in this work, ranging from 7.8 to 8.8 in a typical SBR cycle. This was due either to bicarbonate stripping (pH was higher at high flow rate) and denitrification, and hence, these two processes clearly encourage hydroxyapatite precipitation.

II.4.3 Advantage of HAP accumulation in granular sludge

Hydroxyapatite is a phosphate compound that is much more stable than bacterial polyphosphate. In EBPR systems, sludge containing polyphosphates needs to be extracted and removed rapidly from the system in order to avoid problems with secondary P release, i.e. the release of phosphorus without the presence of external organic carbon (Wouters-Wasiak et al., 1996). This makes it obligatory to restrict the sludge retention time to a reasonable value, and then anaerobic storage is impossible as phosphate would be released in the liquid phase. In contrast, hydroxyapatite accumulation is advantageous because long retention time for granules is possible, as well as storage before agricultural use. In addition, to our experience (data not presented), granules with a mineral HAP core are very stable and can be easily dehydrated.Finally, induced precipitation in granules seems to be completely compatible with biological reactions. In comparison, one of the reported drawbacks of simultaneous phosphorus precipitation in activated sludge process with calcium (lime) is that precipitation occurs at high pH (e.g. 9), which would be out of the optimal pH range for most biological processes (*Carlsson et al., 1997* ; Arvin, 1979). High reactant excess is also necessary to reach very low P concentration at conventional pH. In the Phostrip® process, lime addition is thus performed on a side stream anaerobic reactor (*Brett et al., 1997*). Here, due to important gradients within granules, it is possible to maintain conditions in the core (favorable for precipitation) which are different from those in the external zone. In contrast with previous experience with flocculated sludge, it is shown in this study that hydroxyapatite accumulation in granular sludge is perfectly

compatible with major biological reactions. Future work will be necessary to find the practical conditions which allow advantage to be taken of this process during the treatment of real wastewater.

II.5. CONCLUSIONS

For the first time, different analyses (Raman, SEM-EDX, XRD) have revealed the nature of phosphorus precipitates in an EBPR granular sludge process.

Raman analysis provided a repetitive pattern over a granule core sample. The four main peaks coincided with those of hydroxyapatite ($Ca_5(PO_4)_3(OH)$). SEM-EDX demonstrated the presence of mineral clusters in the core of granules. These clusters concentrated most of calcium and phosphorus and EDX revealed that Ca/P ratios (1.63 ± 0.05) were close to the ratio of hydroxyapatite. XRD analysis of the mineral fraction of the sludge confirmed that the major mineral present was a crystalline hydroxyapatite, although it probably coexists with other minor amorphous calcium phosphates.

This chapter reveals that hydroxyapatite accumulation is an important phenomenon in the EBPR granular sludge process and merits attention in the future. In the conditions tested, it is estimated that about 45% of the P removal was due to biologically induced precipitation. In that sense, next chapter will focus on the operating conditions which could favor hydroxyapatite accumulation as it could become an interesting way of immobilizing and recycling phosphorus.

II.6. ACKNOWLEDGMENTS AND CONTRIBUTIONS

I would like to give a special mention to J. Wan, E. Mengelle, D. Auban, S. Teychene, S. Julien, A. Aguirre, N. Estime and B. Bouillot for their patience and helpful contribution in this work.

II.7. REFERENCES

Adav S. S., Lee D.-J., Show K.-Y. and Tay J.-H. (2008). *Aerobic granular sludge: Recent advances*. Biotechnology Advances 26(5): 411-423.

Arvin, E. Arvin (1979). *The influence of pH and calcium ions upon phosphorus transformations in biological wastewater treatment plants.* Prog. Wat. Technol. 1, 19–40.

Barbillat (2009). *Spectroscopie Raman. Techniques de l'ingénieur*. P2865-1.

Baur R., Prasad R., Britton A. (2008). *Reducing Ammonia and Phosphorus Recycle Loads by Struvite*

Harvesting. Ostara Nutrient Recovery Processes Brochure for WEFTEC 2008.

Bellier N., Chazarenc F. and Comeau Y. (2006). *Phosphorus removal from wastewater by mineral apatite*. Water Research 40(15): 2965-2972.

Bogaert H., Vanderhasselt A., Gearney K., Yuan Z., Thoeye C. and Verstraete W. (1997). A *new sensor based on pH effect of denitrification process.* Journal of Environment Engineering. 123: 884-891.

Brett, S., Guy, J., Morse, G.K. and Lester, J.N. (1997). *Phosphorus Removal and Recovery Technologies*, Selper Publications, London.

Burriel F., Lucena F., Arribas S., Hernández J. (1985) *Química Analítica Cualitativa*. Ed. Thompson. 18th edition.

Carlsson H., Aspegren H., Lee N. and Hilmer A. (1997). *Calcium phosphate precipitation in biological phosphorus removal systems*. Water Research 31(5): 1047-1055.

Cloete T.E., Oosthuizen D.J.(2001). *The role of extracellular polymers in the removal of phosphorous from activated sludge*. Wat. Res. Vol. 35, No. 15, pp. 3595–3598,

Daumer M.-L., Béline F., Spérandio M. and Morel C. (2008). *Relevance of a perchloric acid extraction scheme to determine mineral and organic phosphorus in swine slurry.* Bioresource Technology 99(5): 1319-1324.

De-Bashan L. E. and Bashan Y. (2004). *Recent advances in removing phosphorus from wastewater and its future use as fertilizer (1997-2003).* Water Research 38(19): 4222.

De Kreuk M.K., J.J. Heijnen, Van Loosdrecht (2005). *Simultaneous COD, nitrogen and phosphate removal by aerobic granular sludge.* Biotechnology and Bioengineering. 90(6) 761-769

De Kreuk M.K., van Loosdrech (2007). *Formation of aerobic granules with domestic sewage.* Environment Engineering. 132(1): 694-697.

Demirel B., Yenigun O. and Onay T. T. (2005). *Anaerobic treatment of dairy wastewaters: a review*. Process Biochemistry 40(8): 2583-2595.

Etterer T. and Wilderer P.A. (2001). *Generation and properties of aerobic granular sludge*. Water Science and Technology. 43 (3): 19-26

Giesen A. (1999). *Crystallization Process enables environment friendly phosphate removal at low cost.* Environmental Technology. 20:769-775.

Haas D.W., Lötter DW., Dubery IA. (1988). *An evaluation of the methods used for the determination of ortho-phosphate and total phosphate in activated sludge extracts*. Water Science 15(4), 257-260.

Hollas J. Michael (1996). *Spectroscopie*. Ed. Dunod (3rd edition.)

Hu Z.-r., Wentzel M. C. and Ekama G. A. (2002). *Anoxic growth of phosphate-accumulating organisms (PAOs) in biological nutrient removal activated sludge systems.* Water Research 36(19): 4927-4937.

Ivleva N. P., Wagner M., Haisch C., Niessner R. and Horn H. (2009). *Combined use of confocal laser scanning microscopy (CLSM) and Raman microscopy (RM): Investigations on EPS - Matrix*. Water Research 43(1): 63.

Jardin N. and Johannes Pöpel H. (1996). *Influence of the enhanced biological phosphorus removal on the waste activated sludge production.* Water Science and Technology 34(1-2): 17.

Katsuura H. (1998). *Phosphate recovery from sewage by granule forming process (full scale struvite recovery*

from a sewage works at Shimane Prefecture, Japan). In International conference on phosphorus recovery from sewage and animal waste, Warwick University, UK.

Kohutova A., Honcova P., Podzemna V., Bezdicka P., Vecernikova E., Louda M. and Seidel J. (2010). *Thermal analysis of kidney stones and their characterization.* Journal of Thermal Analysis and Calorimetry 101(2): 695-699.

Larsdotter K., J. La Cour Jansen, G. Dalhammar (2007). *Biologically mediated phosphorus precipitation in wastewater treatment with microalgae.* Environmental Technology (28) 953:960.

Lemaire R. (2007). *Development and fundamental investigations of innovative technologies for biological nutrient removal from abattoir wastewater*. Ph.D Thesis. University of Queensland, Australia.

Li Y. and Liu Y. (2005). *Diffusion of substrate and oxygen in aerobic granule.* Biochemical Engineering Journal 27(1): 45-52.

Lin Y.P., Singer P.C. (2006). *Inhibition of calcite precipitation by ortho-phosphate: speciation and thermodynamics considerations.* Geochimica et Cosmochimica Acta 70 (2006) 2530–2539

Liu Y. and Tay J.-H. (2004). *State of the art of biogranulation technology for wastewater treatment*. Biotechnology Advances 22(7): 533-563.

Maurer M., Abramovich D., Siegrist H. and Gujer W. (1999). *Kinetics of biologically induced phosphorus precipitation in waste-water treatment.* Water Research 33(2): 484-493.

Mostastruc L. (2003). *Modélisation et optimisation d'un réacteur en lit fluidisé de déphosphatation d'effluents aqueux.* Ph.D. Thesis at INPT and UPS Toulouse III.

Montastruc L., Azzaro-Pantel C., Biscans B., Cabassud M. and Domenech S. (2003). *A thermochemical approach for calcium phosphate precipitation modelling in a pellet reactor.* Chemical Engineering Journal 94(1): 41-50

Morgan H., R. M. Wilson, J. C. Elliott, S. E. P. Dowker, P. Anderson. (2000). *Preparation and characterisation of monoclinic hydroxyapatite and its precipitated carbonate apatite intermediate.* Biomaterials, 21 (6) : 617-627

Morgenroth E., Sherden T., van Loosdrecht M.C.M., Hijnen J.J., and Wilderer P.A. (1997). *Aerobic Granular sludge in a sequencing batch reactor.* Water Research. 31(12): 3191-3194.

Mullen, J.W., (2001). *Solutions and Solubility. Crystallization* (4th ed.). pp. 86‑34.

Münch EV., K. Barrm. 2001. *Controlled struvite crystallisation for removing phosphorus from anaerobic digester sidestreams.* 35(1): 151-159.

Musvoto E. V., Wentzel M. C. and Ekama G. A. (2000). *Integrated chemical-physical processes modelling -II. simulating aeration treatment of anaerobic digester supernatants.* Water Research 34(6): 1868-1880.

Ohlinger K.N., Young T.M., Shroeder E.D. (1998). *Predicting struvite formation in digestion*. Water Research. 32 (12): 3607-3614.

Pambrun V.(2005). *Analyse et modélisation de la nitrification partielle et de la précipitation concomitante du phosphore dans un réacteur à alimentation séquencé.* INSA (Toulouse)

Pandolfi D., Pons M.N., da Motta M. (2007). *Characterization of PHB storage in activated sludge extended filamentous bacteria by automated colour image analysis.* Biotechnol. Lett. 29: 1263-1269.

Panswad T., Tongkhammak N., Anotai J. (2007). *Estimation of intracellular phosphorus content of*

phosphorus-accumulating organisms at different P:COD feeding ratios. Journal of Environmental Management, 84(2) :141-145.

Parkhurst D.L., Thorstenson D.C., Plummer L.N.. (1980). PHREEQC - A *computer program for geochemical calculations*. U.S. Geol. Surv. Water Resour. Invest. Rep. 80(96), 210-219.

Rahman R N, Ghaza F M, Salleh A B, et al. (2006). *Biodegradation of hydrocarbon contamination by immobilized bacterial cells.* Journal Microbiology 44(3), 354-359.

Ren T.-T., Liu L., Sheng G.-P., Liu X.-W., Yu H.-Q., Zhang M.-C. and Zhu J.-R. (2008). *Calcium spatial distribution in aerobic granules and its effects on granule structure, strength and bioactivity*. Water Research 42(13): 3343-3352.

Saidou H., Korchef A., Ben Moussa S., Ben Amor M. (2009). *Struvite precipitation by the dissolved CO2 degasification technique: impact of the airflow rate and pH.* Chemosphere. 74 (2): 338-343.

Seckler MM., Bruinsma OSL., van Rosmalen GM. (1996). *Phosphate Removal in fluidized bed I. Identification of physical processes.* Water Research. 30(7): 1585-1588.

Shu L., Schneider P., Jegatheesan V. and Johnson J. (2006). *An economic evaluation of phosphorus recovery as struvite from digester supernatant.* Bioresource Technology 97(17): 2211-2216.

Skoog, Hoeller, Nieman (2003). *Principes d'analyse instrumentale.* Ed. de Boeck (5th edition).

Snoeyink V. L. and Jenkins D. (1980) Water Chemistry. John Wiley and Sons, New York.

Suzuki K., Tanaka Y., Kuroda K., Hanajima D., Fukumoto Y., Yasuda T. (2006). *The technology of phosphorus removal and recovery from swine wastewater by struvite crystallization reaction*. Bioresource Technology 96(14), 1544-1550

Van Rensburg P., Musvoto E. V., Wentzel M. C. and Ekama G. A. (2003). *Modelling multiple mineral precipitation in anaerobic digester liquor*. Water Research 37(13): 3087.

Wan J. (2009). *Interaction entre l'élimination des polluants azotées et la formation des granules aérobies en réacteur biologique séquencé*. PhD thesis, INSA (Toulouse).

Wan J. and Sperandio M. (2009). *Possible role of denitrification on aerobic granular sludge formation in sequencing batch reactor.* Chemosphere 75(2): 220-227.

Wan J, Bessière Y., Spérandio M. (2009). *Alternating anoxic feast/aerobic famine condition for improving granular sludge formation in sequencing batch airlift reactor at reduced aeration rate.* Water Research, 43(20): 5097-5108

Wang T., Dorner-Reisel A. and Müller E. (2004).*Thermogravimetric and thermokinetic investigation of the dehydroxylation of a hydroxyapatite podwer.* Journal of the European Ceramic Society, 24(4): 693-698.

Wang H.L., Yu G.L., Liu G.S., Pan F. (2006). *A new way to cultivate aerobic granules in the process of paper-making wastewater in a sequencing batch reactor*. Biochemical Engineering. 28(11): 99-103.

Wouters-Wasiak K., Heduit A, Audic J.M. (1996). *Consequences of an occasional secondary phosphorus release on enhanced biological phosphorus removal.* Water Research Comission Review, 22(2):91-96.

Yilmaz G., Lemaire R., Keller J., Yuan Z. (2007). *Simultaneous Nitrification, Denitrification and Phosphorus Removal from Nutrient-rich Industrial Wastewater Using Granular Sludge*. Biotechnology and Bioengineering. 100(3): 529-541.

Zhu G., Peng Y., Wu S., Wang S., Xu S. (2007). *Simultaneous nitrification and denitrification in step feeding*

biological nitrogen removal process Journal of Environmental Sciences, (9:19) 1043-1048

CHAPTER III:

STABILITY AND PERFORMANCES OF TWO GSBR OPERATED IN ALTERNATING ANOXIC/AEROBIC OR ANAEROBIC/AEROBIC CONDITIONS FOR NUTRIENT REMOVAL

In this chapter, two aerobic hybrid GSBRs have been compared, working with anoxic/aerobic and anaerobic/aerobic cycles, respectively. Carbon and nutrient removal (N and P) performances will be assessed in this chapter, as well as microbially induced phosphorus precipitation.

This chapter corresponds to an article entitled: "Stability and performances of two GSBRs operated in alternating anoxic/aerobic or anaerobic/aerobic conditions for nutrient removal" (recently accepted in Biochemical Engineering Journal: BEJ-D-11-00811R1) and constitutes a common chapter of two dissertations carried out at LISBP by Ahlem Filali and Angela Mañas.

III.1. INTRODUCTION

The aerobic granular sludge process has been proposed as a promising approach to biological wastewater treatment (De Kreuk et al., 2007). Thanks to their dense structure, aerobic granules have very good settling properties, allowing high biomass retention in the bioreactor. This enables the process to withstand high-strength wastewater loads and results in a small footprint process in comparison to conventional floccular activated sludge systems (Morgenroth et al., 1997, Zheng et al., 2005). Besides, the size and density of granules allow maintaining simultaneous nitrification denitrification and phosphorous removal, i.e. SNDPR (De Kreuk et al., 2005, Lemaire et al., 2008, Yilmaz et al., 2007). However the operating conditions which could guaranty stability of performances and physical properties of aerobic granular sludge, still need further consideration. Although aerobic granulation has been claimed successfully for real wastewater treatment (Liu et al., 2010), the bottleneck of this process is the instability and loss of granules' properties that several actors have reported over the last decade (Coma et al., 2010; Liu et al., 2010; Nor-Anuar et al., 2012) . This drawback is still more relevant among real sewage compared to lab-scale results carried out with purely acetate-fed granules (Dangcong et al., 1999; Coma, 2011). The operating conditions and the reactor system choice, have also an important influence over the development of unstable sludge properties. e.g., SBR reactors have been reported to maintain stable granules for longer operating periods than continuous flow systems (CFR), in spite of the relative low installation costs of the former (Chen et al., 2009).

Different operating parameters have been identified regarding the formation of aerobic granules in aerobic sequenced batch systems, such as the aeration rate, substrate feeding mode, organic loading rate, settling time and cycle operation time (Liu and Tay., 2002; Moy et al., 2002; Liu et al., 2004; Mc Swain et al., 2004 ; Qin et al., 2004). In granular sludge sequencing batch reactors (GSBR) aeration rate plays two major roles: first, it imposes the hydrodynamic conditions in the reactor and secondly, it controls the oxygen mass transfer in the aggregates. High aeration rate was considered to provide high shear force, eroding the surface of granules; as well as to stimulate bacterial strains to secrete more extracellular polymeric substances (EPS) for enhancing structural integrity; to reduce substrate transfer resistance in the liquid boundary layer at the granule surface and to provide enough oxygen for organic substrate degradation (Liu and Tay., 2002; Tay et al., 2004). Different studies brought out that a high aeration rate (expressed by the

superficial upflow velocity, SAV) accelerates the formation of stable aerobic granules, either by promoting fast-growing microorganisms, secreting more EPS or by eroding filamentous bacteria (Liu and Liu, 2006; Lee et al., 2010). Meanwhile, Beun et al (1999) showed that smooth and stable granules could be obtained only with a SAV above 2.0 $cm \cdot s^{-1}$, and in the same line, Tay et al. (2001) reported a minimal of SAV=1.2 $cm \cdot s^{-1}$. Hence, the development of stable aerobic granules in pure aerobic systems is limited because of the high energy demand required for aeration and because efficient nitrogen and phosphorus removal requires the presence of anaerobic or anoxic and aerobic conditions (Tsuneda et al., 2006).

Both alternating anoxic/aerobic and anaerobic/aerobic conditions have been reported to be advantageous for granulation (Wan et al., 2009). Possible explanations for this could be the fact that conversion of readily biodegradable COD to internal stored biopolymers limits the substrate utilization rate during aerobic phase (Van Loosdrecht et al., 1997) or that anoxic growth inside the granule improves heterotrophic growth in the core and thus, improving the density of the aggregates (Wan et al., 2009 and 2010). It appears that alternating a non-aerated feast period followed by an aerated famine period, encourages the selection of slow-growing bacteria (e.g. nitrifiers, Glycogen Accumulating Organisms -GAOs-), being supposed to be positive for the densification of bio-aggregates (Liu et al., 2004). Indeed, the work of Wan et al., (2010) showed that the strategy of feast/famine regime allowed the formation of stable aerobic granules and the simultaneous nitrification denitrification (SND) at the reduced air flow rate of SAV =0.6 cm s^{-1}.

However, in sights of applying the aerobic granular process for treating dairy and cheese wastewater in the future, a preliminary study of the introduction of a feast anaerobic/famine aerobic phase in a GSBR has been carried out in lab-scale. On the other hand, alternating anaerobic/aerobic conditions has been widely reported to promote internal biopolymers storage and to enhance biological phosphorus removal by polyphosphate-accumulating organisms –PAOs-(Levin and Shapiro, 1965; Mino et al., 1995; Janssen et al., 2002). On the other hand, the most part of nitrogen coming from cheese wastewater is in form of ammonium rather than nitrate.

Therefore, the aim of this study is to compare the effect of alternating anoxic/aerobic and anaerobic/aerobic conditions on the performances and stability of an aerobic granular sludge process for the simultaneous carbon, nitrogen and phosphorous

removal. For this purpose, two reactors were followed in parallel, fed with a mixture of different organic substrates and both operated with similar aeration rates. Thus, first reactor (R1) was operated with anoxic/aerobic cycles whereas, the second one (R2), was operated with alternating anaerobic/aerobic conditions. Processes performances as well as the microscale structure of granules were investigated in both reactors.

III.2. MATERIAL AND METHODS

III.2.1. Reactor operating conditions:

The experimental set-up included two geometrically identical Sequencing Batch Airlift Reactors (SBAR) each with a working volume of 17 L (internal diameter =15 cm, total height =105 cm, H/D ratio = 7). Both reactors were inoculated with the same concentration of a stabilized hybrid sludge (containing both flocs and granules) cultivated with alternating anoxic/aerobic conditions. The initial MLSS and MLVSS concentrations were of 19.5 g L^{-1} and 13.1 g·L^{-1}, respectively. The initial SVI was of 22 mL·g^{-1} $_{MLSS}$. Reactor R1 was operated with alternating anoxic/aerobic conditions, whereas the second one (R2) was operated with alternating anaerobic/aerobic conditions and seeded from R1 Each reactor was operated sequentially with a cycle time of 4 h including: 15 min of feeding; 20 min of anoxic or anaerobic phase induced by nitrogen gas blowing; 145 min of aerobic reaction; 30 min settling and 30 min discharge (with a volumetric exchange ratio of 47%). The aeration rate in both reactors was close with a superficial air upflow velocity (SAV) of 1.1 cm s^{-1} and 0.94 cm s^{-1} for R1 and R2, respectively. Both reactors were fed at the bottom of the column as aeration was stopped (static fill). The feed consisted of a synthetic substrate with the following composition: COD of 1000 mg·L^{-1} (consisting a 25 % each of glucose, acetate, propionic acid and ethanol contribution); [PO_4^{3-}] = 30 mgP/L , [Ca^{2+}] = 46 mg L^{-1}, [HCO_3^-] = 100 mg L^{-1}, [$MgSO_4 \cdot 7H_2O$] = 12 mg L^{-1}, [NH_4^+] = 50 mg_N L^{-1}. The ratio COD/N-NH_4^+ maintained was of 20. Nitrate was dosed in R1 in order to maintain anoxic conditions after feeding ([NO_3^-] = 100 mg_N L^{-1}). The pH and DO probes were installed online and the data was gathered every 30 s by computer. pH naturally fluctuated during a reactor cycle from 7.5-9 and from 7-8.5 in R1 and R2, respectively. The temperature was maintained at about 20 ± 2 °C with a water jacket. The reactor performance was monitored through weekly cycle studies, where samples were analyzed at regular intervals during a SBR cycle. Table III.1 summarizes the main operating conditions of both reactors.

Due to annual closure, the supply of influent to the reactors was interrupted for two consecutive weeks and the cycle of operation was modified: the new 2-h cycle consisted of 15 min aeration and 105 min settling. This period (from day 105 to day 120) is referred to as the "starvation period".

Table III. 1: Operating conditions of both reactors

Parameter	R1	R2
Volumetric exchange ratio (%)	47	47
Hydraulic retention time (h)	8.5	8.5
Organic Loading Rate (kg COD·m^{-3}·d^{-1})	2.8	2.8
Ammonia loading rate (kgN-NH_4·d^{-1}·m^{-3})	0.14	0.14
Nitrate loading rate (kg N-NO_3·d^{-1}·m^{-3})	0.28	0
Phosphorus loading rate (Kg P-PO_4·d^{-1}·m^{-3})	0.08	0.08
Superficial upflow velocity of N_2 (cm·s^{-1})	1.1±0.1	0.6±0.1
Superficial upflow velocity of air (cm·s^{-1})	1±0.1	1±0.1
Temperature (ºC)	20±2	20±2
pH (not regulated)	7.5-9.2	7.2-8.5

III.2.2. Analytical characterization of the liquid and solid phases

Physico-chemical analyses were conducted according to standard methods (AFNOR, 1994) for COD (NFT 90-101), MLSS (NFT 90-105) and MLVSS (NFT 90-106). NO_2^-, NO_3^-, PO_4^{3-}, NH_4^+, Ca^{2+}, K^+, Mg^{2+} concentrations were analyzed by Ion Chromatography (IC25, 2003, DIONEX, USA), prior filtering the samples through a 0.2 µm pore-size acetate filters. The Sludge Volume Index (SVI) was measured in the reactor after 30 min of settling. Microscopic observations of sludge samples were performed with a Biomed-Leitz® binocular photonic microscope. XRD analyses of the mineral fraction of R1 and R2 granules were performed with a BRUCKER D5000 diffractometer, with a cobalt tube scattering from 4-70° in 2θ. Samples were taken from both reactors at the end of the aerobic phase, and they were dried and calcined at 500°C for 2 hours before the analysis in order to remove the organic fraction likely to interfere the spectrum.

The proportion of granules by mass and by volume was estimated using Equations III.1 and III.2 respectively:

$$Percentage\ of\ granules\ by\ mass = \frac{MLSS_{granule} 100}{MLSS_{hybrid\ sludge}} \qquad \text{Equation III.1}$$

$$Percentage\ of\ granules\ by\ volume = \frac{V_{granule}.100}{V_{hybrid\ sludge}}$$ Equation III.2

Where MLSSgranule and MLSShybrid sludge are the mixed liquor suspend solids in granules and hybrid sludge respectively. In order to assess the MLSS of granules, sieving at 315 µm was performed as described in Filali et al, (2012). $V_{granule}$ and $V_{hybrid\ sludge}$ represent the apparent volume of granules and hybrid sludge, respectively, in the reactor after 30 minutes of settling.

III.2.3. Microbial characterization

III.2.3.1 FISH probing

Floc and granule samples were fixed as described in Filali et al. (2012). Filamentous bacteria that had developed at the surface of granules were detached with a sterile scalpel and subjected to the same procedure as the flocs. In situ hybridization was performed according to the standard hybridization protocol (Amann et al., 2001). The fluorescently labelled oligonucleotide probes used were as follows: Nso190 and Nso1225 (labelled with FITC) for AOB (Mobarry et al., 1996), Nit3 (labelled with Cy3) for Nitrobacter spp. (Wagner et al., 1996) and Ntspa662 (labelled with Cy3) for Nitrospira spp. (Daims et al., 2000). DAPI (4',6-diamidino-2-phenylindole, dihydrochloride) was used to stain all the DNA-containing organisms. To avoid non-specific staining, unlabelled competitor probes CNit3 and CNtspa662 were added with equimolar amounts of Nit3 and Ntspa662, respectively.

Fluorescent in situ hybridization images were collected with a confocal laser scanning microscope (LEICA SP2, DMRXA2, Germany) using an argon laser (488 nm) for FITC excitation, a helium-neon laser for Cy3 (543 nm) and a diode laser for DAPI (405 nm). Their fluorescence was detected at 498–550 nm, 571–630 nm or 415–450 nm respectively. To obtain images of half-granule sections, 10 to 20 (depending on the size of the granule) overlapping, consecutive images of 1024x1024 pixels were acquired using a 16X oil objective. The final composite image of the granule section was then reconstructed

from all the individual images collected using INKSCAPE open source scalable vector graphics. Images of bacterial clusters were acquired using a 100X oil objective.

III. 2.3.2. PHB staining

Poly-hydroxy butyrate (PHB) staining was carried out using a protocol adapted from Pandolfi et al. (2007). Samples were previously cut at 100µm thickness and spread over a glass plate. Once air-dried, samples were dumped in a solution of black of Sudan during 5 minutes, and then, rinsed with ethanol at 70% vol. Once the sample dried, safranine was dropped covering the whole sample for a contact reaction time of 5 seconds. Afterwards, samples were dried again prior rinsing with distillate water, and observed with the optical microscopy (Biomed-Leitz®). Safranine was used to show up the cytoplasmic membranes in red/pink (bacteria cells), whereas Sudan black stained in blue/black the PHB volutins.

III.3. RESULTS

III.3.1. Performances stability

Fig III.1 and Fig III.2 show respectively the evolution of solids concentration and removal efficiencies of reactors R1 and R2 during the whole operation. Both reactors were initially started with similar seeds, and showed the same suspended solids concentration, i.e. 19.5 gTSS L^{-1} and 13.1 gVSS L^{-1}, as well as very good settling properties (SVI was initially close to 22 $mL \cdot g^{-1}$).

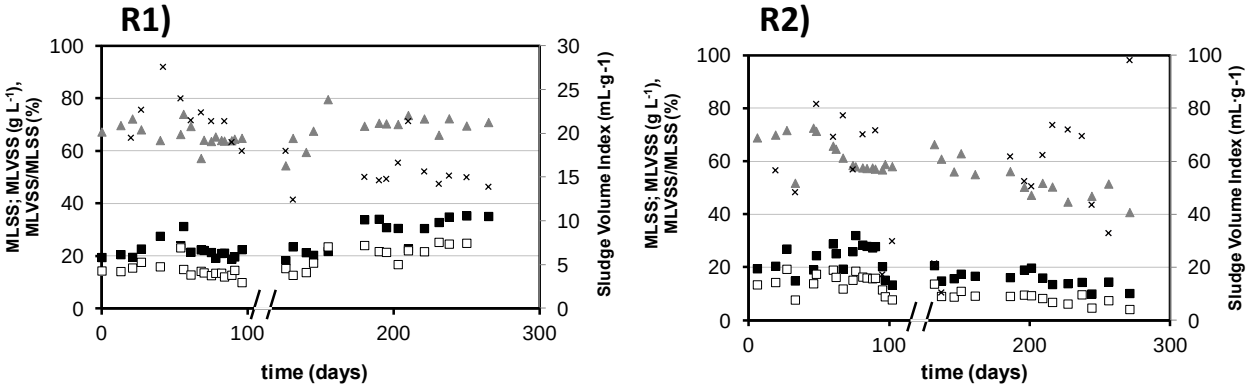

Figure III. 1: Evolution of suspended solids during the reactors run period (■) MLSS; (□) MLVSS; (▲) MLVSS/MLSS and (X) SVI, in R1 and R2. *Cutting off the time axis corresponds to the endogeneous phase (day 105)*

After about 50 days of run and then during the entire period of study (300 days), performances were very stable in the anoxic/aerobic reactor (R1). The removal yields of soluble COD, ammonia and total nitrogen were of 96%, 100% and 89%, respectively. The removal yields of phosphorous gradually increased and stabilized at 45%. Figure III.1 shows that MLSS and MLVSS first stabilized respectively around 21±1.5 and 13.8±1.2 and then, gradually accumulated in the reactor up to 35 gTSS L^{-1} and 25 gVSS L^{-1}, with a ratio VSS/TSS of 65-70%. The suspended solids accumulation was also linked to a decrease of SVI (16 ± 2 mL·g^{-1}). Performances were stable and it is interesting to point out that after a starvation period (without feeding) of 15 days, the reactor was easily started again and it took less than one week for performances to be fully recovered.

Concerning the second reactor (R2), performances initially declined and neither the sludge concentration nor the reactor performances were fully stabilized during the entire study. The MLSS concentration initially increased up to 32 g L^{-1} but then progressively decreased up to less than 10 g·L^{-1}. The sludge volume index (SVI) fluctuated around 60 ± 20 mL g^{-1} during the first 100 days and then increased up to 90 mL·g^{-1}. The COD removal efficiency varied between 90 to 95%, whereas ammonia and total nitrogen removal yields fluctuated from 60% to 100% (mean values of 86% and 84% respectively). Phosphorus removal oscillated from 10 to 80% with a mean efficiency of 42%. In contrast with the first reactor, it was observed that starvation period (15-days) provoked a very significant loss of granules in this second reactor (not shown). The MLVSS/MLSS ratio in this second reactor was decreasing during the whole period, meaning that i) Mineral content increased in this reactor and/or ii) VSS/TSS ratio diminished according to a decrease of MLVSS in the reactor (from 20 g·L^{-1} to 15 g·L^{-1}).

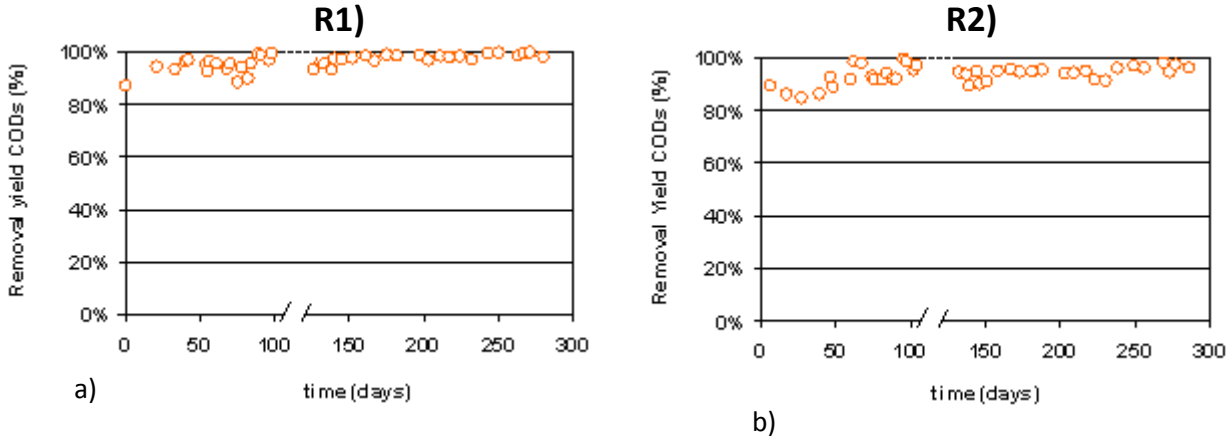

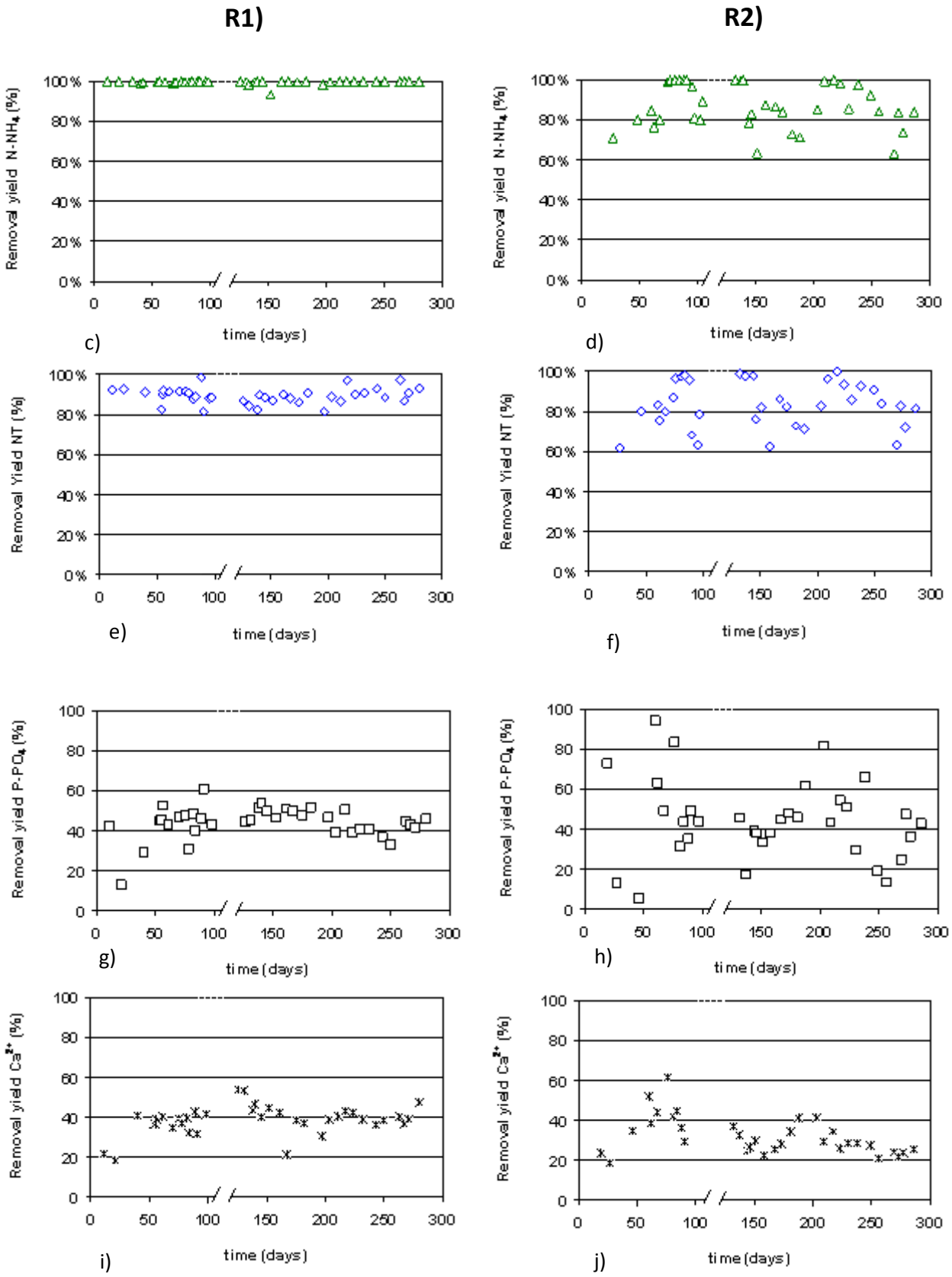

Figure III.2: Evolution of removal yields in R1 (left) and R2 (right) of (○) CODs, (△) N-NH₄, (◇) TN, (□) P-PO₄ and (✳) Ca²⁺. *Cutting off the time axis corresponds to the idle phase (day 105).*

Figure III. 3 plots VSS and the MF/TSS ratio in the mixed liquor of R2. Three different trends can be observed depending on the biomass concentration: for 10 to 20 g/L of VSS, the mineral fraction is almost constant around 40%; at 10 mg/L of VSS, there is a sharp rise of mineral fraction in granules, leading to high mineral accumulation, and finally, a drop of 10 to 5 mg/L of VSS, implies a proportional rise of 20% of mineral content. This effect is noticeable during from day 50-100 (Figure III.1), where a VSS/TSS diminished whilst VSS increased. After that period, we can assume that the drop of VSS/TSS ratio in R2 relays on the decrease of VSS.

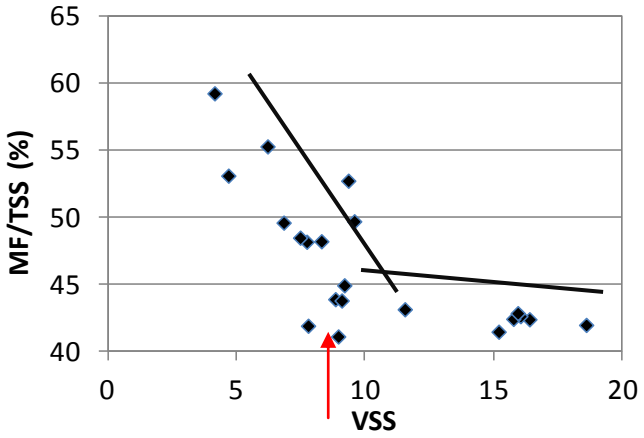

Figure III. 3: Relation between mineral fraction (%) and VSS (g/L) in R2.

III.3.2. Evolution of sludge properties

As both reactors were initially seeded with a mixture of granules and flocs, the evolution of granules percentage in both reactors is an interesting indicator of sludge properties (Figure III.4). A slight enrichment in granules was observed in R1, granule percentage increasing from 60 to 80% of total volume constituting more than 90% of the mass. Granule size also slightly increased (from 1.0 to 3.3 mm). Concomitantly, a part of flocs were maintained during all the study.

In contrast, in R2, sludge properties evolved in a different way. From day 33, an increase of granule fraction by mass was observed, together with a decrease of their fraction by volume, which clearly indicates a strong modification of the aggregate properties and floc washout. First, granules became rapidly bigger (from 2 to 4 mm of diameter) due to a filamentous (fluffy) growth on the surface of the granules. Granular sludge occupying a higher volume in the reactor after settling lead to a floc wash-out and granular sludge proportion initially increased. However progressively, filamentous

suspended growth was also observed generating flocs with poor settling properties. Whilst filamentous bacteria poorly contributed to the total mass of sludge compared to granules, they affected considerably sludge settling (SVI rising up to 90 $mL \cdot g^{-1}$).

As both reactors were seeded initially with a mixture of flocs and granules (being more important the contribution of granules (82% in MLSS or 62% in volume), figure III.4 shows the evolution of granule proportion during the study.

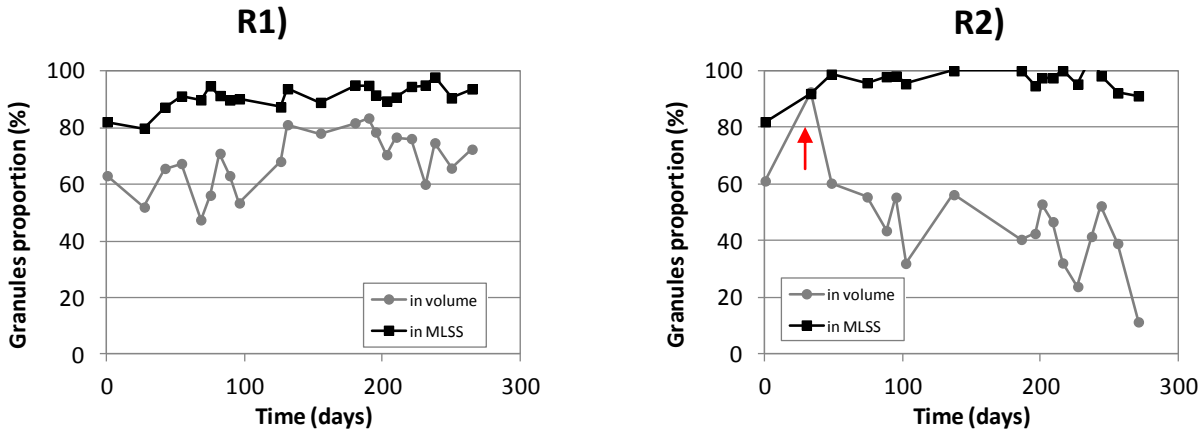

Figure III.4: Evolution of the proportion of flocs (■) and granules (■) in MLSS (a, b) and in volume (c, d) of the hybrid sludge in both reactors

Whereas in R1, the proportion of granules in mass remained constant at about 90%, its contribution in volume raised, probably due to the growth of granules in size (1.0 -3.3 mm), leading to a slight loss of flocs.

In R2, flocs were almost completely washed out on day 33 (indicated by an arrow in figure III.4). Since that day, the proportion of granules in mass and in volume showed different trends: the proportion of flocs decreased in mass, but increased in volume. Moreover, since that day, a floc washout could have taken place, as during that period, the MLSS in the effluent increased up to 300 mg/L. This could be explained, on the one hand, by the fast growth of size that was observed in the granules, and on the other hand, because of the sludge properties changes that were observed. In fact, filamentous growth started to colonize such granules, being responsible in part of their rapid growth of size. However, filamentous bacteria did not contribute in mass as they did conventional flocs, but their effect was noticed in the drop of granule proportion in volume.

Figure III.5 shows the correlation between the MLSS concentration and the percentage of granules in both reactors. It indicates that the MLSS globally increased with the proportion of the volume occupied by the granules and the diminution of suspended biomass growth.

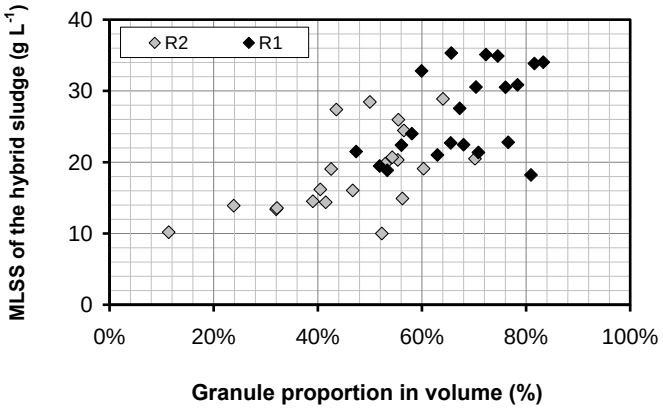

Figure III. 5: Relationship between the MLSS concentration and the granule percentage by volume

Microscopic observations in figure III.6 show that granules from R1 presented a smooth round-shaped surface similar to initial seeded granules in R2 (Figure III. 6.a). On the contrary, as already mentioned, filamentous bacteria outgrew on R2 granules surface (Figure III. 6.b), and this filamentous layer seems to provoke oxygen transfer limitation as suggested by the release of gas bubbles and appearance of a black zone in the internal part (Figure 6.e). Indeed, as suggested by Mosquera-Corral et al. (2005), long-term anaerobic conditions into the granule, could lead to methanogenic bacteria growth. MLSS and MLVSS decreased simultaneously in this reactor (see figure III.1.b).

With time, some of the matured granules from both reactors, presented a cracked broken surface revealing a stronger core (Figures III.6.c and 6.d). Most of the strength of the internal part of granules, could probably be explained by the mineral precipitation as has been demonstrated in chapter II. Whereas in R1 the loss of efficiency due to disintegration of matured granules seems to be compensated by the birth of new small ones, granules from R2 progressively lost density, but no more small granules seemed to be generated in this reactor.

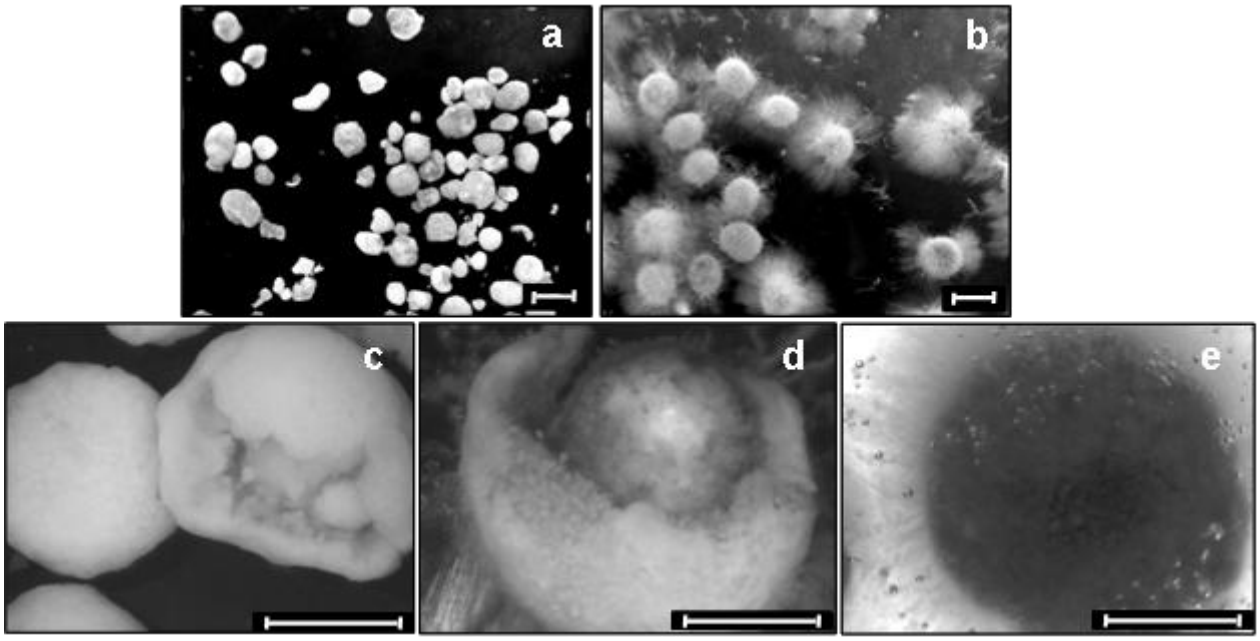

Figure III.6: Microscopic photographs of microbial aggregates at different operating times of a)R1-162 day ; b) R2-162 day; c) R1-238 day; d) R2-238 day; e) R2-250 day. Scale bar = 2mm.

III.3.3. Nitrogen removal

III.3.3.1. Kinetics

Kinetic analyses were performed during the batch cycle to assess COD, nitrogen and phosphorus removal (Figure III.7). The vertical line separates the anoxic and anaerobic phases from the aerobic ones.

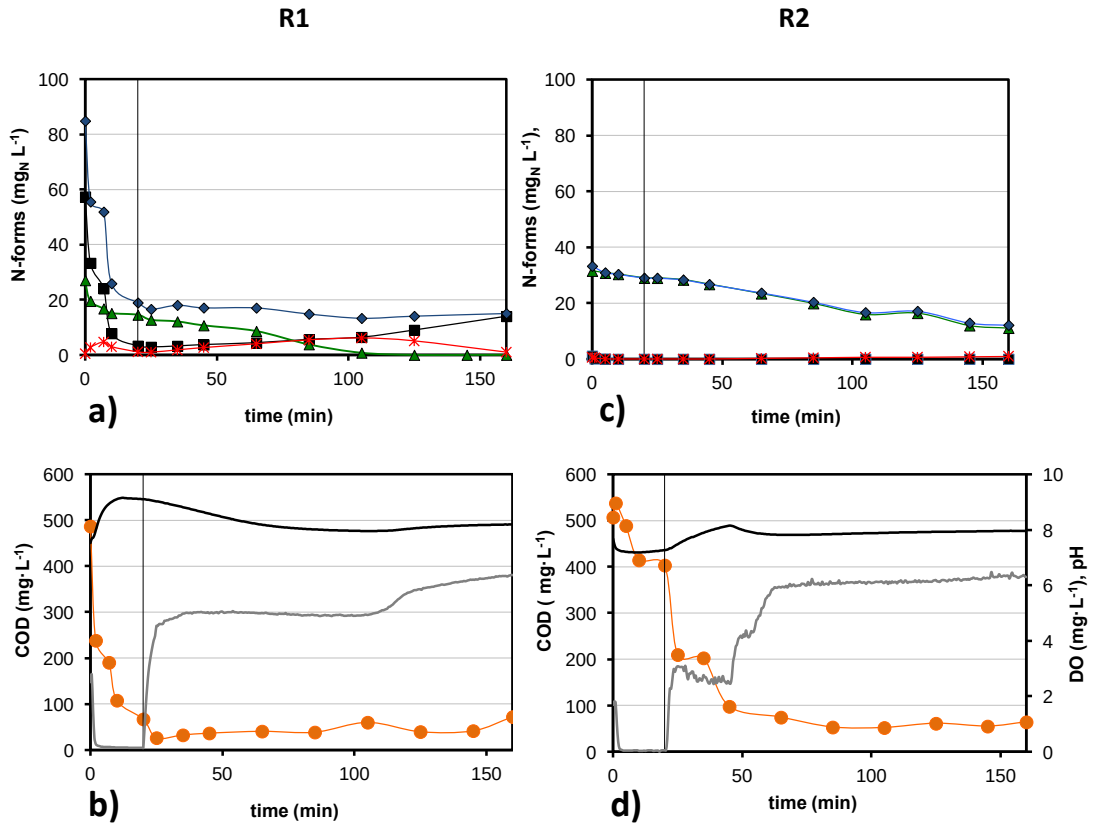

Figure III.7. Evolution of NO_3^- (■), NO_2^- (✳), NH_4^+ (▲), COD (●), TN (◆), pH (—) and DO (—) during a kinetics cycle for R1 (a,b) et R2 (c,d) on day 167th.

During the anoxic phase in reactor R1, COD and nitrate were rapidly depleted. Denitrification occurred at a rate of 350 $mg_N \cdot L^{-1} \cdot h^{-1}$, and nitrite concentration accumulated transiently up to 5 $mg_N\ L^{-1}$. Ammonium was depleted after 1.5 h during the aerobic phase, being the 46% removed by heterotrophic assimilation during the anoxic period and the 54%, aerobically at a rate (AUR) of 8.9 $mg_N\ L^{-1}.h^{-1}$. Nitrite and nitrate were accumulated respectively up to 6 $mg_N\ L^{-1}$ and 14 $mg_N\ L^{-1}$. DO was first stabilized at 5 $mg \cdot L^{-1}$ during nitrification and then increase up to 6.3 mg L^{-1} after ammonia depletion. The stable profile of TN during aerobic period indicates that simultaneous nitrification denitrification did not occur significantly in this reactor. This could be explained by the fact that DO was not enough low and also by the fact that not sufficient organic carbon was stored during the anoxic (feast) phase for allowing denitrification in the granules during aerated phase.

In reactor R2, during the non-aerated phase, COD decreased of 134 mg L^{-1}, reaching a plateau at about 400 mg L^{-1}, which corresponds to the 25% of the COD fed to the system. During the aerated phase, the oxygen profile reaches a first plateau at 2.5

mg·L^{-1}, followed by a second plateau at 4 mg L^{-1}, and then increases to 6.3 mg L^{-1} after 85% of the COD had been removed. pH increases from 7.2 to 8.0 during the first oxygen plateau indicating a probable consumption of VFA and CO_2 stripping phenomena, whereas the second oxygen plateau was due to other substrates. During the second plateau, ammonium is progressively consumed but nitrate and nitrite concentration remained negligible at all times, indicating that SND may occur in granular sludge of reactor R2. Concomitantly, the presence of AOB was demonstrated by FISH analysis in granules from R2 whereas NOB were not detected (see § III.3.3.2). In addition, the nitrification rate was also measured in batch respirometric tests with granular sludge collected from R2 at the end of the aerobic phase (at DO of 5 mg L^{-1}, with ammonia addition of 10 mgN L^{-1}, without addition of organic carbon). AUR was 0.99 mg N.g^{-1}VSS.h^{-1}, no nitrate was observed and nitrite accumulated at a rate of 0.57 mgN.g^{-1}VSS.h^{-1}. These observations encourage us to think that ammonium was simultaneously removed by heterotrophic assimilation and SND during the aerobic phase in the reactor R2. Due to heterotrophic bacteria respiration and growth on storage compounds, the nitrite produced by AOB was fully consumed and some of the ammonia was also assimilated. This is in accordance with the presence of AOB and the absence of NOB in these granules (Filali et al., 2012). Despite the fact that the AUR in R2 is close to the one observed in R1 (8.3 mg_N L^{-1} h^{-1}), the ammonium is not depleted at the end of the cycle because ammonium starts to be nitrified after the COD was depleted. Before that, the oxygen is probably too low in the granules due to the high heterotrophic activity. The final concentration of ammonium in the effluent is here (Figure III. 7.c) of 11 mg_N L^{-1} but varied greatly from one cycle to another, leading to unstable ammonium removal efficiency. Thus, this critical instability of nitrification was probably due to weak proportion of ammonia assimilated during the non-aerated phase and to the strong competition between heterotrophic and autotrophic bacteria for oxygen during the aerobic phase.

III.3.3.2. Spatial distribution of nitrifiers

FISH analysis was performed to assess the microscale structure of granules and the localization of nitrifying bacteria. Figure III.8 shows the images of granules from R1 (a, c and d) and R2 (b and g), together with suspended biomass from R1 (e) and filamentous bacteria from R2 (f). DAPI staining (blue) indicated the presence of heterotrophic bacteria in the granules. Fig. b confirms that granules from R2 were much more irregular than those of R1 (a).

In the first reactor, the localization of nitrifiers in the granules did not change significantly during the run. The image of a half-granule section (Fig 8.a) shows that AOB (magenta) were distributed throughout the granule and, in particular, near large channels and internal voids. The NOB (yellow) were found to be located in deeper layers of the granule (about 250 µm from the surface) and profusely around the internal core of the granule. As observed in previous studies (Ivanov et al., 2005; Zheng et al., 2005), channels and internal voids may play a key role in the transport of oxygen and substrate, which would explain this localization. AOB were found to form dense bacterial clusters with sizes ranging from 10 to 50 µm (Fig 8.c). NOB clusters were dense and small, their size rarely exceeding 10 µm (Fig 8.d). Hybridization of samples of flocs from R1 was also performed (Fig 8.e). AOB were frequently observed in floc samples, forming large, dense clusters, whereas very few NOB were observed.

The spatial distribution of nitrifiers in a half-granule section of R2 (observed on day 227) is reported in Fig 8(b). The distribution of AOB in R2 granules was less extensive than the distribution observed in R1. AOB were located only in the outermost 250µm of the R2 granules. Their distribution was not homogeneous through that layer. AOB clusters colonized some large parts of the aggregate and were totally absent from others. In addition, many of them were found to develop at the surface of the granule. Fig 8.g shows typical dense clusters of AOB that have developed near the surface of the granule. In contrast to R1 clusters, AOB clusters in R2 were relatively small and rarely exceeded a size of 20 µm. The hybridization of NOB with the oligonucleotides Nit3 and Ntspa662 gave a low signal similar to background noise and no typical bacterial clusters could be identified (with a magnification x100). It was thus observed that NOB were not significantly present in granules from R2. The hybridization of samples of flocs and filamentous bacteria that had developed at the surface of the granules (fig 8.f) from R2 indicated that suspended biomass did not contain nitrifying bacteria, be they AOB or NOB (result not shown).

The FISH results corroborate the kinetic assessment that no nitrite nor nitrate was accumulated (§3.3.1), indicating that nitrifiers are difficult to maintain in an anaerobic/aerobic system because of strong competition with heterotrophs for oxygen and space. Furthermore, the absence of NOB in the reactor confirms that SND favours the direct denitrification of nitrite in the core of granules, which progressively limits the development of NOB.

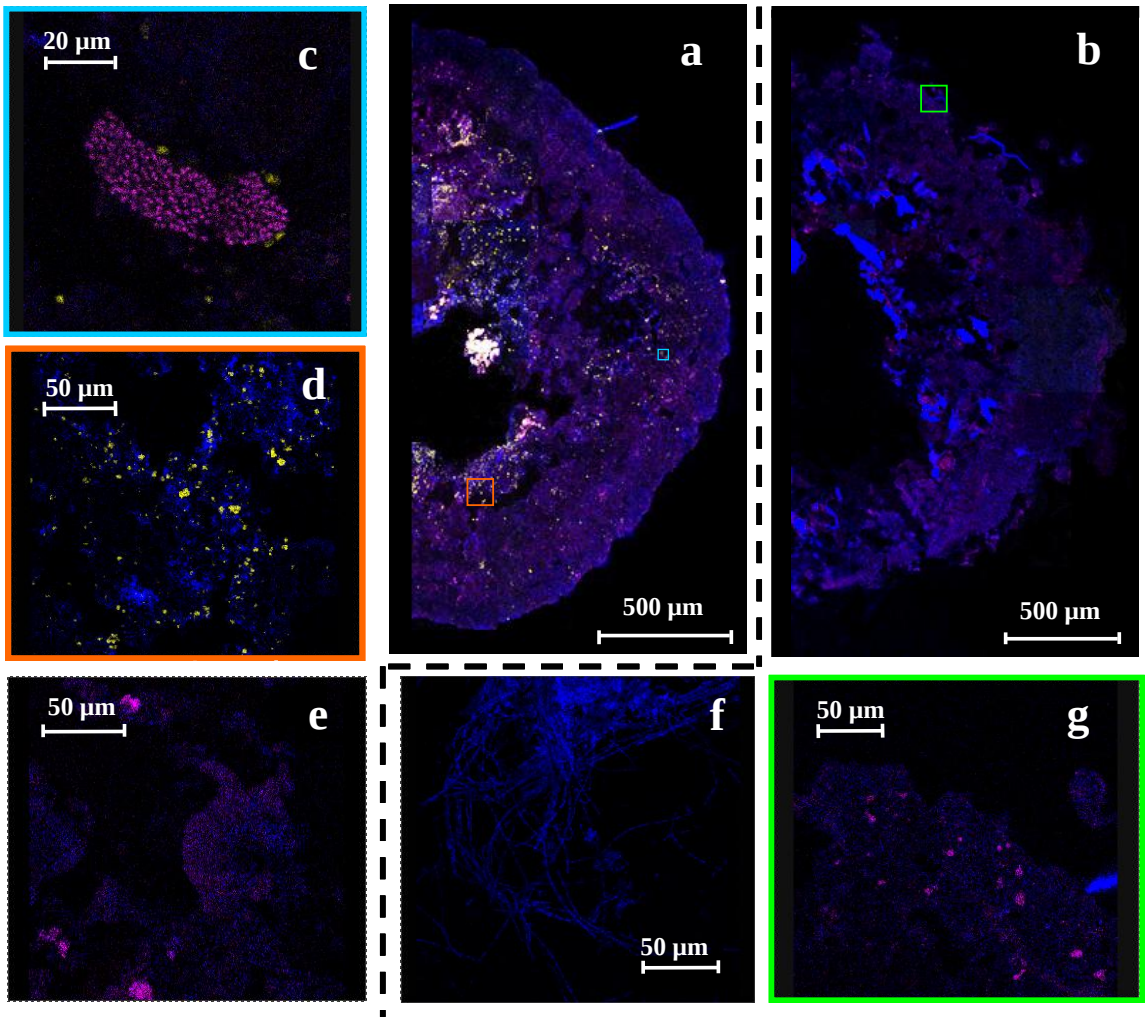

Figure III.8- Confocal laser scanning microscopy images of FISH micrographs of nitrifiers. Half granule section of R1 (a) and part of the section (c and d). Half granule section of R2 (b) and part of the section (g). Confocal laser scanning micrographs of FISH performed on a flocs of R1 (e) and filamentous bacteria of R2 (f). AOB appear in magenta (hybridized with FITC-labelled Nso190 +Nso1225), NOB appear in yellow (hybridized with Cy3-labelled Nit3+Ntspa662), other bacteria appear in blue (DNA staining with DAPI).

III.3.4. Phosphorous Removal

III.3.4.1. Kinetic Assessment

Kinetics carried out over a reactor cycle (figure III.9) showed the different processes regarding dephosphatation. In R1 (fig. 9.a), a rapid decrease of $P\text{-}PO_4$ is observed during the anoxic phase concomitant with pH increase due to denitrification. It was previously demonstrated (chapter II) that calcium phosphate precipitation was responsible of this phenomenon. There is no apparent anaerobic phosphate release in R1

but polyphosphate-accumulating organisms (PAO) activity was supposed anyway. Thus, in order to verify this assumption, specific anaerobic batch tests were performed with sludge from R1 (with acetate as a sole carbon source, without additional calcium, magnesium or ammonium that at high pH (8.5 on average), could entrain precipitation with phosphorus). Three series of 2L- batch reactors were seeded with granules, flocs, and a mixture of flocs and granules, respectively. P release rate for granules, flocs and hybrid sludge was of 2.88, 6.27 and 3.24 $mgP \cdot g^{-1}VSS \cdot h^{-1}$ respectively, which are comparable to those reported by Parker et al. 2001 in EBPR processes. Mino et al., 1998 also reported a value 3.2 $mgP \cdot g^{-1}VSS_{PAO} \cdot h^{-1}$ but in enriched cultures, meaning that even if our culture was not enriched with PAO, their activity was also present in R1. K^+, Mg^{2+} and Ca^{2+} ions were also measured in the bulk, revealing that for each mmol of $P\text{-}PO_4$ released per h, 0.27mmol of Mg^{2+} and 0.51 mmol of K^+ were released for the granule-seeded reactor, whereas similar values (0.24 mmol Mg^{2+} and 0.4mmol of K^+) were released by flocs. A slight release of calcium was also remarked in those tests -it was 3 times more important in granules (0.61 mmol/mmolP released) than in flocs-, arising questions about its role on EBPR. In any case, anaerobic P release and uptake was certainly masked by P precipitation in the GSBR reactor R1. Presence of PAO activity is also visible by potassium concentration which shows a typical profile (release and uptake) explained by its inclusion into polyphosphate structure.

As shown in figure III.9.c, significant anaerobic release of PO_4 takes place in the second reactor (R2). This release continues during the first oxygen step in aerobic phase (DO=2.5ppm), which means that a part of PAO continue to convert substrate (VFA) to internal polymers. This is certainly due to the presence of anaerobic zones into the granule during this phase. P uptake is observed to start as DO increases to 4 mg/L, probably when VFA has been depleted in the reactor. In the following kinetic, final phosphate concentration is similar to those observed in reactor R1. However depending on the cycle, phosphate removal was unstable in R2 due to important variability in the heterotrophic activity at the beginning of aerobic phase.

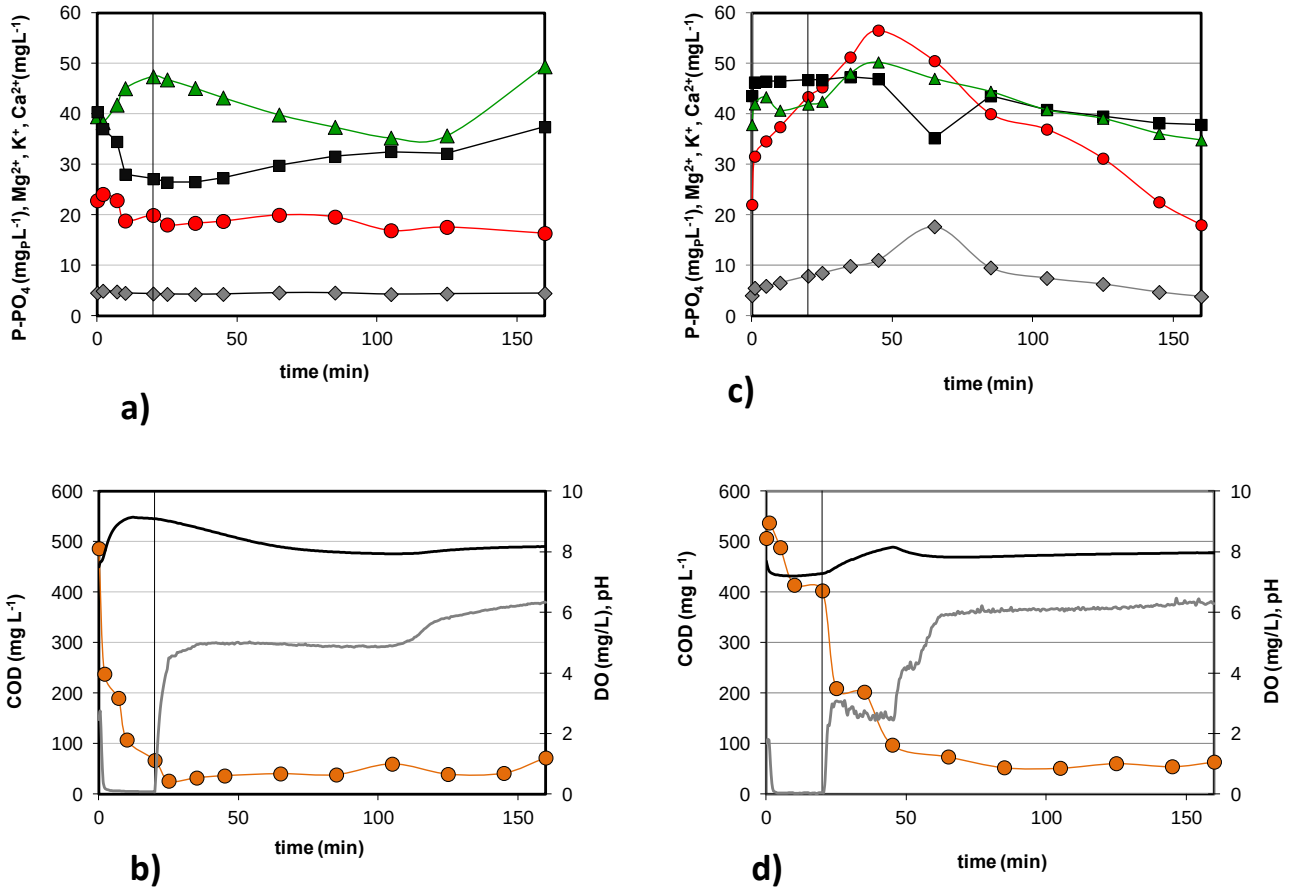

Figure III.9. Evolution of P-PO4 (●), Ca^{2+}(■), Mg^{2+}(◆), K^{+} (▲) , COD (●), pH (—) and DO (—) during a cycle kinetics in (a,b) R1 and (c,d) R2, on day 167.

III.3.4.2. PHB staining

Bacterial intracellular carbon storage was analyzed via PHB staining technique in both reactors. Figures III.10.a and 10.b show two granules sections from R1 and R2 respectively, obtained from samples collected at the end of the aerated phase of each reactor, on day 180. (PHB granules are stained in blue/black whereas cytoplasmic membrane (cells), are stained in pink/red. It should be noted that PHB can be stored by either phosphate accumulating organisms (PAO), whose activity has been demonstrated in the previous section, but also by glycogen accumulating organisms (GAO). PHB is distributed in the peripheral zone of the granules in a thin layer, and in the internal part of the granules, close to internal voids and channels. Comparison of samples from each reactor indicates that PHB in the granules from R2 is more important in the periphery

including the filamentous bacteria outgrown (Fig 10.d), whereas no PHB was reported in some filamentous bacteria from R1 (10.c). This confirms that important heterotrophic activity and carbon storage was present in the surface whereas growth/storage in the center becomes difficult, probably due to the diffusion limitation in granules from R2.

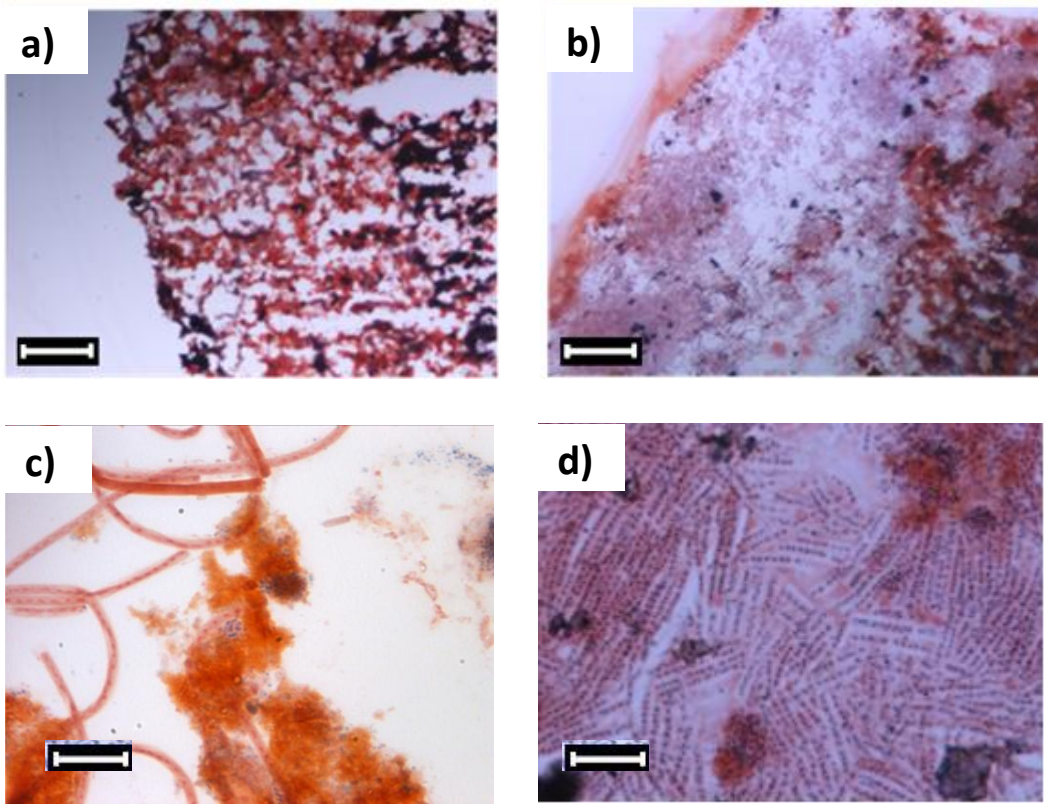

Figure III.10: Microscopic images of the stained 10µm-cut granules: a) R1 ; b) R2; c) R2 filamentous bacteria –external d)R1 filamentous bacteria –internal- filamentous bacteria. The scale bar=100µm for a) and b) and 5 µm for c) and d). PHB granules are stained in blue/black whereas cytoplasmic membrane (cells) are stained in pink/red

III.3.4.3. Phosphate precipitation contribution

Contribution of precipitation in the overall P removal yield can be estimated from calcium behaviour. Several authors claimed that calcium is not implicated significantly in the biological formation of polyphosphate (Jardin and Pöpel; 1996; Pattarkine and Randall, 1999) but precipitates mainly in the form of calcium-phosphate as demonstrated in the precedent chapter. From thermodynamical analysis, amorphous calcium phosphate (ACP) and hydroxy-apatite (HAP) were the most probable minerals. X-ray diffraction

patterns have been compared for granules from R1 and R2, which showed that the most significant mineral was HAP (Ca_5 $(PO_4)_3(OH)$), although in the case of R1 spectrum also indicates a few amount of whytlockite ($Ca_{18}Mg_2H_2(PO_4)_{14}$). A comparison of XDR spectra carried out over the core of granules from R1 and R2, is shown in figure III.11.

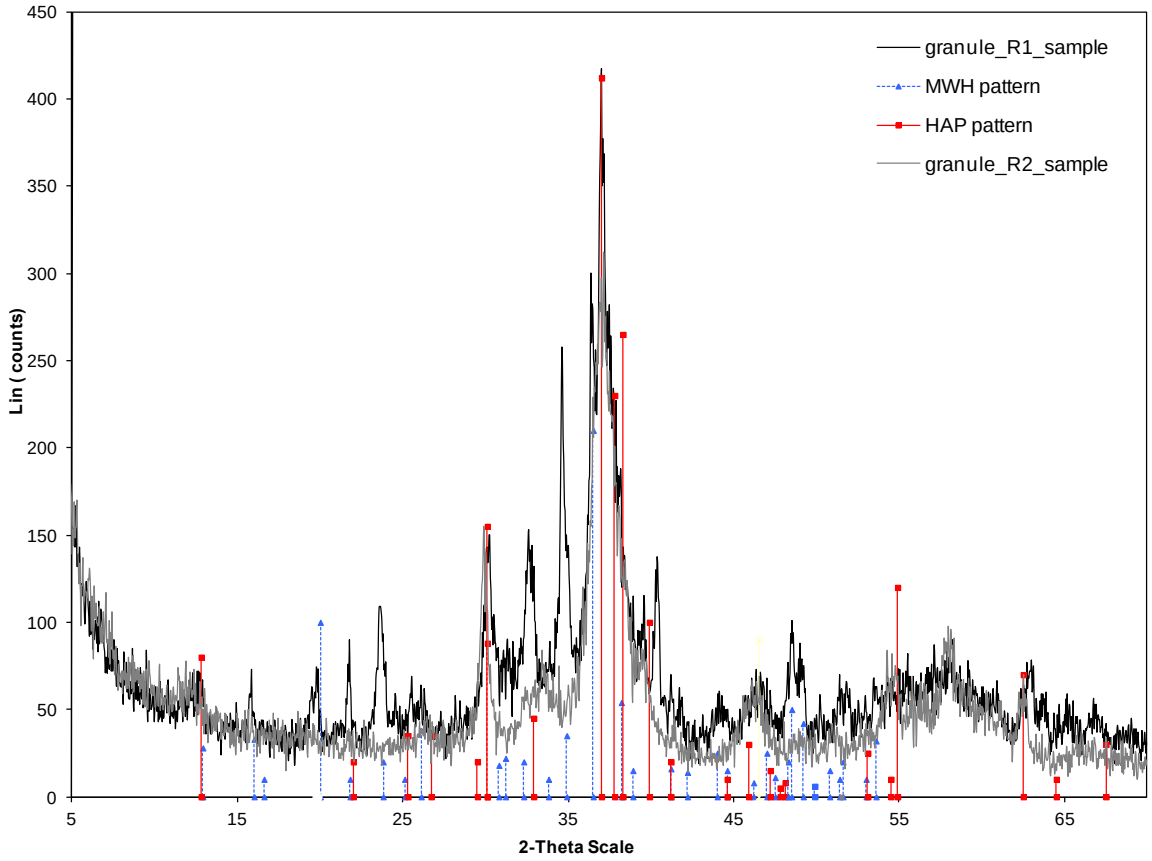

Figure III.11: Comparison of XDR patterns of the core of R1 and R2 granules. R1 (black); R2 (gray).

This figure shows that the precipitation mechanism inside both granules is identical, despite of the different reactor operating conditions, and that the major mineral found in both cases, is hydroxyapatite.

Precipitation is mainly controlled by pH in the bioreactors. Calcium concentration decreases in R1 during the anoxic phase when pH achieves the highest values (close to 9), and it is progressively released during the aerobic period as pH decreases with nitrification (Fig III.9.a). Calcium profile in R2 (Fig III.9.c) remains stable during the anaerobic period with stable pH around 7.5, but decreases during aerobic phase consequently to pH increase up to 8. The whole Ca^{2+} removal was 40% in the reactor R1

(see figure III.2) whereas it progressively decreased to 20% in the reactor R2 (more unstable). This tends to show that calcium phosphate precipitation was more important in the first reactor than in the second one, which is in coherence with the fact that mean pH was higher in the first reactor due to more intense denitrification.

III.4. DISCUSSION

Stability of physical properties is a key issue for ensuring the long-term operation of granular sludge reactor. It is characterized by adequate settleability properties, which guaranties high biomass retention, as well as by no granule washout or breakage for a long period of time. In this study, very low sludge volume index (15 mL g^{-1}) and stable high MLVSS concentration (up to 25 g L^{-1}) were obtained in the GSBR operated with alternating anoxic/aerobic conditions (R1). In contrast, filamentous growth on the surface of granules (and finally in the bulk), progressively deteriorated the properties and performances of granular sludge from reactor R2 operated with alternated anaerobic/aerobic phases (SVI = 90 mL g-1, MLVSS decreased to up to 7g/L) Filamentous growth has been previously observed in aerobic granular sludge SBR, resulting from either a change in the wastewater composition, OLR (organic loading rate) or DO concentration (Tay et al., 2001; McSwain et al., 2004; Schwarzenbeck et al., 2004; Mosquera-Corral et al., 2005; Zheng et al., 2006). It is generally admitted that filamentous growth is favored at low substrate or oxygen availability. For instance Mosquera-Corral et al (2005) reported that aerobic granules lost their stability due to the outgrowth of filamentous bacteria when the DO was reduced to less than 40% saturation. In the present study, despite similar aeration rate was imposed in both reactors, lower DO concentration was obtained in the beginning of the aerobic phase in R2 (anaerobic/aerobic) due to residual COD which was not removed during the non-aerated phase. This leads us to think that filamentous growth is here due to oxygen limited growth of heterotrophic bacteria with easily carbon source (glucose, ethanol or residual acetate or propionate) at the beginning of aerobic phase. The high ratio COD:DO maintained in the bulk at this period makes difficult the growth of a dense biofilm on the surface of the granules. Traditionally, physiological studies revealed that most of filamentous bacteria had strictly aerobic metabolisms, despite limited morphotypes have been claimed to have fermentative metabolisms (Nowak and Brown, 1990), giving them selection advantages in anaerobic/aerobic systems. Plug-flow regime reactor like SBR exerts a selection pressure over floc-forming bacteria due to the high macro-gradients of

substrate preserved and conversion of easily biodegradable substrate to internal polymers (Kuba et al., 1996). In this work with a carbon source composed of glucose, propionate, acetate and ethanol, only a fraction of COD was removed anaerobically and converted to PHB. One specific issue for the use of GSBR with complex mixture of organic carbon is hence to maximize the fraction of COD used during anaerobic period, i.e. increasing pre-fermentation processes being probably one possible solution. Another solution, more energy consuming, would be to increase the aeration rates as shown by Mosquera-Corral et al. (2005). Lower HRT in for R2 could have been selected at the beginning of filamentous growth for promoting their wash out (Morales et al., 2012).

The presence of nitrate during the feast period seemed here critical for the stability of the granules in the first reactor (R1). A first explanation is that COD was fully removed thanks to denitrification which guarantee the absence of COD in the aerobic phase (unlike in R2, in which COD presence at the end of the aerobic phase limits even more the DO difussion in the granules). Moreover as shown by Wan et al., (2009) the anoxic growth of heterotrophic bacteria in the inner layers could encourage aggregates densification. Both are likely to enhance the strengthening of the granule structure and improve their stability.

Consequences on nutrient removal should be also pointed out. First stable full nitrification was maintained in R1 and ammonium nitrifying bacteria (AOB) were found to be distributed evenly throughout the granule. In contrast filamentous heterotrophic bacteria growing in the periphery of granules in R2 make difficult and unstable nitrification due to competition between autotrophs and heterotrophs. FISH analyses confirmed that nitrifying bacteria were located behind the layer of filaments. On the other hand, SND (during aerobic phase) was poorly observed in R1 compared to R2. This can be explained by the fact that less stored COD was available for denitrification during the aerobic period in a system working with pre-anoxic phase (R1). Regarding phosphorus, biological P release was lower in R1 than in R2, which is logically due to less VFA storage by PAO in anoxic conditions (Patel and Nakhla, 2006), but global P removal efficiency was similar and more stable in R1. This was due to the fact that calcium phosphate precipitation was more important in R1, thanks to a higher pH due to denitrification. Despite the fact that some authors have questioned the active role of calcium in EBPR (Barat et al., 2008; Kortstee et al., 1994; Schönborn et al., 2001), the role of calcium precipitation in granular sludge performances and properties still need more

investigations. In this study, assuming that all the calcium removed was co-precipitated with phosphate in the form of HAP in the long term, and based on the general performances graphs (figure III.1), the precipitation mechanism contributed to P removal up to 28% for R1, and 21% for R2.

III.5. CONCLUSIONS

In this study, better performances were observed in a GSBR operated with alternating anoxic/aerobic conditions compared to those working with alternating anaerobic/aerobic phases.

Very good settling properties for granular sludge (SVI ≈ 20 ml/g) and high MLSS concentration were stabilized in the bioreactor with alternating anoxic/aerobic conditions. Full nitrification efficiency was obtained, but SND was poor during aerobic phase due to insufficient internal storage of COD for denitrification.

Despite the fact that alternating anaerobic/aerobic conditions theoretically favors granulation by promoting carbon storage, filamentous bacteria developed at the surface of granules had a negative impact on settleability and nitrification. This was explained by the presence of residual COD during aerobic phase which was not stored during anaerobic period. A critical point with mixture of organic carbon sources is thus to maximize the amount of ready biodegradable substrate used during the un-aerated phase, either anaerobic or anoxic.

Finally comparable P removal yields were observed in both systems. Enhanced biological P removal was more important in anaerobic/aerobic whereas contribution of precipitation (Ca-P) appeared more significant in anoxic/aerobic conditions.

III.6. ACKNOWLEDGMENTS AND CONTRIBUTIONS

I would like to acknowledge my collegue A. Filali, as well as P. Boe, E. Mengelle, D. Delanges and M. Bounouba, for their contribution to this work.

III.7. REFERENCES

Amann., R. (1995). *In situ identification of micro-organisms by whole cell hybridization with rRNA-targeted acid probes.* In: Molecular Microbial Ecology Manual, Edited by A.D.L. Akkermans, J.D. van Elsas & F.J. de Bruijn. London : Kluwer, pp. MMEM-3.3.6/1-MMEM-3.3.6/15.

Barat R., Montoya T., Borrás L., Ferrer J., Seco A. (2008). *Interactions between calcium precipitation and the polyphosphate-accumulating bacteria metabolism.* Water Research, 42 (13): 3415-3424.

Beun J.J., A. Hendriks, Van Loosdrecht M. C. M., Morgenroth E., Wilderer P.A., J. J. Heijnen (1999). *Aerobic granulation in a sequencing batch reactor*, Water Research 33 (10), 2283-2290.

Chen Y.C., Lin C.J., Chen H.L., Fu S.Y., Zhan H.Y. (2009). *Cultivation of Biogranules in a Continuous Flow Reactor at Low Dissolved Oxygen*. Water, Air and Soil Pollution, 9 (4):213-221

Coma M., Biological Nutrient Removal in SBR Technology: from floccular to granular sludge (2011). Ph.D. Thesis, University of Girona, Spain.

Coma, S. Puig, M. D. Balaguer, and J. Colprim, (2010). The role of nitrate and nitrite in a granular sludge process treating low-strength wastewater., Chemical Engineering Journal, 164(1): 208–213.

Daims, H., M. Wagner, P. H. Nielsen, J. L. Nielsen and S. Juretschko (2000). *Novel Nitrospira-like bacteria as dominant nitrite-oxidizers in biofilms from wastewater treatment plants: diversity and in situ physiology*, Water Science and Technology 41 (4-5), 85-90.

Dangcong P., Bernet N., Delgenes J.P., Moletta R. (1999). *Aerobic granular sludge—a case report.* Water Research, 33(3):890-893.

A. Filali, Y. Bessiere, M. Sperandio, (2012). Effects of oxygen concentration on the nitrifying activity of an aerobic hybrid granular sludge reactor RID A-1878-2012, Water Science and Technology, 65(2): 289–29.

Janssen MJ., Meinema K., van der Roest H F.. (2002). *Biological Phosphorus Removal: Manual for Design and Operation*. STOWA IWA Publisher: 186-196.

Jardin, N. and H. J. Popel (1996). *Behavior of waste activated sludge from enhanced biological phosphorus removal during sludge treatment*, Water Environment Research 68 (6), 965-973.

Kortstee G.J.J., Appeldoorn K.J., Cornelus F.C. Bonting, Ed W.J. van Niel, H. W. van Veen (1994). *Biology of polyphosphate-accumulating bacteria involved in enhanced biological phosphorus removal*, FEMS Microbiology Reviews, 15 (2-3):137-153.

de Kreuk, M., Heijnen, J.J. and van Loosdrecht, M.C.M. (2005). *Simultaneous COD, nitrogen, and phosphate removal by aerobic granular sludge*. Biotechnol Bioeng. 90: 761-769.

de Kreuk, MK., Kishida, N., van Loosdrecht, MCM. (2007). *Aerobic granular sludge- state of the art*. Water Sci Technol. 55 (8-9): 75-81.

Kuba, T., Murnleitner, E., van Loosdrecht, MCM., Heijnen, JJ. (1996). *A metabolic model for biological phosphorus removal by denitrifying organisms*. Biotechnol. Bioeng. 52 (6): 685-695.

Lee D.J., Chen Y.Y., Show K.Y., Whiteley C.G., Tay J.H. (2010). Advances in aerobic granule formation and granule stability in the course of storage and reactor operation, Biotechnology Advances, 28(6): 919-934.

Lemaire R. (2007). *Development and fundamental investigations of innovative technologies for biological nutrient removal from abattoir wastewater*. Ph.D Thesis. University of Queensland, Australia.

Lemaire R., Yuan Z.G. and Webb R.I. (2008). *Micro-scale observations of the structure of aerobic microbial granules used for the treatment of nutrient-rich industrial wastewater*, Isme Journal, 2(5): 528-541.

Levin G.V., Shapiro J. (1965). *Metabolic uptake of phosphorus by wastewater organisms*. Journal Water Pollution Control Fed. 37: 800-821.

Liu Y.Q., Moy B., Kong Y.H., Tay J.H. (2010). *Formation, physical characteristics and microbial community structure of aerobic granules in a pilot-scale sequencing batch reactor for real wastewater treatment*, Enzyme and Microbial Technology, 46(6): 520-525.

Liu Y., Tay J.H.. (2002). *The essential role of hydrodynamic shear force in the formation of biofilm and granular sludge*, Water Res., 36 : 1653–1665.

Liu Y.Q., Liu Y. and Tay J. H. (2004). *The effects of extracellular polymeric substances on the formation and stability of biogranules*. Applied Microbiology and Biotechnolog, 65(2):143-148.

Liu Y., Liu Q.S. (2006). *Causes and control of filamentous growth in aerobic granular sludge sequencing batch reactors*, Biotechnology Advances 24 (1): 115-127.

van Loosdrecht M.C.M., Pot M.A., Heijnen J.J. (1997). Importance of bacterial storage polymers in bioprocesses, Water Science and Technology 35 (1), 41-47.

McSwain BS., Irvine RL., Wilderer PA. (2004). *The influence of settling time on the formation of aerobic granules*. Water Sci. Technol. 50 (10): 195-202.

Mino, T., Liu, W-T., Kurisu, F., Matsuo, T. (1995). *Modelling glycogen storage and denitrification capability of microorganisms in enhanced biological phosphate removal processes*. Water Sci Technol. 31(2): 25-34.

Mobarry, B. K., M. Wagner, V. Urbain, B. E. Rittmann and D. A. Stahl. (1996). Phylogenetic probes for analyzing abundance and spatial organization of nitrifying bacteria, Applied and Environmental Microbiology 62 (6): 2156-2162.

Morales N., M. Figueroa, A. Mosquera-Corral, J.L. Campos, R. Méndez (2012). *Aerobic granular-type biomass development in a continuous stirred tank reactor,* Separation and Purification Technology, 89 (22):199-205.

Morgenroth E., Sherden T., van Loosdrecht M.C.M., J.J. Heijnen, P.A. Wilderer. (1997). *Aerobic granular sludge in a sequencing batch reactor*. Water Research, 31(12):3191-3194.

Mosquera-Corral, A., M. K. de Kreuk, J. J. Heijnen and M. C. M. van Loosdrecht (2005). *Effects of oxygen concentration on N-removal in an aerobic granular sludge reactor*, Water Research 39 (12), 2676-2686.Moy, B.Y.P., Tay, J.H., Toh, S.K., Liu, Y., Tay S.T.L. (2002). *High organic loading influences the physical characteristics of aerobic sludge granules*. Lett. Appl. Microbiol. 34, 407-412.

Nor-Anuar A., Z. Ujang, M. C. M. van Loosdrecht, M. K. de Kreuk, and G. Olsson (2012). *Strength characteristics of aerobic granular sludge*. Water Sci. Technol., 65(2): 309–316, 2012.

Nowak, G. and G. D. Brown (1990). *Characteristics of Nostocoida-Limicola and Its Activity in Activated-Sludge Suspension,* Research Journal of the Water Pollution Control Federation 62 (2): 137-142.

Pandolfi D., Pons M.N., da Motta M. (2007). *Characterization of PHB storage in activated sludge extended filamentous bacteria by automated colour image analysis*, Biotechnology Letters 29 (8), 1263-1269.

Patel J., Nakhla G., (2006). *Interaction of denitrification and P removal in anoxic P removal systems*, Desalination, 201(1-3): 82-99.

Pattarkine, V.M., Randall, C.W., (1999). *The requirement of metal cations for enhanced biological phosphorus removal by activated sludge*. Water Sci. Technol. 40, 159–165.

Qin L., Liu Y. and Tay J.-H. (2004). Effect of settling time on aerobic granulation in sequencing batch reactor. Biochemical Engineering Journal. 21(1): 47-52.

Schönborn C., Bauer H.D., Röske I. (2001). Stability of enhanced biological phosphorus removal and composition of polyphosphate granules, Water Research, 35 (13): 3190-3196.

Schwarzenbeck, N., R. Erley and P. A. Wilderer (2004). *Aerobic granular sludge in an SBR-system treating wastewater rich in particulate matter*, Water Science and Technology 49 (11-12): 41-46.

Tay J. H., Liu Q. S. and Liu Y. (2004). *The effect of upflow air velocity on the structure of aerobic granules cultivated in a sequencing batch reactor.* Water Science and Technology 49(11-12): 35-40.

Tay, J. H., Y. Liu and Q. S. Liu. (2001). *Microscopic observation of aerobic granulation in sequential aerobic sludge blanket reactor*, Journal of Applied Microbiology 91 (1): 168-175.

Tsuneda S., T. Ohno, K. Soejima, et A. Hirata. (2006) Simultaneous nitrogen and phosphorus removal using denitrifying phosphate-accumulating organisms in a sequencing batch reactor. Biochemical Engineering Journal, 27(3): 191–196.

Wagner, M., G. Rath, H. P. Koops, J. Flood, R. Amann. (1996). *In situ analysis of nitrifying bacteria in sewage treatment plants*, Water Science and Technology 34 (1-2): 237-244.

Wan J., Bessière Y., Spérandio M. (2009). *Alternating anoxic feast/aerobic famine condition for improving granular sludge formation in sequencing batch airlift reactor at reduced aeration rate*, Water Research, 43 (20): 5097-5108.

Yilmaz G., Lemaire R., Keller J., Yuan Z., (2007). *Effectiveness of an alternating aerobic, anoxic/anaerobic strategy for maintaining biomass activity of BNR sludge during long-term starvation*. Water Research, 41: 2590-2598.

Zheng Y.M., Yu H.Q., Sheng G.P. (2005). *Physical and chemical characteristics of granular activated sludge from a sequencing batch airlift reactor*, Process Biochemistry, 40(2): 645-650.

Zheng, Y.M., Yu H.Q., Liu S.H., Liu X.Z. (2006). *Formation and instability of aerobic granules under high organic loading conditions*, Chemosphere 63 (10): 1791-1800.

CHAPTER IV:

Location and chemical composition of microbially induced phosphorus precipitates in anaerobic and aerobic granular sludge

*This chapter introduces the phenomenon of **biomineralization** in the wastewater treatment field. The aim consists on applying the characterization techniques developed in chapter II, on anaerobic granules coming from industrial UASB reactors from a cheese WWTP, in order to assess the influence that the different supernatants and processes exert to the chemical composition of bioliths found in microbial granules.*

At a second stage, mineral evolution evaluated in aerobic granules grown in the laboratory reactors, gave rise to the need of studying in a greater detail, the different factors influencing the mineral precipitation precursors, consisting the basis of the following chapter.

This chapter constitutes the basis of a national communication proceeding (SFGP 2011, Lille), as well as an extended version of the following article (recently accepted):

Mañas A., Spérandio M., Decker F., Biscans B. (2012). Location and chemical composition of microbially induced phosphorus precipitates in anaerobic and aerobic granular sludge. Environmental Technology: DOI-TENT-OA-2012-0106.

IV.1. INTRODUCTION TO BIOMINERALIZATION PROCESSES

Biomineralization is the process by which microorganisms form minerals. Such processes are very common in Nature since centuries: from the millenary dolomite formations in Earth (Sánchez-Román et al., 2011) to the most sophisticate techniques for applying bioremediation into strengthening cementitious materials (De Muynck et al., 2010), there is a wide range of quotidian processes in which microorganisms are involved in mineral formation: vertebrate bones, dentin and enamel, the undesirable kidney stones disease or the most exotic nacre, shells and pearl formations.

Weiner (1988) distinguished two types of biomineralization processes depending on the environmental conditions influence:

Controlled biomineralization: organisms are directly involved in the mineral formation, and their cellular activity directs the nucleation, growth, morphology and location of the mineral, which nature is unique to that species, regardless of the environmental conditions. e.g.: the intracellular chemically pure magnetite crystals in magnetotactic bacteria (Bazylinski and Frankel, 2004), or silica deposition in the unicellular algae coccolithophores and diatoms (Barabesi et al., 2007).

Induced biomineralization: the type of mineral formed is largely dependent on the environmental conditions that can be locally modified by a wide range of microorganism strains as a result of their metabolic activity. In contrast to controlled biomineralization, no specialized biological structures are thought to be here involved (Barabesi et al., 2007), and precipitation takes place when microorganisms alter almost one of the following abiotic factors: i) Ion concentration; ii) pH; iii) The availability of nucleation sites (Hammes and Verstraete, 2002).

Some authors (Dupraz et al., 2009; Benzerara et al., 2011), also distinguish the term of organomineralization, which is defined as a passive mineral precipitation in the presence of cell surfaces or extracellular polymeric substances (EPS), being the organic matter, the actor responsible of the mineral nature and morphology. Fossilization processes would belong to this group.

The distribution of the biominerals identified to the present, can be categorized as follows: the foremost taxonomic group of mineral-formers are the animals, being 37 the biogenic precipitates identified; then, bacteria (24) followed by plants (11), and finally fungus and protozoa with 10 (Gonzalez-Muñoz et al., 1997). According to their anions, the most abundant biominerals formed are phosphates, followed by oxides and carbonates. However, the

latter group of biominerals are the most referred and studied in the literature, for which the term microbially induced carbonate precipitation (MICP), was already reported a decade ago (Castanier et al., 1999).

When biomineralization started to become interesting in the field of bioremediation and biocementation (following the French Patent FR8903517 in 1989), several groups of research came out since then and, one decade later, different microorganism strains and metabolic pathways were identified and controlled to form different minerals, mainly calcium carbonate: the Calcite Bioconcept was then born (Le Métayer-Levrel et al., 1999). Thus, works focused on microbial mineralization activity involving specific strains (controlled biomineralization): *Bacillus cereus* (Le Métayer-Levrel et al., 1999), *Micrococcus sp. Bacillus subtilis* (Tiano et al., 1999), *Bacillus sphaericus* (De Muynck et al., 2008a and 2008b; Dick et al., 2006), *Pseudomonas putida* (Biobrush®, May, 2005) and *Myxococcus xanthus* (Rodríguez-Navarro et al., 2003), began to appear. The latter species had been proven to induce the precipitation of carbonates, phosphates and sulphates in a wide range of solid and liquid media (Ben Omar et al., 1994). Furthermore González-Muñoz and collaborators, (1993) were the first to report struvite and calcite crystallization by dead cells and cellular fractions of *M. Xanthus and M. Coralloides D.*, although its characterization through Transmission Electron Microscopy analysis (TEM), was difficult because the small crystalline forms of struvite were sometimes destroyed by impact of the electron beam. Ben Omar (1995) had observed the struvite precipitation onto the walls of *M. Xanthus* in a medium at pH=6.5 and rich in magnesium and phosphate concentrations. They had reported struvite formation only in mature and deformed cells, explaining that, in such cells, a phenomenon of "cell-wall relaxation" takes place prior the cell lysis, resulting in extra negative charges that scavenge positive Mg^{2+} and NH_4^+ ions. Regarding hydroxyapatite (HAP) crystallization, *Bacterionema matruchotii* species was reported to produce a lipoprotein, that once extracted and isolated in a culture medium, triggered HAP precipitation (De Muynck et al., 2010). But wherever the nature of the mineral be, matrix studies have highlighted the importance of a unique group of proteins involved in controlling mineral formation in bacteria (Weiner et al., 2008): they were rich in aspartic acid, which is one of the 20 proteogenic aminoacids non-essential in mammals (Lehninger, 1988) and a metabolite in the urea cycle.

The fact that some bacterial strains are related to a specific mineral type, is not only dependent of the aforementioned biological induced macromolecules, but also of the elements involved in their metabolic functions. e.g.: the group of oxyhydroxides so named ferrihydrate and goethite, are known to precipitate spontaneously even at neutral pH, due to the activity of

iron-oxidizing bacteria, that convert the soluble Fe^{+2} form into Fe^{+3} (Hohmann et al., 2010). Another example of how microorganisms can provoke precipitation is by the carbonatation process, which is the displacement of CO_2 into CO_3^{2-} equilibrium diagram, due to a pH increase because of photosynthesis, sulfate-reduction or urea degradation (Warren and Haack, 2001). Thus, bacteria strains involved in the Enhanced Biological Removal Process, such as PAO, can be considered similarly, for their contribution to phosphate precipitation as they have the capacity of modifying the local phosphate concentrations, even if the overall system is undersaturated with respect to these phases.

The role of biomineralization in biological functions remains a matter of debate. Some authors support that it is the accidental result of a metabolic by-product that can cause cell disruption (Knorre and Krumbein, 2000), while others are committed to the fact that it is a specific process with ecological benefits, like providing more strengthening and resistance properties (Ehrlich, 1996; McConnaughey and Whelan, 1997). Accidentally or not, this phenomenon is reported to contribute favorable to the bioremediation field, where several applications for ion removal from wastewaters can be highlighted: groundwater heavy metals removal (Warren and Haack., 2001), radionucleotides (Fujita et al., 2004) and calcium removal from water (Hammes et al., 2003). In this case, we focalized our study in the simultaneous carbon and nutrient removal (nitrogen and P) in a bio reactor with aerobic granulated sludge. The biomineralization is a parallel process that takes place simultaneously in these aggregates, contributing to better operating properties and P removal yields. In the field of dairy agro-food wastewater treatment, UASB reactors seeded with granular sludge, have been reported as a robust and efficient system for reducing the high organic loads that faces this industry (Lettinga et al., 1980; Lemaire, 2007). Moreover, another advantage of driving anaerobic sludge digestion is the sustainable energy production that usually serves to cogeneration. However, anaerobic digestion is not fully effective for nutrient removal as on the one hand, anaerobic effluents are rich in ammonium due to the hydrolysis of proteins, and on the other hand, biological P uptake is not possible with a solely anaerobic compartment. Precipitation in the bulk, of struvite (MAP) is feasible but requires a special design as well as reagents dosing because effluents are usually deficient in Mg and pH requires a strict control (Rensburg et al., 2003). Aerobic granular sludge has been lately developed in order to overcome these deterrents, as it is proven to withstand high organic loads and to perform simultaneous nutrient removal (Liu et al., 2002). Aerobic granules consist of macro-aggregates constituted by a consortium of a wide range of bacteria strains, and that minerals precipitated inside can be the result of local modifications of involved

ion supersaturation and pH factors. This chapter focuses on the induced biomineralization mechanisms, proposing the notion of Microbially Induced Phosphorous Precipitation (MIPP) phenomenon as a side mechanism of P-removal in wastewater treatment. This work is especially dedicated on granular sludge processes applied to high-strength wastewater treatment. Phosphate precipitates were initially demonstrated in aerobic granular sludge process in Chapter II with different techniques (RAMAN, SEM-EDX, XRD and chemical extractions). Here, the same approach was developed on anaerobic granular sludge treating dairy (cheese) wastewaters.

In an attempt to explain the major mechanisms involved in the observed precipitation process, and how the bulk conditions can affect such parameters, a set of characterization assays have been carried out in order to better understand the biomineralization process inside aggregates in granulated sludge for wastewater treatment. This work complements the information already provided by some authors (Bhatti et al., 1995; Langerak van et al. 2000 and 1998), who observed a relation between the ionic concentrations of the mixed liquor from different UASB digesters, and the ash content of their granules. The location of the precipitation process (in the granules or on the reactor walls) is also dealt in this chapter due to its implications in the process: Kettunten and Rintal (1998), reported losses of biomass methanogenic activity with high ash content in the sludge, which constitutes a deterrent for long-stabilization of UASB reactors. Conversely, Iza et al. (1992) observed that some biofilm depositions could take place onto the surface of carbonates precipitated in the bulk and Langerak van et al. (2000) found out that the development of a high ash sludge content contributed to biomass cementation and stabilization.

Most of the anaerobic and aerobic granules investigated in the literature (Ren et al., 2008; Langerak et al., 1998; Svardal, 1991) contained calcium carbonate bioliths inside, whereas aerobic granules cultivated in our laboratory were found to enclose a calcium phosphate core inside (Mañas et al., 2011). The importance of this study relays on the understanding of the parameters that influence the composition and location of the precipitates in granular reactors. Moreover, it emphasizes the contribution of the precipitation mechanism inside granules (so-called MIPP), to the phosphorous dephosphatation process and to the biomass valorization.

Therefore, this work is especially dedicated to the study of the mineral solid compounds found in granular sludge processes (aerobic and anaerobic) applied into high-strength wastewater treatment. A set of characterization analysis has been carried out on different

granule samples collected in five different processes, anaerobic (UASB) or aerobic (GSBR) treating respectively dairy or synthetic wastewaters. The nature and location of the bio-precipitation process is investigated as well as its pros and cons for the process. In an attempt to explain how the bulk conditions can affect such phenomenon, wastewaters characteristics are extensively analyzed and PHREEQC modelling software is used for calculating saturation indexes of the minerals involved.

IV.2. MATERIAL AND METHODS

IV.2.1. Solid characterization and sample preparation:

Anaerobic granule samples from 3 different UASB reactors treating wastewaters produced by cheese factories in southern France were studied. They are referred to as industrial sites 1, 2 and 3. Anaerobic granules came from the anaerobic digester mixed liquor (Methanizer 2 in figure I.5) separated from the supernatant by settling (5 minutes). No purge was made between start-up and the time granule samples were taken; HRTs were 5, 5 and 2.6 days and ORLs were 8.5, 8 and 8 kgCOD·m^{-3}·d^{-1} for sites 1, 2 and 3 respectively.

Concerning aerobic granules, they were sampled from two different GSBR processes (at the end of the aerobic reaction phase) fed with synthetic wastewater. Granular sludge had been inoculated more than one year before sampling, and the processes were operated for more than 100 days with different operating conditions: in anoxic/aerobic batch cycles for Laboratory_R1 and anaerobic/aerobic cycles for Laboratory_R2. The latter was seeded from R1 for quick start-up, as described in Liu Q.S et al. (2005). Organic loading rates and HRT were identical in both aerobic reactors: 3 KgCOD·m^{-3}·h^{-1} and 8.5 h respectively. GSBR cycles were composed of 15 min feeding, 20 min anoxic or anaerobic (mixed with nitrogen gas blowing) period, 145 min aerobic period, 30 min settling and 30 min withdrawal. More details concerning the reactor operating conditions can be found in chapter III. Granules were classified according to their size and color, as in the work shown by Iqbal Bhatti (1995). Granule samples are shown in figure IV.1, and table IV.1 summarizes their characteristics. Because of the great heterogeneity of granules from industrial sites (different colors and sizes), three granules were analyzed for each type of aggregate according to their color: gray, brown, black or white. Conversely, aerobic granules were homogeneous and more than 10 granules were collected from each aerobic reactor,

showing repeatable results. Therefore, only a few of them are shown in table IV.1. Mean diameters (D_G) of individual granules varied from 1 to 4 mm.

All granules sampled were cut into 100-µm slices with a cryo-microtome (Leica CM 30505 Kryostat) and then analyzed with a photon X analyzer (Quantax Technology Silicon Drift) which was coupled with a Scanning Electron Microscope (SEM).

The EDX probe was pointed on to at least 7 different locations in each granule section (see green marks in figure IV.3) in order to ensure the repeatability of the results. The ash content of granules was measured according to standard methods. Samples were taken in triplicate for each site and were washed with distilled water to ensure that the supernatant did not interfere in the measurement.

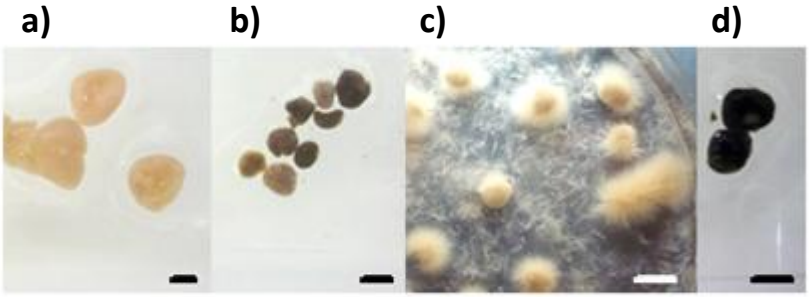

Figure IV.1: Images of the different granules sampled from: a) GSBR_1; b) UASB Industrial Site 1; c) GSBR_2; d) UASB Industrial Site 3. Scale bar=2mm length.

The EDX probe has been pointed on at least 7 different locations in each granule sample in order to ensure the repeatability of the results. The ash content of granules has been measured according to standard methods. Samples have been made in triplicate for each site and they have been washed with distillate water in order to ensure that the supernatant did not interfere in the measurement.

Table IV. 1: Classification of the granules sampled.

Sample name	Site	Condition	Diameter (D_G, mm)	Color	Legend in Figure IV.3
S_1_ana#01	Industrial Site 1 UASB	Anaerobic	3.1	white	3.a
S_1_ana#02			2.7	white	3.b
S_1_ana#03			2.5	grey	3.c
S_1_ana#04			1.2	brown	3.d
S_1_ana#05			2.6	black	3.e
S_2_ana#06	Industrial Site 2 UASB	Anaerobic	1.6	brown	3.f
S_2_ana#07			3.1	grey	3.g
S_2_ana#08			3.4	black	3.h
S_3_ana#09	Industrial Site 3 UASB	Anaerobic	4.0	grey	3.i
S_3_ana#10			2.1	grey	3.j
S_3_ana#11			2.5	black	-
S_4_aer#12	Lab Site 4 GSBR_1	Alternating Anoxic/Aerobic	2.4	brown	3.k
S_4_aer#13			1.2	brown	3.l
S_4_aer#14			1.5	brown	3.m
S_5_aer#15	Lab Site 5 GSBR_2	Alternating Anaerobic/Aerobic	3.7	brown	3.n
S_5_aer#16			2.8	brown	3.o
S_5_aer#17			3.2	brown	3.p

IV.2.2. Characterization of liquid phases and calculation of SI:

The influent and effluent of each reactor were characterized according to the standard methods (AFNOR, 1994), and results are shown in table IV.3 (ANNEX IV.1). The analytical results provided the input data for the geochemical software PHREEQC® version 2.17, which was used for calculating the concentration of the chemical species in equilibrium for each liquid phase (acid/base, ion pairs). SI for each mineral considered was calculated according to the equation IV.1, which considers the term *j* (in contrast with default calculation with PHREEQC®), which is the number of ions contained in the mineral formula considered [Paraskeva et al., 2000; Montastruc, 2003].

$$SI = \log\left(\frac{IAP}{K_{sp}}\right)^{1/j} \qquad \text{(Equation IV.1)}$$

Where *IAP* is the Ionic Activity Product of the ion activities involved in the mineral precipitation, and *Ksp* refers to the thermodynamic mineral precipitation constant at a given temperature. Modification from the default database (Minteq v4) has been proposed in order to include the thermodynamic data of some important minerals: struvite (MAP), amorphous

calcium phosphate (ACP), hydroxydicalcium phosphate (HDP) and Magnesium Whitlockite (MWH) as shown in table IV.2.

In annex IV.3, a complete database of a research over the different mineral precipitation constants at 25ºC, is shown.

Table IV. 2: Thermodynamic constants of the main minerals considered for this study (modifications on the Minteq v4 database are indicated)

Parameter	Chemical formula	Ksp Value in Modified Database	Ca/P	Ca/O	Mg/P
CAL	$CaCO_3$	6.35[2] for Ic>0.02 8.48[2] for Ic<0.02	-	0.33	-
ARAG	$CaCO_3$	8.3[7]	-	0.33	-
DOL (ordered)	$CaMg(CO_3)_2$	17.09[**]	-	0.17	-
MWH*	$Ca_{18}Mg_2H_2(PO_4)_{14}$	104.4[8]	1.29	0.02	0.14
MAP*	$MgNH_4PO_4:6H_20$	13.26[1]	-	-	1.00
NEW	$MgHPO_4:3H_2O$	5.8[2, 6]	-	-	1.00
DCPD	$CaHPO_4 : 2H_2O$	6.62[2]	1.00	0.25	-
DCPA	$CaHPO_4$	6.9[4]	1.00	0.25	-
OCP	$Ca_8(HPO_4)_2(PO_4)_4:5H_2O$	49.6[5]	1.33	0.33	-
HDP*	$Ca_2HPO_4(OH)_2$	22.60[3]	2.00	0.33	-
ACP*	$Ca_3(PO_4)_2:xH_2O$	28.92[2]	1.50	0.38	-
TCP	$Ca_3(PO_4)_2$	32.63[6]	1.50	0.38	-
HAP	$Ca_5(OH)(PO_4)_3$	58.33[1,2]	1.67	0.38	-

**: not included in the initial Minteq V4 database; **: default database References: [1] Ohlinger et al., 1998; [2] NIST database at 25°C; [3] Maurer et al., 1999; [4] Heughebaert et al., 1984; [5] Frèche, 1989; [6] Murray and May., 1996; [7] Wang et al., 2010; [8] Shellis et al., 2004*

IV.3. RESULTS

IV.3.1. Wastewater and process characteristics:

The influent and effluent of each reactor were analyzed and characterized according to section IV.2, and results are shown in table IV.3 (Annex IV.1). The processes could be considered to have reached the steady state, as they had been operated for more than one year before the sampling period. All the bioreactors showed high organic removal efficiency as more than the 95% of the COD was removed in these systems.

Whey and dairy wastewaters are rich in phosphate and proteins, reflected by the high organic nitrogen content (Demirel B. et al., 2005). In the anaerobic digesters, proteins are hydrolyzed, explaining the decrease of COD and VSS and the increase of ammonium concentration in the effluents of each site.

In the aerobic reactors, organic compounds were oxidized to carbon dioxide, ammonium was converted into nitrite and nitrates (nitrification) which were further converted into gaseous N_2 (denitrification). Phosphates were partially removed by *Biological Enhanced Phosphorus Removal* (EBPR). Alkalinity was produced in the anaerobic reactors during methane production and in the aerobic reactors during the denitrification processes. This contributed to the pH rise which was also encouraged by stripping processes (carbon dioxide) in the aerobic reactors. Phosphate removal was observed in all the systems, probably due to precipitation processes in the anaerobic reactors, whereas both precipitation and biological phosphorus removal were shown to occur in the aerobic reactors.

For all sites, the mineral content of the suspended solids in the effluent was higher than those of the influent and, simultaneously, calcium concentration in the liquid decreases in all the systems. The high quantity of suspended solids in UASB processes is linked with the high mineral content (42.6 to 80%). In these reactors, mineral content seemed to be correlated to pH: the highest pH for site 2 corresponded to the highest mineral content (80%); the lowest pH for site 1 corresponded to the lowest mineral content (42.6%). Microscopic observations of the anaerobic effluent from site 2, shows that precipitated particles are visible in the reactor bulk (figure IV.2). Microbial aggregates detached from the supernatant coming from the effluent of reactor 2 (stained in red with safranine) appeared with a non-organic prismatic structure (circled).

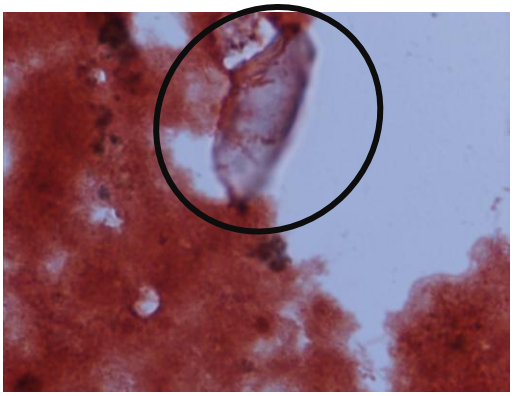

Figure IV. 2: microscopic image stained from digester 2. Red: bacterial cells; in the circle, a possible mineral precipitated in the bulk.

In contrast, no minerals were found in the supernatant of the aerobic reactors. Finally, the ash content (SMF) of the different granules has been quantified in table IV.3, pointing out that in aerobic systems, the quantity of minerals embedded in granules is strongly influenced by the process, as illustrated in GSBR 1 and GSBR 2: both reactors have similar mineral fractions in

the mixed liquor (33.7 and 38.7 % respectively), but the latter presents higher mineral content in the granules (the double), being at the same time, the reactor in which EBPR process was more remarkable (see Chapter III). In anaerobic sites, the sludge ash content is also different, varying from 28-81%. In UASB, where SMF achieved the highest values (sites 1 and 2), efficiency removal yields problems have been reported and reactors needed to be re-seeded.

IV.3.2. Analysis of mineral bioliths in granules:

Figure IV.3 shows the different SEM images taken from the different sectioned granule samples. SEM and EDX probes testing at different locations of the samples, confirmed that almost all of the granules (except two, the black ones) presented mineral inorganic concretions. These precipitates were easily detectable due to their geometrical shape, brightness and low organic matter content. In the photographs, crystallized minerals appear lighter than the organic fraction. They were mainly observed inside the granules, but in some cases precipitates were formed at the surface, as in figs.3.a and 3.b., in which a mineral layer envelops the anaerobic microbial granule. Finally, samples in figs.3.e and 3.h, did not present any sign of mineral deposition either embedded in, nor surrounding the bio-aggregate.

Bioliths found in the anaerobic granules were randomly distributed (figs. 3.c, d, f, g, i and j), although they formed a biofilm of at least 400µm beyond the aggregate surface. The bioliths in aerobic granules (figs. 3.k-3.p), constituted a large solid fraction centered in the core at least 300µm from the surface layer for figs. 3.k and l; and 800µm for figs. 3.m,n,o and p.

In the case of the granules from figures 3.a and 3.b, the mineral shell that covered the aggregates was around 400-800 µm thick on average, which represented a considerable fraction probably affecting the diffusion of nutrients and the bacterial activity. More information about EDX elemental scanning is provided in Annex IV. 2.

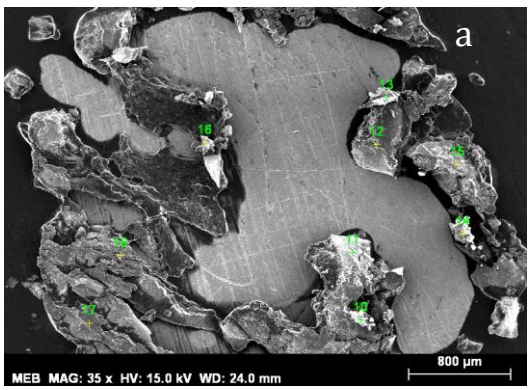

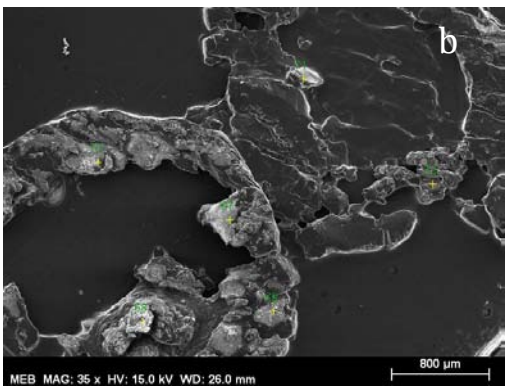

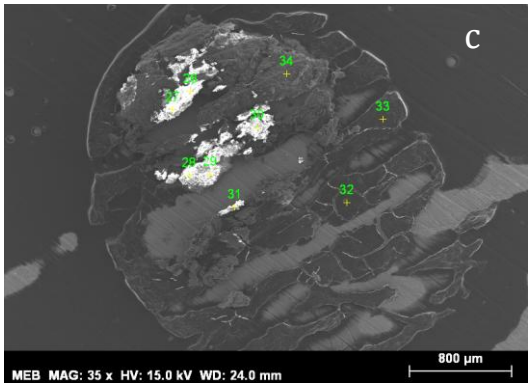
c
MEB MAG: 35 x HV: 15.0 kV WD: 24.0 mm
800 µm

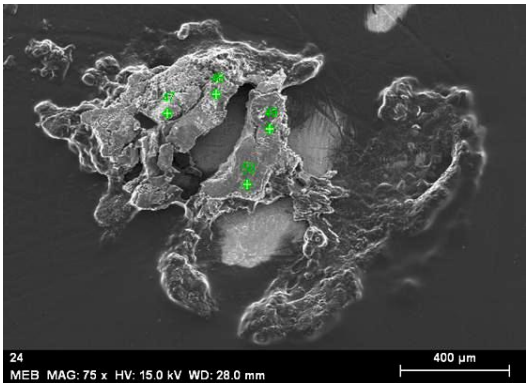
24
MEB MAG: 75 x HV: 15.0 kV WD: 28.0 mm
400 µm

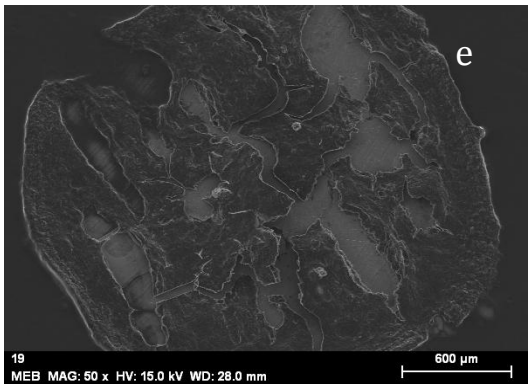
e
19
MEB MAG: 50 x HV: 15.0 kV WD: 28.0 mm
600 µm

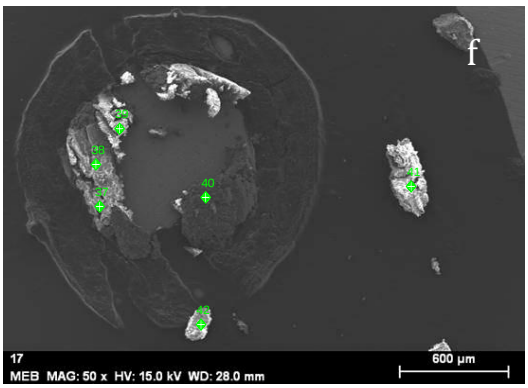
f
17
MEB MAG: 50 x HV: 15.0 kV WD: 28.0 mm
600 µm

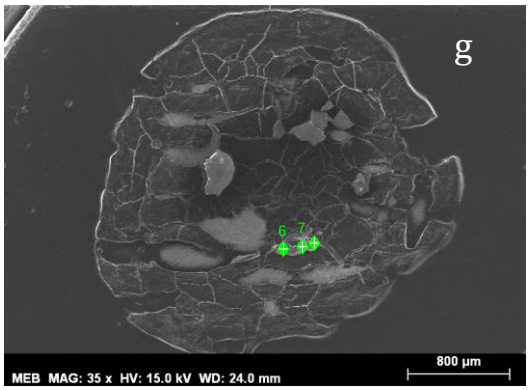
g
MEB MAG: 35 x HV: 15.0 kV WD: 24.0 mm
800 µm

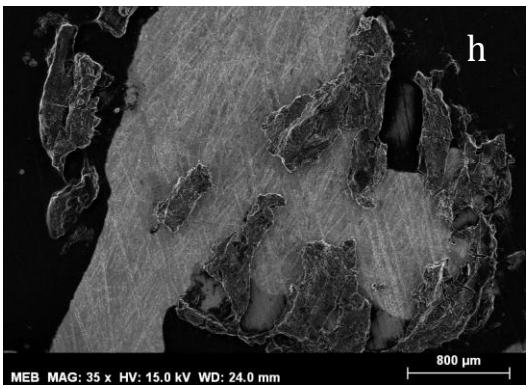
h
MEB MAG: 35 x HV: 15.0 kV WD: 24.0 mm
800 µm

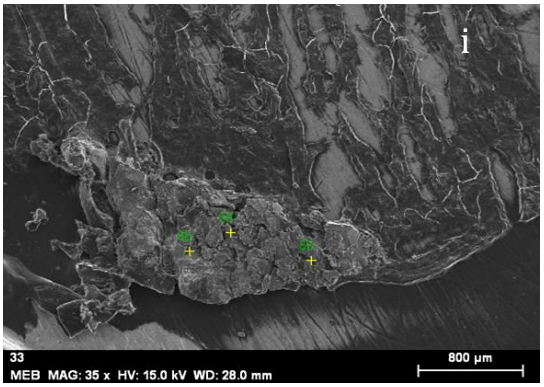
i
33
MEB MAG: 35 x HV: 15.0 kV WD: 28.0 mm
800 µm


j
27
MEB MAG: 35 x HV: 15.0 kV WD: 28.0 mm
800 µm

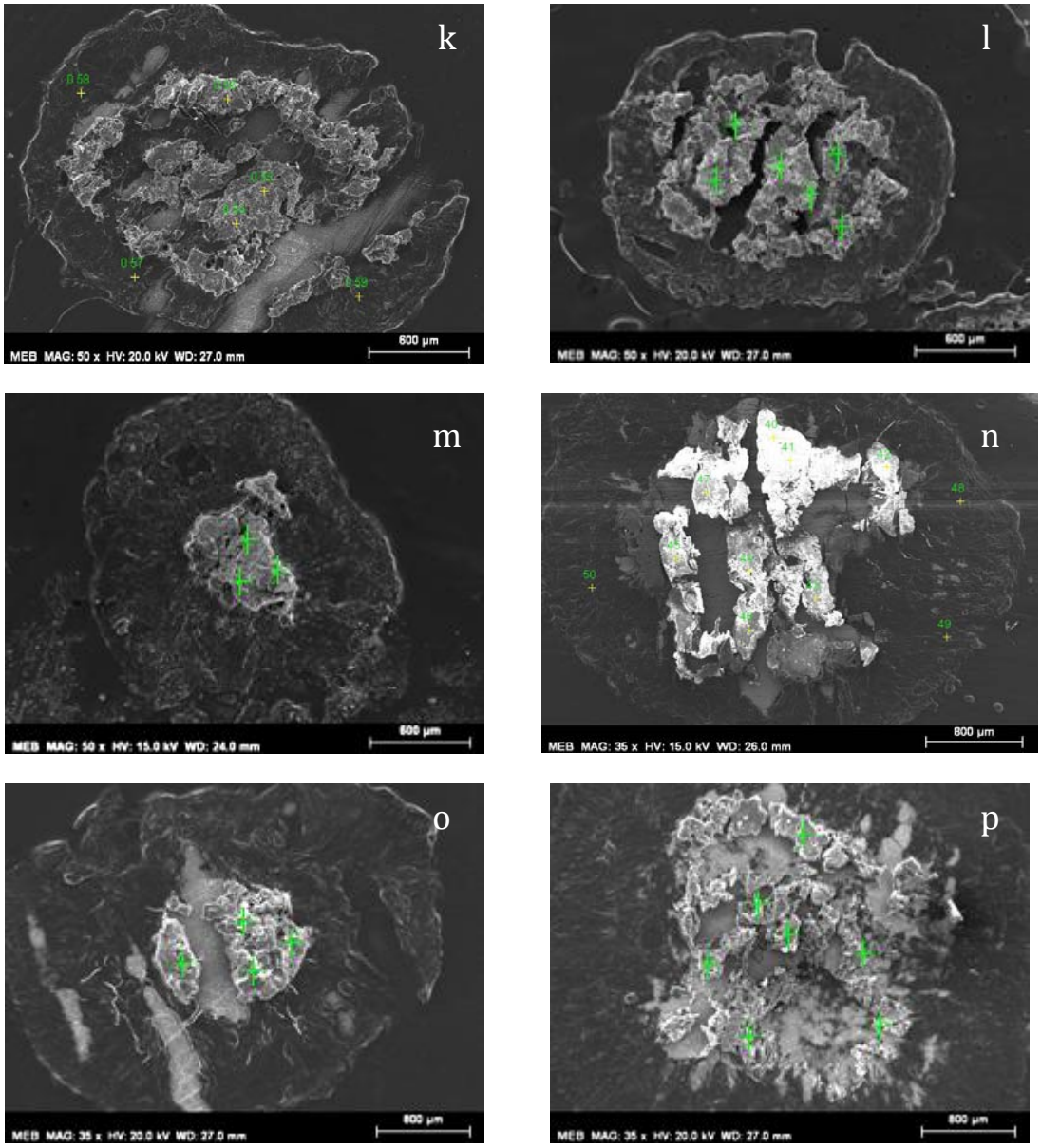

Figure IV. 3: SEM images from the granules samples. a) S1_ana#01; b) S1_ana#02; c) S1_ana#03; d) S1_ana#04; e) S1_ana#05; f) S2_ana#06; g) S2_ana#07; h) S2_ana#08; i) S3_ana#09; j) S3_ana#10; k) S4_aer#12; l) S4_aer#13; m) S4_aer#14; n) S5_aera#15; o) S5_aer#16; p) S2_aer#17. Scale bar = 800µm for (a, b, c, f, g, i, j, k, n, o, p); 600 µm for h, e, l, m; 400µm for d.

Analyses were carried out with EDX probes pointed over the mineral clusters (marked with small crosses) revealing the major element composition, and indicating the nature of the most probable mineral formed (table IV.4). A number of local analyses (at least seven) were carried out for each granule at different locations in the mineral clusters. Average values and standard deviation are shown as well in table IV.4.

It was clear that after oxygen, calcium was the major constituent of the mineral fraction, varying from 22 to 49% for anaerobic granules and from 17 to 38% for aerobic granules. The other major constituent was phosphorus, except for the granules collected in UASB reactor 2. Phosphorus content varied from 0.06 to 24% and from 7 to 15% for anaerobic and aerobic granules respectively. The magnesium content of the clusters was smaller (< 1%) and nitrogen was sparsely found in variable concentrations (0 to 4%) in some granules.

The data indicated that the molar Ca:P ratio varied from 1.25 to 1.68 in the different granules (except for those from site 2, in which no significant phosphorus was found). These values are evocative of several calcium phosphates with varying theoretical Ca:P ratios: OCP (1.33), ACP (1.5), TCP (1.5), HAP (1.67). For some samples Ca:O ratio were also of the same order of magnitude as theoretical values of calcium phosphate or calcium carbonate (0.33 to 0.38 see table IV. 2) but the Ca:O ratio showed much greater deviation than that of Ca:P, making its interpretation more difficult.

Table IV. 4: EDX analysis of mineral clusters found in anaerobic and aerobic granules (mean values from at least 7 analysis for each granule): Elemental composition (percentage in mass), molar ratios, most probable solid phase.

Sample	% Ca	% P	%Mg	% N	%O	Ca/P (molar)	Ca/O (molar)	Mineral (probable)
S1_ana#1	27.77±5.70	11.62±2.53	0.35±0.19	1.71±1.46	44.33±6.22	1.40±0.05	2.86±0.30	ACP/TCP
S1_ana#2	31.91±7.21	13.37±2.42	0.51±0.15	2.86±3.55	39.29±4.14	1.47±0.01	0.52±0.11	ACP/TCP
S1_ana#3	46.92±17.36	0.17±0.16	0.02±0.06	0.51±0.60	48.81±4.66	-	0.99±0.28	CAL/ARAG
S1_ana#4	48.99±5.93	24.02±1.65	-	-	33.36±16.81	1.25±0.12	0.68±0.25	OCP
S1_ana#5	-	-	-	-	-	-	-	-
S2_ana#6	31.25±8.57	0.06±0.14	0.06±0.10	-	49.59±3.38	-	0.26±0.03	CAL/ARAG
S2_ana#7	29.43±7.11	0.26±0.18	0.24±0.17	2.06±1.80	47.65±1.88	110±59	0.28±0.12	CAL/ARAG
S2_ana#8	-	-	-	-	-	-	-	-
S3_ana#10	26.28±4.29	11.10±2.29	0.19±0.14	-	31.64±4.27	1.44±0.08	0.33±0.01	ACP/TCP
S3_ana#11	22.40±8.90	9.36±2.99	0.39±0.05	-	42.89±0.00	1.42±0.12	0.21±0.08	ACP/TCP
S4_aer#12	32.18±8.68	13.42±2.61	0.34±0.16	-	40.55±0.15	1.65±0.10	0.38±0.18	HAP
S4_aer#13	32.55±4.98	12.37±1.94	0.24±0.28	-	41.07±0.89	1.68±0.04	0.39±0.21	HAP
S4_aer#14	38.17±11.61	14.45±3.07	0.67±0.19	-	46.05±14.32	1.62±0.05	0.64±0.20	HAP
S5_aer#15	25.80±3.07	11.38±1.01	0.43±0.13	-	46.65±3.46	1.64±0.04	0.31±0.07	HAP
S5_aer#16	16.46±1.58	7.19±0.49	0.31±1.20	4.26±1.51	39.9±0.07	1.53±0.07	0.17±0.02	ACP/TCP
S5_aer#17	32.73±5.07	11.96±1.64	0.10±0.09	0.42±0.55	34.43±5.86	1.60±0.04	0.31±0.07	HAP

"-" : mineral not found or element not detectable

The solid phase most probably formed in the granules, according to their Ca:P and Ca:O molar ratios are suggested in the last column of table IV.4. Calcium phosphates ACP, TCP, HAP were the most probable solids in the granules, except for those from UASB number 2, which seemed to contain calcium carbonate (ARAG or CAL). Almost all the aerobic granules had Ca:P ratios close to that of HAP, except for one sample from GSBR-2, in which the Ca:P ratio was closer to ACP (or TCP). As ACP and TCP are both possible precursors of HAP, further work needs to be carried out for discarding which is the one that forms inside the granules, as they have identical Ca:P ratios (See Chapter V). The same problem remains for discarding between ARAG or CAL, two calcium carbonate polymorphs.

At the anaerobic sites, results showed heterogeneity in the chemical composition of the different granules sampled for each given site. Indeed, granules from anaerobic sites were different in color and size (see table IV.1), and the nature of minerals found inside the aggregates were also different in one same reactor. For instance, at site 1, we found different granules containing calcium carbonate and calcium phosphates. At site 2, all granules containing mineral bioliths appeared to be made up of calcite or aragonite. Anaerobic granules from site 3 all contained calcium phosphates, probably ACP or TCP.

IV.3.3. Ca- P distribution during granule growth: case of GSBR

By focusing on the granular sludge from the aerobic systems (GSBRs), it was observed that small granules were continuously generated in the reactor and grew progressively with microbial activity (this process is much slower in the case of anaerobic methanogenic bacteria whose growth rate is more than ten times lower than those of aerobic bacteria). Therefore, different aerobic granules with different sizes were sampled from the two GSBR reactors (GSBR_1 = site 4, and GSBR_2 = site 5), assuming that biggest granules would be more mature than the small ones. Only the central sections are shown in figure IV.4, illustrating the evolution of the mineral formation inside the microbial aggregates from small granules to mature ones.
It can be noted that solid mineral precipitated in the center of the small granules and increased progressively, at the same time as microbial biofilm developed at the surface of the granule. In the biggest granules, successive rings of mineral were finally visible, indicating past growing periods (reminiscent of the rings of a tree trunk).

It should be noted that the stretch marks in figure IV.4 are due to the cut blade.

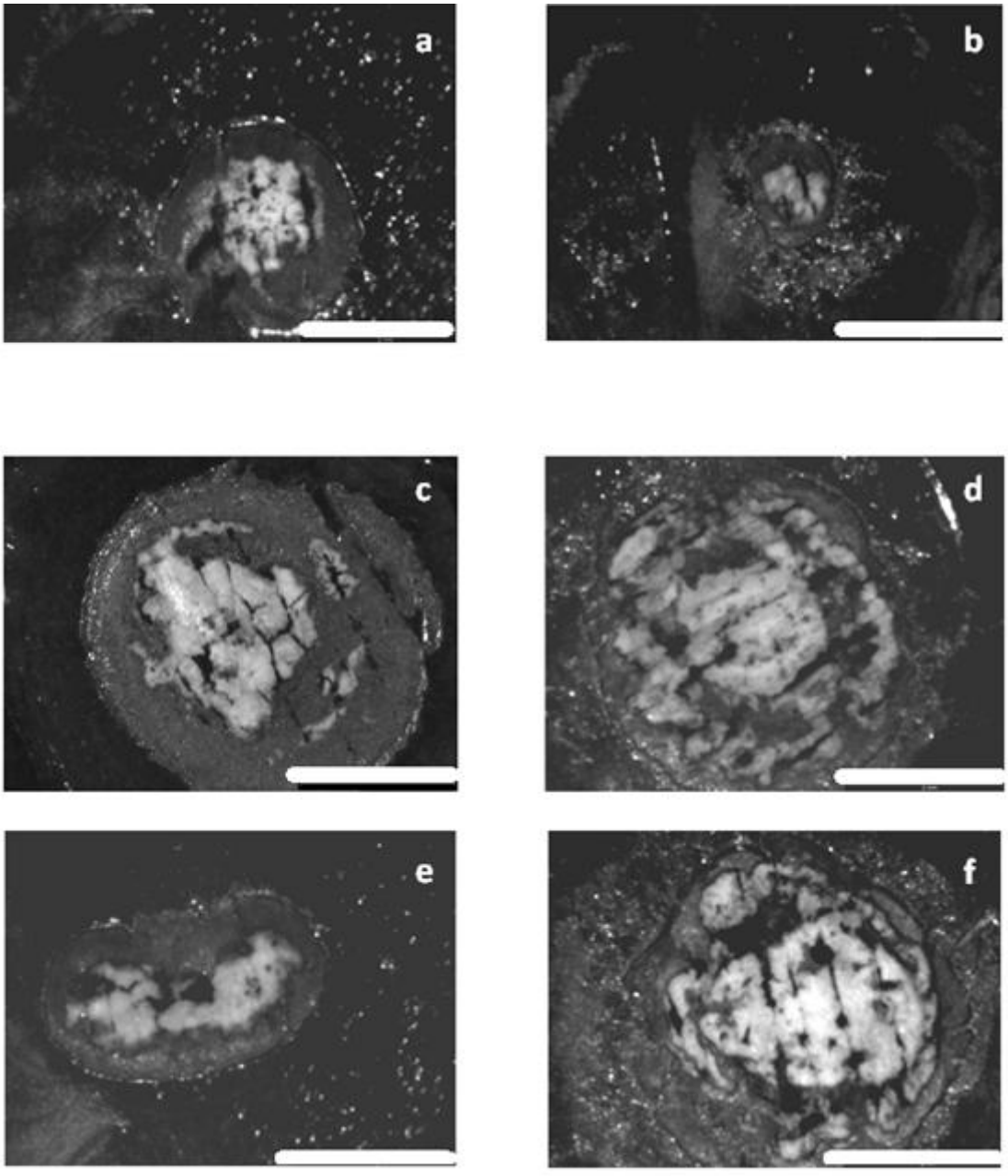

Figure IV.4: Binocular images of central slices of different granules from the GSBRs, classified from the smallest to the biggest ones. a) S_4_aer#18; b) S_5_aer#19; c) S_4_aer#20; d) S_5_aer#21; e S_4_aer#22; f S_5_aer#23. The bar scale is 2mm length.

Different mature granules from both reactors presenting a mineral-ring distribution were analyzed with an EDX probe, according to figure IV.5.

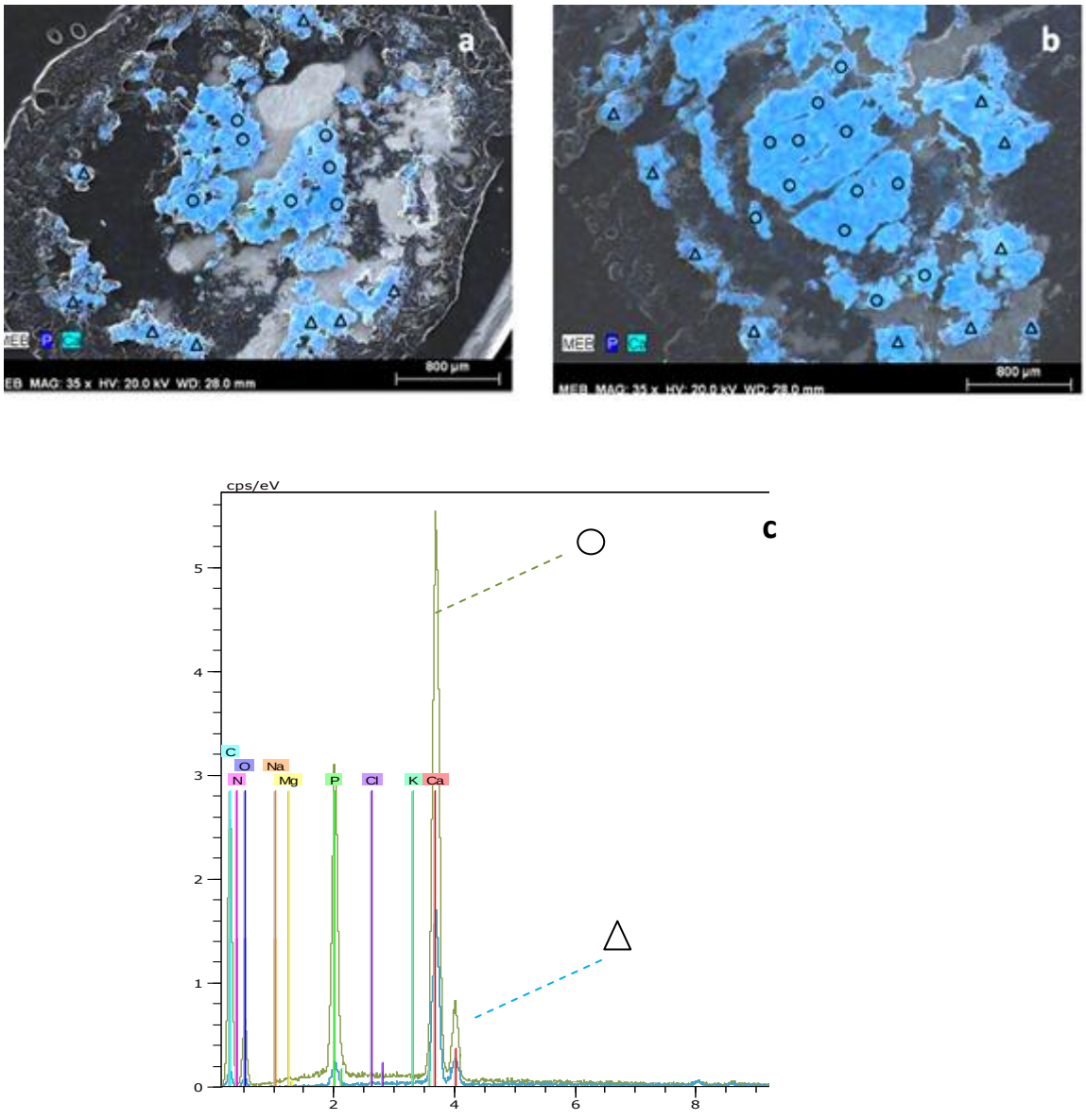

Figure IV.5: EDX analysis of the mineral layers in granules from the GSBRs. a) granule from GSBR_1; b) granule from GSBR_2; c) Inner and outer layer-patterns with EDX analysis from fig.5.a.The different "Δ" and "O" marks represent the probe pointing at the outer and inner parts respectively.

A detailed analysis with EDX probes was performed in two different zones of the mineral core of the granules: in the central zone and in the external rings as indicated in figure IV.5. The results show that mineral precipitates have slightly different compositions in the inner part compared to the external layer. In the granule shown in figure 5.a, the mean value of Ca:P ratio part of the internal layer was close to that of HAP (1.69±0.19) whereas the mineral in the

outer layer showed a lower mean Ca:P ratio of 1.52±0.20, close to that of the precursor forms ACP or TCP (theoretical Ca:P=1.5). In the second example shown in figure IV.5.b, there are three concentric layers. Lower Ca:P ratio was found in the outer layer of mineral (1.29±0.05) whereas the inner part had a Ca:P molar ratio of 1.50±0.16.

These results indicate a possible conversion from calcium phosphate precursors with lower Ca-P ratio (ACP, TCP or OCP) to the moret stable calcium phosphate hydroxyapatite (HAP) with the highest ratio found in the center (theoretical Ca:P ratio = 1.67). These results are consistent with the traditional idea that HAP formation is not the result of spontaneous nucleation but of a progressive conversion of less stable calcium phosphates, indicating that a minimal retention time in the granule is necessary to convert the precursor phases (probably ACP, TCP, or OCP) into HAP.

A zoom over the mineral fraction of aerobic granules was performed with SEM, finding out a porous honeycomb structure as can be observed in figure IV.6.

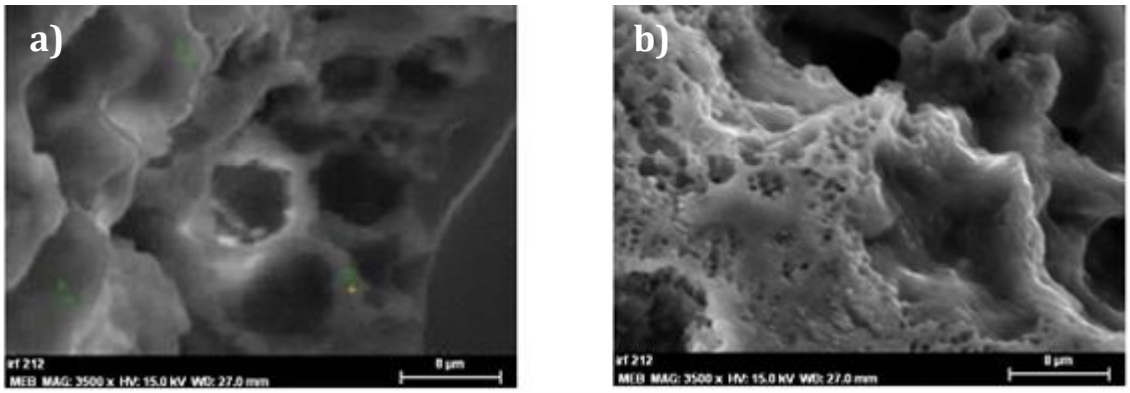

Figure IV.6: SEM images of aerobic granules. The scale bar=8µm

The holes in the bioliths may have been due to the bacterial colonies that have been progressively disappearing (the diameters of the small holes in figure 6.b are evocative of the pore sizes that would be produced by such a phenomenon) or from gaseous metabolite exchanges (CO_2, N_2, etc.). These assumptions will be further discussed in section IV.4.

IV.3.4. Calculation of saturation index in the different reactors

The saturation indexes of the minerals that could precipitate were calculated with PHREEQC software according to the liquid composition of each reactor stream. pH and temperature values used in the calculations were those of the reactor outputs. It was assumed that the conditions inside each reactor are similar to that of the outlet if proper mixing was imposed in the reactor, which considering the different scale, is more realistic in the case of lab scale reactors (GSBRs from sites 4 and 5) than in the full scale UASB reactors (sites 1, 2, 3).

The results (shown in table IV.5) indicated the compounds with a positive SI which were likely to precipitate. Concerning calcium phosphate, results confirmed that hydroxyapatite (HAP), amorphous calcium phosphate (ACP), tricalcium phosphate (TCP) and ordered dolomite (DOL), were systematically supersaturated in all the samples, which is in accordance with the analysis of the solid phase.

Calculations also showed that struvite (MAP) was under-saturated in all the reactors as were newberite (NEW), magnesium whitlockite (MWH) and octacalcium phosphate (OCP). Finally, brushite (DCPD) and monetite (DCPA), both precursors of HAP, were found to be supersaturated in some anaerobic reactors, but not in aerobic ones (GSBRs). Calcium carbonates, be they calcite (CAL) or aragonite (ARAG), were supersaturated in most of the systems, except for UASB 1. The higher SI value achieved was in site 2, where calcium carbonates had been detected in the solid phase. It must also be noticed that either Calcite (CAL) or Aragonite (ARAG), were supersaturated in the GSBR (sites 4 and 5), whereas no calcium carbonates were found in the aerobic granules. This indicated either (i) the possible effect of precipitation inhibitors (e.g. phosphates), or (ii) the fact that ARAG or CAL precipitates in another zone (reactor walls, recirculation pipes), but not in the microbial granules. Another possibility is the precipitation of calcium carbonate in the bulk, with possible nucleation on suspended solids or free bacteria (flocs). Crystals were not observed in the supernatant of aerobic granular sludge process, in contrast to anaerobic sites, in which solid crystals were detected in some samples (figure IV.2).

Table IV. 5: SI values for the mineral phases calculated with PHREEQC in the effluent

Mineral phase	*UASB_site 1*	*UASB_site 2*	*UASB_site 3*	*GSBR_site 4*	*GSBR_site 5*
ARAG	-0.09	**0.44**	**0.18**	**0.23**	**0.20**
CAL	-1.08	-0.55	-0.81	**0.33**	**0.29**
DOL(ord)	**0.02**	**0.49**	**0.15**	**0.18**	**0.14**
MWH	-2.72	-2.50	-2.78	-2.45	-2.48
MAP	-0.27	-0.10	-0.45	-	-0.61
NEW	-0.37	-0.46	-0.73	-0.94	-0.98
DCPD	**0.06**	**0.09**	-0.04	-0.18	-0.20
DCPA	**0.18**	**0.22**	**0.10**	-0.03	-0.05
OCP	-5.63	-5.27	-5.71	-5.27	-5.33
HDP	-0.24	**0.00**	-0.26	**0.15**	**0.13**
ACP	**0.25**	**0.55**	**0.26**	**0.73**	**0.70**
TCP	**1.04**	**1.32**	**1.02**	**1.45**	**1.41**
HAP	**0.92**	**1.23**	**0.92**	**1.44**	**1.41**
Ic (mol/kg)	0.05	0.10	0.08	0.02	0.01
pH	6.67	7.4	6.88	8.41	7.85
T(°C)	33	30	29	21	21

Carbonate saturation is encouraged by accumulation of mineral carbon produced by microbial reactions. Higher SI values were observed for anaerobic site 2, at which the pH (7.4) was slightly higher than in other anaerobic processes (sites 1 and 3). In aerobic systems, because aeration encouraged carbon dioxide stripping and nitrification consumed alkalinity, inorganic carbon concentration was lower than in anaerobic reactors. However, the relatively high pH at which both GSBR worked explained the supersaturation of calcium carbonate at sites 4 and 5.

The SI values in the effluent indicate the mineral that is still super-saturated after the process. However, due to a long retention time and possible rapid precipitation (especially in anaerobic systems), equilibrium can be reached in the reactors, leading to a reduction of SI (stabilized around zero). Thus, the variation of SI (namely ΔSI) was calculated between the SI calculated for outlet concentrations and the SI calculated for the inlet concentrations of the volume control (each reactor).

$$\Delta SI = SI_{effluent} - SI_{influent}$$

Of all the minerals included in the simulation, only those with positive SI in least one stream were considered for the ΔSI calculation in figure IV.7. Thus, a ΔSI<0 could indicate a possible SI decrease in the effluent due to precipitation. Although alkalinity was produced during the anaerobic processes, a decrease of SI was observed in UASB 2, which indicated that calcium carbonate should precipitate, in accordance with previous local observations. ΔSI of calcium phosphates (DCPD, DCPA, HDP, ACP, TCP, and HAP) decreases in all the aerobic systems, which can be explained by the precipitation of some of these compounds, also confirmed by previous granules analysis. Similarly, in the case of the anaerobic sites, HDP precipitation seems to be discarded.

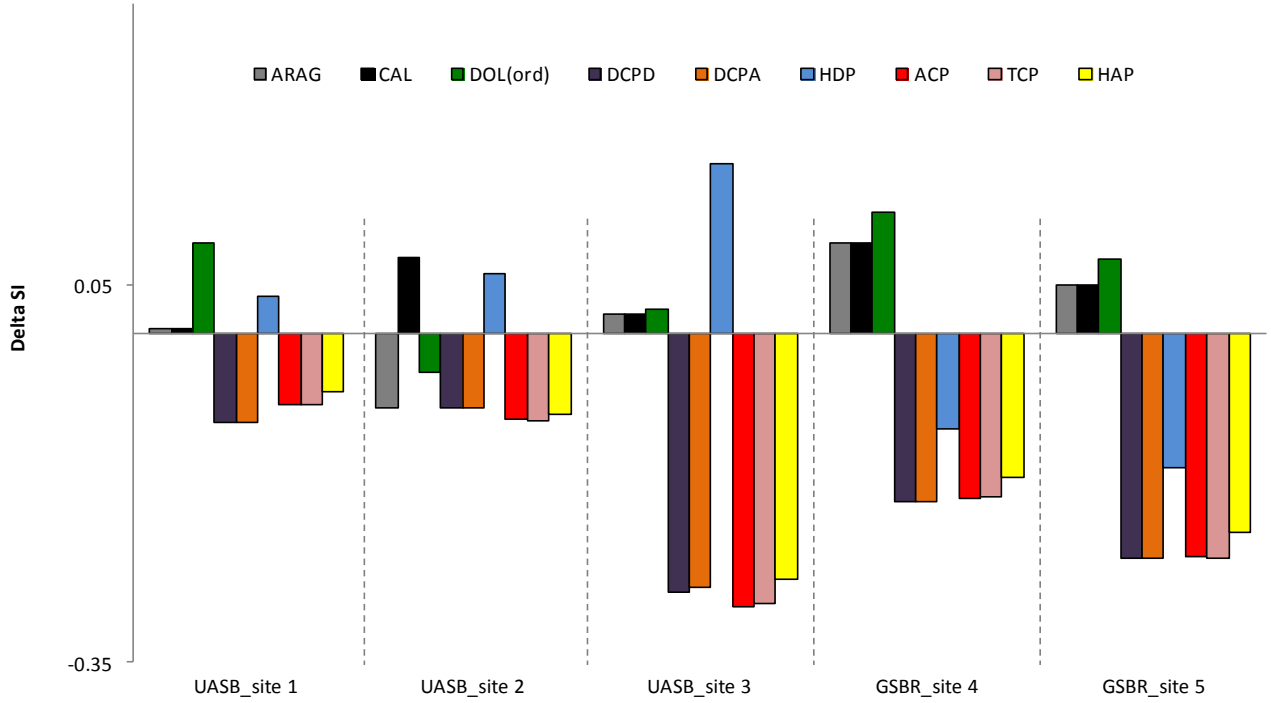

Figure IV.7: ΔSI for the different minerals that can precipitate in the different reactors considered.

IV.4. DISCUSSION

IV.4.1. Nature of precipitates: consistency between the local analysis observation and the Saturation Indexes.

SEM-EDX analysis demonstrated that calcium phosphates were the major precipitates found in the granules, both aerobic or anaerobic. More specifically solid composition was close to those of hydroxyapatite (HAP), amorphous calcium phosphate (ACP) or tricalcium

phosphates (TCP). This was consistent with the analysis of Saturation Index in the liquid phase, indicating that these minerals were systematically saturated.

Concerning other calcium phosphate precursors only one sample (brown-type ones, S1_ana#4) shows Ca:P and Ca:O ratios which could implicate an OCP precursor. This seems consistent with the fact that pH in site 1 is the lowest one, and Gao and co-workers (Gao et al., 2010) reported the formation of HAP through OCP precursor at acidic pH. However, of all the calcium phosphate precursors proposed in the literature for acidic pH (DCPD, DCPA and OCP), only OCP was not observed to be saturated in the bulk according to PHREEQC calculations.

Calcium carbonates were only observed in some granules, mainly in site 2 coinciding with the higher pH and alkalinity values among the anaerobic sites. In the aerobic reactors, despite pH values are higher than in the anaerobic ones, alkalinity is reduced by the nitrification reactions, explaining the lower carbonate precipitation potential. Carbonates are well-known competitors of phosphates for calcium bounding, competing for the active nucleation and crystal growth sites (Langerak, 1998; Plant and House, 2002). Moreover, it is known that this competition is severely influenced by pH (House, 1987). Working with digester supernatant, Battistoni and co-workers (1997) reported that a pH between 7-8.5 would favor phosphate precipitation, whereas a higher pH (9-11), would favor carbonates. At dissolved concentrations higher than 20μmol/L (which is the case of all industrial sites), P is supposed to inhibit calcite or aragonite precipitation (Plant and House, 2002). In this study, P and Ca concentration measured in the bulk are relatively similar in all industrial reactors but pH and alkalinity was slightly higher in site 2. The simultaneous presence of carbonate or phosphate in the same reactor could be also possibly due to local heterogeneities. Therefore carbonate would preferentially precipitate in granules, where the microbial activity would induce proper pH for carbonate deposition (or in zones were alkalinity accumulates).

In contrast with calcium precipitates, neither magnesium phosphate nor magnesium carbonate was significantly observed in the microbial granules. The effect of calcium as the main inhibitory factor for magnesium phosphate precipitation, has been widely reported. Moreover, Shen et al., (2001) made different experiments with dairy wastewater showing that high Ca:Mg ratios were not inhibitory for struvite concentration if enough magnesium and pH concentration were present in the wastewater. Therefore, he demonstrated struvite precipitation in such effluents by adding a calcium chelating agent (EDTA) or calcium oxalate, for previous magnesium and phosphate release prior struvite precipitation. He demonstrated that it was possible even with Ca:Mg initial ratios of 1.46 (note that Ca:Mg ratios of UASB 2

=1.43); and that rather than adding Mg to lower the ratio, it was more efficient to decrease calcium concentration by sequential precipitation with other minerals free of phosphate.

Especially the case of struvite should be pointed out: struvite was never found in the granules despite the high concentration of ammonium and phosphorus in the anaerobic effluents. It was thermodynamically under-saturated in all of the liquid phases of the processes studied, either aerobic or anaerobic. This can be explained by the fact that pH in the UASB is not high enough to let struvite precipitation, whereas higher pH conditions (e.g. strong stripping) lead to struvite crystal formation in the bulk (results not shown). Indeed struvite precipitation rate is rapid, which could lead to its precipitation in the bulk, or in specific zones when proper pH is achieved (notably > 7.4) (Ohlinger et al., 1998).

IV.4.2. Location of mineral bioliths: a possible role of microbial reactions?

The discussions above suggest that another important aspect is the location of the inorganic deposits in the different granular sludge processes. By modelling calcite precipitation, Langerak and co-workers (2000) established different physical or chemical conditions for operating a UASB favoring precipitation in the bulk rather than in granules: 1) a low Ca:Na ratio, 2) small granule diameter 3) a high mineral crystallization rate constant and 4) An influent [Ca^{2+}] < 390 mg/L. In our case, information provided about the industrial effluents of the different sites and the number of samples are not sufficient to confirm most of these statements (Ca:Na, granule size, …). However from a general point of view, the location of mineral crystals certainly depends either on physico-chemical and biological phenomena. The major one, as stated by Langerak, is probably the crystallisation rate constant. In our case, information provided about the industrial effluents of the different sites and the number of samples were not sufficient to confirm most of these statements (Ca:Na, granule size, …). However, from a general point of view, the location of mineral crystals certainly depends on both physicochemical and biological phenomena. The major one, as stated by Langerak, is probably the crystallization rate constant.

Indeed, it should be noted that the mineral crystallization rate of hydroxyapatite is clearly the lowest in calcium phosphate according to the literature, and this form was shown to accumulate in the core of granules. In contrast, the other forms (ACP, TCP, OCP), which could be formed rapidly, were mainly observed in the periphery of aggregates, and could also be formed rapidly in the supernatant (see chapter V). A first example is provided by the “white” granules

from UASB site 1 (S1_ana#01 and S1_ana#02), in which a mineral concretion was precipitated at the surface (ACP or TCP). This was also illustrated by the detailed analysis of granules from GSBR (sites 4 and 5), revealing that Ca:P ratios similar to those of HAP were mainly found in the central part of granules whereas more unstable but more rapidly formed phases (ACP, TCP, OCP) were found at the periphery.

Precipitation can be also related to the local conditions imposed by microbial reactions. Bacterial activity contributes to biomineralization by modifying local supersaturation, because ion and proton exchanges in the environment generate some gradients within the bio-aggregates. The spatial distribution of mineral clusters in the granules seems to show that local conditions in the core of microbial granules are favorable for calcium phosphate accumulation (especially HAP). Another observation (figure IV.2) is that, for granules from aerobic reactors (GSBR), precipitates (bioliths) are found in the central part of the aggregates, whereas they are randomly distributed in the granules from anaerobic processes (UASB). A possible explanation is that local microbial modification of pH, carbonate and phosphate concentration, could encourage this precipitation.

According to microbial analysis over cross-section of anaerobic granules (Batstone et al., 2006; Quarmby and Foster, 1995), these bacteria are stratified as follows: acidogens are located in the outer part of the granules, while acetoclastic methanogens form clusters in the central part. Hydrolysis, acidogenesis and acetogenesis tend to release protons, while methanogenesis consumes protons (0.25 mmolH+ release/1 mmol acetate or H_2 uptake). These observations lead us think that a pH increase in the environment of methanogens clusters could generate favorable conditions for precipitation.

Similarly in aerobic granular sludge processes, whereas nitrification takes place in aerobic zones of granules, denitrification consumes protons in their anoxic zones.(Wan et al., 2009; Mañas et al., 2009). Calcium phosphate precursors initially formed in the periphery are progressively converted into a stable form (hydroxyapatite) in the core. Future work would be necessary to discover how microbial reactions could modify the local pH and so play a role in this precipitation phenomenon. In addition, another possible interaction would be due to polyphosphate accumulating bacteria (PAO), whose ability to release phosphate during anaerobic periods transiently increases the calcium phosphate saturation in their environment.

IV.4.3. Consequences of precipitation.

From a general point of view, the role of biomineralization in microbial functions remains uncertain. Some authors support that it is the accidentally result of a metabolic by-product that can cause cell disruption (Knorre and Krumbein, 2000), while others are committed to the fact that it is a specific process with ecological benefits, like providing more strengthening and resistance properties (*Ehrlich, 1996*; *McConnaughey and Whelan, 1997*). Accidentally or not, this phenomenon is reported to contribute favorably to the bioremediation field, where several applications for ion removal from wastewaters have been pointed out at the introduction of this chapter.

In aerobic GSBR, the biomineralization of calcium phosphates is a side dephosphatation process that takes place simultaneously in these aggregates, contributing to increase the settling velocity and to the P removal yield (Mañas et al., 2011). Driving the precipitation inside granules instead of in the bulk could entrain other advantages like the control of the spontaneous precipitation in pipelines and walls, responsible of clogging and high operational costs (Borgerding, 1972). In anaerobic processes, Langerak found out that the development of a high ash sludge content contributed to biomass cementation and stabilization, which is an important parameter for operating UASB reactors. However, this process should be accurately controlled as negative consequences can be also reported. Kettunten and Rintal (1998) reported losses of biomass methanogenic activity with high ash content in the sludge, constituting a deterrent for long-stabilization of UASB reactors. In the industrial cases studied, when precipitation took place at the surface of the aggregates, the methane production performance decreases and the UASB reactor had to be restarted with new fresh granules if a regular sludge extraction is not performed. In our case, both UASB containing the higher SMF sludge, were reported to lose removal efficiency and thus, needed to be restarted with fresh granules, stressing importance over the bioavailability losses that take place at higher mineral fraction. In aerobic site 5, mineral content in sludge was also relevant (68%), and some instability problems (VSS decrease) were remarked. Thus, a compromise should be adopted and a regular granule extraction must be done in order to operate stable and efficient GSBR systems, which implicates an exhaustive SRT control, which have an impact not only over the mineral phases, but also on the microbial communities that perform nitrogen removal. In any case, the use of thermo-chemical databases for estimating saturation indexes can give an indication of the precipitation potential. However the location of precipitation is still complex to predict, involving either physico-chemical driving mechanisms (kinetic) and microbial induced phenomena. From a

modelling point of view, future work will be necessary to be able to predict the exact calcium phosphate precursors that finally form HAP and how can microbially induced phosphorus precipitation (MIPP) be controlled with operating conditions in the reactor.

IV.5. CONCLUSIONS

Local analysis of mineral precipitation in microbial granules from anaerobic and aerobic reactors, has lead to the following conclusions:

Calcium phosphates were the major precipitates found in the granules sampled. SEM-EDX analysis demonstrated that solid composition is close to hydroxyapatite (HAP), amorphous calcium phosphate (ACP) or tricalcium phosphates (TCP). This was consistent with the analysis of the Supersaturation Index in the liquid phase, indicating that these minerals were systematically saturated in the bulk.

Calcium carbonate was only found in the granules from the anaerobic UASB 2 with the highest operating pH (treating industrial wastewater). Struvite was not found in the granules and it was thermodynamically saturated in all the processes studied, be they aerobic or anaerobic.

Spatial distribution of mineral clusters in the aerobic granules seems to point out that local conditions in the core of microbial granules are favorable for calcium phosphate accumulation (especially HAP), whereas other minerals (like calcium carbonates) could rather appear in the bulk. Results also indicate that calcium phosphate precursors initially formed in the periphery are progressively converted on the core into a more thermodynamically stable form (hydroxyapatite). These phenomena could be explained not only by differences in the crystallization kinetics, but also by the local pH modification within the granules due to microbial activity (anaerobic or anoxic).

To conclude, the supernatant composition can contribute to predicting the nature of the bioliths developed in granular sludge, but it is not the sole determinant factor, as it does not explain the differences found in different granules grown in the same reactor. This places emphasize on the role of microbial reactions over all the mechanisms contributing to the biomineralization phenomenon.

IV.6. ACKNOWLEDGMENTS AND CONTRIBUTIONS

I would like to highlight and thank VALBIO Company and specially F. Decker and D. Auban for their helpful contribution in this work.

IV.7. REFERENCES

Abbona F., H.E. Lundager Madsen, R. Boistelle. (1982). Crystallization of two magnesium phosphates, struvite and newberyite: Effect of pH and concentration. J. Crys. Growth, 57: 6‑14.

AFNOR, 1994. Recueil de normes française-Qualité de l'eau.

Barabesi, C., Galizzi, A., Mastromei, G., Rossi, M., Tamburini, E., Perito, B. (2007). Bacillus subtilus gene cluster involved in calcium carbonate biomineralization. *Journal of Bacteriology* 189: 228–235.

Batstone D.J., Picioreanu C., van Loosdrecht M.C.M. (2006). Multidimensional modelling to investigate interspecies hydrogen transfer in anaerobic biofilms. Water Research 40(16):3099-3108.

Battistoni P., Fava G., Pavan P., Musacco A., Cecchi F. (1997). Phosphate removal in anaerobic liquors by struvite crystallization without addition of chemicals: Preliminary results. *Water Research* 31 (11): 2925-2929.

Bazylinski, D.A., Frankel, R.B., (2004). Magnetosome formation in prokaryotes. *Nature Reviews Microbiology* 2: 217–230.

Benzerara K., Miot J., Morin G., Ona-Nguema G., Skouri-Panet F., Férard C. (2011). *Comptes Rendus Geoscience* 343: 160-167.

Ben Omar N., M. Entrena, M.T. González-Muñoz and J.M. Arias. (1994). Effects of pH and phosphate on the production of struvite by Myxococcus xanthus. *Geomicrobiology Journal* **12** (2).

Ben Omar N., Martínez-Cañamero M., González-Muñoz M.T., Arias J.M., Huertas F. (1995). Myxococcus xanthus' killed cells as inducers of struvite crystallization. Its possible role in the biomineralization processes, Chemosphere, 30 (12): 2387-2396.

Bhatti Iqbal Z., Furukawa K., Fujita M. (1995). Comparative composition and characteristics of methanogenic granular sludges treating industrial wastes under different conditions. *Journal of Fermentation and Bioengineering* 79 (3): 273-280.

Bordering, J. (1972). Phosphate deposits in digestion systems. J. Water Pollution Control Federation, 44(5): 813-819.

Burns J.R., B. Finlayson (1982). Solubility product of magnesium ammonium phosphate hexahydrate at various temperatures, Journal of Urology, 128 (2): 426‑428.

Castanier S., G. Le Metayer-Levrel and J.-P. Perthuisot, (1999). Calcium carbonates precipitation and limestone génesis: the microbiogeologist point of view. *Sedimentary Geology*. 126 (1-4):9-23.

Demirel B., O. Yenigun, T. Onay, Anaerobic treatment of dairy wastewaters: a review. (2005). Process Biochemistry, Vol. 40: 2583-2595.

De Muynck W., de Belie N., Verstraete W. (2010). Microbial carbonate precipitation in construction materials: A review. *Ecological Engineering* 36(2): 118-136.

De Muynck W, Cox K., De Belie N., Verstraete W. (2008a). Bacterial carbonate precipitation as an alternative surface treatment for concrete , Construction and Building Materials, 22(5): 875-885.

De Muynck W, Debrouwer D., K., De Belie N., Verstraete W. (2008b). Bacterial carbonate precipitation improves the durability of cementitious materials, Cement and Concrete Research, 38 (7): 1005-1014.

Driessens F.C.M., R.M.H. Verbeeck (1981). Metastable states in calcium phosphate - aqueous phase equilibrations. Journal of Crystal Growth, 53(1):55-62

Dupraz, C., Reid, R.P., Braissant, O., Decho, A.W., Norman, R.S., Visscher, P.T. (2009). Processes of carbonate precipitation in modern microbial mats. Earth-Science Reviews 96: 141–162.

Ehrlich H. (1996). Geomicrobiology: its significance for geology. *Earth-Science reviews* 45(1-2): 45-60.

Frèche M., (1989). Contribution à l'étude des phosphates de calcium ; Thesis I.N.P. Toulouse.

Fujita, Y., Redden, G.D., Ingram, J.C., Cortez, M.M., Ferris, F.G., Smith, R.W. (2004). Strontium incorporation into calcite generated by bacterial ureolysis. *Geochemica Cosmochimica Acta* 68(15):3261–3270.

Gao R., van Halsema F.E.D. Temminghoff E.J.M. van Leewen H.P., van Valenberg H.J.F. Eisner M.D., Giesbers M., van Boekel M.A.J.S. (2010). Modelling ion composition in simulated milk ultrafiltrate (SMUF). I: Influence of calcium phosphate precipitation. Food Chemistry 122(3):700-709

González-Muñoz, M., Arias, J.M., Montoya, E., Rodriguez-Gallego, M. (1993). Struvite production by Myxococcus coralloides D. *Chemosphere* 26 (10), 1881–1887.

González-Muñoz M.T., Ben Omar N., Martínez-Cañamero M., López Galindo A., Arias J.M. (1997). Struvite and calcite crystallization induced by cellular membranes of Myxococcus xanthus. *Journal of Crystal Growth 1*63 (4-2): 434-439.

Hammes F. Verstraete W. (2002). Key roles of pH and calcium metabolism in microbial carbonate precipitation. *Reviews in Environmental Science and Biotechnology* 1(1):3-7

Hammes F., Boon N., Villiers J., Verstraete W., Douglas Siliciano S. (2003). Strain-Specific Ureolytic Microbial Calcium Carbonate Precipitation. *Applied and Environmental Microbiology* 69(8):4901-4909.

Heughebaert J.C., J.F. De Rooij, G.H. Nancollas (1986). The growth of dicalcium phosphate dihydrate on octacalcium phosphate at 25°C. *Journal of Crystal Growth* 76(1): 192-198.

Hohman C., Winkler E., Morin E., Kappler A. (2010). Anaerobic Fe^{2+}-oxidizing bacteria show as resistance and immobilize As during Fe^{3+} precipitation. *Environmental Science Technology*. 44: 94-101.

House W. A. (1987). Inhibition of calcite crystal growth by inorganic phosphate. J. Colloid and Interface Science. 119 : 505-511.

Iza J., Keenan P. J. and Switzenbaum M. S. (1992). Anaerobic treatment of municipal solid waste landfill leachate: operation of a pilot scale hybrid UASB/AF reactor. Wat. Sci. Technol 25 : 255-264.

Kettunen R.H., Rintal J.A. (1998). Performance of an on-site UASB reactor treating leachate at low temperature, Water Research, Vol. 32: 537-546.

Knorre H.V., Krumbein W.E. (2000). Bacterial calcification in microbial sediments. Springer-Verlag Berlin: 25-31.

Langerak van E. P. A., H. Ramaekers, J. Wiechers, A. H. M. Veeken, H. V. M. Hamelers, G. Lettinga (2000). Impact of location of CaCO3 precipitation on the development of intact anaerobic sludge. Water Research 34 (2): 437-446

Langerak van E. P. A., Beekmans M. M. H., Beun J. J., Hamelers H. V. M. and Lettinga G. (1998) Influence of phosphate and iron on the extent of calcium carbon- ate precipitation during anaerobic digestion. Control of Calcium Carbonate Precipitation in Anaerobic Digestion. Thesis, Wageningen Agricultural University, The Netherlands.

Lehninger A. (1988). Bioquímica. 2nd Edition, Omega Publishers.

Le Métayer-Levrel G., Castanier S., Orial G., Loubière J.F., Perthuisot J.P. (1999). Applications of bacterial carbonatogenesis to the protection and regeneration of limestones in buildings and historic patrimony. *Sedimentary Geology* 126(1-4):25-34.

Lemaire, R.L.G. (2007). Development and fundamental investigations of innovative technologies for biological nutrient removal from abattoir wastewater. PhD Thesis, Advanced Water Management Centre. Brisbane, University of Queensland.

Lettinga, G., van Nelsen, A.F.M., Hobma, S.W., de Zeeuw, W., Klapwijk, A., (1980). Use of the upflow sludge blanket (USB) reactor concept for biological wastewater treatment, especially for anaerobic treatment. Biotechnology and Bioengineering, 22 : 699-734.

Y.P. Lin, P.C. Singer (2006). Inhibition of calcite precipitation by ortho-phosphate: speciation and thermodynamics considerations. Geochimica et Cosmochimica Acta, 70:. 2530‑2539

Liu, Y., Tay, J.-H., (2002). The essential role of hydrodynamic shear force in the formation of biofilm and granular sludge. Water Research 36: 1653-1665.

Liu Q.S., Liu Y., Tay S.T.L., Show K.Y., Ivanov V., Moy B.Y.M, and Tay J.H., (2005) *Startup of pilot-scale aerobic granular sludge reactor by stored granules*, Environmental Technology Jounal, 26: 1363-1370.

Loewenthal R. E., Kornmuller U. R. C. and Van Harden E. P. (1994). Struvite precipitation in anaerobic treat- ment systems. Water Sci. Technol. 30(12), 107±116.

Mamais D., Pitt P. A., Cheng Y. W., Loiacono J. and Jenkins D. (1994) Determination of ferric chloride dose to control struvite precipitation in anaerobic sludge digester. Water Environ. Research 66(7), 912±918.

Mañas A., Sperandio M., Biscans B. (2009). Inducing mineral phosphate precipitation in biological aggregates for wastewater treatment and phosphorus recovery in a Sequencing Batch Reactor. Congrès National SFGP, Marseille 2009.

Mañas A., Biscans B., Spérandio M. (2011). Biologically induced phosphorus precipitation in aerobic granular sludge process . Water Research, 45(12):3776-3786

Maurer M., D. Abramovich, H. Siegrist, W. Gujer,. Kinetics of biologically induced phosphorus precipitation in wastewater treatment, Water Research, Vol.,33 (1999), 484-493.

McConnaughey T.A. and Whelan J. F. (1997). Calcification generates protons for nutrient and bicarbonate uptake. *Earth-Science. Reviews*. 42: 95-117.

H. McDowell, T.M. Gregory, W.E. Brown (1977). Solubility of $Ca_5(PO_4)_3OH$ in the system $Ca(OH)_2$‑H_3PO_4‑H_2O at 5, 15, 25, and 37º C . J. Res. Natl. Bur. Stand., 81A :273‑281

Montastruc L. (2003). Modélisation et optimisation d'un réacteur en lit fluidisé de déphosphatation d'effluents aqueux. Ph.D. Thesis at INPT and UPS Toulouse III

Murray K. and May P. M. (1996) Joint Expert Speciation System (JESS). An international computer system for determining chemical speciation in aqueous and non-aqueous environments. Supplied by Murdoch University, Australia.

Musvoto E.V., M.C. Wentzel, R.E. Loewenthal, G.A. Ekama (2000a)Integrated chemical–physical processes modelling—I. Development of a kinetic-based model for mixed weak acid/base systems Water Research, 34(6): 1857-1867

Musvoto E.V., M.C. Wentzel, G.A. Ekama (2000b) Integrated chemical–physical processes modelling—II. simulating aeration treatment of anaerobic digester supernatants . Water Research, 34 (6): 1868-1880.

NIST database: Searchable bibliography of Fundamental Constants. Available at: http://www.nist.gov/pml/data/physicalconst.cfm (consulted on January 2011).

Nordstrom D.K., J. W. Ball, R. J. Donahoe, D. Whittemore (1989). Groundwater chemistry and water-rock interactions at Stripa. Geochimica et Cosmochimica Acta, Volume 53 (8):1727-1740.

Ohlinger, K.N., Young, T.M., Shroeder, E.D. (1998). Predicting struvite formation in digestion. Water Research 32 (12): 3607-3614.

Paraskeva C.A., Charalambous P.C., Stokka L.E., Klepetsanis P.G., Koutsoukos P.G., Read P, Ostvold T., Payatakes A.C. (2000). Sandbed Consolidation with Mineral Precipitation. *Journal of Colloid and Interface Science* 232 : 326–339.

Plant L.J., House W.A. (2002). Precipitation of calcite in the presence of inorganic phosphate. *Colloids and Surfaces A: Physicochemical and Engineering Aspects* 203(1-3): 143-153

Quarmby J., C. F. Forster (1995). An examination of the structure of UASB granules. *Water Research* 29(11):2449-2454

Ren T.T., Liu L., Sheng G.P, Liu X.W., Yu H.Q., Zhang M.C., Zhu J.R. (2008). Calcium spatial distribution in aerobic granules and its effects on granule structure, strength and bioactivity. Water Research, 42 (13): 3343-3352

Rensburg van P., Musvoto E. V., Wentzel M. C., Ekama G. A. (2003). Modelling multiple mineral precipitation in anaerobic digester liquor. Water Research 37(13):3087-3097.

H.M. Rootare, V.R. Deitz, F.G. Carpenter. (1962). Solubility product phenomena in hydroxyapatite-water systems. J. colloid. Sci., 17: 179‑206.

Seckler M.M., Bruinsma S.L., van Rosmalen G.M. (1996). Phosphate removal in a fluidized bed I. Identification of physical processes. Water Research 30(7):1585-1588.

Shellis R.P., R.M. Wilson, Apparent solubility distributions of hydroxyapatite and enamel apatite, journal of Colloid and Interface Science, 278 (2004), pp. 325-332.

Shellis R.P. (1996). A scanning electron-microscopic study of solubility variations in human enamel and dentine. Archives of Oral Biology, 41(5):473-484.

Shen Y., J. A. Ogejo, K. E. Bowers (2011). Abatting the effects of calcium on struvite precipitation in dairy liquid manure. American Society of Agricultural and Biological Engineers. 54(1):325-336.

Snoeyink, V.L., Jenkins, D. (1980) Water Chemistry, John Wiley & Sons, New York.

Stumm, W. and Morgan, J.J. (1981) Aquatic Chemistry, 2nd Ed, John Wiley & Sons Inc. ISBN 0 471 09173-

1.

Svardal K. (1991). Calcium carbonate precipitation in anaerobic waste water treatment. Wat. Sci. Technol 23 : 1239-1248.

Taylor A.W., E.L. Gurney, A.W. Frazier (1963). Solubility products of magnesium ammonium and magnesium potassium phosphates. Trans. Faraday Soc., 487 : 1580‑1583

Tiano, P., Biagiotti, L., Mastromei, G. (1999). Bacterial bio-mediated calcite precipitation for monumental stones conservation: methods of evaluation. *Journal of Microbiology Methods* 36 (1–2): 139–145.

Wan J., Y. Bessière, M. Spérandio. (2009). Alternating anoxic feast/aerobic famine condition for improving granular sludge formation in sequencing batch airlift reactor at reduced aeration rate, Water Research, 43:5097-5108.

Wang P., A. Anderko, R.D. Springer, J.J. Kosinski, M.M. Lencka, (2010). Modeling chemical and phase equilibria in geochemical systems using a speciation-based model, Journal of Geochemical Exploration, Vol. 106, pp. 219-225.

Warren L., and Haack E. (2001). Biogeochemical controls on metal behaviour in freshwater environments. *Earth-Science Reviews* 54(4): 261-320.

Weiner S. (2008). Biomineralization: A structural perspective. *Journal of Structural Biology* 163 (3):229-23.

ANNEX IV.1: Liquid characterization of the influent and effluents from the reactors (UASB or GSBR)

Table IV. 3: characterization of the influent and effluent streams of each bioreactor.

			Site 1 UASB Anaerobic		Site 2 UASB Anaerobic		Site 3 UASB Anaerobic		Site 4 GSBR-1 Anoxic/Aerobic		Site 5 GSBR-2 Anaerobic/Aerobic	
			Influent	**Effluent**	**Influent**	**Effluent**	**Influent**	**Effluent**	**Influent**	**Effluent**	**Influent**	**Effluent**
Liquid phase	Cl^-	mg/L	652	658	754	641	464	451	181	164	175	170
	$N\text{-}NO_2^-$	mg/L	1.10	-	1.20	-	0.21	0.29	-	0.095	0	0.08
	$N\text{-}NO_3^-$	mg/L	4.60	3.30	6.20	2.35	6.41	1.08	111	16.14	1.13	0.25
	$P\text{-}PO_4^{3-}$	mg/L	191	118	121	114	107	73.0	31.2	17.04	31.25	15.9
	Na^+	mg/L	145	515	304	410	302	710	391	348	209	208
	$N\text{-}NH_4^+$	mg/L	122	323	71.7	315	0.86	320	64.6	0	59.08	9.93
	K^+	mg/L	167	442	441	415	418	512	45.1	33.9	45.2	35.1
	Mg^{2+}	mg/L	15.55	32.53	22.7	21.95	19.39	11.04	4.39	3.63	4.19	2.98
	Ca^{2+}	mg/L	80.9	76.5	132	90.9	150	88.7	46.0	29.1	43.6	24.3
	TKN	mg/L	831	968	558	422	nd	nd	64.6	nd	59.1	nd
	COD	mg/L	29120	240	16380	120	23760	2705	1000	45	1000	75
	TIC	mg/L	-	363	-	919	-	nd	23.3	-	24.00	50.7
	pH	-	3.62	6.67	3.54	7.4	3.61	6.88	7.54	8.22	7.6	7.9
	T	°(C)	15	33	15	30	15	29	12	21	12	21
	Ca/P	mol/mol	0.33	0.50	0.85	0.62	1.08	0.94	1.14	1.32	1.08	1.18
	Ca/Na	mol/mol	0.56	0.15	0.43	0.22	0.50	0.12	0.12	0.08	0.21	0.12
	Ca/Mg	mol/mol	3.16	1.43	3.53	2.51	4.71	4.87	6.35	4.85	6.31	4.94
Suspended solids	SS	g/L	20.8	5.59	18.28	3.15	12.86	5.42	-	0.3	-	0.4
	VSS	g/L	17.64	3.21	15.98	0.63	10.07	2.12	-	0.1	-	0.2
	MF	% (mass)	15.19	42.58	12.58	80.00	21.70	60.89	-	33.65	-	38.70
Granular sludge	SMF Ash content	% of dry mass	81.0±0.4		71.7±1.2		28.2±0.5		33.5±0.4		68.4±2.2	

ANNEX IV.2: SEM-EDX images of granules from UASB or GSBR

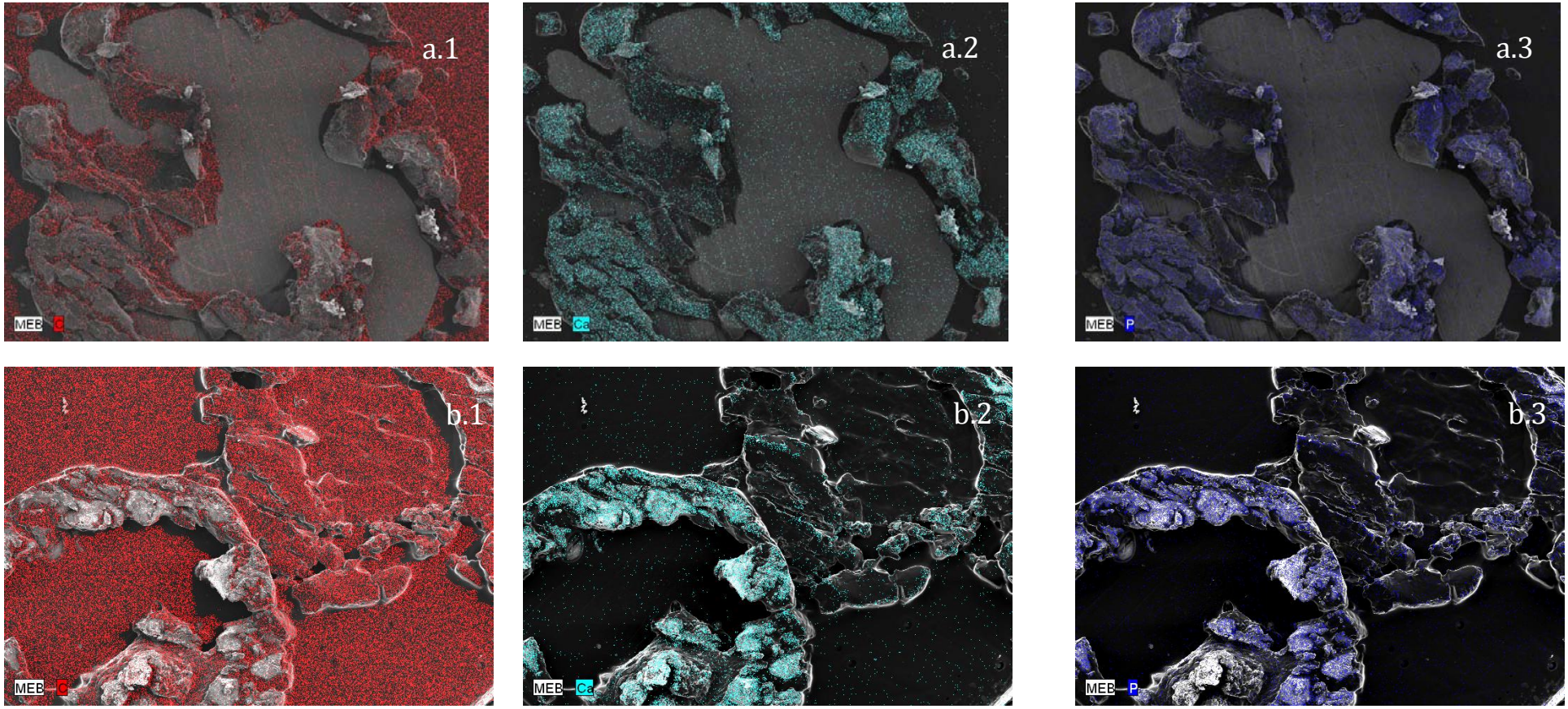

Figure IV.A.2: SEM-EDX Images from the granules from Fig. IV.2. Legend: Red, for organic fraction (carbon), Light blue for Ca, dark blue for P.

ANNEX IV.2: SEM-EDX images of granules from UASB or GSBR

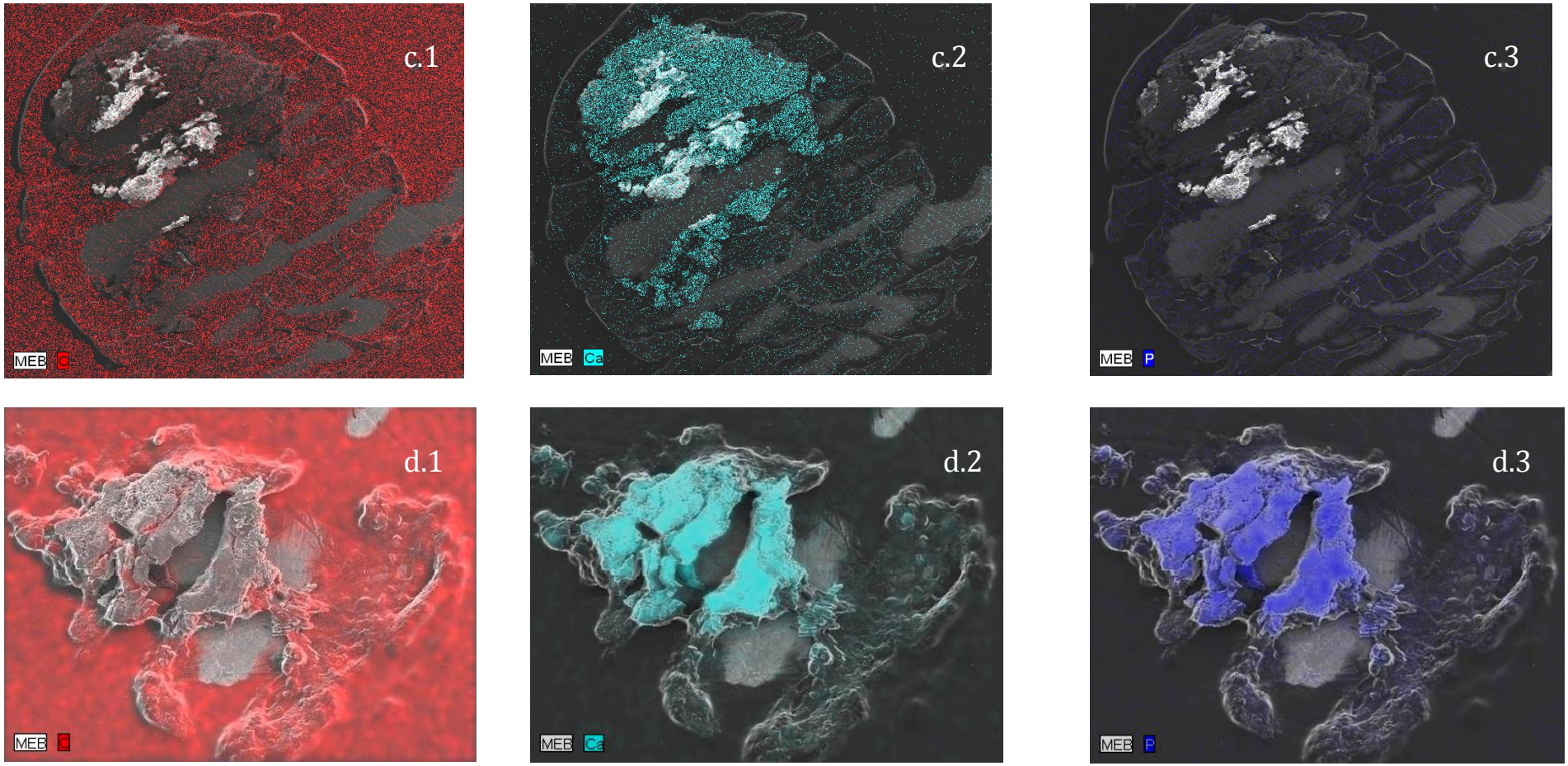

Figure IV.A.2: SEM-EDX Images from the granules from Fig. IV.2. Legend: Red, for organic fraction (carbon), Light blue for Ca, dark blue for P.

ANNEX IV.2: SEM-EDX images of granules from UASB or GSBR

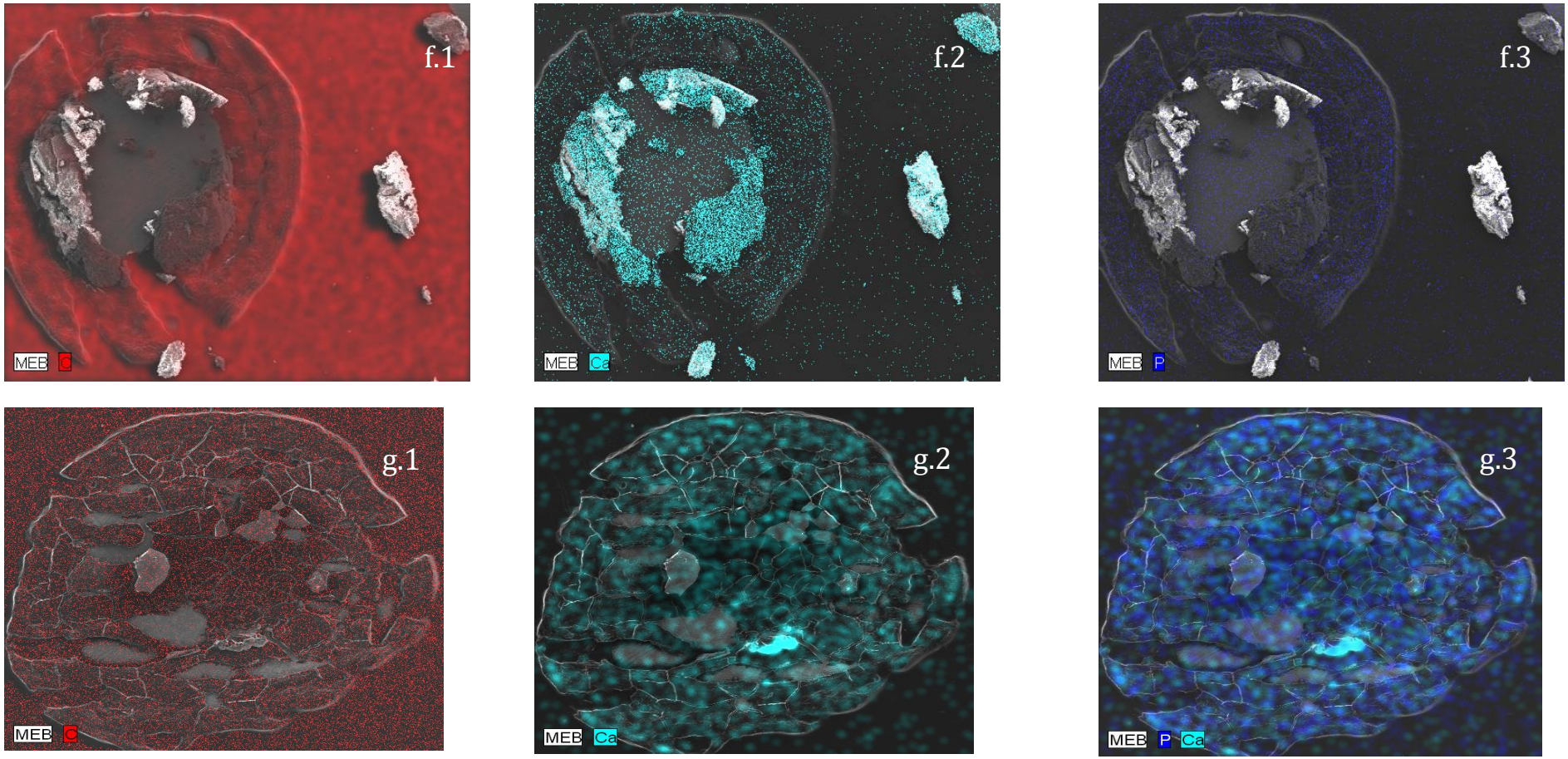

Figure IV.A.2: SEM-EDX Images from the granules from Fig. IV.2. Legend: Red, for organic fraction (carbon), Light blue for Ca, dark blue for P.

ANNEX IV.2: SEM-EDX images of granules from UASB or GSBR

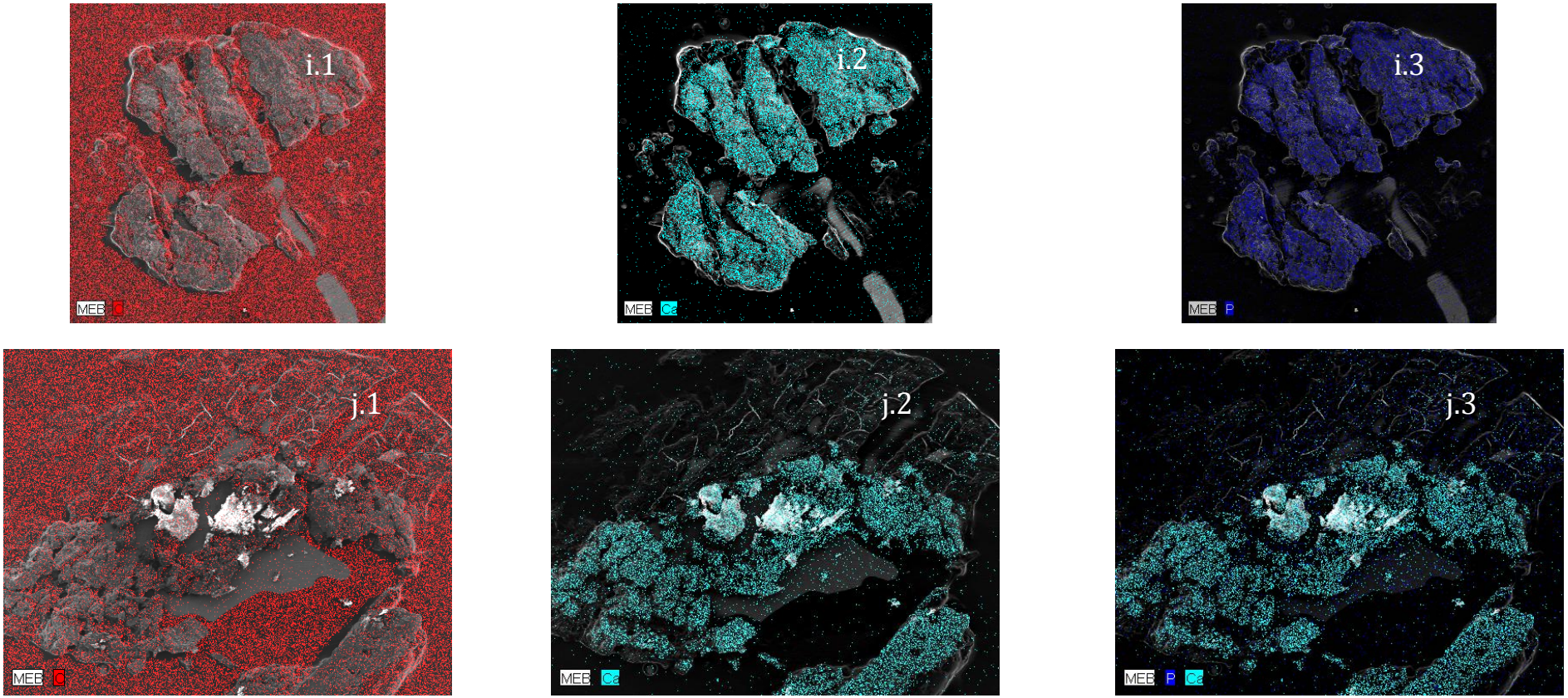

Figure IV.A.2: SEM-EDX Images from the granules from Fig. IV.2. Legend: Red, for organic fraction (carbon), Light blue for Ca, dark blue for P.

ANNEX IV.2: SEM-EDX images of granules from UASB or GSBR

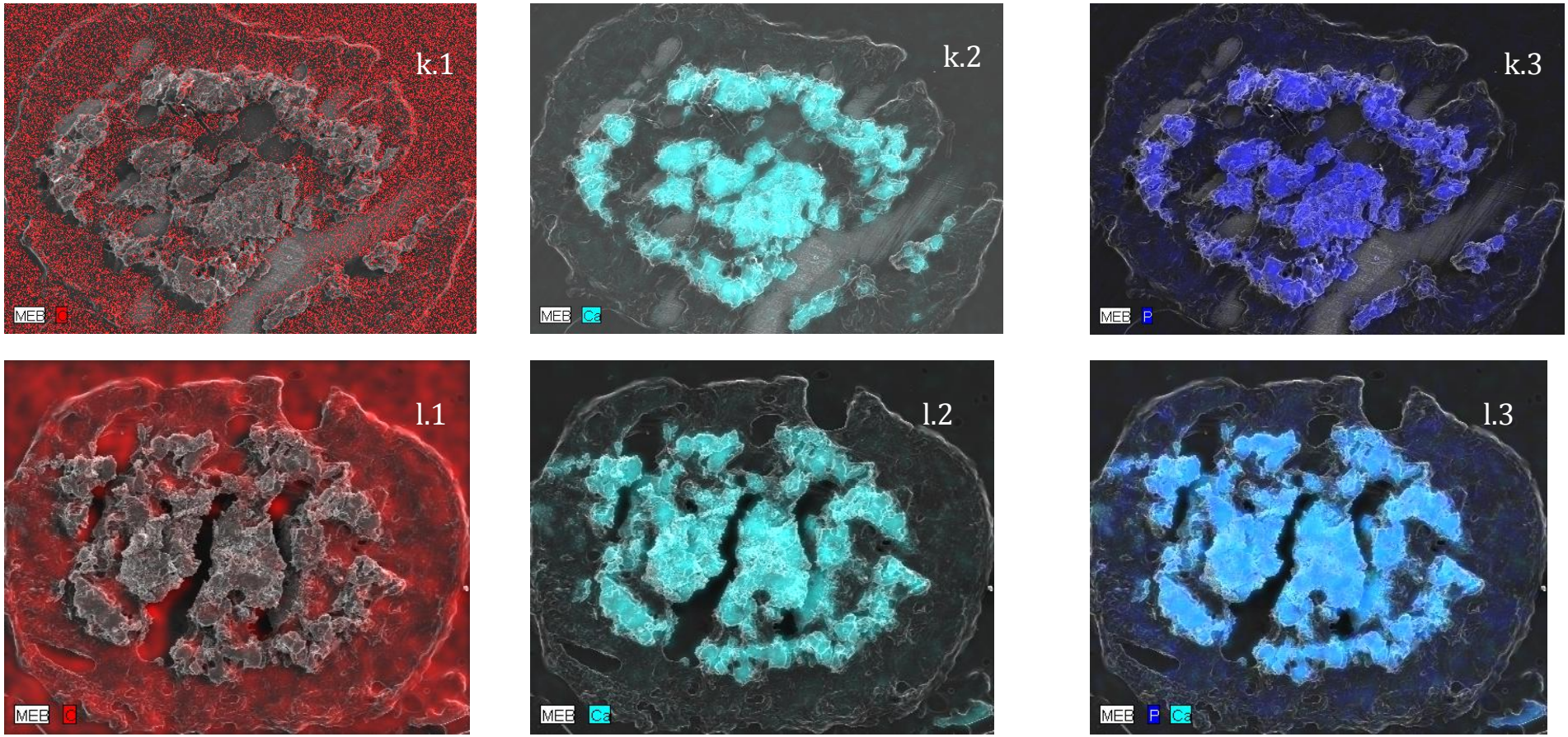

Figure IV.A.2: SEM-EDX Images from the granules from Fig. IV.2. Legend: Red, for organic fraction (carbon), Light blue for Ca, dark blue for P.

ANNEX IV.2: SEM-EDX images of granules from UASB or GSBR

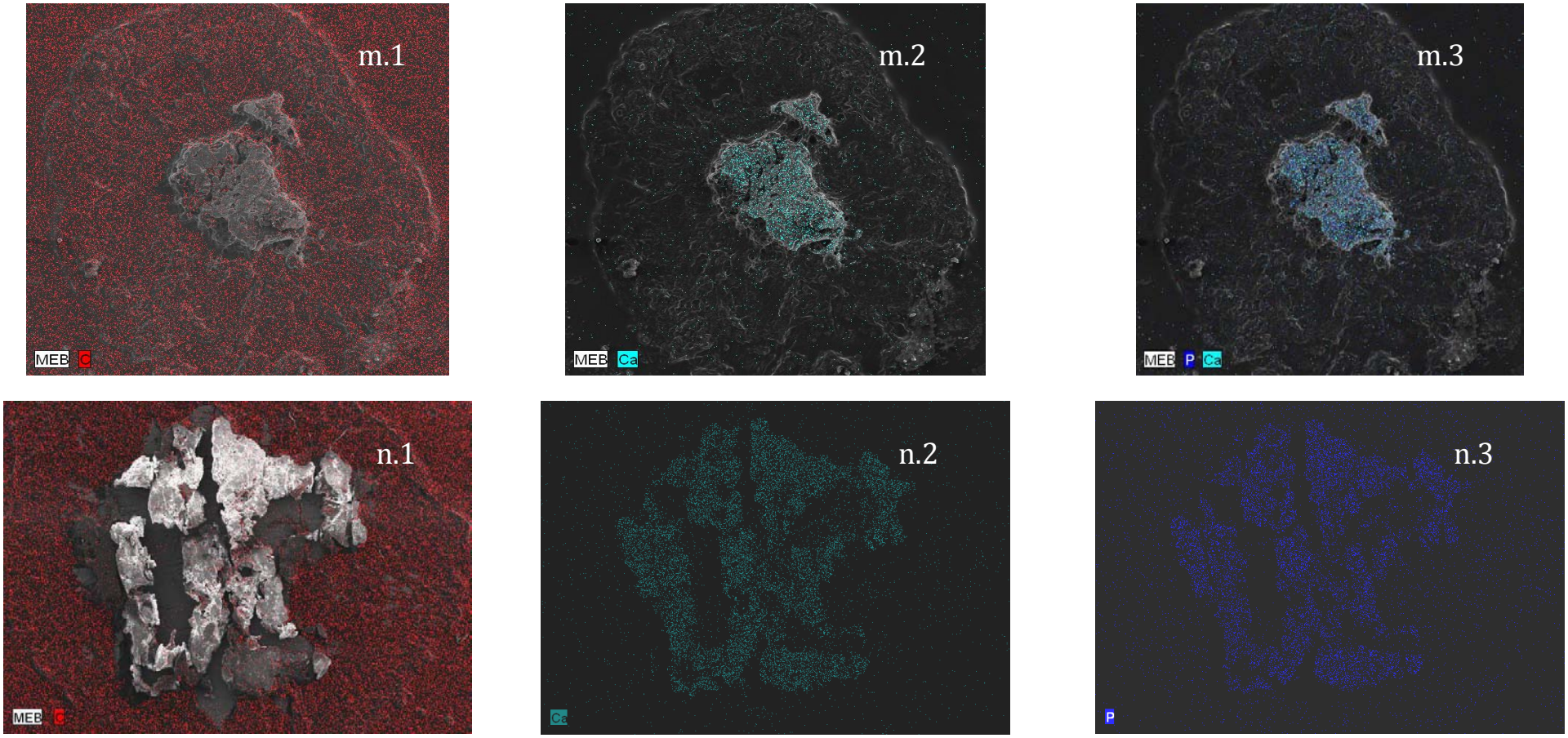

Figure IV.A.2: SEM-EDX Images from the granules from Fig. IV.2. Legend: Red, for organic fraction (carbon), Light blue for Ca, dark blue for P.

ANNEX IV.2: SEM-EDX images of granules from UASB or GSBR

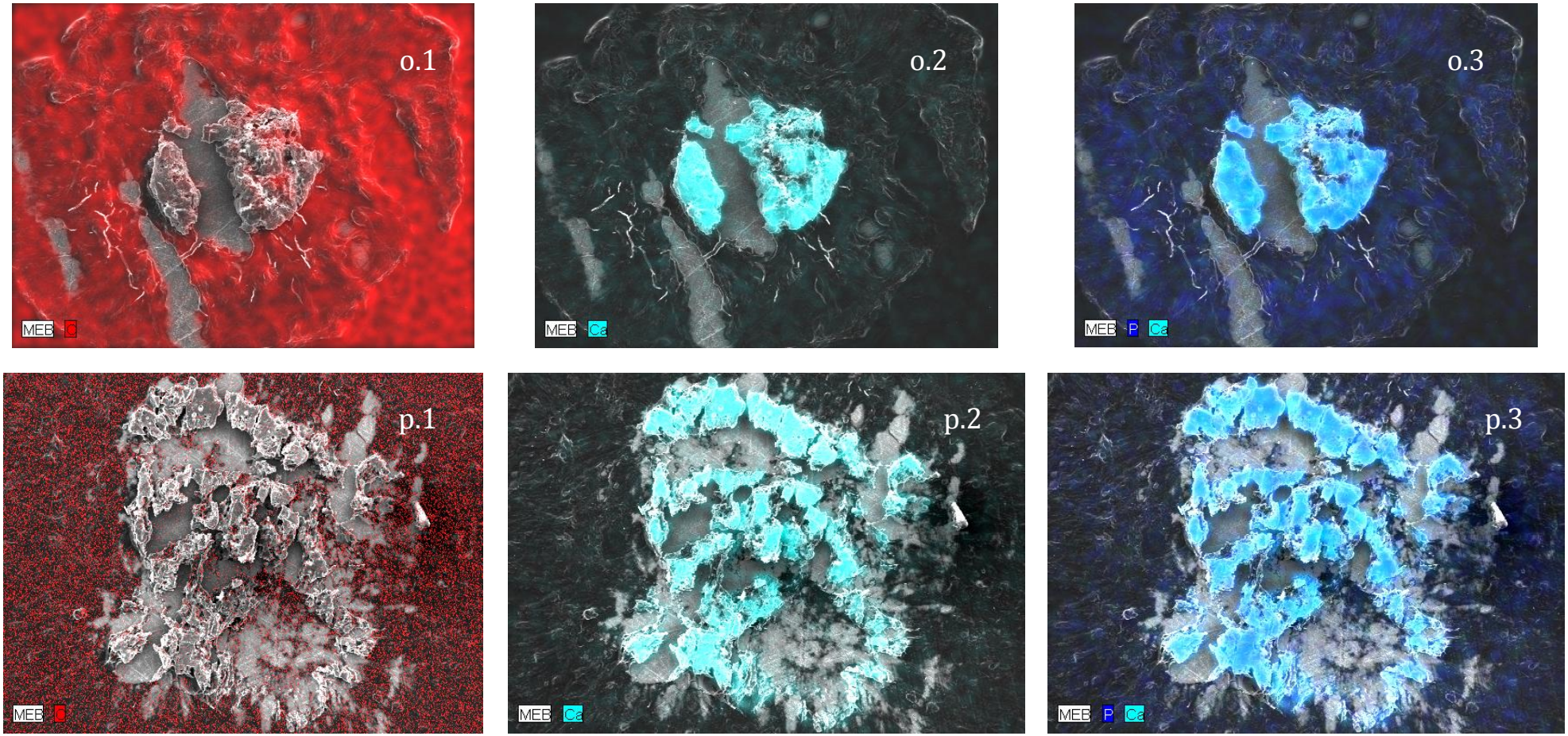

Figure IV.A.2: SEM-EDX Images from the granules from Fig. IV.2. Legend: Red, for organic fraction (carbon), Light blue for Ca, dark blue for P.

ANNEX IV.3: Database from literature of mineral precipitation constants at 25ºC

Table IV.6: Database of the mineral precipitation constants at T=25ºC. *Values used for simulations in this thesis are marked in bold.*

Code Reference	Mineral	Abreviation	Formula	pK_{sp} (25°C)								
				A	B	C	D	E	F	G	H	I
0	Struvite	MAP	$MgNH_4PO_4x6H_20$	9.41	**13.26**	13	12.6	12.60-13	10.08	9.94	12.6	13.16
1	Calcium phosphate tribasic (hydroxyapatite)	HAP	$Ca_5(PO_4)_3(OH)$	114	57.5	58.33	**58.33**	3.421	58.52			
2	Calcium Phosphate dibasic dihydrated (brushite)	DCPD	$CaHPO_4 x 2H_2O$	6.69	6.6	6.5	**6.62**					
3	Magnesite	MAG	$MgCO_3$	7.46	8.2	**7.46**						
4	Calcite	CAL	$CaCO_3$	8.42	8.48	8.5	6.45	11.44	**6.35**	8.48		
5	Hydroxy-dicalcium phosphate	HDP	$Ca_2HPO_4(OH)_2$	**22.6**	27.3							
6	Newberite	NEW	$MgHPO_4x3H_2O$	5.8	**5.8**							
7	Phosphate dicalcic anhydrous	DCPA	$CaHPO_4$	6.9								
8	Octocalcium phosphate	OCP	$Ca_4H(PO_4)_3x2.5H_2O$	49.6								
9	Tricalcium phosphate	TCP	$Ca_3(PO_4)_2$	26	**32.63**							
10	Amorphous calcium phosphate	ACP	$Ca_3(PO_4)_2 x XH_2O$	25.46	26.52	25.2	**28.92**					
11	Potassium struvite	MKP	$MgKPO_4x6H_20$									
12	Dolomite	DOL	$CaMg(CO_3)_2$	**9.8**								
13	Aragonite	ARAG	$CaCO_3$	**8.36**								
14	Vaterite	VAT	$CaCO_3$	**7.91**								
15	Whitlockite	MWH	$Ca_{18}Mg_2H_2(PO_4)_{14}$	**104.4**	104.4	98.15-111.47						

ANNEX IV.3: Database from literature of mineral precipitation constants at 25ºC

Table IV.7: Codification of the references above

pK_{ps} reference			
Code Ref.	**Reference**	**Code Ref.**	**Reference**
0.A	Bordering, 1972	4.B	Nordstrom et al., 1989
0.B	Ohlinger et al., 1998	4.C	Murray and May, 1996
0.C	Mamais et al., 1994	4.D	Musvoto et al., 1999b
0.D	Loewenthal et al., 1994	4.E	Musvoto et al., 1999a
0.E	Snoeyink and Jenkins, (1980); Burns and Finlayson., 1982	4.F	NIST database (strong Ic)
0.F	Taylor et al., 1963	4.G	NIST database (weak Ic)
0.G	Abbona et al., 1982	5.A	Maurer et al., 1999
0.H	Stumm and Morgan, 1981	5.B	Rootare et al., 1962
0.I	Murray and May, 1996	6.A	Murray and May, 1996
1.A	Stumm and Morgan, 1981	6.B	NIST DATABASE (weak Ic)
1.B	Murray and May, 1996	7.A	Freche, 1989
1.C	Freche, 1989	8.A	Freche, 1989
1.D	NIST database	9.A	Ringbom, 1967
1.F	Mc Dowell et al., 1977 = (PHREEQC default)	9.B	Murray and May, 1996
1.E	Lin and Singer, (2006)	10.A	Hoffman, 1977
2.A	Freche, 1989	10.B	Seckler et al., 1996
2.B	Stumm and Morgan, 1981	10.C	Meyer et al., 1982
2.C	Murray and May, 1996	10.D	NIST database
2.D	NIST database	12.A	Garrels et al., 1960
3.A	Stumm and Morgan, 1981	13.A	Wang et al., 2010
3.B	Murray and May, 1996	14.A	Wang et al., 2010
3.C	NIST DATABASE (weak Ic)	15.A	Shellis et al., 2004; 1996
4.A	Stumm and Morgan, 1981	15.B	Driessens and Verbeeck, 1981
		15.C	Shellis et al., 1996

CHAPTER V:

PARAMETERS INFLUENCING CALCIUM PHOSPHATE PRECIPITATION IN GRANULAR SLUDGE SEQUENCING BATCH REACTOR

In this chapter, the major parameters influencing calcium phosphate precipitation have been assessed in a GSBR operating with anaerobic/aerobic cycles during a working stable period.

The aim of this chapter is to provide information about the mechanisms of crystal formation inside aerobic granules, moreover, the precursors that could induce such precipitation in sights of further modeling.

This chapter corresponds to the article: Mañas A., Pocquet M., Spérandio M., Biscans B. (2011). "Parameters influencing calcium phosphate precipitation in granular sludge sequencing batch reactor", submitted on September 2011 at Chemical Engineering Science Journal (Accepted on January 2012). It also constituted the basis of an international oral communication at ISIC18 (about crystallization) Congress, Zurich, September 2011.

V.1. INTRODUCTION

A recent report of the United Nations Environment Program highlights phosphorus management as one of the main emerging problems to be faced in 2011 (United Nations of Environmental Program yearbook 2011): the demand for phosphorus is increasing, the available resources are scarce, the use needs to become more efficient and the recycling more widespread. On the other hand, it is found in excess in wastewater effluents, damaging aquatic ecosystems and the quality of water. In a wastewater treatment plant, biological processes are mandatory for meeting carbon (COD) and nitrogen (N) quality standards of the effluent (Giesen, 1999). Biological dephosphatation by polyphosphate accumulating organisms (PAOs) have to be intensively employed but still needs to be combined with physicochemical treatment to isolate phosphate in a solid form. Therefore, research is now focusing increasingly on combined processes that remove phosphorous from wastewaters and successively recover it in the form of a valuable product (De Bashan et al., 2004), for example struvite ($MgNH_4PO_4 \cdot 6H_2O$) or hydroxyapatite ($Ca_5(PO_4)_3(OH)$).

The aerobic granular sludge process is a promising technology for wastewater treatment, performing simultaneous nitrogen and phosphorus removal (Liu and Tay, 2004; Lemaire, 2007; Morgenroth et al., 1997). The granular sludge process is based on dense microbial aggregates containing different bacterial communities. Recent studies indicate that calcium phosphate can also precipitate and accumulate in the core of granules, playing a role in the global performance of the process (Wan and Spérandio, 2009; Manas et al., 2011). In this work, research focuses on this induced biological phosphorus precipitation inside biological aggregates. Until now, only a few studies have been dedicated to this mechanism, focusing on general mineral precipitation on the walls of pure bacterial strains by changing either pH or ion concentration (Dupraz et al., 2009; Bazylinski, 1996; Weiner, 2008). This work aims to gain insight into the parameters that influence microbial induced phosphorus precipitation in granular sludge for wastewater treatment. Major questions concern the nature of the precursors in the Ca-P precipitation and the influence of the microbial reactions on the precipitation in relation with pH.

Previous work has identified the chemical composition of the mineral clusters found inside aerobic granules (Mañas et al., 2011). Hydroxyapatite (HAP) was the major crystallized compound and the presence of amorphous precipitates was also suggested by X-ray Diffraction Analysis. Boskey and Posner, 1974) and Nancollas and Koutsoukos (1980) stated that HAP could form without any precursors at low ionic strength (Ic) but its

formation is normally preceded by different mineral phases depending on the pH, the ionic strength and the presence of other ions (Nancollas and Wu, 2000). Octacalcium phosphate (OCP) was identified as the precursor of HAP at physiological pH (Tomazic et al., 1975; Brown et al., 1981; Elliot, 1994). However, brushite (DCPD) was later reported by several authors (Abbona et al.,1986; Gao et al., 2010) as the hydroxyapatite precursor in acidic conditions, and OCP was also found to form in low-pH medium. While Posner and co-workers (1975) found tricalcium phosphate (TCP) to be the main HAP precursor in aqueous solutions at ambient temperature, Amjad et al. (1981) did not find the same results with a constant composition study. Grases et al. (1996) found TCP to be a precursor of human calculi at pH between 6 and 7, although Johnson and Nancollas (1992) stated that β-TCP is not formed at ambient temperature. Posner and Betts (1975) stated that hydroxyapatite formation is preceeded by a poor crystal solid which consists of calcium phosphate clusters with the formula $Ca_9(PO_4)_6$. Finally, amorphous calcium phosphate (ACP), was first observed by Eanes (1965) and, since then, several authors have observed it in different pH ranges: between pH = 5-7.5, according to Madsen et al., (1995) and Tsuge et al., (2002); in the neutral pH range (Madsen and Christensson, 1991); at pH>7.4, where ACP was the only phase reported by Montastruc (2003) and Seckler et al., (1996); and even at high pH (9.5-12) in a report by Lazic (1995). Normally, models consider the precipitation of the most thermodynamically stable phase as a function of the precursor formation but there is some disagreement about its choice. Maurer and Boller (1999) and Maurer et al., (1999) stated that calcium phosphate precipitation took place simultaneously with bio-dephosphatation processes throughout hydroxyl dicalcium phosphate (HDP) formation but gave no demonstration to support their claim. In contrast, Barat et al. (2011) assumed that amorphous calcium phosphate (ACP) was the first calcium phosphate precursor for modeling HAP precipitation in EBPR processes.

Musvoto et al., (2000b) succeeded in modeling phosphate precipitation in digester supernatant. Barat et al., (2011) showed that satisfying prediction of phosphorus removal by simultaneous biological and chemical process was obtained with ASM2d model coupled with ACP precipitation.In view of the broad differences of opinion in the literature concerning the nature of HAP precursors in similar conditions, in this chapter, experiments were carried out with granular sludge in which HAP has been observed to accumulate in the core of granules (Chapter II). From literature it comes that HAP is not directly formed but precipitation is assumed to be controlled by precursor precipitation.

The objectif of this chapter is to investigate the operating conditions which can influence this first step of precipitation.

V.2. MATERIAL AND METHODS

V.2.1. Biological reactor operating conditions

Reactor kinetic tests were first carried out in two lab-scale continuously running Granular Sequenced Batch Airlift Reactor (GSBR), called R1 and R2 in what follows for simplicity. Details can be consulted in chapter II. Most of the following results were collected on GSBR noted R2 which was operated in 4-hour cycles with anaerobic/aerobic conditions as follows: 15 min of feeding; 20 min of anaerobic reaction (nitrogen gas injection); 145 min of aerobic reaction; 30 min settling and 30 min withdrawal (with a volumetric exchange ratio of 47%). The synthetic feed had the following composition: 1000 mg/L COD consisting of a 25% each of glucose, acetate, propionic acid and ethanol contribution, nutrients and salts ($[PO_4^{3-}]$ = 30 mgP/L, $[Ca^{2+}]$ = 46 mg/L, $[HCO_3^-]$ = 100 mg/L, $[NH_4^+]$ = 50 mgN/L). A COD/N-NH_4^+ ratio of 20 was maintained. The reactor had a working volume of 17 L. The temperature was maintained at 20±2ºC, and pH varied during the process cycle (from 7.2 to 8.5 on average). These last parameters, together with DO, were measured and recorded on line for more than 250 days of reactor operation. During this period, pH evolved naturally in the bulk under the influence of biological reactions (denitrification, nitrification) and physicochemical processes (CO_2 stripping, precipitation, etc). During this operation, three kinetic tests were followed at different pH values: (1) a normal cycle where pH was not controlled during the kinetic batch cycle, (2) a cycle at the high pH value of 8.4 ± 0.2 (by NaOH dosing), (3) a cycle at the low pH value of 7.4 ± 0.2 (by NaOH and HCl dosing).

V.2.2. Batch precipitation in abiotic experiments

Batch tests were carried out in parallel to assess the precipitation of calcium phosphate from the all the P removal mechanisms separately (without biological reactions). For this purpose, a 2L-volume reactor (figure V.1) was seeded with aerobic granules from the GSBR-R2 reactor, and the kinetics was determined after an endogenous stage (sludge was aerated without feeding). The endogenous period depended on the test and the objective was to deplete the nutrients as far as possible at the kinetics starting

point, ensuring a stable and low respirometric activity and stable evolution of ions in the bulk. At the end of the endogeneous period, pH was 8.15; and the ions concentrations were constant and as follows: [Ca^{2+}]=12.29 mg/L, [PO_4^{3-}]=2.94 mgP/L; [Cl^-]=171.58 mg/L, [NO_2^-]=4.66 mgN/L; [NO_3-]=8.99 mgN/L, [Na^+]=237.97 mg/L, [K^+]=22.54 mg/L, [Mg^{2+}]=0.23 mg/L and [NH_4^+]=0 mgN/L. Calcium and phosphorus were added to the batch reactors at different amounts, maintaining a regime of constant mixing (260 rpm) and an air flow rate of 60 L/h. A pH and a DO probe were placed in the reactor and data were acquired online every 5 s (DO was stable at 6±0.01 mg/L). All batch tests were performed at a temperature of 25ºC. No ammonium, magnesium or carbonates were added in the tests, in order to avoid the co-precipitation of other species and to limit the study to the calcium phosphate system. A different set of tests were carried out in order to evaluate the parameters reported to influence the precipitation mechanisms in the literature (pH, ionic strength, Ca/P concentrations, VSS and time). All the experiments carried out in the physicochemical reactor can be classified in two sets including different periods (P0, P2, P3, etc.). Each set was performed at a different initial VSS concentration (S1=3.73 and S2= 0.51 g/L) and, in each period, a change of a parameter (pH, Ic, [Ca], [P], Ca/P ratio, etc.) was studied. Table V.1 summarizes the experiments. Ca and P concentrations were analyzed at different times for each experiment in order to evaluate the ΔCa/ΔP disappearing from the bulk, and experimental ratios were then compared to the theoretical ones for the minerals most likely to precipitate according to the SI calculation (see section V.2.3).

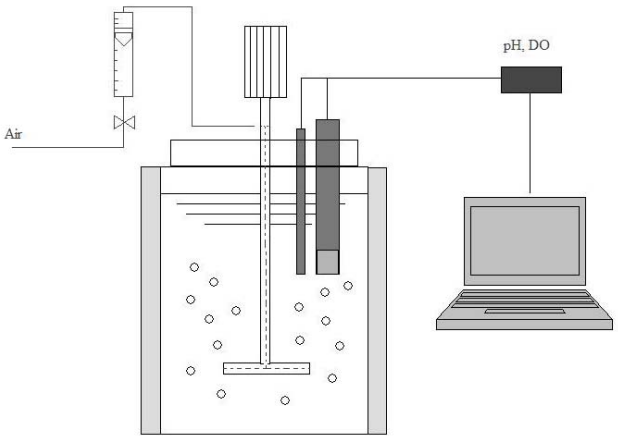

Figure V. 1: Batch test scheme used for abiotic precipitation tests.

Table V.1: Precipitation experiments in the 2-L reactor (batch) with different parameters.

Experiment	VSS_{init} (g/L)	TSS (g/L)	pH_{init}	pH_{mean}	Ic_{init} $_{x10^{-2}}$	Ca_{init} mg/L	P_{init} mg/L	Ca/P_{init} molCa/molP	Total Duration min
S1P1	3.73	7.4	7.95	7.95	1.29	34.20	14.98	1.77	12
S1P2	3.73	9.6	6.83	6.86	2.32	86.01	114.20	0.58	280
S1P3	3.73	12.6	6.43	6.72	3.33	210.62	45.90	3.56	77
S1P4	3.73	15.8	6.71	6.62	3.39	89.34	104.83	0.66	7
S1P5	3.73	18.4	7.26	7.33	3.40	54.44	84.01	0.50	1173
S1P6	3.73	36.3	7.24	7.09	3.69	21.86	64.61	0.26	39
S2P1	0.51	2.66	7.78	7.77	1.20	33.40	14.27	1.81	1530
S2P2	0.51	2.86	7.77	7.30	1.77	71.10	32	1.72	467
S2P3	0.51	2.86	8.6	8.01	1.61	36.76	12.66	2.25	67
S2P4	0.51	2.86	9.17	8.77	1.60	22.73	8.49	2.53	15
S2P5	0.51	6.47	8.5	7.25	6.91	474.30	484.28	0.76	12
S2P6	0.51	6.47	6.5	6.48	5.71	92.32	315.54	0.23	31

V.2.3 Characterization of liquid and solid samples

Samples were filtered with 0.2 µ-pore-size acetate filters before being analyzed by ionic chromatography (IC25, 2003, DIONEX, USA), in which NO_2^-, NO_3^-, PO_4^{3-}, NH_4^+, Ca^{2+}, K^+, Mg^{2+} concentrations were determined. COD, MLSS and VSS were analyzed according to standard methods (AFNOR 1994).

Solid samples were collected at the end of each batch of tests. Granules were separated from suspended particles by rapid settling (5 min). Granule samples and suspended solids were characterized separately. After calcination at 500°C for 2 hours, samples were analyzed by X-Ray Diffraction (XRD) (BRUKER D5000), with a cobalt tube scattering from 4-70° in 2θ.

EDX analysis was performed with a photon X analyzer (Quantax Technology Silicon Drift) having a detection limit of 127 eV. It was coupled to a SEM (JEOL 5410 LV) which allowed working in a partial pressure chamber.

V.2.4 Calculation and modeling

The ionic strength (I_c) and saturation index (SI) of the minerals considered were calculated using the geochemical software PHREEQC (Parkhurst et al., 2000), with a

modified database taking into account the pK_{sp} of the different minerals from the NIST database at the temperature at which the tests were conducted (25°C).

A dynamic model was developed to predict calcium phosphate precipitation based on differential equations as described in Annex V.1 written in the form of a *Petersen* matrix. The model was solved with AQUASIM software. Based on the work of Musvoto et al. (2000a and 2000b), the model included acid-base reactions and ion pair formation, described by a combination of the forward and reverse reactions of dissociation. Selection of ion pair species was based on exhaustive species decomposition with the PHREEQC software (Minteq v4 database, modified). For a more accurate prediction of phosphorus concentration in solution, two ion pairs containing phosphorus were added to the dynamic model proposed by Musvoto: MgH_2PO_4 and $NaHPO_4$. Both softwares were used successively. PHREEQC software allows first to decompose the concentrations obtained from the experimental analysis with ion chromatography (total calcium, magnesium, phosphorus, etc…) into aqueous species and ion pairing complexes. The output values of PHREEQC serve as inputs for initializing the differential equations described in AQUASIM, ensuring a better accuracy of the results (otherwise the dynamic simulations initially show an equilibrium period of a few minutes). Precipitation equation for the precursor was described using the nomenclature of Koustoukos and co-workers (1980), according to the equation *V.*1.

$$\frac{d}{dt}M_{v+}A_{v-} = K_{MA}\left[\left(\left(M^{m+}\right)^{v+}\left(A^{a-}\right)^{v-}\right)^{1/v} - \left(10^{-pKsp\_MA}\right)^{1/v}\right]^{n} \qquad \text{Equation V.1}$$

Where $M_{v+}A_{v-}$ represent the soluble salt, ACP (or TCP) in this case; *K_MA* is the kinetic constant; (M_{m+}) and (A_{a-}) are the ion activities; v+ and v- the number of cationic and anionic species ($v=v^+ + v^-$) in the salt; *n* the number of different ion species in the salt; and *pKsp_MA* is the negative log value of the dissociation constant. As precipitation is a surface limited reaction, the kinetic constant is dependent on the amount of solids present in the system. It was fitted to the experimental data for each assay. The *pKsp_MA* is the thermodynamic constant and it is specific to the mineral phase and the given temperature. It is normally provided in the literature.

SI for each mineral considered was calculated according to the equation V.2, which considers the term *j* (in contrast with default calculation with PHREEQC®), which is the

number of ions contained in the mineral formula considered (Paraskeva et al., 2000; Montastruc, 2003).

$$SI = \log\left(\frac{IAP}{K_{sp}}\right)^{1/j} \qquad \text{(Equation V.2)}$$

Where *IAP* is the Ionic Activity Product of the ion activities involved in the mineral precipitation, and *Ksp* refers to the thermodynamic mineral precipitation constant at a given temperature. Values were thus compared to 0, being probable to precipitate those minerals which SI were positive in the bulk. Ionic coefficients are calculated according Davies expression (Loewenthal et al., 1989):

$$\log f_i = -AZ_i^2\left(\frac{I_c^{1/2}}{1+I_c^{1/2}} - 0.3I_c\right) \qquad \text{(Equation V.3)}$$

$$I = \frac{1}{2}\sum C_i Z_i^2 \qquad \text{(Equation V.4)}$$

$$A = 1.825\cdot 10^6 \left(78.3\cdot T\right)^{-1.5} \qquad \text{(Equation V.5)}$$

Being f_i, the activity coefficient for ionic species, (f_m, f_d or f_t), monovalent, divalent or trivalent, respectively, I (or Ic), the ionic strength in the solution; *A*, the temperature-dependant constant; C_i, the concentration of the i^{th} ionic species (in mol/L); Z_i, the charge of the i^{th} ionic species; *T*, the temperature (in Kelvin). A simplified version of the physico-chemical model is provided in Annex V.1, where CO_2 stripping and NH_3 expulsion were also considered according to the following equations:

$$\left[H_2CO_3^*\right] = \left[CO_2 dissolved\right] + \left[H_2CO_3\right] \qquad \text{(Equation V.6)}$$

$$\frac{d}{dt}\left[H_2CO_3^*\right] = \left(\frac{D_{CO_{2(g)}}}{D_{O_2}}\right)^{0.5} \cdot Kla_{O2} \cdot \left(K_{H,CO_{2(g)}} \cdot \rho_{CO_{2(g)}} - \left[H_2CO_3^*\right]\right) \qquad \text{(Equation V.7)}$$

$$\frac{d}{dt}\left[NH_3\right] = Kla_{NH3} \cdot \left(-\left[NH_3\right]\right) \qquad \text{(Equation V.8)}$$

Being $\rho_{CO_{2(g)}}$ the partial pressure of CO_2 and $K_{H,CO2}$ the Henry's law constant for CO_2. For the stripping of NH_3, the partial pressure of this gas is neglected. Only expulsion of NH_3 is considered in the model.

V.3. RESULTS

V.3.1 Ca and P behavior in the biological reactors: influence of pH

Under normal operating conditions (figure V.2.), two successive stages were observed during the GSBR cycle. First K^+, Mg^{2+} and PO_4^{3-} were released during the anaerobic phase, whereas calcium was nearly constant (slight increase). During this phase, polyphosphate accumulating organisms (PAOs) consumed volatile fatty acids (a fraction of the COD) at the expense of energy release by the breakage of intracellular polyphosphate, composed of K^+, Mg^{2+} and PO_4^{3-} (Jardin and Pöpel, 1996; Barat et al., 2005). Then, in the subsequent aerobic phase, phosphorus was taken up by the PAOs, thus reconstituting the polyphosphate source and resulting in a net phosphorus removal from the bulk at the end of the aerobic cycle. Figure V.2.b also shows the pH profile during the course of the cycle: pH first slightly decreases during anaerobic phase due to proton release (as observed by Serralta et al., 2004) and then increased to 8.2 at the beginning of the aerobic period due to volatile fatty acids consumption and CO_2 stripping. At the end of COD consumption, aerobic respiration declined and pH decreased. This could be explained by proton release during biological nitrification and also a possible acidification can be due to calcium phosphate precipitation. Calcium remained constant during the pH plate profile and then decreased, the decrease coinciding with the maximum phosphate concentration in the bulk.

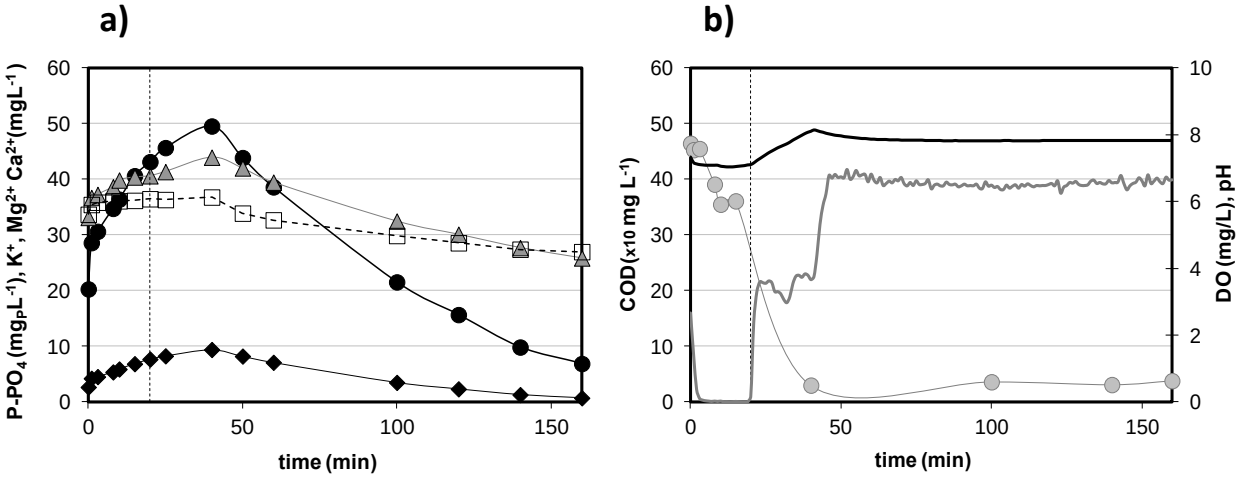

Figure V.2: Kinetic cycle in GSBR (R2) operated at normal conditions (without pH control). **a)** ***Evolution of PO_4^{3-} (●), Ca^{2+}(□), Mg^{2+}(◆), K^+ (▲); b) COD (○), pH (—) and DO (_) during a cycle run.***

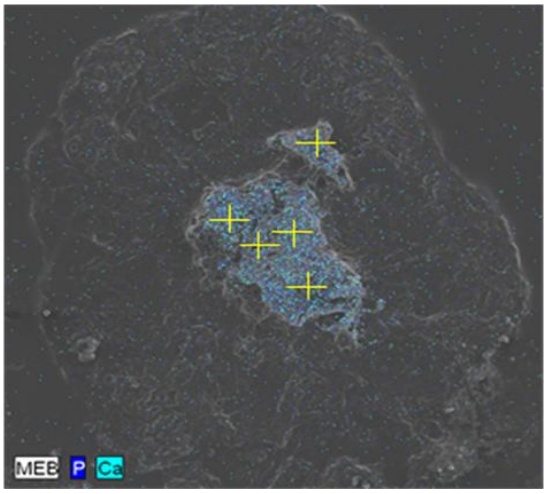

Figure V.3: Granule cut analyzed with SEM-EDX Analysis showing calcium phosphate inside

Simultaneous storage of a part of the phosphates from the bulk occurred in the form of calcium phosphate precipitates inside biological granules, demonstrated by SEM-EDX analysis (figure V.3). A Ca:P molar ratio of 1.64±0.09 was found in the mineral core which was close to that of HAP (1.67) (see details in chapter II). This second mechanism contributing to phosphorus removal and immobilization is noted as *Microbial Induced Phosphorus Precipitation* (MIPP).

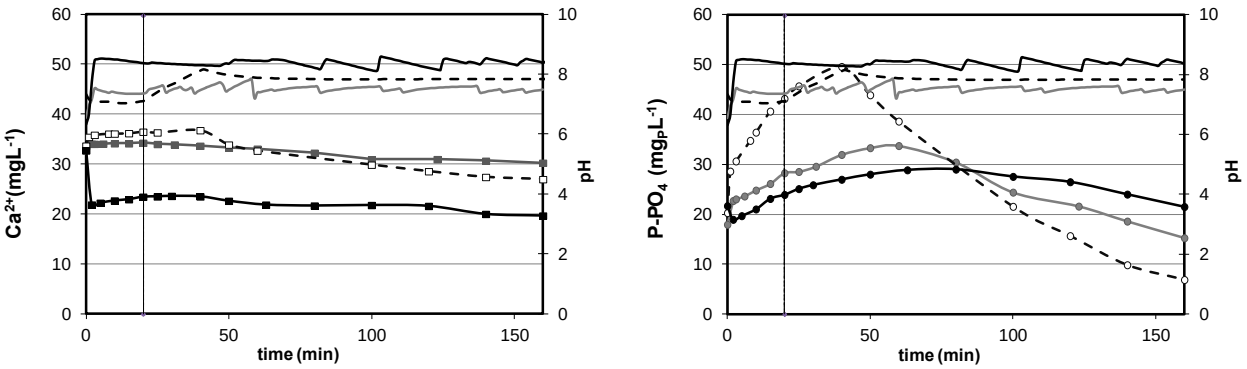

Figure V.4: Kinetic tests in biological reactor at different pH a) calcium and pH; b) phosphorus and pH. Legend: Ca□), P ○), pH(-); normal kinetics (black, dotted line); high pH (black); low pH (gray).

Three experiments were carried out in the biological GSBR, with pH controlled at 8.4±0.2 and 7.4±0.2 and another, at the normal pH evolution. Calcium and phosphate profiles in the supernatant are shown in figures 4.a and 4.b. Initial examination suggested that pH strongly influenced the phosphate profile (Fig. 4b). Experiments at high or low pH both led to a decrease of the phosphate release and uptake. A better P removal yield was

finally achieved when pH was not controlled. A first reason is probably that micro-organisms (PAOs) are disturbed by a sudden change of pH in the reactor (here the final pH was 0.5 units higher or lower than in the normal cycle). A second explanation may be that precipitation is favored at high pH, masking the EBPR process. Given that two processes (MIPP and EBPR) are responsible for the total phosphate behavior, the contribution of precipitation could be evaluated with respect to calcium removal. The higher the pH in the bulk, the lower the calcium concentration obtained, strengthening the contribution of precipitation to the whole process.

In order to evaluate whether pH drives the calcium phosphate precipitation, figure V.5 shows the variation of calcium concentration versus pH, obtained from different kinetics carried out at different moments during the running period. We extended the analysis to two GSBRs: R1 (operated in anoxic/aerobic conditions) in which pH reached higher values induced by a higher denitrification activity, and R2 (operated in anaerobic/aerobic conditions). Figure 5.a compares the effect of pH induced biologically in two reactors, GSBR R1 and R2. The details of the first reactor will not be addressed here but the main difference with respect to R2 relies in the introduction of an anoxic phase (with the presence of nitrate as electron acceptor) instead of the anaerobic one of R2, as seen in chapter III. Thus, in R1, biological denitrification induced higher pH increase (from 7.5 to 9.2) than in R2, resulting in a higher contribution of the precipitation phenomenon. Figure 5b shows that, when pH increases to 9 in R1 (at the end of anoxic phase), calcium concentration decreases in the bulk as a consequence of precipitation, reaching the lowest value observed (around 22 mgCa/L). Meanwhile, there is calcium release when the pH decreases. The same figure for R2 shows a different trend: calcium concentration increase is followed by a flat stable period during which pH increases (until the end of phosphate release by PAO), then calcium decreases during the aerobic phase, probably due to precipitation. At the end of the cycle, calcium concentration reaches a similar value (25-26 mg/L) in both reactors, as final pH values are also similar (7.9-8). Finally these data point out the important influence of the biological reaction on pH and its consequences on precipitation.

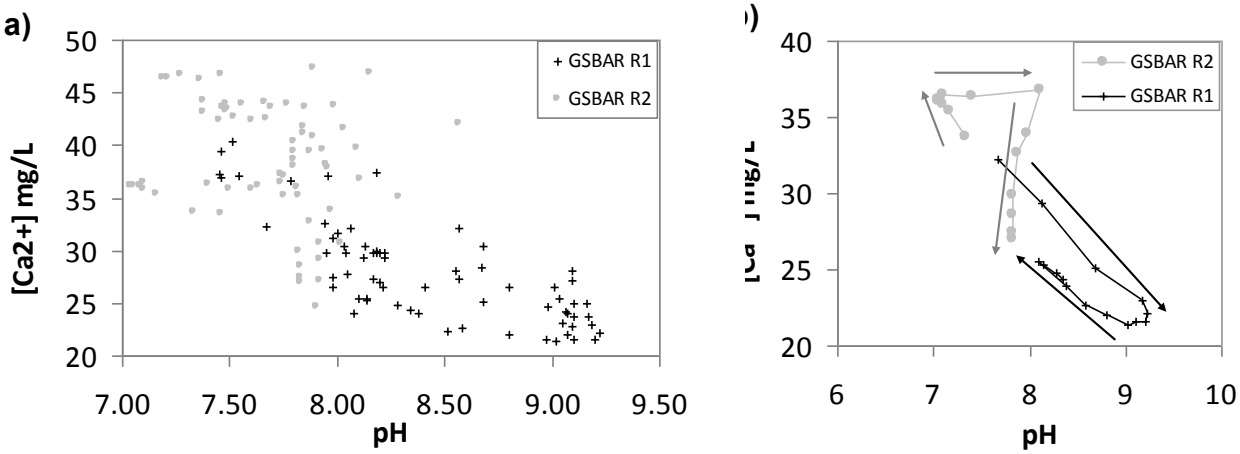

Figure V.5: calcium concentration versus pH in two biological GSBR: a) set of points corresponding to different kinetics during the reactor running period, b) comparison of the tendency of calcium profiles with pH during a kinetic course in both reactors

V.3.2. Calcium precipitation in the batch tests.

In order to assess the calcium precipitation kinetics separately from EBPR reactions, batch tests were performed individually with sludge samples maintained aerated and mixed in endogenous conditions. Various pH, ionic strengths, TSS and initial calcium and phosphorus concentrations were tested. Simulations with PHREEQC software considering the supernatant quality at the starting point of each test indicated the minerals that were supersaturated in the bulk (SI>0 in table V.2).

In all tests, hydroxyapatite (HAP), amorphous calcium phosphate (ACP) and tricalcium phosphate (TCP) were systematically supersaturated in the bulk. Aragonite, which is one of the polymorphs of calcium carbonate, was only thermodynamically susceptible to form in tests with high pH and low VSS, or initially at high VSS concentration, when inorganic carbon was not already depleted. Neither octacalcium phosphate (OCP), nor newberite and magnesium phosphate. Brushite (DCPD), phosphate dicalcic anhydrous (DCPA) andhydroxidicalcium phosphate (HDP) were only supersaturated for some of the tests (coinciding with aragonite saturation).

Table V.2: ***Supersaturation Indexes with respect to different minerals in the bulk at the beginning of the batch precipitation tests calculated with PHREEQC at T=25ºC.***

	supersaturated solid phases calculated by PHREQC										
test	**HAP**	**ACP**	**HDP**	**TCP**	**OCP**	**DCPD**	**DCPA**	**CAL**	**ARAG**	**NEW**	**$Mg_3(PO_4)_2$**
S1P1	1.28	0.57	0.05	1.31	-5.43	-0.18	-0.04	-0.87	0.11	-1.62	-1.79
S1P2	1.06	0.45	-0.22	1.19	-5.40	0.20	0.34	0.29	-0.38	-1.29	-1.97
S1P3	1.81	1.03	0.54	1.77	-4.88	-0.24	-0.10	0.60	0.51	-1.04	-0.57
S1P4	1.02	0.40	-0.26	1.14	-5.48	0.17	0.31	-0.39	-0.48	-1.01	-1.64
S1P5	1.19	0.54	-0.10	1.28	-5.32	0.13	0.27	-0.19	-0.28	-0.97	-1.41
S1P6	0.92	0.25	-0.29	1.00	-5.80	-0.13	0.02	-0.39	-0.48	-1.16	-1.62
S2P1	1.18	0.48	-0.03	1.22	-5.55	-0.20	-0.06	-1.00	-0.03	-1.26	-1.44
S2P2	1.43	0.75	0.13	1.49	-5.07	0.09	0.23	-0.88	0.10	-1.04	-1.24
S2P3	1.52	0.77	0.28	1.51	-5.21	-0.24	-0.10	-0.60	0.38	-1.20	-1.02
S2P4	1.59	0.80	0.39	1.54	-5.27	-0.44	-0.30	-0.43	0.55	-1.33	-0.91
S2P5	2.26	1.64	0.76	2.38	-3.65	0.73	0.87	0.72	0.63	-1.59	-0.87
S2P6	0.98	0.38	-0.31	1.13	-5.44	0.28	0.42	-0.58	-0.67	-0.84	-1.72

Only the batch tests in which pH values coincided with the range of pH observed in the GSBR (6.5-9.1) were considered for evaluating Ca:P stoechiometry. Figure V.5 shows the variation of calcium versus phosphate, indicating the experimental Ca:P stoichiometry in the different tests. For each point, relative standard deviation was 25% (mainly due to chromatography analysis). The sets of experiments were correlated to a straight line, the average slope of which gave a Ca:P ratio of 1.43 ± 0.03.

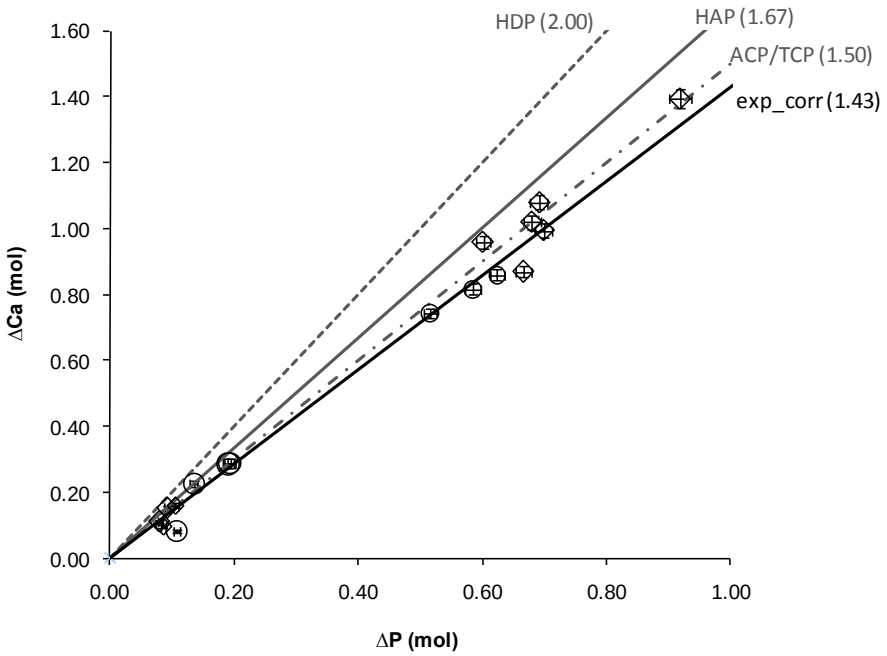

Figure V.6: experimental ΔCa versus ΔP (mmol) precipitated in the batch tests, compared to the reference ratios for minerals that were supersaturated in the bulk.

It can be seen that most of the points are arranged in a row close to that of the theoretical mineral ACP/TCP (Ca:P=1.5), indicating that the last two phases are the most likely to precipitate prior to HAP crystallization in the different conditions tested. No significant influence of pH (range 6.5-9.1), calcium and phosphorus concentrations (range 20-300mg/L) or ionic strength (range $1.2 \cdot 10^{-2}$-$5.7 \cdot 10^{-2}$) was found on this ratio. Since ACP and TCP have the same molar Ca/P ratios, the above methodology does not distinguish between the two minerals. Considering the fact that pH could vary between 6.5 and 9 in a biological reactor, figure 7 shows the influence of pH on the SI of the three major supersaturated phases according to PHREEQC: ACP, TCP and HAP. Simulations were conducted with the concentrations corresponding to experiment S2P1, comparable to those in the range measured in the biological reactor (33 mg/L for Ca and 14 mg/L for P).

The SI of the minerals increased proportionally to the pH in the bulk, revealing for all of them, one pH value at which HAP, then TCP and finally ACP started to become supersaturated, the other parameters remaining constant. Since the Ca:P ratios of ACP and TCP were similar due to the similarities in their chemical formula, modeling was further evaluated to isolate the most probable precursor driving HAP crystallization in aerobic granules.

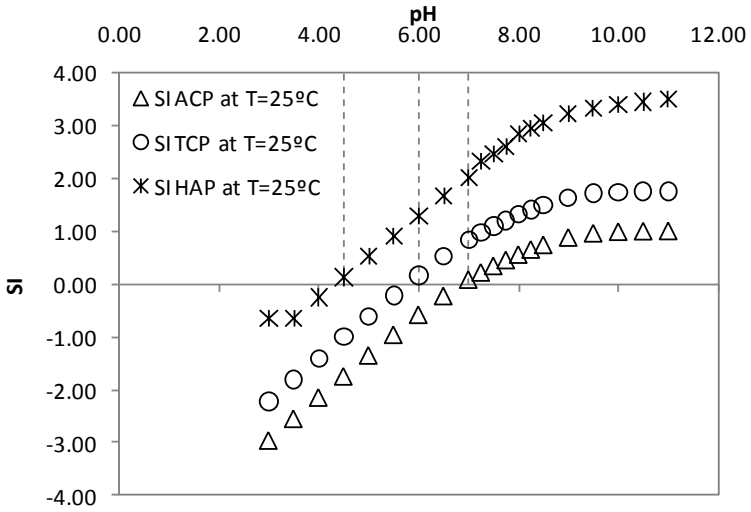

Figure V.7: pH influence on ACP, TCP and HAP supersaturation index calculated by PHREEQC® for test S2P1.

V.3.3 Modelling calcium phosphate precipitation

Based on the batch tests, three experiments (S2P1 and S2P2 at low VSS concentration, and S1P5 at high VSS concentration) were modeled using AQUASIM software, combined with PHREEQC for the initial conditions. The kinetic constant rate of the mineral (K) and the thermodynamic constant were fitted in the model as the values proposed for the last one in literature vary widely according to the different authors (table V.3).

Table V.3: Thermodynamic precipitation constants of ACP and TCP from the literature

Mineral phase	pKsp (T=25ºC)	Reference
ACP	25.46	Hoffmann, 1977
	26.52	Seckler et al., 1996
	25.20	Meyer and Weatherall 1982
	28.92	NIST database, 2011
B-TCP	32.63	Murray and May, 1996
	32.70	NIST database, 2011
	28.77	Song et al., 2001

Figure V.8 shows the calcium and phosphorus profiles modeled in the aforementioned tests compared to the experimental points. The adjusted model matches

the experimental data well, and the kinetic constants together with the pKsp fitted for each experiment are shown in table V.4.

Table V.4: Thermodynamic precipitation and kinetic rate constants deduced from the model.

Assay	TSS(g/L)	pKsp value	Kinetic constant rate (min^{-1})
S1P5	18.40	28.36	$3.81 \cdot 10^{7}$
S2P1	2.86	27.99	$4.13 \cdot 10^{5}$
S2P2	2.66	27.88	$1.16 \cdot 10^{5}$

Results show that the higher the TSS concentration in the bulk, the higher the kinetic constant rate of precipitation. In contrast, pKsp values were very similar in all the experiments. An average value of $\mathbf{pK_{sp}=28.07\pm0.58}$ was obtained. Considering a single pKsp for all the experiments, a satisfactory pKsp value was obtained from the mean of the previously fitted values, allowing the thermodynamic constant of the precursor phase to be found.

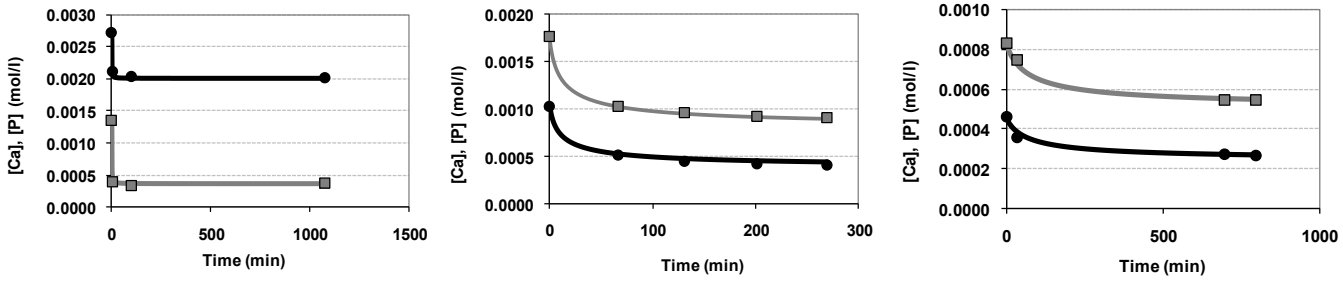

Figure V.8: Comparison of experimental and modeled assays at different MLSS concentrations: a) 18.4 g/L; b) 2.66 g/L; c) 2.86 g/L. Legend: [Ca] in gray; [P] in black.

The sensitivity of the model to pKsp value is evaluated in figure V.9. The three sets of tests chosen were modeled taking 3 different pK_{sp} values into account according to table V.3: the minimum provided in the literature (25.2), the maximum provided (32.63) and the mean value calculated above from the experiments modeled (28.07). It can be seen that the model (with a pKsp=28.07±0.58) described the observations correctly for different initial Ca:P ratios.

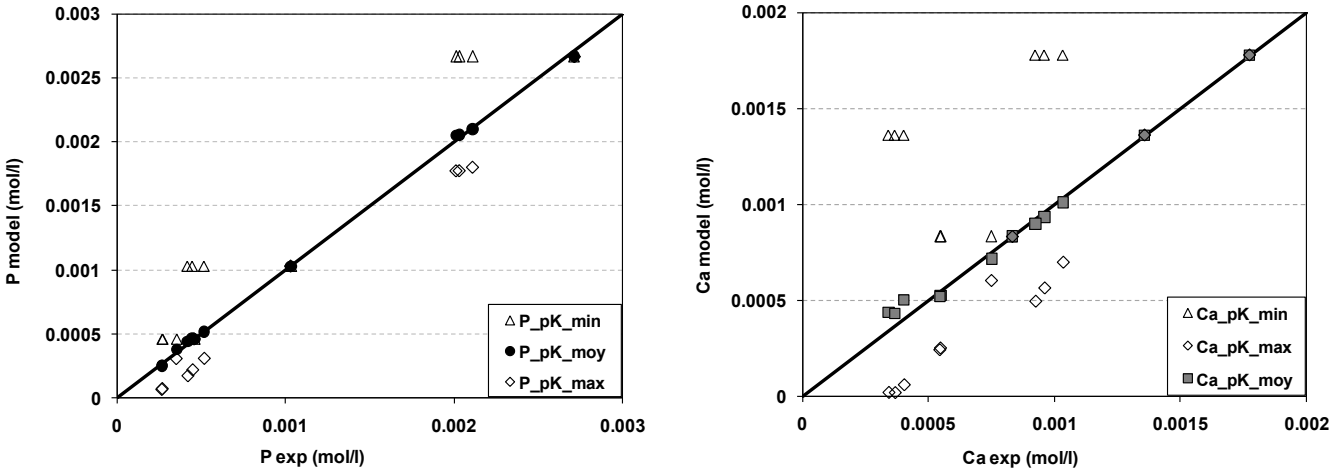

Figure V.9: Model sensitivity to the different precipitation constants (pKsp) (a) [P] prediction; (b) [Ca]

V.3.4 Analysis of the solid phases

Precipitates were collected and analyzed at the end of each experimental series and were representative of the cumulated mineral matter in the 2L reactor.

Figure V.10 shows the XRD analysis conducted on two samples: the suspended matter precipitated (black), and the sample of biological granules. Both samples were compared to the most coincident mineral patterns in the database of the software used (EVA®). The XRD spectra highlighted two coincident patterns with clear individual peaks: hydroxyapatite (HAP) and sylvite (KCl). Sylvite (KCl) was only observed in the suspended matter. It is a very soluble salt which was certainly not precipitated in the reactor initially but was formed during the evaporation of the sample (the presence of K^+ and Cl^- in the solution was due to the potassium phosphates and calcium chloride used for batch tests). The HAP spectrum was the one that explained the major peaks for both granules and suspended solids samples. In addition, the spectra indicated the probable presence of amorphous phases, which could explain the large peaks that do not exactly match any crystalline forms.

The most important conclusion is that both sample patterns match and coincide with that of HAP almost perfectly, despite the black peak at 33º, 47º and 58º in the 2θ abscissa axis, which corresponds to that of the sylvite mentioned above. Another conclusion is that, whatever the precursor is, the final phase crystallized seems to be HAP, both in the bulk and in the granules, and that the time scale for its precipitation is less than 7 days. These results confirm the similarities between the precipitated phases found in the supernatant during the batch tests and those observed inside the granules.

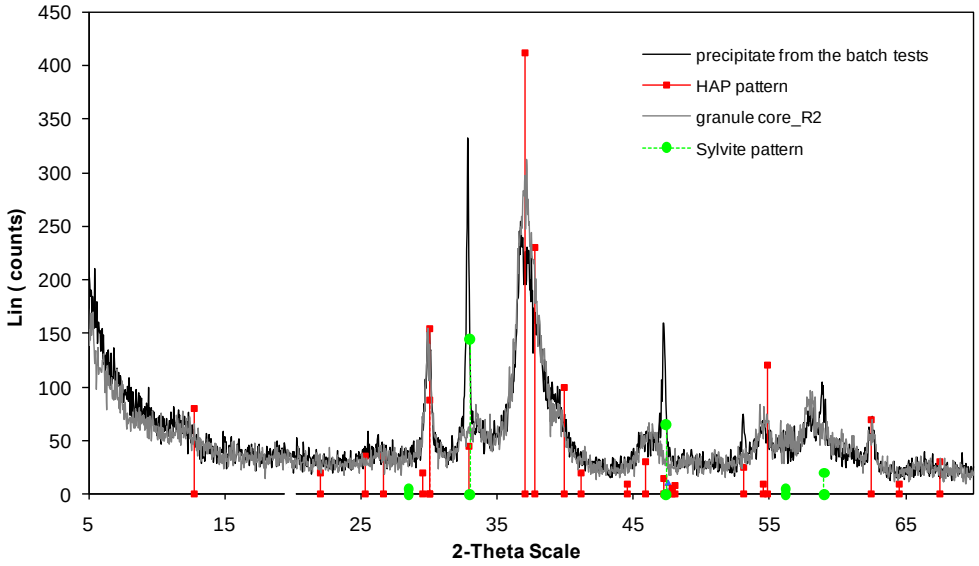

Figure V.10: Comparison of the mineral precipitated at the end of the batch tests and mineral fraction in the core of biological granules.

V.4. DISCUSSION

V.4.1. ACP: the precursor of HAP in granular sludge processes

The results globally confirm that HAP is the major crystallized mineral accumulated in the granular sludge in the long term. But data also indicate that calcium phosphate precipitated first during each batch cycle, due to super-saturation in a precursor form which was probably ACP. According to House and Donaldson (1986), HAP precipitation crystallizes through a precursor when heterogeneous nucleation takes place, which was the case here. Although different precursors are proposed in the literature, ACP or TCP seems to be the one that can be formed at a wider pH range, and different ionic strengths. Results obtained in this paper for the precipitation batch tests (in which

biological activity was limited), led to a calcium phosphate precursor with Ca:P molar ratios between 1.38-1.59, with a mean value of 1.43±0.03, which fits with ACP or TCP. Modeling different assays at different MLSS concentrations revealed that the pKsp that best fitted the data was $pKsp_{25ºC}$ = 28.07±0.58. The thermodynamic constant was compared to that provided in the literature (table V.3) and corresponds to ACP for the NIST database, whereas TCP, which has the same Ca/P ratio, should theoretically present a higher pKsp. Regarding the precursor phases able to form in acidic conditions (Gao et al., 2010), neither brushite (DCPD), nor monetite (DCPA) and octacalcium phosphate (OCP) were likely to form in the batch tests from a thermodynamic point of view, considering the SI negative values. This result first contrasts with the model by Maurer and Boller, 1999, who proposed the HDP as a precursor form, with Ca:P molar ratio = 2. In our work, the only test in which the Ca:P removal ratio was close to 2 could be explained by a simultaneous precipitation of calcium carbonate, probably aragonite at high pH, which is supported by the supersaturation index (SI) calculated with PHREEQC (see table V.2). Thus, our results confirm the approach of Barat et al., 2011, and those of Musvoto et al., 2000a and 2000b, who considered ACP, as the first step of calcium phosphate precipitation.

Finally, modeling ACP formation by the Koutsoukos model (1980), predicted calcium and phosphate behavior during the batch tests quite well. These assays were predicted only for the short term (from 3 to 15 h) and it should be noted that the progressive formation of HAP should also be included in the long term as it was demonstrated to accumulate after several days.

V.4.2. Operating pH conditions influencing MIPP in GSBR

Supersaturation with respect to Ca and P concentrations and pH were the major parameters that influenced precipitation, in agreement with Mulkerrins et al., (2004).

In order to evaluate how pH drives calcium phosphate precipitation, figure V.11 shows the evolution of calcium concentration as a function of pH, obtained by modeling different pH values over different kinetics during the running period in order to assess the contribution of P precipitated with calcium at each pH in equilibrium. Simulations were carried out using the model described above, which allowed the calculation of the equilibrium concentration for Ca^{2+} and PO_4^{3-} at the different pH tested between 6.5 and 9.5. Different Ca:P ratios and initial concentrations were tested in the influent, in order to

assess the limiting conditions for the maximum P removal fraction by precipitation (in the case that no biological P removal takes place).

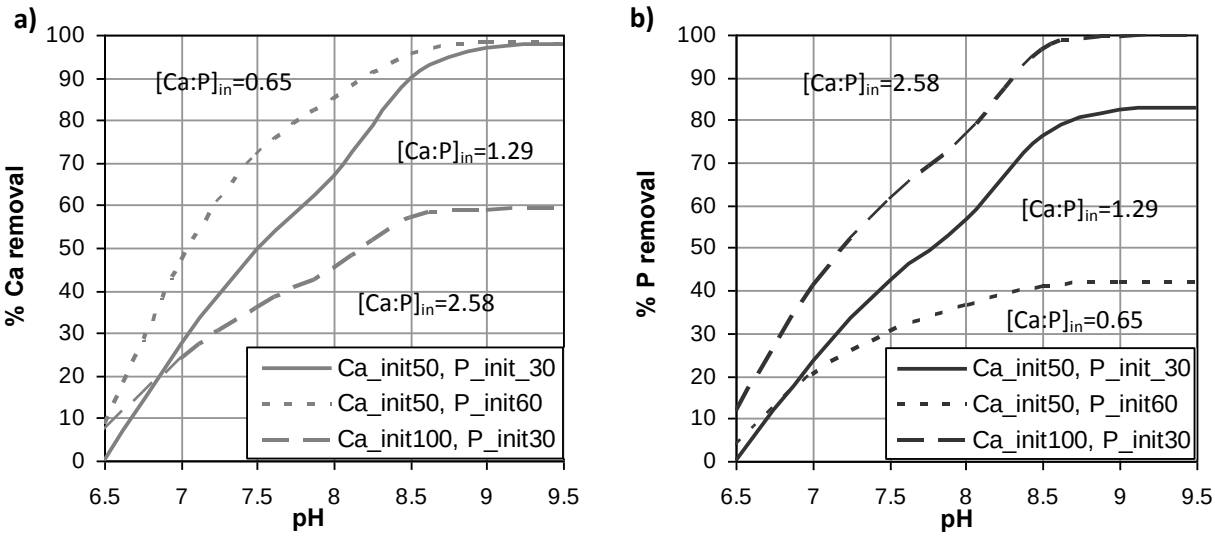

Figure V11: Contribution of calcium phosphate precipitation within different pH attained at the end of each kinetic phase in the GSBR. Ca:P ratios in the inlet are in mol. a) % of Ca removed by precipitation (gray); b) % of P removed by precipitation (black)

The results in figure V.11 pointed out that in the current influent conditions ([Ca] = 50 mg/L and [P]= 30 mg/L), the maximum fraction of P that could be removed by precipitation achieves the 55% at final pH=8. This is under the assumption that no interference with EBPR process took place. Indeed in the bioreactor, experimental kinetics showed a higher P removal but a lower contribution of the precipitation mechanism (39.6 %), which is due to simultaneous biological P removal (EBPR). Figure 11.b confirms that pH seriously influences the Ca-P precipitation: variation of one pH unit from 7.5 to 8.5 leads theoretically to an increase from 40% to 75%, at the GSBR working pH range. Therefore, P removal by Ca-P precipitation can vary a lot depending on the final pH attained at the end of the cycle. For example, varying 25% to 85% of P could precipitate varying pH in a range from 7 to 9 in the model. As indicated in Figure V.11, precipitation was observed in the sequencing batch reactor due to an enough level of calcium and phosphate achieved in the influent (50 mg/L of Ca and 30 mg/L of P). The amount of calcium-phosphate formed in the reactor is first driven by the amount of calcium and

phosphate present in the bulk. Finally, figure V.11 also shows how the amount of P removed by precipitation increased as the influent Ca/P ratio increases.

V.4.3. Influence of biomass and bioreactions on precipitation

The precipitation process is also influenced by biomass in different ways: (1) bio-aggregates play a catalyzing role at the nucleation sites, (2) some of the bioreactions modify the pH locally and transiently, (3) some of the bio-reactions transiently release phosphates (coming from internal polyphosphate).

Identification of the model parameters indicated that the kinetic rate of calcium phosphate precipitation increased with suspended solids concentration. Obviously, it is well-known that precipitation is a surface-controlled process and the differences in the values of the kinetic constants can be due to the surface available for crystal nucleation. Moreover no precipitates were observed in batch tests without any sludge addition (VSS=0, results not shown) whereas crystal formation was observed in tests with even lower initial Ca and P concentrations and even lower pH but previously seeded with microbial aggregates, leading to the conclusion that heterogeneous nucleation onto the suspended biological aggregates constitutes a first step towards the MIPP process. Figure V.12 shows different images of microscopic observations over the different experiments in the batch reactor.

At the end of a normal cycle in the bioreactor, no crystals were found in the supernatant (figure 12.a). In contrast, in the batch assays, nucleation began (figure 12.b) and some crystals started appearing on the bioaggregates interface (figure 12.c). Different crystallization forms were observed during the physicochemical tests (figs. 12.d, e and f), all converging in dendritic crystals centered in rhombohedral structures that finally superposed to form rectangular terraces like the HAP formation reported by (Chakhmouradian and Mitchel, 1999; Elliott, 1994).

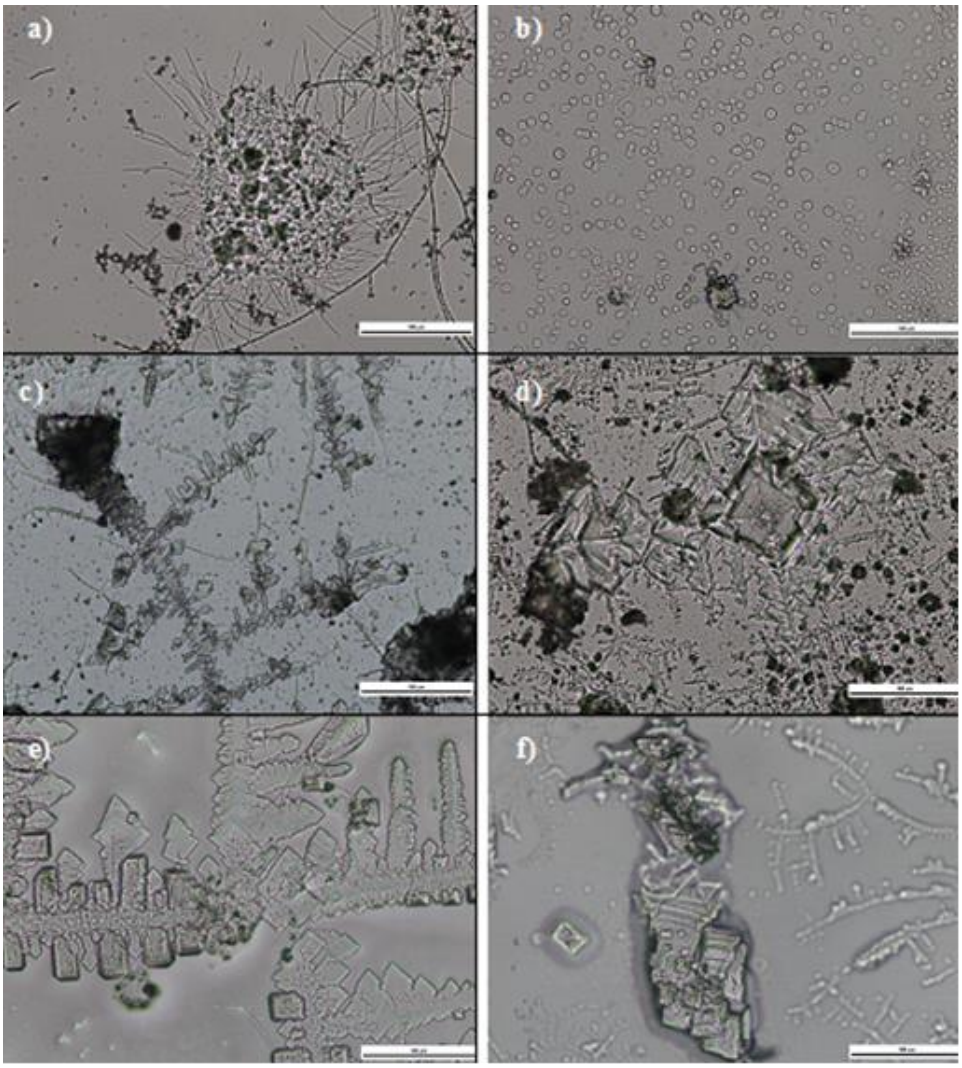

Figure V.12: Mineral precipitation in the batch tests at different periods (Scale bar =100 µm): *a) at the end of the aerobic period in the biological reactor, b) beginning of the batch test with low VSS concentration; c) dendritic growth of precipitates that have nucleated on organic sludge filaments; d) rhombohedral shape of calcium phosphate growing at the crossing point of the dendritic crystals; e) illustrates a co-precipitation of another phase onto the previous crystals and f) shows the final helicoidal crystal growth of presumed HAP.*

As calcium phosphate in the form of HAP was observed in the center of granules, it is likely to think that bioreactions could locally increase the supersaturation either by a pH increase or an anaerobic phosphate release. In the beginning of the GSBR cycle when pH starts to increase due to denitrification (and also acetate consumption) and when P is released by PAO, heterogeneous nucleation of ACP probably begins on the surface walls of bacterial and maybe also in the internal pore of aggregates where anoxic or anaerobic

activities are the most important. Partial solubilization of ACP at the surface of the bioaggregates could also take place during subsequent aerobic period as the nitrification provokes a proton release. On the other hand, the pH in the center could be maintained relatively high due to oxygen limitation favoring simultaneous denitrification, and amorphous calcium phosphate could be progressively converted to HAP in the core of granules. ACP cannot be detected by XRD (Banu, 1995), so no peaks of the precursor could be observed in the core of granules, only those of the crystallized HAP have been demonstrated. However, previous analysis with EDX probes showed that Ca and P content in the external part of bioliths was lower than those measured in the center (Mañas et al. 2011). Thus, HAP would probably crystallize with time and grow in an organic confined medium that would store it as a stable phosphate resource until granule breakage or purge.

V.5. CONCLUSIONS

In this work, experiments were conducted to investigate calcium phosphate precipitation in an EBPR process with granular sludge.

Short term calcium phosphate precipitation was characterized by a Ca:P stoichiometry of 1.43±0.03 which is close to those of ACP or TCP. Calcium and phosphate behavior were successfully modeled considering a mean pKsp value adjusted to 28.07±0.58, which is in accordance with the literature and comparable to that of ACP. After several days, amorphous calcium phosphate was converted to HAP, which was detected by XRD analysis.

The contribution of P removal by precipitation, which is linked to the MIPP mechanism responsible of the phosphate bioliths found in granules, is basically influenced by pH and Ca and P concentrations. In the conditions tested, a maximal contribution of precipitation between 40 % to 75 % of the P removed could take place depending on the final pH achieved in the biological reactor.

The presence of biomass influenced calcium phosphate precipitation in different ways: heterogeneous precipitation took place on bio-aggregates which formed the nucleation site, and the kinetic rate is hence proportional to suspended solid concentration (no signs of precipitation were found in the test carried out without biomass). Bioreactions that produce alkalinity, i.e. denitrification or VFA consumption,

encourage precipitation in the bioreactor and also probably in the core of microbial granules, where hydroxyapatite is observed to accumulate.

V.6. ACKNOWLEDGMENTS AND CONTRIBUTIONS

I would like to give a special mention to M. Pocquet, E. Mengelle, D. Auban, M. Bounouba and D. Delanges for their helpful contribution in this work.

V.7. REFERENCES

Abbona F., Lundager Madsen H.E., Boistelle R. (1986). *The initial phases of calcium and magnesium phosphates precipitated from solutions of high to medium concentrations.* Journal of Crystal Growth 74(3):581-590.

Amjad Z., Koutsoukos P.G., Nancollas G.H. (1981). *The crystallization of fluoroapatite. A constant composition study*. Journal of colloid and Interface Science 82(2):394-400.

Banu Mihai (2005). *Mise en forme d'apatites nanocristallines: ceramiques et ciments*. PhD thesis INP Toulouse.

Barat R., Montoya T., Seco A., Ferrer J. (2011). *Modelling biological and chemically induced precipitation of calcium phosphate in enhanced biological phosphorus removal systems.* Water Research, 45(12): 3744-3752.

Bazylinski, D.A., (1996). *Controlled biomineralization of magnetic minerals by magnetotactic bacteria.* Chem. Geol. 132 (1-4): 191–198.

Benzerara,. K.,Miot,J.,Morin,G.,Ona-Nguema, G.,Skouri-Panet,F., Ferrard, C. (2011). *Comptes Rendus* Geosci. 343, 160–167.

Boskey, A.L., Posner, A.S., (1974). *Magnesium stabilization of amorphous calcium phosphate: a kinetic study.* Mater. Res. Bull. 9 (7): 907–916.

Brown W.E., Matthew M., Tung M.S. (1981). *Crystal chemistry of OCP*; Prog Crystal Growth Charact., 4: 59-8.

Chakhmouradian A.R. and R.H. Mitchell (1999). Niobian Ilmenite, Hydroxylapatite and sulfatian monazite. *Alternative hosts for incompatible elements in calcite kimberlite from International'Naya, Yakutia*. The Canadian Mineralogist 37:1177-1189.

De-Bashan L. E. and Bashan Y. (2004). *Recent advances in removing phosphorus from wastewater and its future use as fertilizer (1997-2003).* Water Research 38(19): 4222.

Dupraz S., Parmentie M., Ménez B., Guyot F. (2009). *Experimental and numerical modelling of bacterially induced pH increase and calcite precipitationn in saline aquifers.* Chemical Geology 265: 44-53.

Eanes E.D., Gillessen I.H., Posner A.S. (1965). *Intermediate states in the precipitation of hydroxyapatite.* Nature 208: 365-367.

Elliott J.C. (1994). *Structure and Chemistry of the Apatites and Other Calcium orthophosphates; Studies in Inorganic Chemistry* 18, Amsterdam, London, New York, Tokyo: Elsevier.

Gao R., van Halsema F.E.D. Temminghoff E.J.M. van Leewen H.P., van Valenberg H.J.F. Eisner M.D., Giesbers M., van Boekel M.A.J.S. (2010). *Modelling ion composition in simulated milk ultrafiltrate (SMUF). I: Influence of calcium phosphate precipitation.* Food Chemistry 122(3):700-709

Giesen A. (1999). *Crystallization process enables environmental friendly phosphate removal at low costs.* Environmental Technology 20(7): 769-775.

Grases F., Söhnel O., Vilacampa A.I., March.G. (1996). *Phosphates precipitating from artificial urine and fine structure of phosphate renal calculi.* Clinica Chimica Acta 244(1):45-67.

Hoffman R. J. (1977) *Phosphorus removal in the modified activated sludge process*. Research Report W22, Dept. of Civil Eng., Univ. of Cape Town, Rondebosch, 770 1, South Africa.

Jardin H., Pöpel J. (1996), *Influence of the enhanced biological phosphorus removal on the waste activated sludge production*, Water Science and Technology 34 (1–2):17.

Johnsson, M.S.A., Nancollas, G.H., (1992). *The role of brushite and octacalcium phosphate in apatite formation*. Crit. Rev. Oral Biol. Med. 3 (1-2): 61–82.

Koutsoukos P., Amjad Z., Tomson M. B. and Nancollas G. H. (1980). *Crystallization of calcium phosphates: a constant composition study.* J. Am. Chem. Soc. 27: 1553-1557.

Lazic S. (1995). *Microcrystalline hydroxyapatite formation from alkaline solutions*. Journal of Crystal Growth 147(1-2):147-154.

Lemaire R. (2007). *Development and fundamental investigations of innovative technologies for biological nutrient removal from abattoir wastewater.* Ph.D Thesis. University of Queensland, Australia.

Liu, Y., Tay, J.-H., (2004). State of the art of biogranulation technology for wastewater treatment. Biotechnology Advances 22 (7): 533-563.

Lundager-Madsen H.E., Christensson F. (1991). *Precipitation of calcium phosphate at 40° C from neutral solution.* Journal of Crystal Growth 114(4):613-618.

Lundager-Madsen H.E., Christensson F., Chernoc A.A., Polyak L.E., Suvrova E.I. (1995). *Crystallization of calcium phosphate in microgravity*. Advances in Space Research 16(8):65-68.

Mañas A., Spérandio M., Biscans B. (2011). *Biologically Induced phosphorus precipitation in aerobic granular sludge process.* Water Research 45: 3776-3786.

Maurer M., Boller M. (1999). *Modelling of phosphorus precipitation in wastewater treatment plants with enhanced biological phosphorus removal*. *Water Science and Technology* 39(1):147-163.

Maurer M., Abramovich D., Siegrist H., Gujer W. (1999). *Kinetics of biologically induced phosphorus precipitation in waste-water treatment.* Water Research 33(2):484-493.

Meyer J.L., Weatherall C.C. (1982). *Amorphous to crystalline calcium phosphate phase transformation at elevated pH.* Journal of Colloid and Interface Science 89(1):257-267.

Monstastruc L. (2003). *Modélisation et optimisation d'un réacteur en lit fluidisé de déphosphatation d'effluents aqueux.* Ph.D. Thesis, INPT and UPS Toulouse III.

Morgenroth, E., Sherden, T., Van Loosdrecht, M.C.M., Heijnen, J.J., Wilderer, P.A., (1997). *Aerobic granular sludge in a sequencing batch reactor.* Water Res. 31 (12), 3191–3194.

Mulkerrins D., Dobson A.D.W., Colleran E. (2004). *Parameters affecting biological phosphate removal from wastewaters*. Environment International 30:249-259.

Murray K. and May P. M. (1996) Joint Expert Speciation System (JESS). *An international computer system for determining chemical speciation in aqueous and non-aqueous environments.* Supplied by Murdoch University, Murdoch 6150, Western Australia and the Division of Water Technology, CSIR, PO Box 395, Pretoria, South Africa.

Musvoto E.V., M.C. Wentzel, R.E. Loewenthal, G.A. Ekama (2000a). *Integrated chemical–physical processes modelling—I. Development of a kinetic-based model for mixed weak acid/base systems.* Water Research, 34(6): 1857-1867

Musvoto E.V., M.C. Wentzel, G.A. Ekama (2000b) *Integrated chemical–physical processes modelling—II. simulating aeration treatment of anaerobic digester supernatants*. Water Research, 34 (6): 1868-1880.

Nancollas G.H. and Koutsoukos P.T. (1980). *Calcium phosphate nucleation and growth in solution.* Progress in Crystal Growth and Characterization 3(1):77-102.

Nancollas, H.G., Wu, W., (2000). *Biomineralization mechanisms: a kinetics and interfacial energy approach.* J. Cryst. Growth 211: 137–142.

NIST database: Searchable bibliography of Fundamental Constants. URL: http://www.nist.gov/pml/data/physicalconst.cfm (consulted on January 2011).

Parkhurst D.L. (2000). *PHREEQC 2.2- A computer Program for Speciation, Reaction-Path, Advective transport and Inverse Geochemical calculation*. U.S. Geological Survey, Colorado 2000.

Posner AS, Betts F. (1975). *Synthetic amorphous calcium phosphate and its relation to bone mineral structure*. Acc Chem Res 8:273–81.

Seckler M.M., Bruinsma S.L., van Rosmalen G.M. (1996). *Phosphate removal in a fluidized bed I. Identification of physical processes.* Water Research 30(7):1585-1588.

Y. Song, H.H. Hahn, and E. Hoffmann, (2001). "*The effects of pH and Ca/P ratio on the precipitation of calcium phosphate", Second international conference on Recovery of Phosphate from sewage and animal wastes,* Holland, 12th and 13th March.

Tomazic B., Tomson M., Nancollas G.H. (1975). *Growth of calcium phosphates on hydroxyapatite crystals: The effect of magnesium.* Archives of Oral Biology, 20(12):803-808.

Tsuge H., Tanaka Y., Yoshizawa S., Kuraishi T. (2002). *Reactive Crystallization Behavior of Calcium Phosphate With and Without Whey Protein Addition.* Chemical Engineering Research and Design 80(1):105-110.

United Nations of Environment Program Yearbook (2011): Emerging Issues in our Global Environment.

Wan J. and Sperandio M. (2009). *Possible role of denitrification on aerobic granular sludge formation in sequencing batch reactor.* Chemosphere 75(2): 220-227.

Weiner, S., (2008). *Biomineralization: a structural perspective*. J. Struct. Boil. 163 (3): 229–234.

Table V.5: Petersen matrix simplified for aqueous species in the solution: acid/base equilibria, ion pairing and $Ca_3(PO_4)_2$ precipitation.

	CO_3^{2-}	HCO_3^-	H^+	OH^-	$H_2PO_4^-$	HPO_4^{2-}	PO_4^{3-}	Mg^{2+}	Ca^{2+}	Na^+	NH_3	pK	Kr (s^{-1})
H_2O			1	1								14	10^{10}
H_2CO_3		1	1									(3404.7/T)-14.8435+T*0.03279	10^7
HCO_3^-	1		1									(2902.4/T)-6.498+T*0.02379	10^{10}
H_3PO_4			1		1							(799.3/T)-4.5535+T*0.01349	10^8
$H_2PO_4^-$			1			1						(1979.5/T)-5.3541+T*0.01984	10^{12}
HPO_4^{2-}			1				1					12.02	10^{15}
NH_4^+			1								1	(2835.8/T)-0.6322+T*0.00123	10^{12}
$CaOH^+$				1					1			-1.22	10^7
$CaCO_3(aq)$	1								1			-3.20	10^7
$CaHCO_3^+$		1							1			-1.26	10^7
$CaPO_4^-$							1		1			-6.46	10^7
$CaHPO_4$						1			1			-2.73	10^7
$CaH_2PO_4^+$					1				1			-1.41	10^7
$MgOH^+$				1				1				-2.20	10^7
$MgCO_3$	1							1				-3.40	10^7
$MgHCO_3^+$		1						1				-1.16	10^7
$MgHPO_4$						1		1				-2.50	10^7
$MgPO_4^-$							1	1				-3.13	10^7
$MgH_2PO_4^+$					1			1				-1.51	10^7
$NaHPO_4^-$						1				1		-1.05	10^7
$Ca_3(PO_4)_2$							2		3			**	**

** Needs to be determined by this method

Table V.6: Kinetic rate of the forward and reverse equations for dissolved species.

	Rate of the forward dissociation	Rate of the reverse dissociation
H_2O	K_r_w*((10^(-pK_w))/(fm^2))	K_r_w*S_OH*S_H
$H_2CO_3^*$	K_r_c1*((10^(-pK_c1))/(fm^2))*S_H2CO3star	K_r_c1*S_H*S_HCO3
HCO_3^-	K_r_c2*((10^(-pK_c2))/fd)*S_HCO3	K_r_c2*S_H*S_CO3
H_3PO_4	K_r_p1*((10^(-pK_p1))/(fm^2))*S_H3PO4	K_r_p1*S_H*S_H2PO4
$H_2PO_4^-$	K_r_p2*((10^(-pK_p2))/fd)*S_H2PO4	K_r_p2*S_H*S_HPO4
HPO_4^{2-}	K_r_p3*(((10^(-pK_p3))*fd)/(ft*fm))*S_HPO4	K_r_p3*S_H*S_PO4
NH_4^+	K_r_n*(10^(-pK_n))*S_NH4	K_r_n*S_H*S_NH3
$CaOH^+$	K_r_ca1*S_CaOH	K_r_ca1*((10^(-pK_caoh))*fd)*S_Ca*S_OH
$CaCO_3(aq)$	K_r_ca2*S_CaCO3aq	K_r_ca2*((10^(-pK_caco3))*(fd^2))*S_Ca*S_CO3
$CaHCO_3$	K_r_cahco3*S_CaHCO3	K_r_cahco3*((10^(-pK_cahco3))*fd)*S_Ca*S_HCO3
$CaPO_4^-$	K_r_capo4*S_CaPO4	K_r_capo4*((10^(-pK_capo4))*fd*ft/fm)*S_Ca*S_PO4
$CaHPO_4$	K_r_cahpo4*S_CaHPO4	K_r_cahpo4*((10^(-pK_cahpo4))*(fd^2))*S_Ca*S_HPO4
$CaH_2PO_4^+$	K_r_cah2po4*S_CaH2PO4	K_r_cah2po4*((10^(-pK_cah2po4))*fd)*S_Ca*S_H2PO4
$MgOH^+$	K_r_mgoh*S_MgOH	K_r_mgoh*((10^(-pK_mgoh))*fd)*S_Mg*S_OH
$MgCO_3$	K_r_mgco3*S_MgCO3	K_r_mgco3*((10^(-pK_mgco3))*(fd^2))*S_Mg*S_CO3
$MgHCO_3^+$	K_r_mghco3*S_MgHCO3	K_r_mghco3*((10^(-pK_mghco3))*fd)*S_Mg*S_HCO3
$MgHPO_4$	K_r_mghpo4*S_MgHPO4	K_r_mghpo4*((10^(-pK_mghpo4))*(fd^2))*S_Mg*S_HPO4
$MgPO_4^-$	K_r_mgpo4*S_MgPO4	K_r_mgpo4*((10^(-pK_mgpo4))*fd*ft/fm)*S_Mg*S_PO4
$MgH_2PO_4^+$	K_r_mgh2po4*S_MgH2PO4	K_r_mgh2po4*((10^(-pK_mgh2po4))*fd)*S_Mg*S_H2PO4
$NaHPO_4^-$	K_r_nahpo4*S_NaHPO4	K_r_nahpo4*((10^(-pK_nahpo4))*fd)*S_Na*S_HPO4

CHAPTER VI:

CONCLUSIONS AND PERSPECTIVES

"Tout ce qu'un homme est capable d'imaginer, un jour, d'autres hommes seront capables de le réaliser." Jules Verne

***

This short chapter overviews the main outcomes of this thesis, the work that has not been valorized as result chapters yet, as well as some guidelines for future work.

VI.1.GENERAL CONCLUSIONS AND RESULTS

This thesis has been focused on phosphorus removal in biological aerobic granular sludge reactors, and particularly, on a particular phenomenon observed, namely by the first time: ***Microbially Induced Phosphorus Mineralization*** **(MIPP)**, consisting on the bioaccumulation of phosphate minerals inside granules.

The first strategy consisted on evaluating the performances and the different processes that took place in a GSBR which contained a mixture of flocs and granules, and working with anoxic/aerobic cycles. During 500 days of study, COD, N-NH_4 and phosphorus removal yields varied from 92-97%, 93-100% and 30-70% respectively. The assessment of different reactor kinetics cycles, and the absence of solid minerals in the bulk, lead us think that some biomineralization processes could take place inside aerobic granules.

According to this, a set of tests with different analytical techniques (Raman, SEM-EDX, XDR, MPL, chemical extractions) were carried out in the research of mineral deposits in the flocs matrix, in the supernatant and in different granule-cut slices.

The observation of the granules with microscopic polarized light (MPL), first revealed a crystalline structure in the internal slices of aerobic granules grown in the afore-mentioned GSBR. Raman, XRD and SEM-EDX analysis converged that a calcium phosphate crystal in the major form of hydroxyapatite [$Ca_5(PO_4)_3(OH)$], precipitated in the core of granules.

In the third chapter, the stability and performances of two GSBR were studied. *GSBR1* was the same precedent reactor (working with anoxic/aerobic cycles), whereas *GSBR2* was seeded with biomass from *GSBR1*, and it was run in anaerobic/aerobic cycles, encouraging bio-P removal. At the end of the 250 days of study, a part of the biomass in *GSBR2* was washed out, due to the filamentous bacteria outgrowth on granules surface (associated with the fast growth of granules' size up to 4mm). Conversely, the parent reactor maintained its good properties. *GSBR1* was stable during the course and achieved good COD and nitrogen removal yields (99 and 100% respectively), whereas GSBR2 achieved 97% of COD removal and 86% on average of nitrogen removal, being very variable this last performance. Regarding phosphorus, both reactors attained similar yields on average (45%), although GSBR2 was more unstable. The contribution of precipitation in both reactors was of 28 and 21 % of the incoming phosphorus for GSBR1 and GSBR2, respectively, based on average calcium removal yields. Therefore, precipitation phenomena seemed to be more important in GSBR1, which was assumed to be enhanced by the higher pH achieved (up to 9.2) during the denitrification stage.

In chapter IV, the analytic techniques developed in chapter II, were applied for anaerobic granules originated from different full scale UASB treating wastewater from cheese industry. Granules from anaerobic processes presented a broad heterogeneity of samples, some contained mineral bioliths sparsely inside, others outside and some samples did not contain bio-minerals neither inside nor wrapping the granule. But most of the samples contained either calcium phosphate concretions inside, probably ACP or TCP (considered like HAP precursors); or calcium carbonate, for the UASB working at the highest pH. The calculation of supersaturation indexes for the minerals assessed in the bulk of all reactors (UASB and GSBR) and SEM-EDX analyses, lead to think that calcium phosphate tended to cumulate inside granules due to the more favorable local conditions induced by biological reactions. In any case, struvite does not appear to precipitate neither in the bulk nor inside granules of any reactor (anaerobic nor aerobic). Aeration tests over the effluent coming from different anaerobic digesters (Annex VI.1), showed that struvite could form if proper pH was attained by CO_2 stripping (aerating the effluent). Despite of the higher pH achieved in aerobic reactors, ammonium is depleted via nitrification during the aerobic phase, and magnesium concentrations were not high enough to precipitate struvite at the end of the cycles, although figures II.9 and II.11 show that it could be transiently formed during the anaerobic/anoxic phase.

It is assumed that in aerobic granules, calcium phosphates were formed gradually by means of a precursor of the most thermodynamic stable phase, as suggested with SEM-EDX analysis. The research of such precursors is important regarding modeling, and it was thus assessed in chapter V.

Therefore, different precipitation batch tests were carried out in order to assess physicochemical precipitation at different pH, TSS and calcium and phosphorus concentrations. A physicochemical model was used for modeling the different set of tests. Those experiments revealed that the most probable precursor of HAP in the operating conditions of the GSBR reactor was ACP, providing a pKsp constant of 28.07 ± 0.58; and a kinetic constants varying with the TSS concentration.

Phosphorus removal by Ca-P precipitation can vary depending on the final pH reached at the end of the cycle, varying from 25% to 85% in a pH range from 7 to 9 according to the model. The free evolution of pH from 7.2 to 8.5 during the kinetic cycle course in GSBR2, seems to be the best strategy to encourage bio-P removal, and with the current synthetic effluent

concentrations, the maximum fraction of P that could be removed by precipitation achieves the 55% at final pH=8.

The bio-precipitation process is influenced by biomass in different ways: (1) bio-aggregates play a catalyzing role as nucleation sites, (2) some of the bioreactions modify the pH locally and transiently, (3) some of the bacteria (PAO) transiently release phosphates (coming from internal polyphosphate). The first point was illustrated by the fact that no crystal precipitation was found in physicochemical experiments with TSS = 0 g/L. The second point could explain the stratification of calcium phosphates in the core of granules, as denitrification (responsible of pH rise) takes place in the anoxic zones of the granule (Mañas et al., 2009).

Summarizing, this thesis has contributed to two different aspects: from a fundamental point of view, it has been evaluated the mechanisms of biomineralization in aerobic granules, developing some analytical techniques for characterizing the nature of the bioliths. A physico-chemical model as well as some calculation softwares, have been coupled in order to provide thermodynamic information for the comprehension of the different phenomena. From an applied point of view, it has been evaluated the performances and stability of different reactor configurations, in sight of applying the process for a real case of industrial wastewater effluent.

VI.2.PERSPECTIVES

Finally, providing information about the mineralization phenomenon in aerobic granular sludge, this work sheds light on the possibility of treating calcium and phosphorus-rich effluents, like those coming from the dairy and cheese industry, with aerobic granules cultivated in SBR, for several reasons: 1) in order to achieve better nutrient removal yields 2) in order to facilitate sludge valorization with a phosphate-rich, stable and easily dewatering mineral 3) driving mineral precipitation inside granules can provide them stable settling properties. And finally it could reduce the clogging problem in pipes, pumps and reactor walls.

Nevertheless, work is now in progress in order to evaluate some aspects that have not been possible to assess during this Ph.D dissertation:

1) The use of a real effluent with higher concentrations of nutrients and calcium is now planned in a SBR with a volume of 345 L (figure VI.1) located in one of the cheese wastewater treatment plants. It will be placed after the anaerobic digester, and a VFA by-pass stream could

be envisaged in order to provide more easily biodegradable carbon sources and avoid the filamentous bacteria growth that destabilized reactor GSBR2, and to enhance EBPR. This process will be combined and compared with a struvite crystallizer.

Figure VI. 1: GSBR (right) and crystallizer (left) pilots for real wastewater treatment coming from the cheese industry.

Even if some commercial technologies (see chapter I) aim hydroxyapatite pellet formation, hydroxyapatite is one of the most thermodynamic stable phases among calcium phosphates, thus, phosphate bio-availability is considered insufficient for direct fertilization. A post-treatment process of granules withdrawn, could consist on an acid solubilization of smashed dried granules in water (figure VI.2), used for irrigating the fields.

Figure VI. 2: Air-Dried granular sludge purged from GSBR1.

2) Another perspective of this thesis consists on the coupling of the physicochemical model and the biological one in order to assess the precipitation phenomenon inside granules. Preliminary results using the ASM3 model for GSBR1 showed proton gradients inside these aggregates, and they were compared to titrimetric results that had been found in the literature (Mañas et al., 2009). However, future work implies the coupling of both models in aerobic granules (that has not been done to the present). Given that biological phosphorus removal takes place in the reactor, the choice of a suitable biological model must be considered (like ASM2d including pH calculations –Henze et al., 1999; Serralta et al., 2004; García-Usach et al., 2010). We have chosen the possibility of using ASM3+bio-P model (Rieger et al., 2001) and research is now focused on this aspect.

3) Another axis that should be envisaged is the use of pH microsensors for measuring pH gradients inside the granules. Some trials with O_2 probes were performed on granules embedded on an agar gel (results not here shown), revealing that O_2 was depleted immediately in the first 100 μm from the granule surface, and further work needs to be done, especially regarding the granule fixation methods and the medium. The goal of carrying out the set of tests performed with oxygen microsensors, was to i) prove the microprobes resistance when passing through the mineral core ii) verifying that the channels created by the microsensors did not affect the internal gradients in the granule (by creating a macropore channel). The results ensured the resistance of the sensor to the internal solid core as well as the minimum influence of the macropore created.

4) Finally, the biomineralization potential of granules could be explored for different particular cases of polluted effluents, like in the metal bioremediation field. Metals are involved in different industrial waste effluents (textile, tannery and dyes, painting, metallurgical, paper-ink industry, etc.) and some experiments with aerobic granules have been proven to accumulate higher metal concentrations than other sorbents, like alginate (Maiti et al., 2009), bacterial spp. (Qiu et al., 2009), or activated sludge biomass (Boswell et al ., 2001). Moreover, the advantage of the use of granules for this purpose relies on the easy solid-liquid separation conversely to activated sludge. Aerobic granules have been investigated for their capacity of accumulate divalent metals like Ni^{2+}, Cu^{2+}, Zn^{2+} (Liu et al., 2002; Liu and Xu, 2007), Cr^{2+} (Yao et al., 2009), Co^{2+} (sun et al., 2009) and Cd^{2+} (Xu and Liu, 2008). They established that precipitation and ion-exchange mechanisms could be responsible of this phenomenon, and some of them identified some functional groups like alcohol, carboxyles, amines and phosphates as metal binding sites.

However, further work could be made in order to enhance metal accumulation potential phenomenon in granules for detoxification processes and better understanding the metal-binding mechanisms in these aggregates and the knowledge of the functional groups involved.

In fact, the porous structure of bio minerals revealed for the bioliths precipitated inside granules, could constitute a proper matrix for scavenging and entrapping metals inside, without the redisolubilization problem.

5) A last research axis that this thesis could provide as a starting point (introduced in chapter IV), is the use of bio-genetic tools for driving the precipitation of a desired mineral (struvite for example, rather than hydroxyapatite). The study of the lipoproteins rich in aspartic acid (Weiner et al., 2008; de Muynck et al., 2010), as well as the enrichment of sludge with bacterial spp. like *M. Xanthus and M. Coralloides D.* (Ben Omar, 1995 and González-Muñoz, 1993), could be promising for this purpose.

VI.3.REFERENCES

Ben Omar N., Martínez-Cañamero M., González-Muñoz M.T., Arias J.M., Huertas F. (1995). *Myxococcus xanthus' killed cells as inducers of struvite crystallization. Its possible role in the biomineralization processes,* Chemosphere, 30 (12): 2387-2396.

Boswell CD, Dick RE, Eccles H, Macaskie LE. (2001). *Phosphate uptake and release by Acinetobacter johnsonii in continuous culture and coupling of phosphate release to heavy metal accumulation*. J Ind Microbiol Biotechnol, 26(6):333–40.

De Muynck W., de Belie N., Verstraete W. (2010). *Microbial carbonate precipitation in construction materials: A review.* Ecological Engineering 36(2): 118-136.

García-Usach F., Ribes J., Ferrer J., Seco A. (2010). *Calibration of denitrifying activity of polyphosphate accumulating organisms in an extended ASM2d model.* Water Research, 44(18):5284-5297

González-Muñoz, M., Arias, J.M., Montoya, E., Rodriguez-Gallego, M. (1993). *Struvite production by Myxococcus coralloides D*. Chemosphere 26 (10), 1881–1887.

Henze M., Gujer W., Mino T., Matsuo T.,. Wentzel M.C., Marais G.R., Van Loosdrecht M.C.M. (1999). *Activated sludge model No.2D, ASM2D.* Water Science and Technology, 39(1): 165-182.

Liu Y, Yang SF, Tan SF, Lin YM, Tay JH. (2002). *Aerobic granules: a novel zinc absorbent*. Lett Appl Microbiol. 35(6):548–551.

Liu Y, Xu H. (2007). *Equilibrium thermodynamics and mechanisms of Ni2+ biosorption by aerobic granules*. Biochem Eng J 2007;35(2):174–82.

Maiti SK, Bera D, Chattopadhyay P, Ray L. (2009). *Determination of kinetic parameters in the biosorption of Cr (VI) on immobilized Bacillus cereus M116 in a continuous Packed Bed Column Reactor*. Appl Biochem Biotechnol, 159(2):488–504.

Mañas A., Sperandio M., Biscans B. (2009). *Inducing mineral phosphate precipitation in biological aggregates for wastewater treatment and phosphorus recovery in a Sequencing Batch Reactor*. Congrès National SFGP, Marseille 2009.

Qiu RL, Zhao BL, Liu JL, Huang XF, Li QF, Brewer E, Wang SZ, Shi N. (2009). *Sulfate reduction and copper precipitation by Citrobacter sp. isolated mining area.* J Hazar Mater, 164(2–3):1310–1315.

Rieger L., Koch G., Kühni M., Gujer W. and Siegrist H. (2001). *The eawag bio-P module for activated sludge model No.3.* Wat. Res., 35 (16): 3887-3903.

Serralta J., Ferrer J., Borrás L., Seco A. (2004). *An extension of ASM2d including pH calculation*. Water Research, 38(19): 4029-4038.

Sun XF, Wang SG, Zhang XM, Paul Chen J, Li XM, Gao BY, Ma Y. (2009). *Spectroscopic study of Zn2+ and Co2+ binding to extracellular polymeric substances (EPS) from aerobic granules.* J Colloid Interface Sci., 335(1):11–17.

Weiner S. (2008). *Biomineralization: A structural perspective*. Journal of Structural Biology 163 (3):229-23

Xu H, Liu Y. (2008). *Mechanisms of Cd2+, Cu2+ and Ni2+ biosorption by aerobic granules*. Sep Purif Technol, 58(3):400–11.

Yao L, Ye ZF, Tong MP, Lai P, Ni JR. (2009). *Removal of Cr3+ from aqueous solution by biosorption with aerobic granules*. J Hazard Mater, 165(1–3):250–5.

1. DESCRIPTION:

Aeration test with the effluent from a UASB digester from a dairy industrial wastewater treatment plant (Site 2, according to Chapter IV).

2. MATERIAL AND METHODS:

A batch stirred reactor of 2.5L-volume has been aerated during 24 hours in order to promote pH changes due to the stripping phenomenon. (Stirring: 300 rpm; air flow: 120 L/h). pH has been followed during the course, and samples were taken regularly for the physico-chemical characterization according to AFNOR 1994. The instantaneous concentrations of Ca^{2+}, PO_4^{3-}, Mg^{2+}, K^+, Cl^-, Na^+, NH_4^+, NO_2^- and NO_3^- have been determined by Ionic chromatography (IC25, 2003, DIONEX, USA), prior filtering the samples through a 0.2 µm pore-size acetate filters. Microscopic observations of drops sampled at regular intervals have been performed during the kinetics, and the final precipitate has been dried and analyzed with XDR and SEM-EDX, similarly as in the precedent chapters. Initial TSS concentrations were of 730 mg/L (mainly due to floccular biomass) and initial VSS=462 mg/L.

3. RESULTS AND DISCUSSION:

3.1. Kinetics

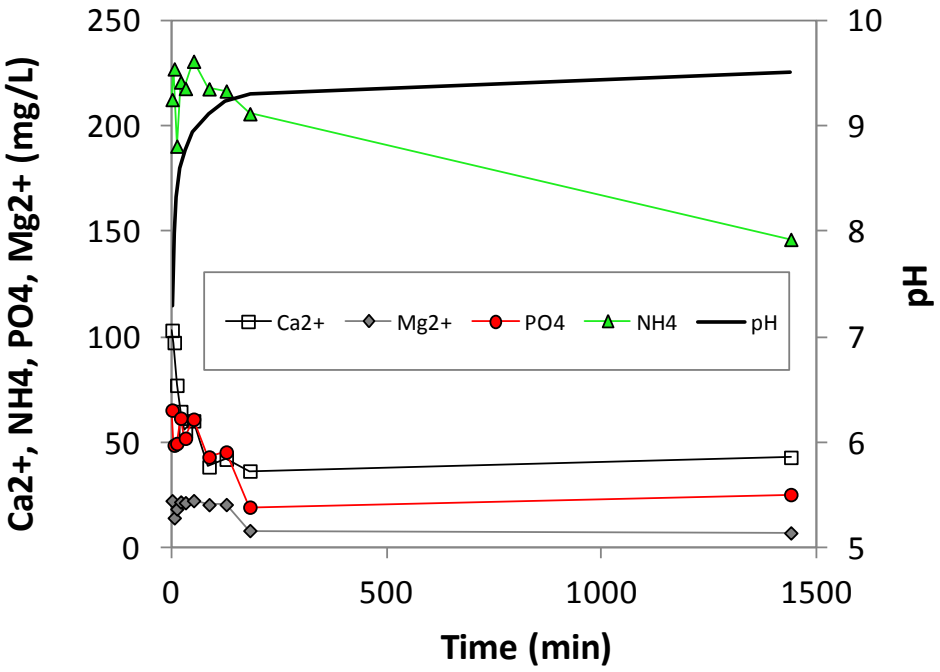

Figure A.VI.1: Evolution of pH, Ca^{2+}, Mg^{2+}, NH_4^+, P-PO_4^{3-} concentration during the batch kinetics at 120L/h and 300 rpm.

Figure A.VI.1 shows the evolution in the bulk of different ions involved in struvite and calcium phosphate minerals. All ions considered decrease during the course as pH rises due to the CO_2 stripping phenomenon, being 1.50, 1.29, 4.74 and 0.63, the Ca^{2+}, PO_4^{3-}, NH_4^+ and Mg^{2+} diminutions, respectively. Ammonium depletion could be due to simultaneous struvite precipitation, and ammoniac stripping (as pH rises up to 9).

3.2. Solid phase analysis

Samples taken during the kinetic course were observed with a microscope in order in the research of crystal structures (figure A.VI.2). The crystals shown have the same appearance as struvite crystals.

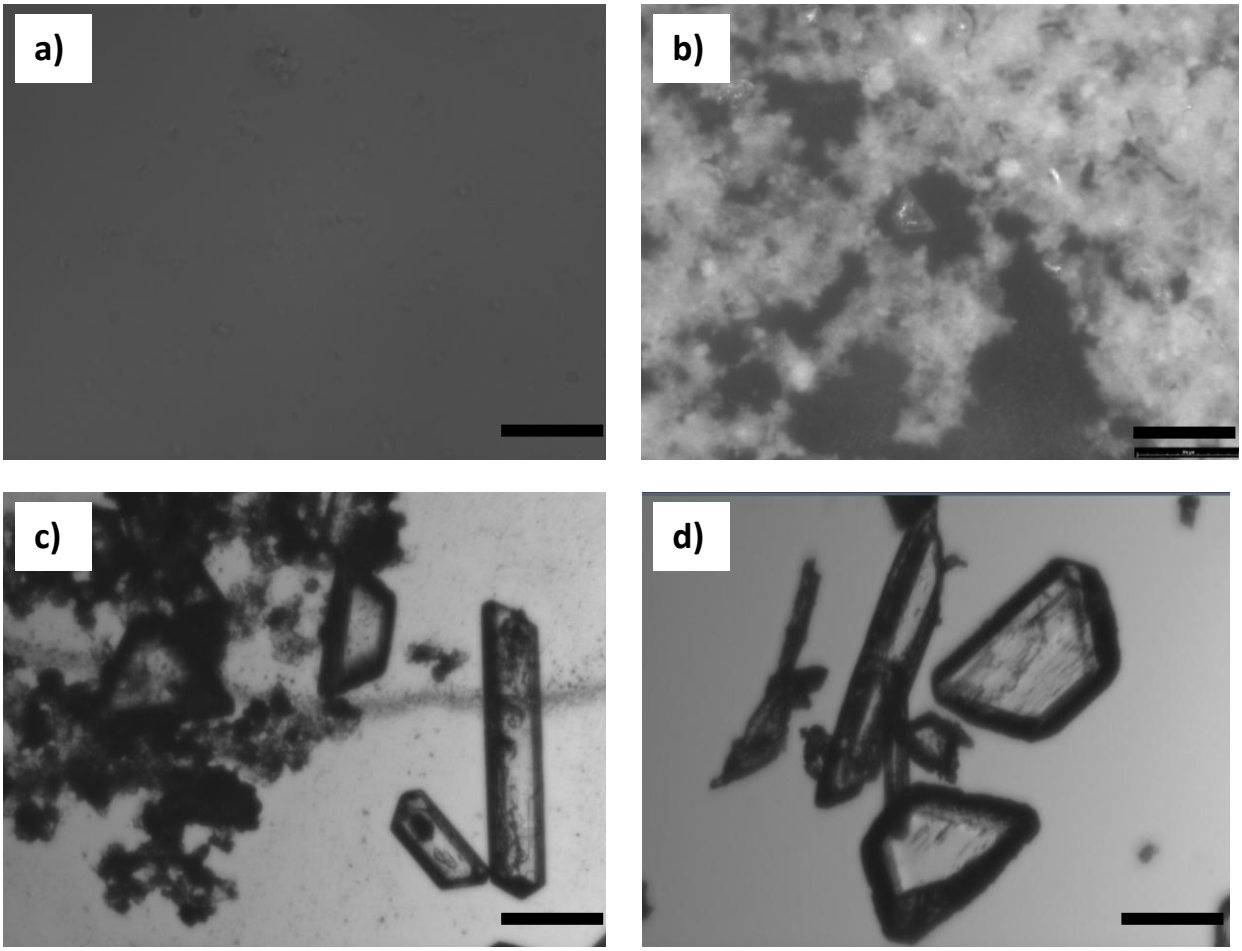

Figure A.VI.2: Microscopic observations of the bulk at a) 0min; b) 45 min; c) 2 h; d) 24h

Figure A.VI.3. shows the XDR analysis carried out over the air-dried solid phase collected at the end of the aeration test. Conversely to the methods used in the precedent chapters, the sample was not calcined, and the organic matter could have interferred the spectrum, and no MAP or HAP patterns from the database matched with the sample.

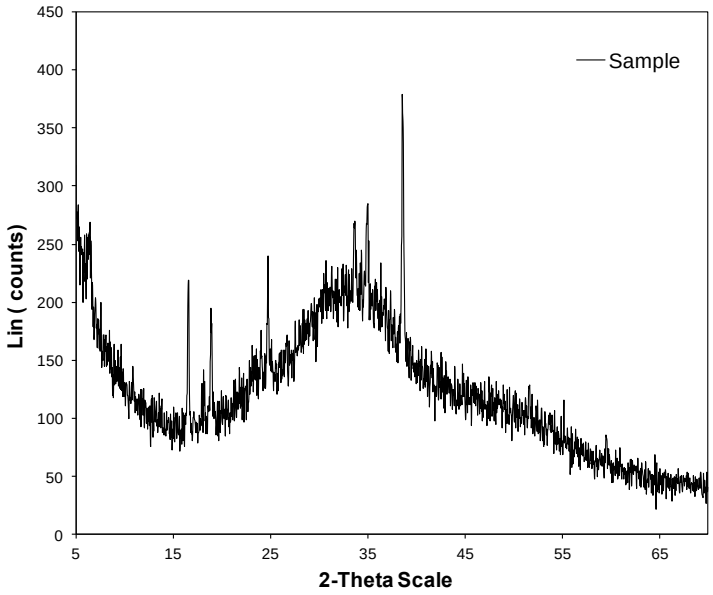

Figure A.VI.3: XDR pattern of the sample solid phase

3.3. Influence of different operating conditions (aeration and stirring rates)

Another test performed at higher aerating rates and stirring velocities (150L/h and 520 rpm) were tested in order to compare the phosphorus removal yields, which are shown in table A.VI.1.

Table A.VI. 1: Comparison of the ion removal yields(%) at two different operating conditions

Ion	Test 1: 300rpm/120L·h^{-1}	Test 2: 520rpm/150L·h^{-1}
Ca^{2+}	58	73
PO_4^{3-}	61	60
Mg^{2+}	68	72
NH_4^{+}	31	0

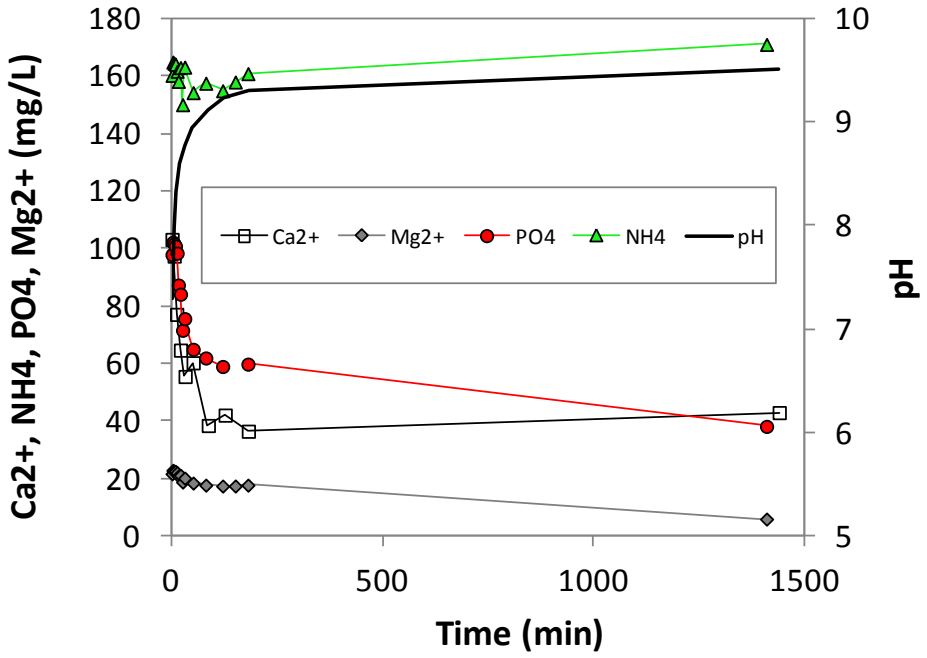

Figure A.VI.4: Evolution of pH, Ca^{2+}, Mg^{2+}, NH_4^+, P-PO_4^{3-} concentration during the batch kinetics at high aeration and high stirring conditions (150L/h and 520 rpm).

4. CONCLUSIONS:

Preliminary tests with real effluents have been conducted for assessing the precipitation potential by pH rise induced by aeration. Table A.VI.1 reveals similar removal yields for phosphorus, slightly higher removal yields for calcium and magnesium in the second test, and a probable struvite redisolubilization phenomenon in the second test. Indeed, conversely to the first test, ammonium is not removed at the end of the course, probably due to the competition of phosphorus for the calcium and magnesium phosphates.

These observations bear out that mineral precipitation takes place in the bulk when there is higher pH values than 7.4 and ions supersaturation. It was also useful to validate the physico-chemical model.